

ABSTRACT

INELASTIC PROTON SCATTERING

FROM ^{48}Ca

By

Carl Jerome Maggiore

Inelastic proton scattering from the nucleus ^{48}Ca has been performed at four energies: 25.11, 29.83, 35.00, and 40.21 MeV, using the proton beam from the MSU sector-focused cyclotron. Cross sections were taken every five degrees from 13° to 100° with Ge(Li) counters fabricated at this laboratory. The overall resolution obtained was less than 30 kev at all energies.

The elastic scattering from ^{48}Ca was compared with the elastic scattering from ^{40}Ca using the optical model. It was found that the relative matter distributions are in agreement with the predictions of the $A^{1/3}$ law.

The inelastic scattering revealed several previously unreported excited states in ^{48}Ca . Angular momentum transfers for most of the states were obtained by comparison of the shapes of the angular distributions to those of known L. Where possible, spin assignments are inferred on the basis of this and other data.

The experimental angular distributions are compared with calculated distributions using the collective model distorted wave Born approximation. The nuclear deformations obtained are used to calculate the vibrational model parameters and the reduced transition probabilities. The results are compared with previous inelastic alpha scattering experiments and inelastic electron scattering

results. The energy dependence of the results and the sensitivity of the deformations to the optical model parameters were studied.

INELASTIC PROTON SCATTERING

FROM ^{48}CA

By

Carl Jerome Maggiore

A THESIS

Submitted to
Michigan State University
in partial fulfillment of the requirements
for the degree of

DOCTOR OF PHILOSOPHY

Department of Physics

1971

For Jan

ACKNOWLEDGEMENTS

I would like to give special thanks to Charles Gruhn, my advisor, for his patient and unlimited willingness to help throughout the last four years. I am unable to adequately express the debt of gratitude that I owe him.

Special thanks are also due to Barry Freedom for help with the calculations, the data taking, and being there when needed. To Thomas Kuo who worked closely with me throughout the experiment many thanks are due. Without him the work could not have been done.

And for help and understanding in the non-technical aspects of this work my deepest thanks to my parents and my wife, Jan.

TABLE OF CONTENTS

Acknowledgments	iii
List of Tables	vi
List of Figures	vii
1. Introduction	i
2. Experimental Procedures	iii
2.1 Modifications to the Goniometer	iii
2.2 Target Storage System	iv
2.3 Cyclotron and Beam Transport	vi
2.4 Detectors	ix
2.5 Electronics	x
2.6 Data Acquisition	xi
3. Data Analysis	xviii
3.1 Angle Calibration	xviii
3.2 Normalization	xix
3.3 Excitation Energies	xxii
3.4 Cross Sections	xxv
4. Optical Model Studies	xxvi
4.1 Optical Model for DWBA Calculations	xxvi
4.2 Optical Model Difference between ^{40}Ca and ^{48}Ca	xxxii
5. Theoretical Analysis	xlvi
5.1 DWBA Theory	xlvi
5.2 Collective Model	xlix

5.3 Vibrational Model	1
5.4 Calculations	liii
6. Results	lx
6.1 States below 5 MeV	lx
6.2 States between 5 and 6 MeV	lxvi
6.3 States between 6 and 7 MEV	lxviii
6.4 States between 7 and 8 MeV	lxxiii
6.5 States between 8 and 9 MeV	lxxiv
6.6 Summary	lxxviii
6.7 Comparison with Theory	lxxxii
Bibliography	lxxxiv
Appendices	
I. Detector Fabrication and Testing	lxxxvii
I.1 Choice of Ge(Li)	lxxxvii
I.2 Fabrication	lxxxviii
I.3 Packaging	xcii
I.4 Testing	xcv
I.5 Radiation Damage	xcvii
I.6 Other Ge(Li) Detectors	ciii
II. Experimental Data	cviii
II.1 Theoretical Angular Distributions	cviii
II.2 Plotted Angular Distributions	cxiii
II.3 Tabulated Angular Distributions	cxliv
II.4 Tabulated Nuclear Deformations	clxxvi
II.5 Quantities Calculated from the Nuclear Deformations	clxxxii

LIST OF TABLES

2.1	Contributions to the energy resolution	xiii
3.1	Isotopic analysis of the target	xxi
3.2	Contributions to the uncertainty in absolute normalization	xxi
3.3	Excitation energies of ^{48}Ca	xxiv
4.1	Fricke's average optical parameters	xxvii
4.2	Potential well depths using Fricke geometry	xxviii
4.3	Potential well depths with equal real and imaginary geometries	xxviii
4.4	Differences in the optical model parameters for ^{48}Ca and ^{40}Ca	xxxviii
6.1	Upper limits on the 0^+ cross sections	lxvii
6.2	Comparison of the nuclear deformations	lxxxi
I.1	Contributions to the energy resolution	c

LIST OF FIGURES

2.1	Cyclotron and beam layout	vii
2.2	Ge(Li) electronics	xii
2.3	Typical 25 MeV spectrum	xiv
2.4	Typical 30 MeV spectrum	xv
2.5	Typical 35 MeV spectrum	xvi
2.6	Typical 40 MeV spectrum	xvii
4.1	Optical model fit with $R = I$ geometry	xxix
4.2	Optical model fit with Fricke geometry	xxx
4.3	40 MeV χ^2 surface	xxxiv
4.4	35 MeV χ^2 surface	xxxx
4.5	30 MeV χ^2 surface	xxxvi
4.6	25 MeV χ^2 surface	xxxvii
4.7	Ratio of elastic angular distributions	xl
4.8	Optical model radii with $U_{sym} = 0$	xli
4.9	Optical model radii with $U_{sym} = 4.4$ MeV	xlii
4.10	Optical model radii with $U_{sym} = 0$ and unequal geometries	xliii
4.11	Optical model radii with $U_{sym} = 4.4$ MeV and unequal geometries	xliv
5.1	DWBA calculations for $L = 2$ states	lv
5.2	DWBA calculations for $L = 3$ states	lvi
5.3	DWBA calculations for $L = 4$ states	lvii
5.4	DWVA calculations for $L = 5$ states	lviii
6.1	Comparison of ^{48}Ca and ^{50}Ti	lxI
6.2	Comparison of ^{48}Ca and ^{52}Cr	lxii
6.3	$L = 3$ states	lxv
6.4	$L = 5$ states	lxix
6.5	$L = 4$ states	lxxi
6.6	Comparison with other experiments	lxxxix

6.7	Experimentally determined β^2	lxxx
I.1	Surface barrier geometry	xc
I.2	Detector mount	xciii
I.3	Slit scattering	xciv
I.4	^{137}Cs spectrum	xcvi
I.5	Alpha particle spectra	xxviii
I.6	Proton resolution at 40 MeV	xcix
I.7	Proton radiation damage	ci
I.8	Relative efficiency curve	cvi

1. INTRODUCTION

^{48}Ca is a doubly closed shell nucleus and is used as the core for a large number of nuclei in the $f_{7/2}$ region of the periodic table. Relatively little work has been done on ^{48}Ca because of the difficulty obtaining targets.* Inelastic alpha scattering performed at 42 MeV (Pe 65) and 31.5 MeV (Li 67) has identified the spins and parities of the strongly excited states, but the resolution of ~ 100 keV is not able to resolve many of the weak or high lying states. The $^{46}\text{Ca}(\text{t},\text{p})^{48}\text{Ca}$ reaction has been used to study the level structure of ^{48}Ca (Bj 67) and detects a large number of levels, but the experiment was only able to positively identify the 0^+ levels in ^{48}Ca . Inelastic proton scattering is able to identify angular momentum transfer reasonably well if the data are clean, and has the advantage of being a useful probe of the microscopic structure (Gl 66). Therefore the present experiment involving inelastic proton scattering was undertaken.

The ability of the (p,p') reaction to identify angular momentum transfer increases as the incident beam energy increases, also the direct reaction theory is expected to be more correct at higher energies where compound nuclear effects are small. The experiment was performed at four energies to check the consistency of the DWBA

* ^{48}Ca is a stable nucleus, but constitutes only 0.18% of the natural abundance of Ca.

method of analysis and the collective model calculations.

The experiment was performed with Ge(Li) counters because these detectors are able to give 30 keV resolution at 40 MeV, and they have the dynamic range needed to obtain the data in a reasonable period of time. A magnet spectrograph can yield better resolution, but at the time was not available. Stacks of Si(Li) counters, while able to detect 40 MeV protons, cannot do so with 30 keV resolution and clean valleys.

The experiment was performed with the goniometer of Ken Thompson (Th 69), which was designed specifically for use with Ge(Li) detectors. The detectors were fabricated in this laboratory. A discussion of the fabrication techniques is presented in Appendix I.

2. EXPERIMENTAL PROCEDURE

2.1 Modifications to the Goniometer

In order to obtain the data for this experiment in a "reasonable" period of time it was decided that a detection system that would allow simultaneous data taking at two angles was needed. Other requirements were that small angle data into 15° be taken, and that the only windows the scattered protons traverse be the 1/4 mil aluminized mylar windows on the detector cryostats. Therefore it was necessary to design a new 16" target chamber with a sliding seal for use with the goniometer (Th 69).

The modular design of the goniometer makes it particularly convenient for modification to particular experimental requirements. The details of the 16" target chamber are shown on MSUCL drawing HA-110-901-H. The basic design calls for input and exit ports compatible with the taped beam pipe and slip-fit O-ring seals used previously. The data taking window extends from 10° to 110° . There are two viewing ports opposite the data taking window that extend from 20° to 70° and from 110° to 160° . There is also a fixed Leybold fitting at 90° on this side of the chamber. On the data taking side of the chamber, there are two BNC feed throughs at 145° and 155° , and another Leybold fitting at 135° .

This particular design allows data to be taken from about 12° to 110° . If one wants to take data at scattering angles larger than 110°

the chamber may be rotated 180° and data taken from 70° to 170°. The monitor counter may be set on the secondary arm at any angle to view the beam through the monitor ports or at either of the fixed Leybold fittings.

The sliding seal is composed of a 1/8" O-ring inset in the chamber and a sliding steel strap made of 9 mil shimstock. Pressure sensitive teflon tape was applied to the chamber and the clamping ring to provide a smooth non-stick surface for the steel strap. In practice it was necessary to glue the O-ring into the groove in the chamber to prevent movement of the O-ring when the steel strap was moved. In addition the strap and O-ring were well lubricated with Dow Corning silicone high vacuum grease. No particular problems were encountered with the sliding seal in use as long as it was kept clean and lubricated.

The vacuum feed throughs to the detector cryostat caps were short sections of 3/4" copper tubing. The tubing was soldered into a brass block which was in turn soldered to the steel strap. The cryostat caps were coupled to the copper tubing using a simple O-ring slip fitting.

To provide the counter torque needed when the sliding seal is in motion, the target chamber was rigidly attached to a quadrupole support stand with a 1" X 5" aluminum arm. This same quadrupole support stand, which was bolted to the floor, was used to support the vacuum diffusion pump for the goniometer.

2.2 Target Storage System

The target used in this experiment was relatively expensive and

it would oxidize completely if exposed to the atmosphere for a few hours. Therefore, it was necessary to design and build a vacuum storage system for the target. The goniometer was initially designed with a target transfer lock which could be used to transfer a target into the target chamber without breaking vacuum (Th 69), therefore the target storage system was designed to be compatible with the transfer unit of the goniometer.

A modular design consisting of three basic units was used. A cryogenic pumping system with three ports, a transfer valve, and a storage chamber are the three basic units. The details for the target storage system are shown on MSUCL drawings HA-114-100-F to HA-114-106-F.

The cryogenic pumping system is based on a Linde LD-10 cryosorption pump attached to three NRC 1253-1 1/8" valves which are coupled to the standard 4" Marmon flanges. A cryosorption pump was used because a system was needed which was independent of probable university-wide power failures. While it is true that the pump must always be kept at liquid nitrogen temperature, it was not felt that this was a particular disadvantage, since the detectors also had to be stored at liquid nitrogen temperature and could be kept at the same dewar.

The second unit in the storage system is the storage-transfer valve. This is a vacuum valve which has 4" Marmon flanges on both sides, can hold a vacuum on either side, and is wide enough to allow passage of a 1 1/4" target frame in the open position.

The third unit is the storage chamber itself which is merely an aluminum chamber with a lucite window and a target holder.

To make a target transfer from the storage system to the goniometer

the portable storage system is moved out to the experimental area near the goniometer. The storage valve is closed and the storage chamber and valve removed from the cryosorption pump. The transfer unit (Th 69) is attached to the storage valve and then evacuated. The valve is opened and the target moved into the transfer unit. The valve is closed and the storage chamber is removed from the valve. The transfer unit with the target is now attached to the goniometer. When the goniometer is evacuated, the transfer valve is opened and the target is transferred to the target ladder of the goniometer. The complete transfer in vacuum requires about 45 minutes.

2.3 Cyclotron and Beam Transport

The Michigan State University sector-focused cyclotron (Bl 66) was used to produce the proton beams used in this experiment. The machine is a variable energy, isochronous cyclotron utilizing an electrostatic deflector and magnetic channel for single turn extraction. The experiment was performed with an internal beam of 1 to 5 microamps. The extraction efficiency varied from 70% to 100%. The beam current on target was varied from 3 to 90 nanoamps depending on the scattering angle.

The extracted beam is focused and energy analysed by the beam transport system shown in Figure 2.1. The two horizontal bending magnets, M1 and M2, are used to center the beam on the object slit, S1, and to align the beam parallel to the beam pipe axis. The quadrupole doublets, Q1 and Q2, are used to focus the beam on slit S1. The divergence of the beam is defined by slits S1 and S2 which are separated

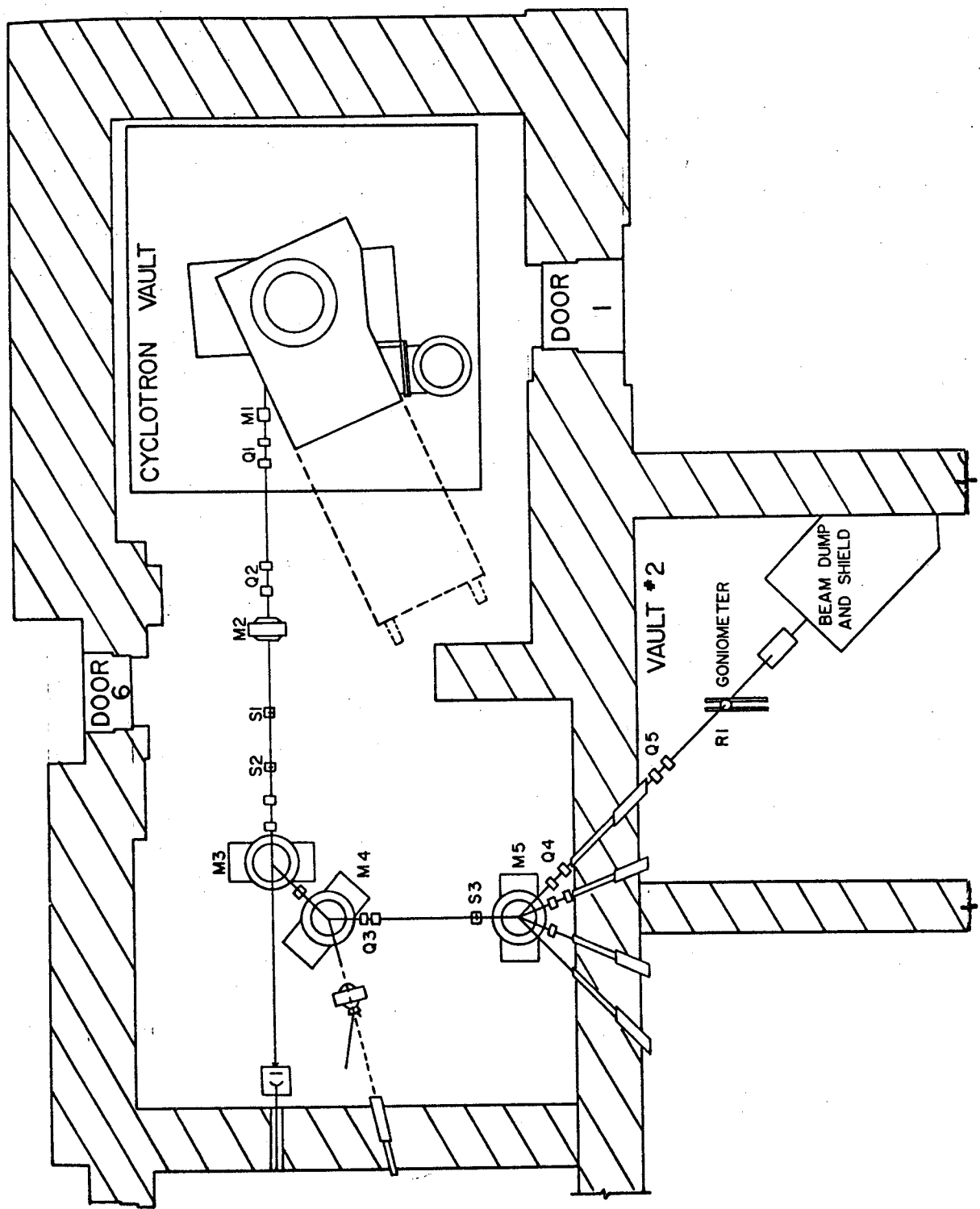


Figure 2.1 Cyclotron and beam layout.

by 48 inches. M3 and M4 are two 45° bending magnets which are the primary elements of the analysis system. The quadrupole doublet Q3 focuses the beam on slit S3. M5 is another 45° bending magnet which deflects the beam into the goniometer. The quadrupole doublets Q4 and Q5 focus the beam onto the target. More complete descriptions of the properties of the energy analysis system have been published elsewhere (Ma 67) (Sn 67). During this experiment the slits S1 and S3 were set at 15 mils for energy resolution of 10 keV. S2 was set at 100 mils to yield a beam divergence of ± 2 mrad.

For the final beam preparation a scintillator with a 1/8 inch hole in the center was inserted in the target ladder of the goniometer. The beam spot was viewed with a television camera to check for proper focus and centering. In addition a tantalum ring, R1, with a 1/2 inch hole was located 16 inches in front of the target on the beam axis. The beam current on this ring was monitored throughout the experiment. The criteria used to insure proper alignment of the beam were: a well focused and centered beam on the scintillator, minimum current on the ring, maximum current in the Faraday cup, and minimum neutron background in the experimental room.

During the experiment the beam spot on target was approximately 1/16 inch wide and 3/8 inches high. The current on the ring was always less than 1% of the beam dumped in the Faraday cup and was usually 0.1% or less. The current on the ring was probably due to slit scattering from S3. The neutron background in the experimental area provided a very sensitive test of the alignment of the beam into

the goniometer. If the beam scraped the beam pipe, the input snout, or the exit snout it would increase the neutron background by 2 or 3 orders of magnitude.

The Faraday cup used in this experiment is actually only a shielded beam dump and as such was not intended to measure absolute charge accurately. A 12 foot section of beam pipe, insulated from the goniometer by a Delrin spacer, with a 1/2 inch thick aluminum cap was used. It was surrounded by concrete and parrafin shielding described elsewhere (Th 69a) to reduce the neutron background seen by the detectors.

The Faraday cup was in contact with the parrafin and concrete shielding blocks and was probably subject to some leakage current to ground. The Faraday cup was connected to an Ortec model 439 current digitizer used with an Ortec model 430 scaler to integrate the charge. The current digitizer outputs a logic pulse for every 10^{-10} Coulomb of integrated charge. This logic pulse is then fed into the scaler to record the total integrated charge. This arrangement provided relative numbers for the total incident charge for each run; these numbers were used as a check on the monitor counter which was used for the actual normalization.

2.4 Detectors

The detectors used in this experiment were lithium drifted germanium counters of the surface barrier geometry designed specifically for this experiment. (See Appendix I) The two detectors were

separated by 14.6°. The small angle counter was 13.25 inches from the target and had a final 30 mil Ta collimator that was 6.6 mm high and 2.2 mm wide. The large angle counter was 11.25 inches from the target and had a final 30 mil Ta collimator that was 6.2 mm high and 2.2 mm wide. The two detectors were operated at 1500 V and 1200 V bias respectively with leakage currents of less than 0.1 na.

The monitor counter used in this experiment was also of the Ge (Li) type, but since optimum resolution was not required, it was used in the side entry geometry. The detector was mounted in a Harshaw cryostat of the "sausage" type (Model 15). The monitor counter was mounted at a fixed angle on the secondary arm of the goniometer. The protons scattered into the monitor counter traversed an air space of about 1/2 inch between the 1/2 mil Kapton window on the target chamber of the goniometer and the 1/4 mil aluminized mylar window on the cryostat.

2.5 Electronics

The electronic equipment used in this experiment is shown in Figure 2.2. At the time the experiment was performed, it was necessary to use rather unconventional arrangement of the electronics to obtain acceptable resolution. It was our experience that with commercially available electronics, after amplification to the required 5 to 10 volt output signal, the rms noise level would be 3 to 4 mV, thus yielding a precision of 0.04% to 0.06% in the voltage measurement. At 40 MeV this corresponds to a contribution of 16 to 24 keV to the overall resolution. This was not acceptable.

It was found that by using a modified Ortec 109A preamplifier and the second stage of the Tennelec TC200 amplifier, the total electronic noise as measured with a Canberra stabilized pulser (Model 1501) was less than 6 keV at 40 MeV. The outputs of the amplifiers were fed into two Northern Scientific NS 629 analog-to-digital converters. The ADCs were interfaced to a Sigma 7 computer which was used to store the data. The ADCs were set to provide 8192 channel conversion gain. Only the upper 4096 channels of information were stored by using the 4096 channel digital offset. Using this configuration spectra were obtained with about 5 keV per channel.

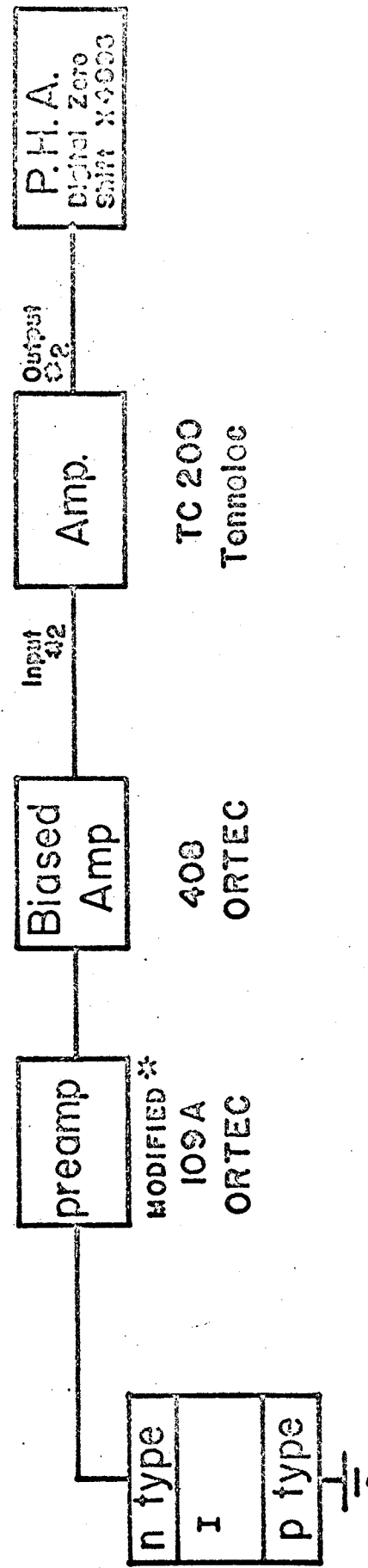
Conventional electronics were used with the monitor counter: Ortec 109A preamplifier, Ortec 410 linear amplifier, Ortec biased amplifier and into a Nuclear Data 160 multichannel analyser.

To make the dead time corrections two Ortec 420 single channel analysers were used. A window was set on the elastic peak from the monitor counter; the output of the single channel analyser was used to feed an Ortec 430 scaler and the channel zero of each NS 629 ADC. The Ortec 416 gate and delay generator was used to provide proper pulse shaping for the ADCs. The dead time correction was made by comparing the number of counts in the scaler with the number of counts in channel zero. A similar arrangement was used to make the dead time corrections for the monitor counter. The dead times throughout the experiment were always less than 5%.

2.6 Data Acquisition

The data were acquired during two three day runs. Data for

Electronics for Ge(Li) detector



Typical precision of electronics: 0.015% at 40 MeV

* Modified by Joel B. Ayres, ORTEC

Figure 2.2 Ge(Li) electronics.

each energy were taken at 20 angles in 5° steps from about 13° to 100° . The data at 28° and 73° were taken twice, once with each put in position for aligning the beam at the next energy. The counters were removed during the alignment procedure to prevent radiation damage from the neutron background.

The resolution obtained during this experiment was between 25 and 30 keV (FWHM). The contributions to this energy resolution are listed in Table 2.1. Notice that the straggling contributions from the windows add directly rather than in quadrature, and they are the largest contribution to the energy resolution.

Table 2.1 Contributions to the energy resolution

Source	ΔE (keV)	ΔE^2 (keV 2)
Electronics	6.0	36
Ion pair statistics	6.2	39
Nuclear collisions	0.7	
Straggling		
Target	5	
Package window	5.3	18.3
Detector window	8	337
Beam	10	100
Kinematics	10	100
Total	24.5	602

Representative spectra at each energy are shown in Figures 2.2 - 2.5.

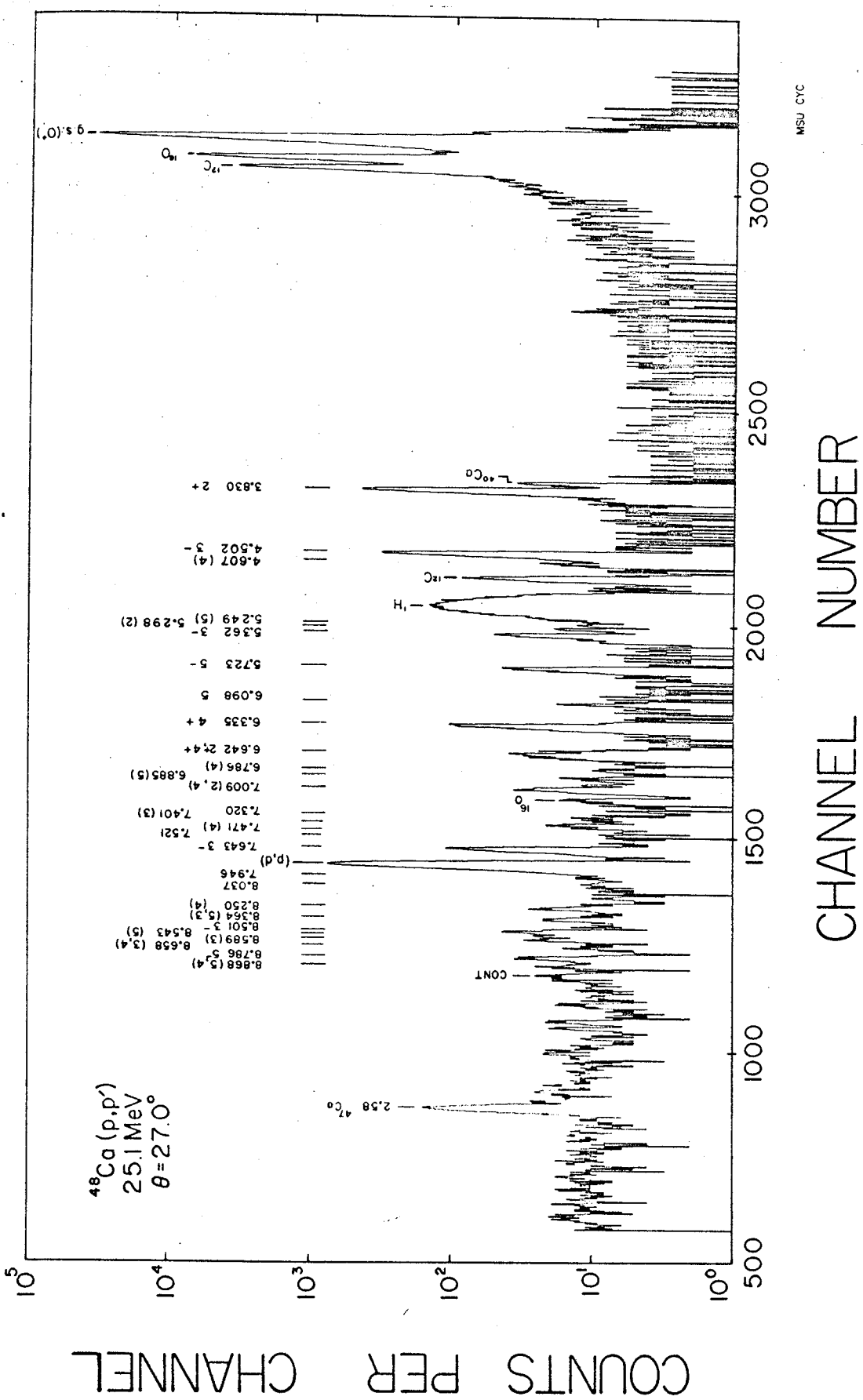
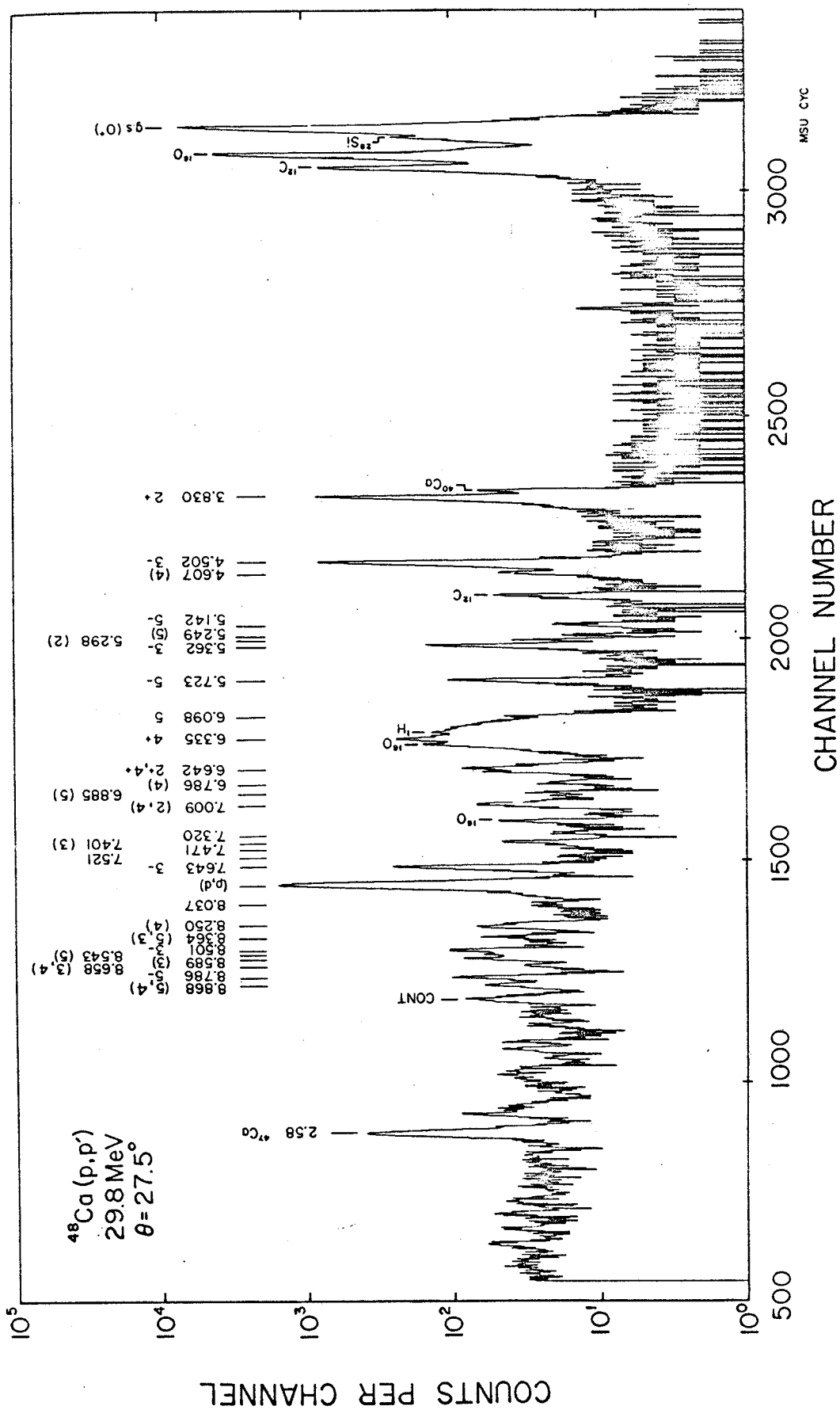


Figure 2.3 Typical 25 Mev spectrum.



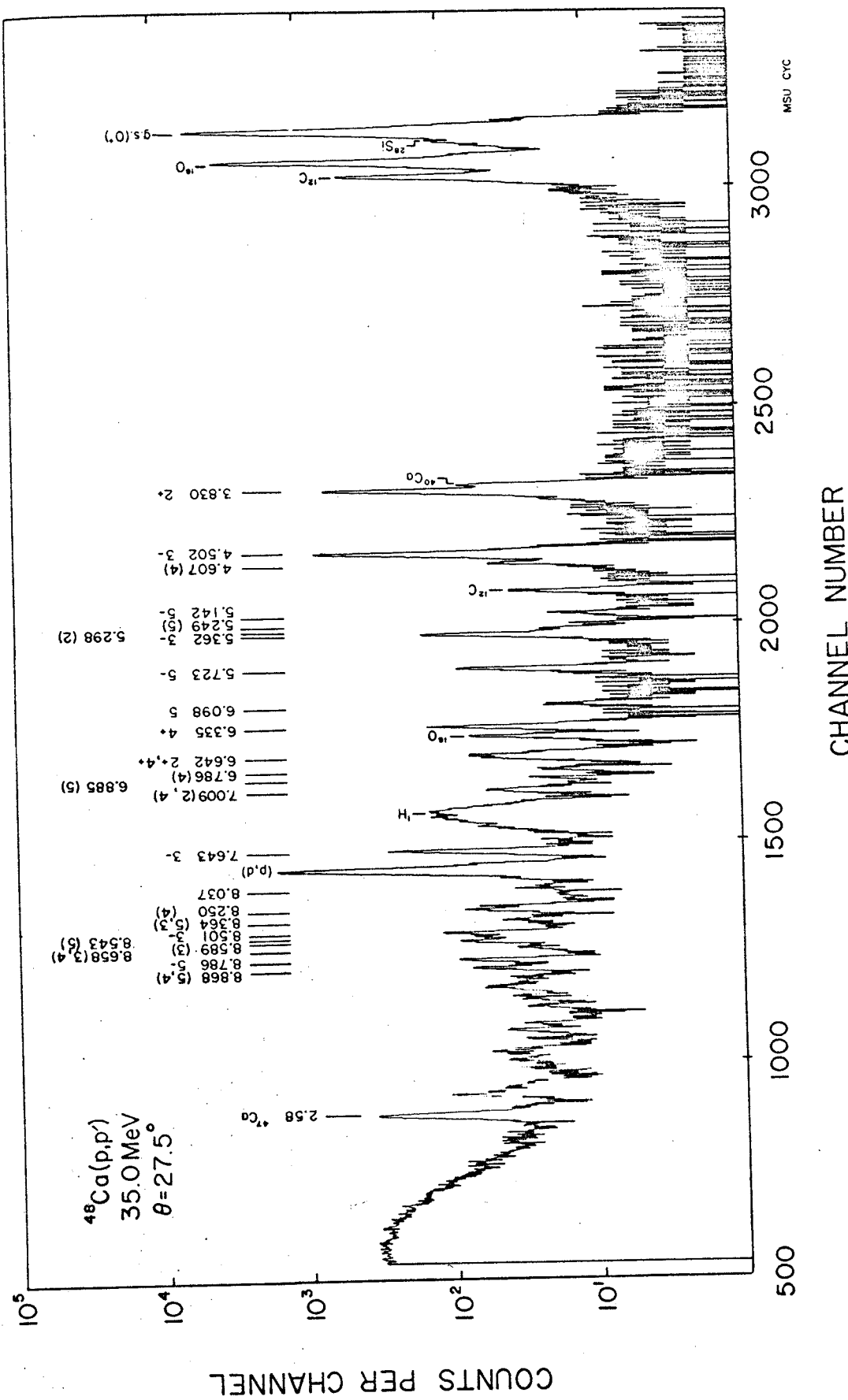


Figure 2.5 Typical 35 Mev spectrum.

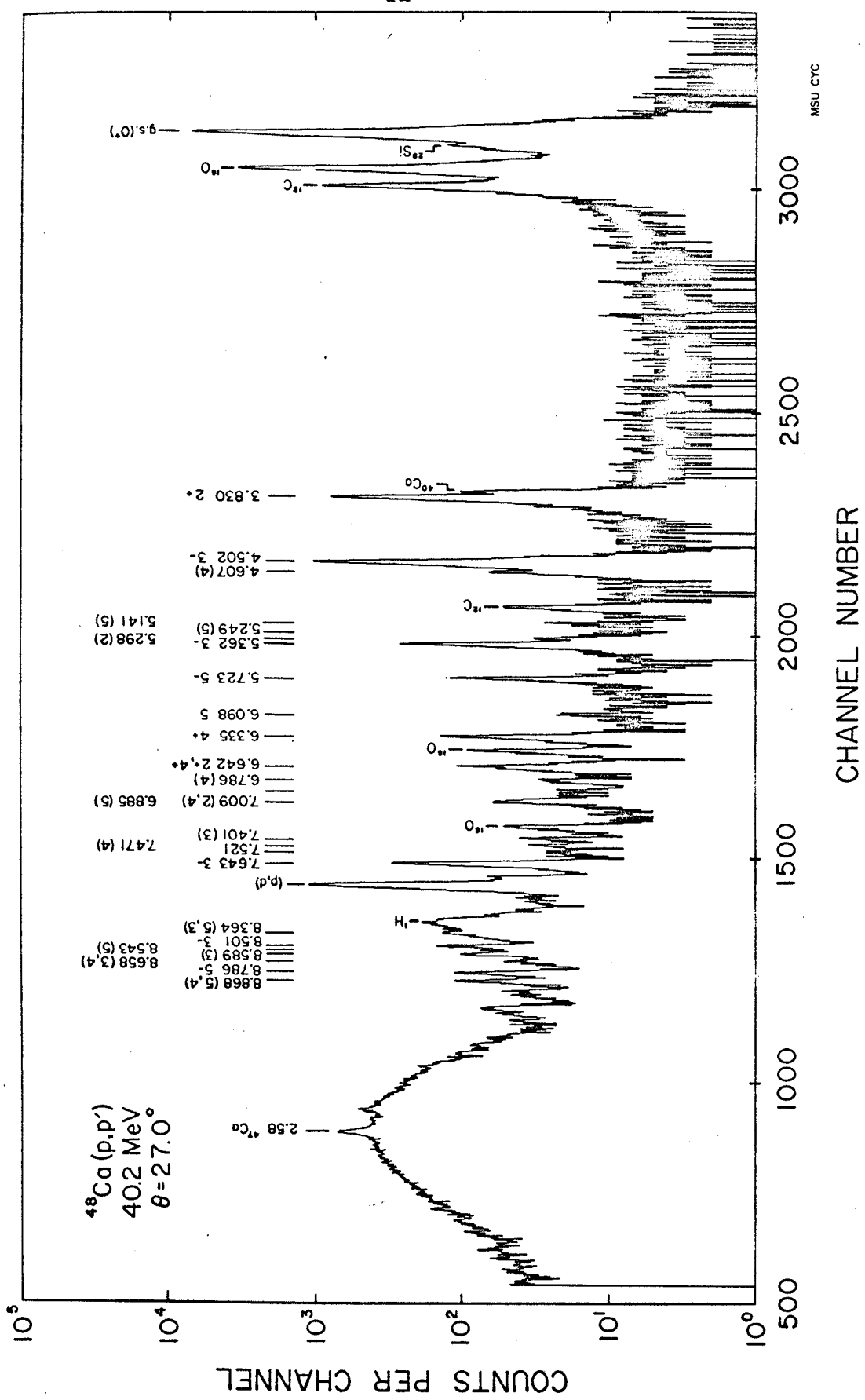


Figure 2.6 Typical 40 Mev spectrum.

3. DATA ANALYSIS

In this experiment the relative cross sections were measured using a monitor counter for normalization. The absolute cross sections were obtained by normalizing the ^{40}Ca elastic scattering, observed at large angles, to previous work and using the ratio of isotopic abundances in the target (c.f. Sec. 3.2).

The use of a monitor counter at a fixed angle to provide the relative normalization for each run eliminated the need to know the exact areal density of the target, solid angles of the detectors, target angle, and total incident charge.

The relative normalization between the two detectors used in this experiment was determined by taking data at a number of overlap angles. Dead time corrections were made for both detector ADC's as well as the monitor counter ADC.

3.1 Angle Calibration

The program, PEAKSTRIP, written by R. A. Paddock, was used to obtain the centroid, net counts, and statistical error in the counts for each peak in the spectrum. The input consisted of the two channel numbers, defining the edges of each peak, and the backgrounds at these boundary channels. A linear background is assumed under the peak. If there were more than 30 counts in the peak, the centroid was determined using the top two-thirds of the peak; otherwise the total peak was used.

The fractional standard error for the counts in each peak was determined by the formula

$$\Delta N = \frac{(N + 2B)^{1/2} - N}{N}$$

where

N is the total number of counts and

B is the total background count.

To determine the scattering angle for each spectrum the computer program, ANGCAL, was written. The program input consists of the centroids of three uncontaminated peaks, one of which is moving kinematically faster than the other two. The two slowly moving peaks are used for energy calibration, the third peak is used to determine the angle. An initial guess is made for the angle, and then, through an iterative procedure, the actual scattering angle is determined. The process usually converges within four iterations. Relativistic kinematics, calculated by the program KINE, written by P. J. Plauger, are used throughout. Typically elastic scattering from H or ^{12}C was used for the fast moving peak, and the ground state and known excited states of ^{48}Ca (Ma 66) (Bj 67) were used for the kinematically slow moving peaks. The angle calibration determined by the above procedure is believed accurate to $\pm 0.1^\circ$; the major limitations are the accuracy with which the centroid can be determined, the uncertainty in the energy calibration curve, and the uncertainty of the incident beam energy.

3.2 Normalization

The relative normalization for each run was obtained by

normalizing to the total counts in the elastic peak observed by the monitor counter. In each monitor spectrum the edges of the elastic peak were chosen at a constant fraction of the total peak height. The ratio of monitor counts to the integrated current for each run was calculated and found to be constant to within 5%. It is believed that the monitor counter yields the better relative normalization since the current digitizer and Faraday cup were subject to some leakage current.

Since data were taken simultaneously at two angles during the experiment it was necessary to determine the relative normalization between counters. This normalization is determined by the difference in solid angle subtended by the two counters and any difference in the detection efficiency of the two counters. The relative normalization between counters for this experiment was determined by taking data over the same angular range with each counter and then normalizing one angular distribution to the other. This was done at each energy and found to be constant within 2%. If a large error were made in the relative normalization between counters, the error would show up as systematic discontinuities in the angular distributions of all states at the overlap angles where one counter started taking data and the other stopped. No such discontinuities in the angular distributions were observed.

At scattering angles greater than 65° this experiment was able to completely resolve the elastic scattering from ^{40}Ca and ^{48}Ca . Table 3.1 lists the composition of the target used in this experiment.

Table 3.1 Isotopic analysis of the target.*

Isotope	Atomic %	Precision
40	3.58	± 0.05
42	0.05	± 0.01
43	0.01	
44	0.11	± 0.02
46	< 0.01	
48	96.25	± 0.05

* Determined by the Stable Isotopes Division of the Oak Ridge National Laboratory where the target was made.

Table 3.2 Contributions to the uncertainty in absolute normalization.

Source	%
Target composition	2
Normalization of ^{40}Ca	5
Statistics: ^{40}Ca peak	7
Monitor peak	3
Total	$\sim 10\%$

It can be seen that ^{40}Ca is the major contaminant and the relative amount is determined to within 5%. Accurate elastic scattering data for ^{40}Ca already exists (Fr 67); therefore it was decided to normalize the present ^{48}Ca data using the ratio of isotopic abundances in the target. As can be seen from Table 3.2, the absolute cross sections determined in this manner are accurate to $\pm 10\%$. The principal contributions to the uncertainty are the statistics of the ^{40}Ca elastic peak and the absolute normalization of the ^{40}Ca elastic scattering.

3.3 Excitation Energies

To determine the excitation energies of the various states observed, the program FOILTARCAL, written by R. A. Paddock, was used. The input was the output of PEAKSTRIP plus information concerning target composition, target orientation, the reaction involved, the detector angle, and a set of standard reference peaks. The program uses the reference peaks to determine a calibration curve of given order, which is then used to find the excitation energies of the unknown peaks. The program accounts for target thickness and uses relativistic kinematics throughout.

The reference peaks used for calibration purposes were the ground states of ^{48}Ca , ^{16}O , ^{12}C , the 4.44 MeV state of ^{12}C , the excited states of ^{48}Ca listed in Table 3.3, and the (p,d) ground state. Only reference peaks that were free of contaminants were used.

In order to use the deuteron peak as a calibration point in

the proton spectrum it was necessary to make a correction for the window in front of the detector. Since the deuteron loses more energy than a proton of the same energy in traversing the 1/4 mil aluminized mylar window, it was necessary to calculate the difference in energy loss between a proton and deuteron of the same energy and add this correction factor to the excitation energy of the deuteron. This correction factor varied from 20 to 60 kilovolts depending on the energy and angle of the scattered deuteron.

Both linear and quadratic energy calibration curves were tried. It was found that both linear and quadratic calibration curves yielded excitation energies for known states that agreed with those of Marinov and Erskine (Ma 66) to within the calculated uncertainties. As might be expected the quadratic curve yielded a better absolute fit to the known excited states up to 7 MeV in excitation energy.

As a check on the calibration curve above 7 MeV, the deuteron peak corresponding to the 2.580 - 2.600 doublet in ^{47}Ca was used. Again the necessary corrections to make the deuteron look like an equivalent energy proton were made. The linear calibration curve predicted the position of the deuteron doublet to within 7 keV with an uncertainty of ± 11 keV. The quadratic calibration curve predicted an excitation energy for the doublet that was approximately 50 keV high.

Without strong evidence to indicate that a quadratic or higher order calibration curve was needed, it was decided that the linear energy calibration curve would be used. These results indicate that

Table 3.3 Excitation Energies of ^{48}Ca .

L* (MeV) Present Data	E* (MeV) Ma 66 (p, p')	E* (MeV) La 66 (p, p')	E* (MeV) Bj 66 (p, t)
3.830±0.005	3.833†	3.818	3.827†
	4.284	4.272	4.281
4.502±0.004	4.506†	4.498	4.496†
4.607±0.006	4.613	4.604	
5.142±0.004	5.146	5.13	
5.249±0.003		5.266	
5.298±0.007			
5.362±0.005	5.368†	5.37	5.459
5.723±0.004	5.728	5.724	
6.098±0.003	6.106	6.096	
6.335±0.005	6.338†	6.34	6.329†
6.642±0.009		6.61	6.645
6.786±0.008		6.79	6.793
6.885±0.008			
7.009±0.008			
7.320±0.025			
7.401±0.025			
7.471±0.025			
7.521±0.025			
7.643±0.006			7.650
7.786±0.007			
7.940±0.006		7.97	
8.037±0.009			8.018
8.250±0.008			8.237
8.364±0.010			8.268
8.501±0.008			8.473
8.543±0.008			8.513
8.589±0.007			8.538
8.658±0.010			8.604
8.786±0.008			8.697
8.868±0.008			8.782

† Points used to determine the energy calibration curve.

the detectors and electronics used in this experiment yielded a data taking system which was linear to within 0.1% over a 10 MeV range of excitation energy.

3.4 Cross Sections

The program RELTOMOM, written by R. A. Paddock, was used to convert the PEAKSTRIP output and the monitor counts into the center-of-mass cross section for each peak. It was at this point that spurious data points were reanalyzed. Whenever possible, corrections were made for contaminated peaks.

In particular ^{12}C , ^{16}O , and ^{40}Ca were subtracted from the forward angle elastic scattering. To make these corrections the cross sections of the elastic scattering from ^{12}C and ^{16}O were used, where kinematically separated, to determine the relative amounts of carbon and oxygen on the target at each energy. Using the known ^{12}C and ^{16}O cross sections (Ca 67), the background subtraction could be made at smaller angles. The total amount of ^{12}C and ^{16}O on the target was approximately constant throughout the experiment. The same technique was used to subtract the excited states of ^{40}Ca from the ^{48}Ca excited states when they were not kinematically separated.

4. OPTICAL MODEL STUDIES

In order to perform the distorted wave Born approximation calculations, it is necessary to obtain the optical potential which describes the elastic scattering at each energy, because it is used to define part of the wave function in the entrance and exit channels. The optical potential is also of interest in itself because the parameterization used to describe the optical potential defines a radius which is usually associated with the matter distribution. Since good proton elastic scattering data exist for ^{40}Ca (Ku 70) (Fr 67) the study of the difference between elastic scattering from ^{40}Ca and ^{48}Ca and its relation to the optical model was undertaken.

4.1 Optical Model for DWBA Calculations

A commonly used optical potential, which has been found adequate to describe cross section and polarization data throughout the periodic table (Fr 67), is of the form

$$V(r) = V_c(r) - V_o f(x_o) - i(W_o - 4W_D \frac{d}{dx_I}) f(x_I) + (h/m_c)^2 V_s \frac{(1-d)}{r} \frac{d}{dr} f(x_s) l.s$$

V_c is the Coulomb potential for a uniformly charged sphere of radius $1.25 \text{ \AA}^{1/3}$. The geometry is of the Woods-Saxon form, that is

$$f(x_i) = [1 + \exp(x_i)]^{-1} \text{ where}$$

$$x_i = (r - r_i^{1/3})/a_i.$$

Fricke et. al. found a set of average optical potential parameters which fit a large number of targets. These parameters are listed in Table 4.1.

Table 4.1 Fricke's average optical parameters.

$r_o = 1.16F$	$a_o = 0.75F$
$r_I = 1.37F$	$a_I = 0.63F$
$r_s = 1.06F$	$a_s = 0.738F$
$V_s = 6.04 \text{ MeV}$	

It was found that by using these average geometry parameters a reasonable fit to the elastic scattering data could be found by searching on the potential well depths V_o , W_o , and W_D . The optical model search code, GIBELUMP, was used to minimize χ^2 by varying the potential well depths. The quantity χ^2 is a measure of the goodness of fit of the theory to the data.

$$\chi^2 = \frac{1}{N} \sum_{i=1}^N [(\sigma_{\text{Th}}(\theta_i) - \sigma_{\text{Ex}}(\theta_i)) / \Delta\sigma_{\text{Ex}}(\theta_i)]^2$$

where N is the number of points, $\sigma_{\text{Ex}}(\theta_i)$ and $\sigma_{\text{Th}}(\theta_i)$ are the experimental and theoretical cross sections at the angle θ_i , and $\Delta\sigma_{\text{Ex}}(\theta_i)$ is the experimental error associated with the i^{th} data point. The final parameters used at each energy are listed in Table 4.2.

Table 4.2 Potential well depths using Fricke geometry.

Energy (MeV)	V_o (MeV)	W_o (MeV)	W_D (MeV)	χ^2/N
25.11	50.98	0.60	6.04	11
29.83	49.93	3.96	3.61	11
35.00	43.80	5.24	2.34	7
40.21	47.67	5.24	2.35	4

The fits provided by these parameters to the data are shown in Figure 4.1.

In extracting a deformation parameter f for the inelastic scattering (see Section 5.) there is a possible ambiguity due to the fact that the real and imaginary geometries are not equal. Therefore, a set of optical parameters were found with the additional constraint that the real and imaginary geometries be equal. In this analysis $r_o = r_I = 1.20F$ and $a_o = a_I = 0.68F$. The optical strength parameters are listed in Table 4.3.

Table 4.3 Potential well depths with equal real and imaginary geometries.

Energy (MeV)	V_o (MeV)	W_o (MeV)	W_D (MeV)	χ^2/N
25.11	51.72	0.36	6.95	13
29.83	45.93	0.15	6.57	6.4
35.00	46.50	3.49	4.62	3.6
40.21	46.58	4.13	4.57	2.0

The fits to the data are shown in Figure 4.2.

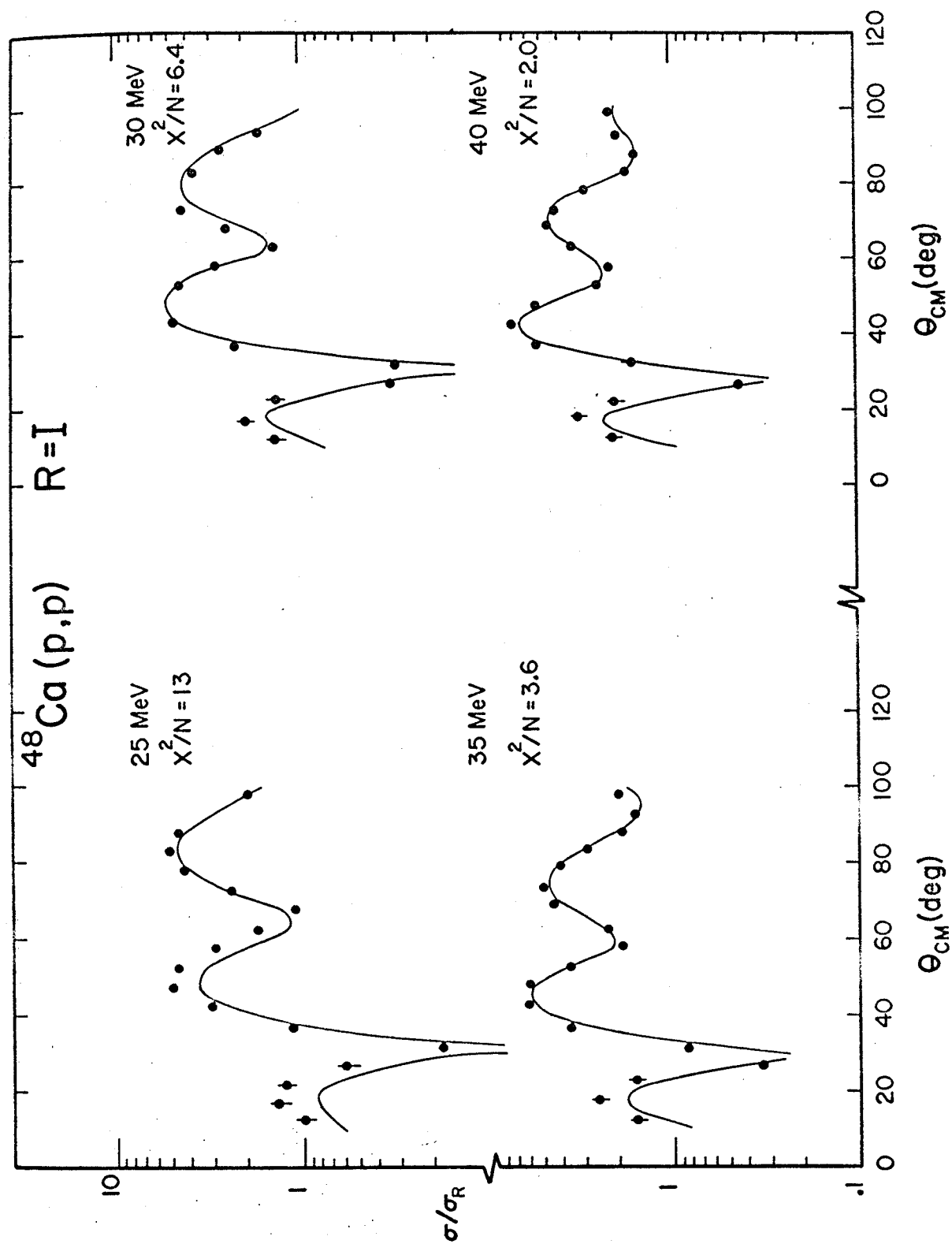


Figure 4.1 Optical Model fit with $R=I$ geometry.

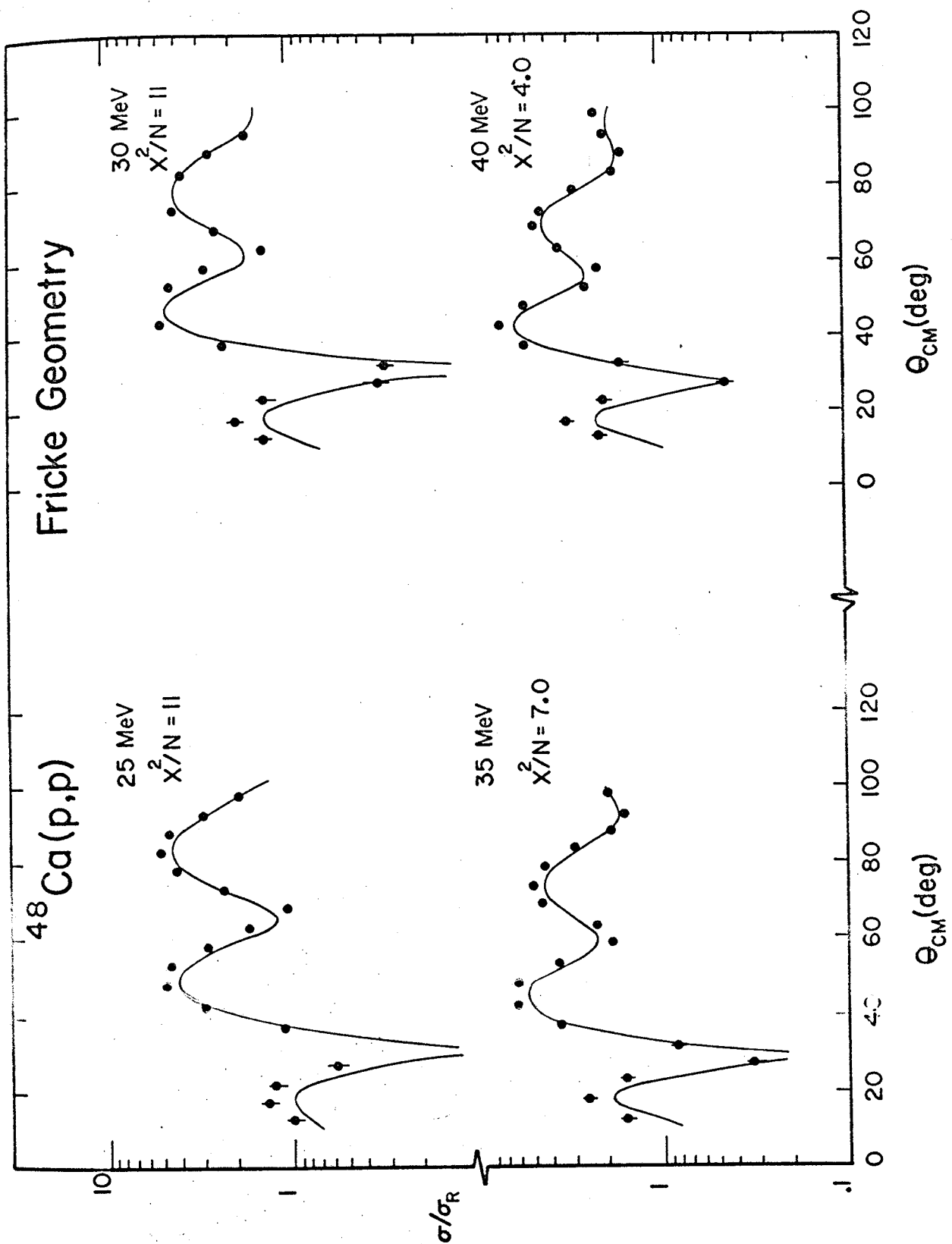


Figure 4.2 Optical model fit with Fricke geometry.

4.2 Optical Model Difference Between ^{40}Ca and ^{48}Ca

Electromagnetic studies of the relative charge distributions of the calcium isotopes indicate that for ^{48}Ca relative to ^{40}Ca , the half density point of the charge distribution (R_{op}) increases by 0.15F and the surface diffusivity decreases by 12%. (Fr 68) Recent optical model analyses of 30 MeV elastic alpha scattering from these nuclei by Bernstein, et. al. indicate that $\Delta R_{\text{op}} = R_{\text{op}}(^{40}\text{Ca}) = 0.15\text{F}$ and the surface diffusivity is essentially unchanged (Be 69).

Fernandez and Blair have calculated a strong absorption radius for 42 MeV elastic alpha scattering and also find $\Delta R \approx 0.15\text{F}$ with the diffusivity being a constant. (Fe 70)

If one assumes that the matter distribution is related to the geometry of the optical potential used to fit the elastic scattering, then one may be able to determine differences in the matter distribution by looking at differences in the optical potential. We have therefore used the optical model to fit the ^{40}Ca data and fix the potential well depths at each energy. The ^{48}Ca data are then fit by using the potential strengths obtained from the ^{40}Ca analysis and performing a search which grids the parameters determining the geometry of the optical model. Such a grid search was performed so that the sensitivity of the fit to the radius and diffusivity would be determined.

The optical model with its large number of parameters presents a problem in itself since many of the parameters are known to be coupled. It was therefore decided to simplify the potential as much

as possible. The spin-orbit potential did not improve the fit to the data, particularly since polarization and large angle data were not being fit. Therefore, the spin orbit terms were eliminated entirely with no effect on the results presented here. One possible optical potential would have a Coulomb term and either a surface or a volume imaginary term along with the real volume term. In this potential the real and imaginary terms have the same geometry. As a first try, therefore, a potential of the following form was used:

$$U(r) = U_C(r) - [V_R - i4W_D \frac{d}{dx}]f(x)$$

$$f(x) = (1+e^x)^{-1} \text{ where } x = \frac{(r-r_0)^{1/3}}{a}$$

This is essentially the same potential used by Bernstein et. al. in their alpha particle analysis except that a surface absorption rather than volume absorption term is used. The procedure was to fix the geometry for the ^{40}Ca analysis ($r_0 = 1.25$ fm, and $a = 0.65$ fm) and search on V_R and W_D to obtain the best fit at each energy. Then a "geometric" analysis of the ^{48}Ca data was made by holding V_R and W_D the same for both isotopes and performing a grid search on r_0 and a .

An immediate objection to the procedure of holding V_R the same for both nuclei can be made since there is a symmetry term in the real central potential of the form $V_{\text{SYM}} \frac{(N-Z)}{\Lambda}$. (Sl 68) This is particularly important if one is trying to describe differences in the elastic scattering by differences in the geometry because of the Vr^2 ambiguity in the optical model. (Pe 62) Therefore a grid search

was also performed for the ^{48}Ca data where $V_R(^{48}\text{Ca}) = V_R(^{40}\text{Ca}) + V_{\text{SYM}}^A(N-Z)$. The value of V_{SYM}^A used was 26.4 MeV (Fr 67) which added 4.4 MeV to the real well depth of ^{40}Ca . The results of a grid search on r_o and a are most easily visualized using an iso- χ^2 plot as in Figure 4.3. It can be seen that the radius has a more well defined minimum in χ^2 space than the diffusivity and that the two parameters are slightly coupled. Plots at the other energies are shown in Figures 4.4, 4.5, and 4.6. Notice that the minimum in χ^2 for the 25 MeV data is not well defined as a function of diffusivity.

To investigate the sensitivity of the results to the form of the imaginary potential, the same calculations were performed using volume absorption only and a combination of volume and surface absorption. The quality of the fit at any given energy varied depending on the form of the imaginary potential. The higher energy data was fitted better with more volume absorption and the lower energy data was fitted better with more surface absorption. The geometry parameters yielding a best fit in each case were, however, approximately independent of the form of the imaginary potential at each energy.

Elastic proton scattering is often fit with an optical model having a different real and imaginary geometry. The sensitivity of the results to the requirement that the real and imaginary geometries be equal was investigated by using the geometry parameters of Fricke, et. al. (Fr 67) for the ^{40}Ca data. The results at each energy are listed in Table 4.4 and are in reasonable agreement with the results obtained by holding the real and imaginary geometries equal. The

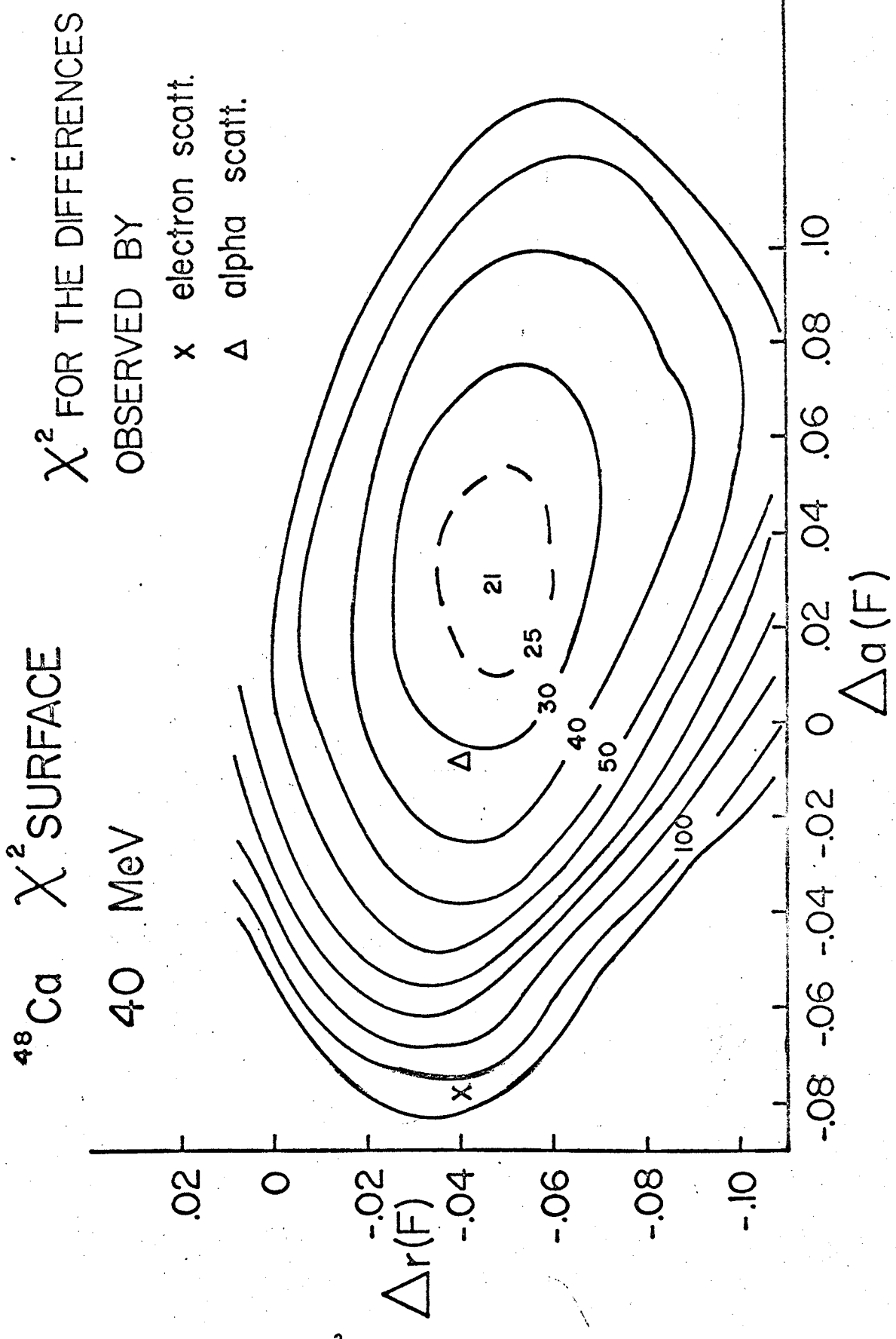
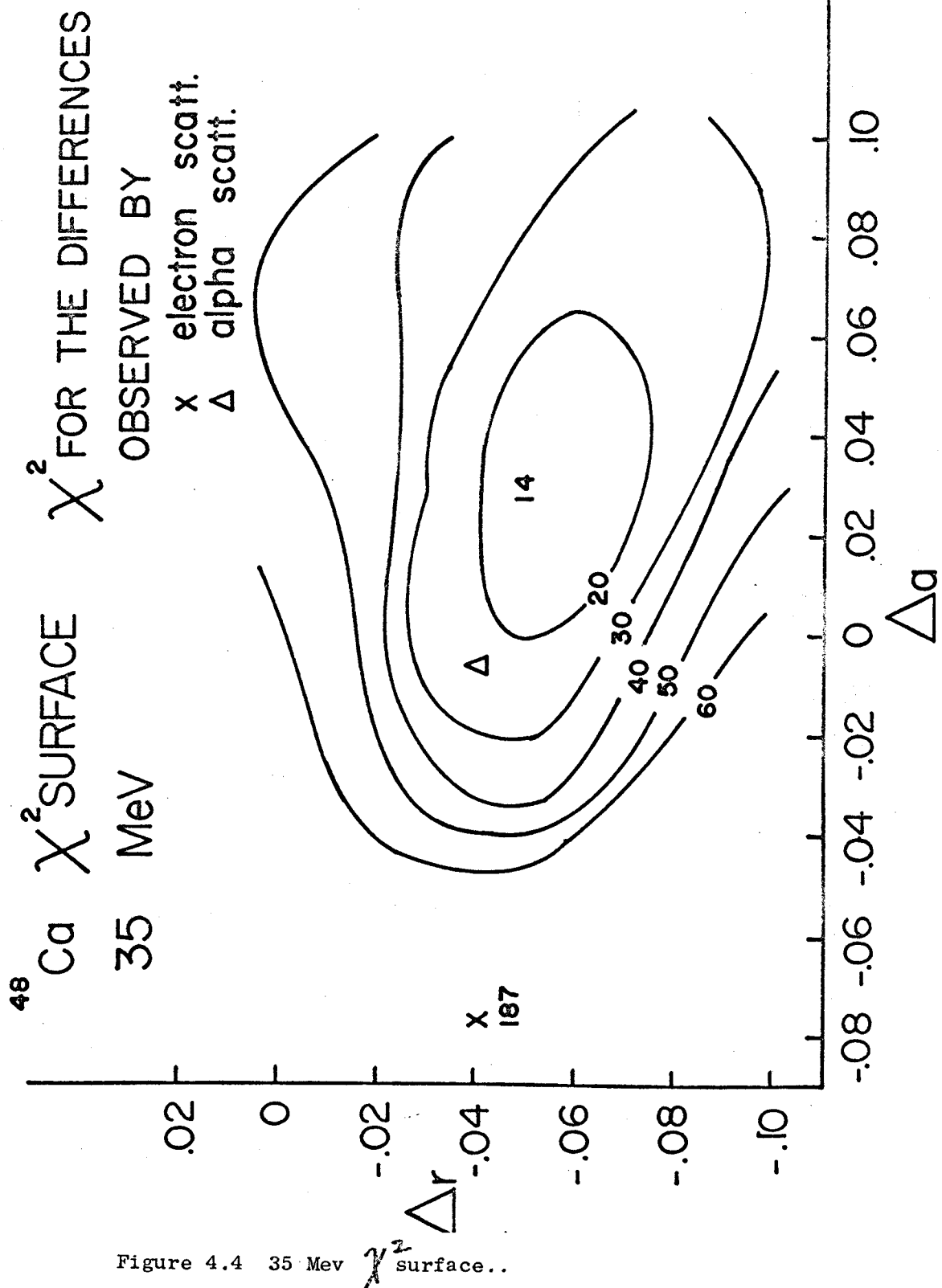


Figure 4.3 40 Mev χ^2 surface.



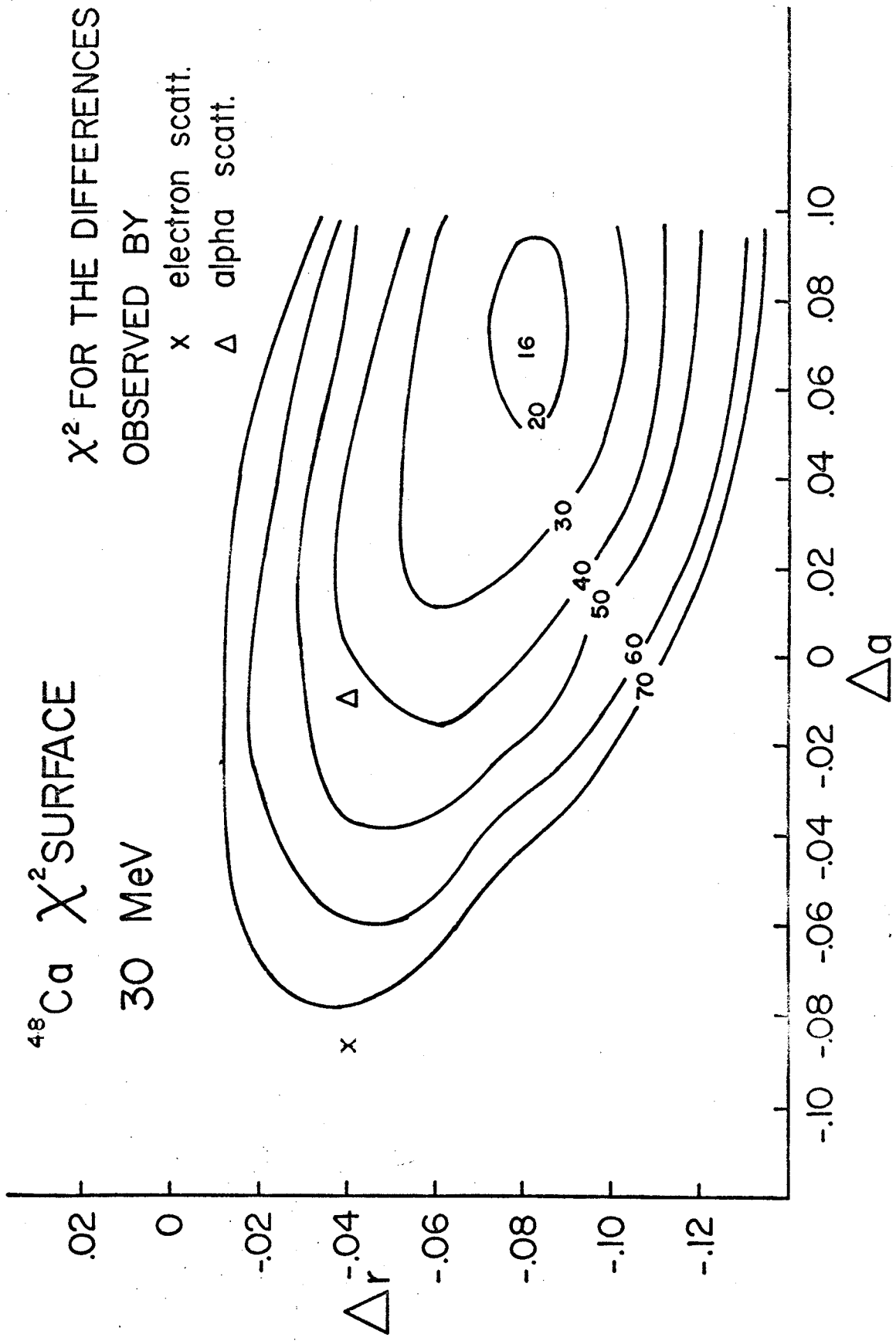


Figure 4.5 30 Mdv χ^2 surface.

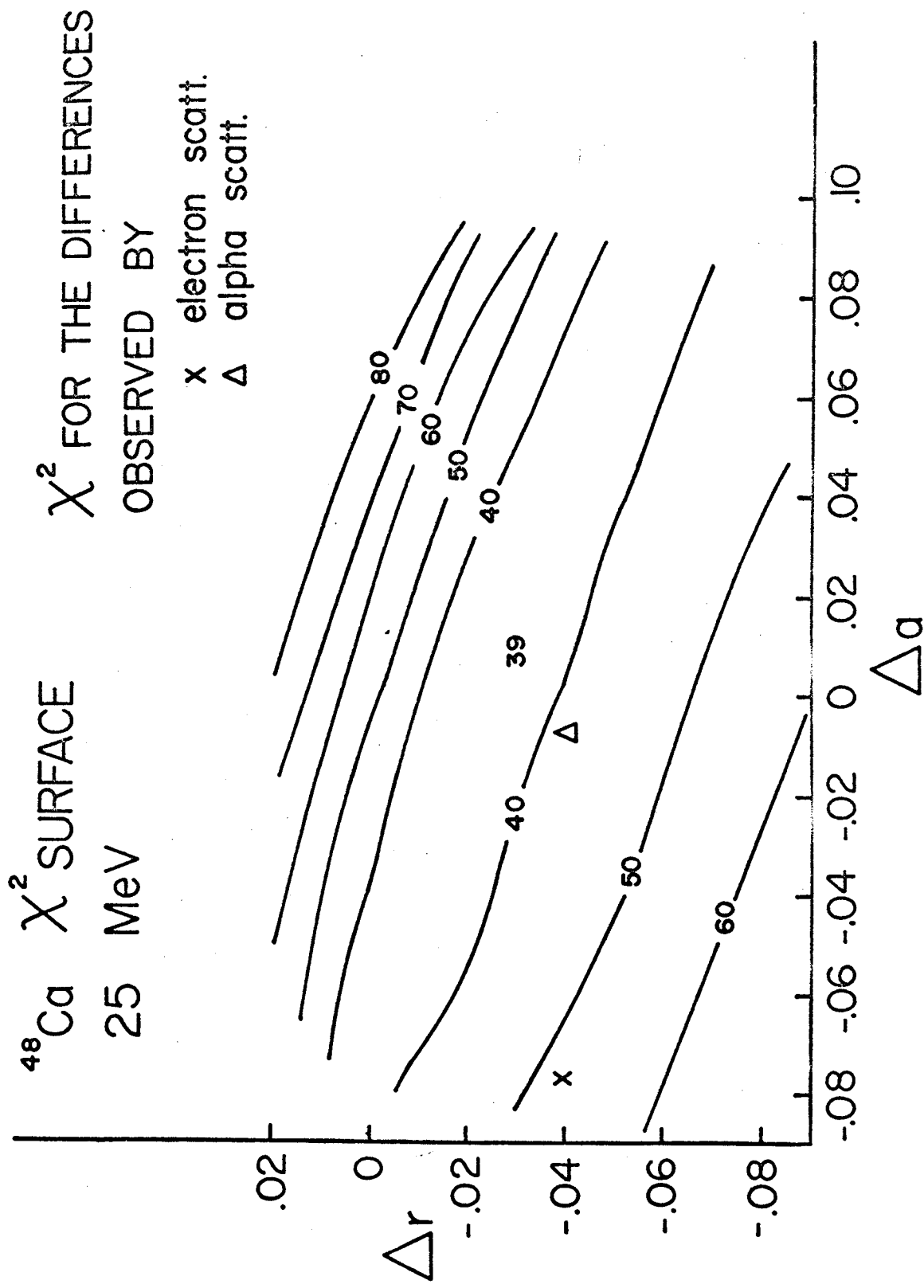


Figure 4.6 25 Mev χ^2_{surface} .

Table 4.3 Differences in the optical model parameters for ^{48}Ca and ^{40}Ca

^{40}Ca : $r_o = r_I = 1.25$		^{40}Ca : $r_o = 1.16, r_I = 1.37$										
$a_o = a_I = 0.65$		$a_o = 0.75, a_I = 0.63$										
$\langle R^2 \rangle_{\text{op}}^{1/2} = 4.08$		$\langle R^2 \rangle_{\text{op}}^{1/2} = 4.14$										
$U_{\text{SYN}} = 0.0 \text{ MeV}$												
E(MeV)	ΔR	Δa	ΔR_{MSR}	$U_{\text{SYN}} = 4.4 \text{ MeV}$		$U_{\text{SYN}} = 0.0 \text{ MeV}$		$U_{\text{SYN}} = 4.4 \text{ MeV}$				
	ΔR	Δa	ΔR_{MSR}	ΔR	Δa	ΔR	Δa	ΔR	Δa			
25	0.27	0.05	0.30	0.17	0.01	0.14	0.24	0.01	0.30	0.10	0.06	0.21
30	0.17	0.03	0.18	-0.01	0.07	0.16	0.18	0	0.11	-0.04	0.06	0.13
35	0.35	-0.03	0.17	0.09	0.03	0.13	0.32	0.02	0.14	0.10	0.04	0.15
40	0.35	-0.03	0.17	0.08	0.03	0.13	0.39	-0.04	0.14	0.14	0.02	0.13

$$\left. \begin{aligned} \Delta R &= R(^{48}\text{Ca}) - R(^{40}\text{Ca}); \quad R = r_o A^{1/3} \\ \Delta a &= a(^{48}\text{Ca}) - a(^{40}\text{Ca}) \\ \Delta R_{\text{MSR}} &= \langle R(48)^2 \rangle_{\text{op}}^{1/2} - \langle R(40)^2 \rangle_{\text{op}}^{1/2} \end{aligned} \right\}$$

All units in fm

cases where the radii and diffusivities were changed by the same absolute amounts and by the same percentage amounts were found to differ negligibly.

Figure 4.7 shows the ratio $\sigma(^{48}\text{Ca})/\sigma(^{40}\text{Ca})$ versus the center-of-mass scattering angle for each energy. It is indicative of how well the ratio of cross-sections is fit with the geometric search procedure and the optical model having equal real and imaginary geometries. The results one would obtain if one used the differences in the proton distributions determined by electron scattering are also shown. The electromagnetic differences do not fit the data, particularly at higher energies.

Greenlees, Pyle, and Tang (Ge 63) (Ge 63a) have pointed out that the geometric quantity which is best determined by the optical model is the root mean square radius. Our results, listed in Table 4.4 are in good agreement with this fact if one neglects the results for the 25 MeV data. One can justify neglecting this 25 MeV data because the minimum in χ^2 space for r and a is not well defined at this energy, but consists of a broad trough, the minimum of which does not correspond to a line of constant rms radius.

The results shown in Figures 4.8 - 4.11 indicate that the half density point of the radius and the diffusivity are not uniquely determined by the present optical model analysis. The sign and the magnitude of the differences depend on the energy of the incident protons and whether or not a symmetry term is added to the real potential. The average difference in the rms radii of ^{48}Ca and ^{40}Ca observed by this optical model analysis is 0.15 fm which equals the

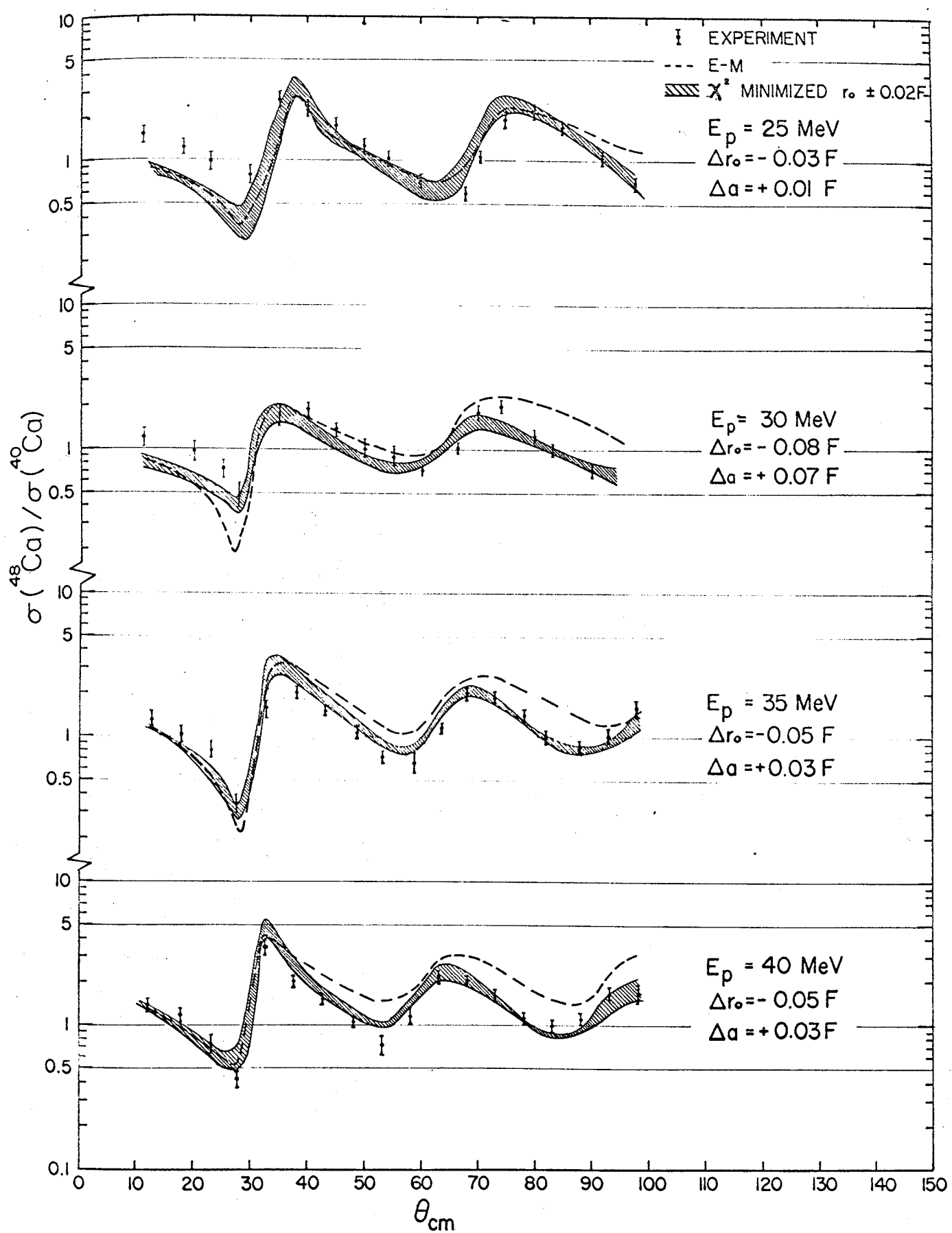


Figure 4.7 Ratio of elastic angular distributions.

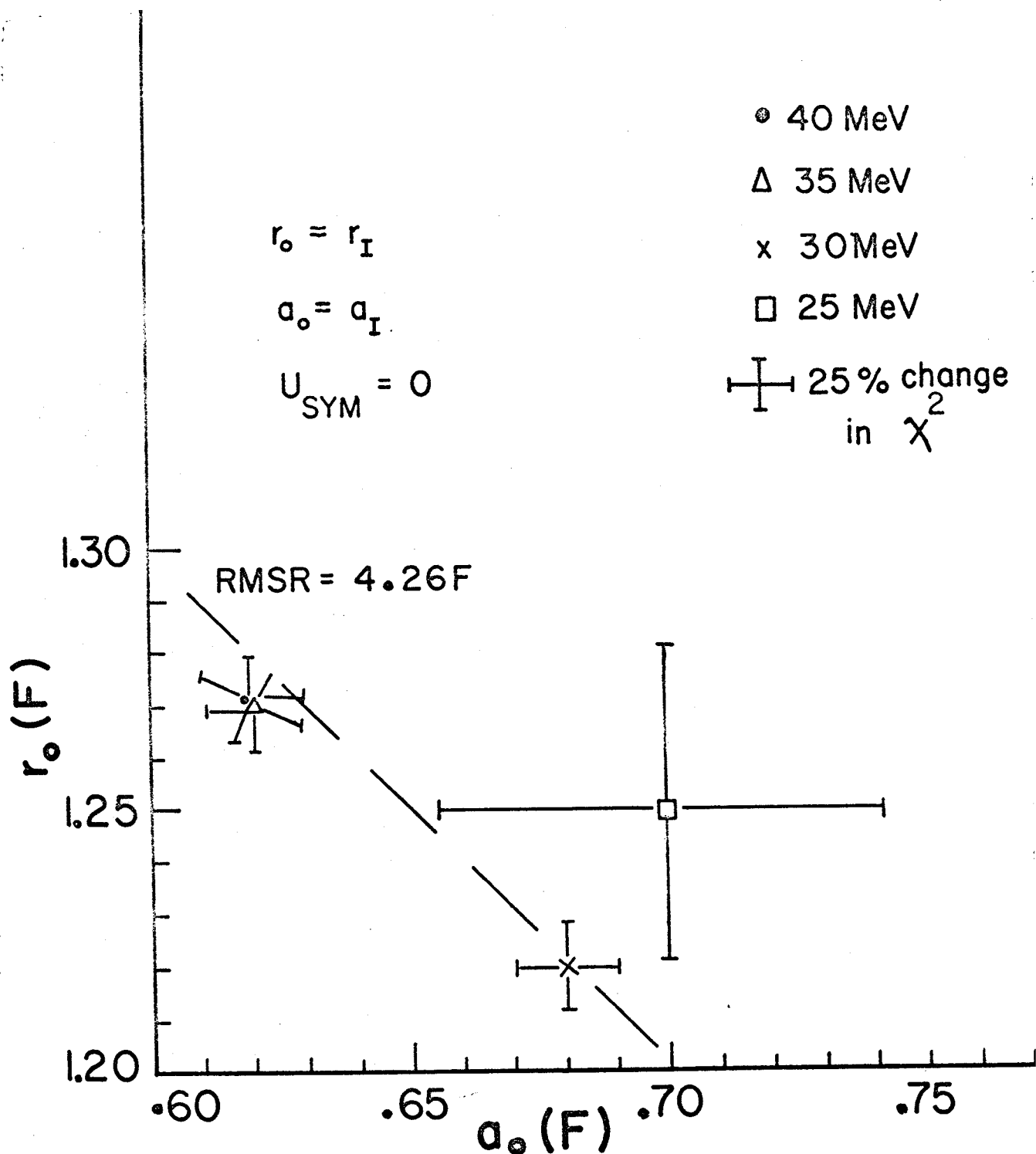


Figure 4.8 Optical model radii with $U_{sym} = 0$.

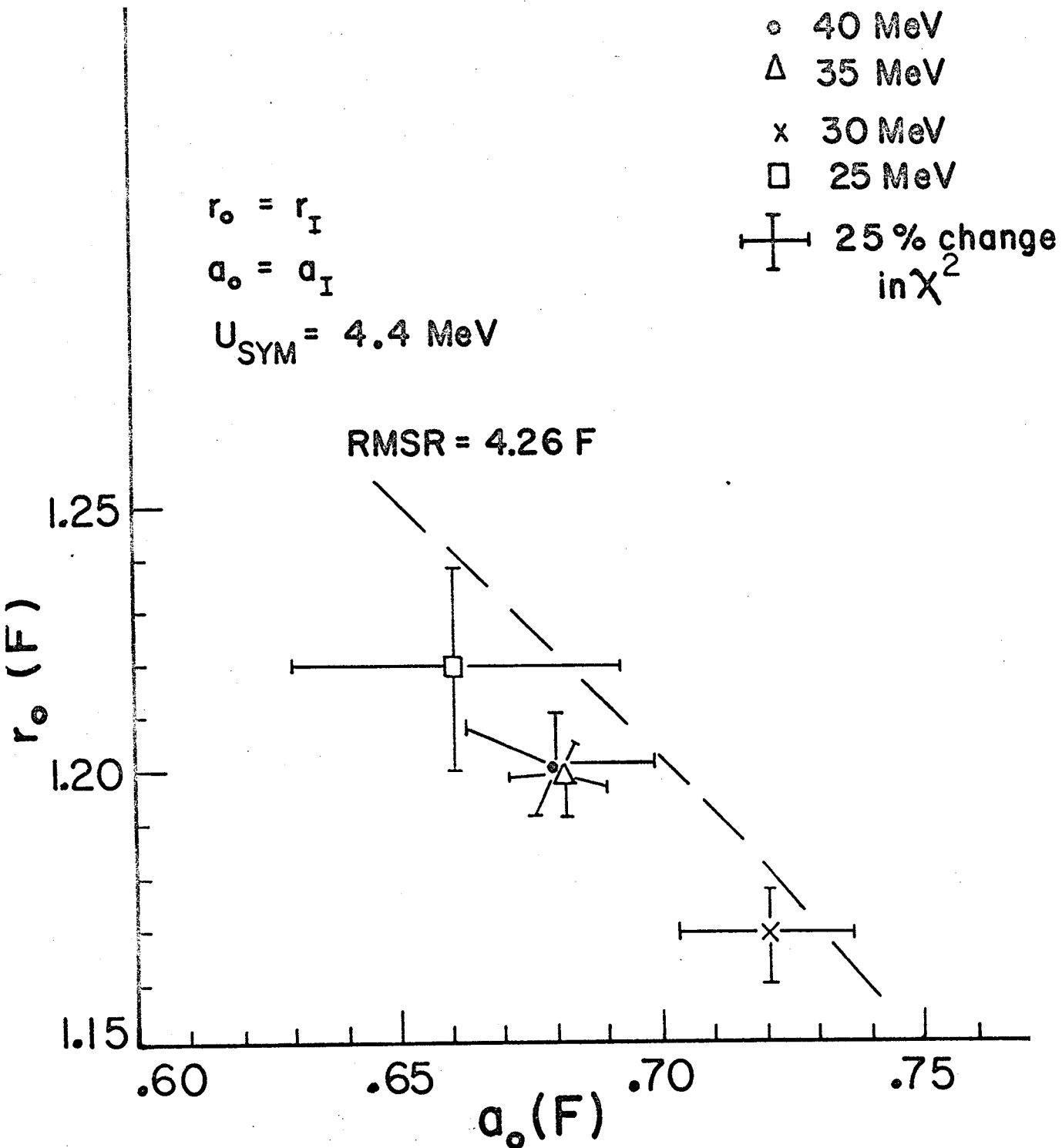


Figure 4.9 Optical model radii with $U_{sym} = 4.4 \text{ Mev.}$

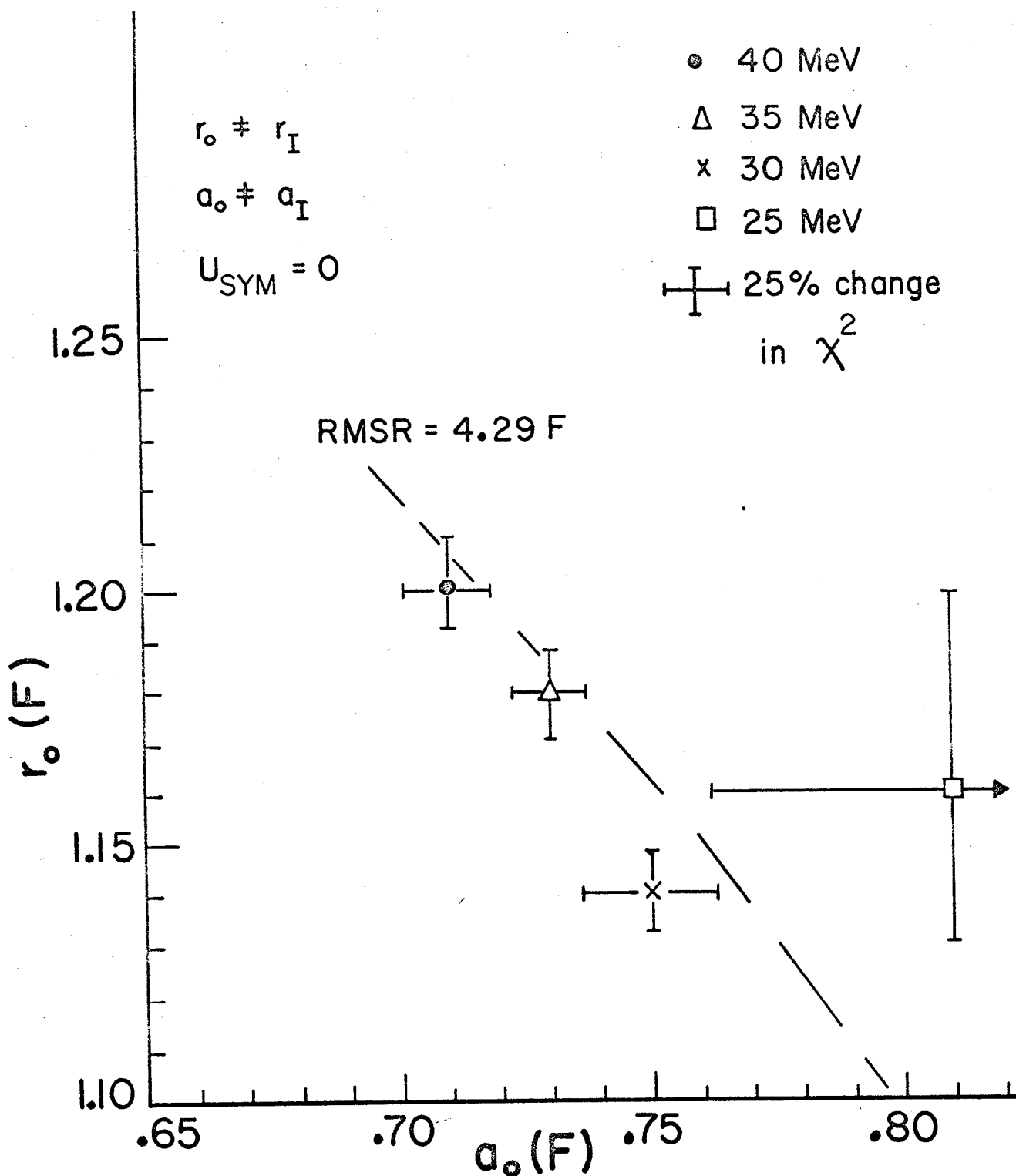


Figure 4.10 Optical model radii with $U_{\text{sym}} = 0$ and unequal geometries.

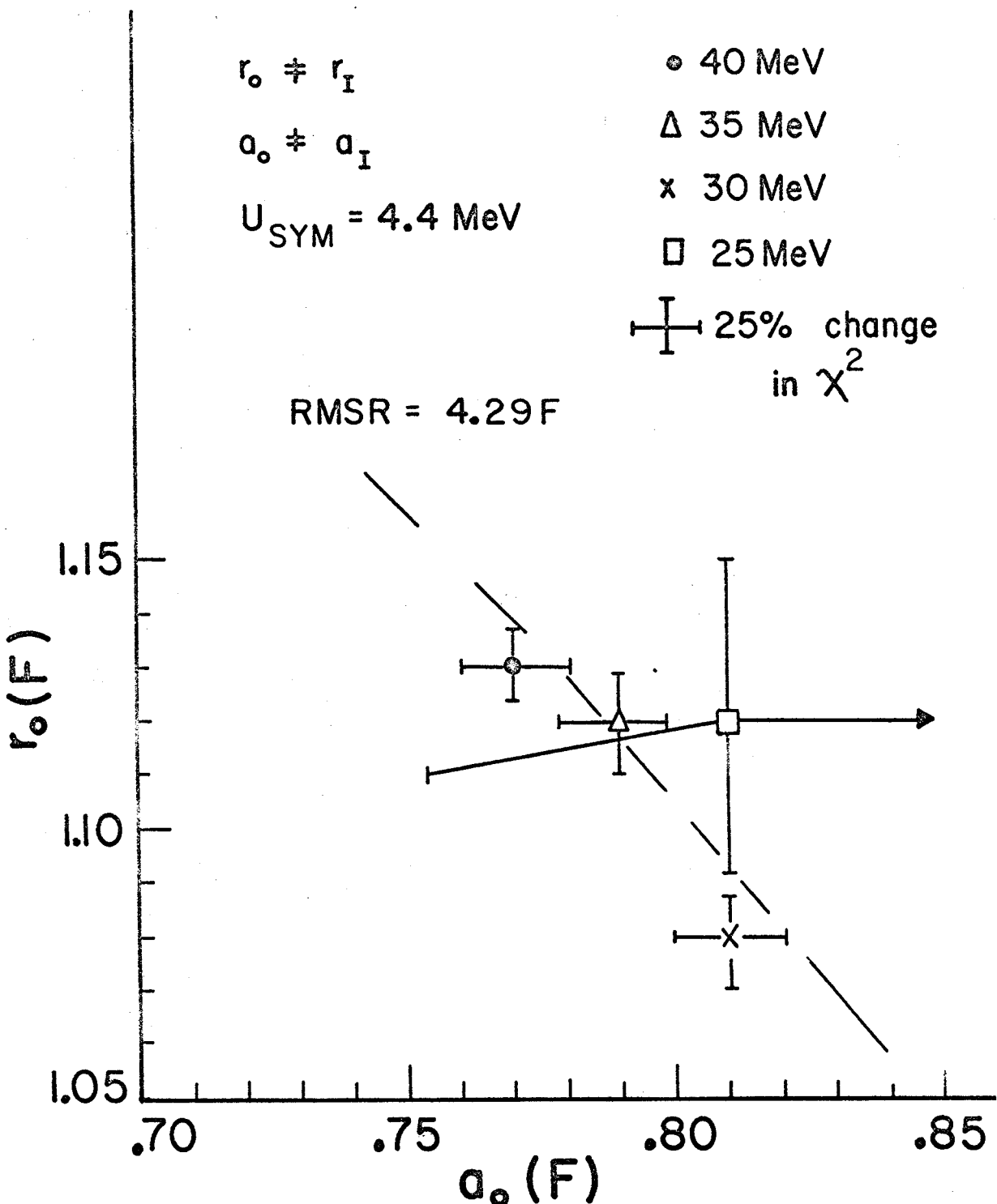


Figure 4.11 Optical model radii with $U_{SYM} = 4.4$ Mev and unequal geometries.

difference in the rms radii predicted by the $\Lambda^{1/3}$ law. This result is not in agreement with the elastic alpha particle scattering data.

If one assumes that the rms radius of the matter distribution is related to the rms radius of the optical potential via a constant interaction distance; then the difference in the optical model radii equals the difference in the rms matter radii. If one further assumes that the rms radius of the proton distribution is given by the rms radius of the charge distribution determined by electron scattering, then our results, in conjunction with the electron scattering results,* indicate that the ^{48}Ca nucleus has an excess neutron density in the surface region. This agrees with the conclusions based on Coulomb energy differences, (No 68) shell model calculations, (El 67) and Hartee-Fock calculations. (Ta 68)

*Frosch et. al. found that the rms charge radius of ^{48}Ca is 0.01 fm smaller than $^{40}\text{Ca}.$ ¹

5. THEORETICAL ANALYSIS

The data were compared to the predictions of the collective model using the formalism of the distorted wave Born approximation. Details of the theory are described elsewhere (Ba 62) (Ro 61) (Sa 64). An outline of the theory is presented below.

5.1 DWBA Theory

For inelastic scattering the form of the reaction is

$$A(a, a^1) A^*$$

where a is the projectile and A is the target nucleus. The total Hamiltonian for the system is

$$H = H_0 + T_0 + U(r_0) + V(r_0, \xi)$$

where ξ represents the internal coordinates of the projectile and target.

T_0 is the relative kinetic energy for the two parts of the system.

$U(r_0)$ is the optical potential describing the elastic scattering

r_0 is the separation vector between the projectile and the target.

$V(r_0, \xi)$ is the potential producing the inelastic scattering.

The eigenfunctions of the total Hamiltonian, Ψ , are solutions of the Schröedinger equation

$$(E - H) \Psi = 0 \quad 5.1$$

Similarly, the eigenfunctions, $v(\xi)$, of the Hamiltonian, $H(\xi)$, are solutions to the equation

$$[E_n - H(\xi)] v_n(\xi) = 0$$

and represent the internal states of the target and projectile.

The subscript, n, represents either the initial states, i, or the final states, f.

The solution to equation 5.1 has the following asymptotic form

$$\Psi^+ \underset{(r \rightarrow \infty)}{\longrightarrow} v_i(\xi) \exp(i k_i \cdot r_0) - \sum A_{if} v_f(\xi) \exp(ik_f r_0) / r_0$$

It is composed of an incident plane wave and an outgoing spherical wave. The cross section for the final state, f, is given by

$$\left| \frac{d\sigma}{d\Omega} \right| = |A_{if}|^2$$

The usual procedure is to define a transition amplitude such that

$$t_{if} = \left\langle v_f(\xi) \right| \chi_f^{-1} \left| V(r_0, \xi) \right| \Psi^+ \quad 5.2$$

Then the cross section for inelastic scattering is given by

$$\frac{d\sigma}{d\Omega} = \left(\frac{\mu_i/\mu_f}{2\pi\hbar^2}\right)^2 \frac{k_f}{k_i} \sum |t_{fi}|^2$$

where μ is the reduced mass of the system and the summation is an average over spins of the initial states and a sum over spins of the final states. The function χ_f^- is the solution to the Schröedinger equation

$$\left[-\nabla^2 + \frac{2\mu}{\hbar^2} U_f(r_o) - k_f^2 \right] \chi_f^- = 0,$$

i.e. the optical model wave functions describing the elastic scattering.

Since the solution of equation 5.2 requires a knowledge of the total wave function Ψ^+ , it cannot be calculated exactly. The Born approximation

$$\Psi^+ \approx v_i(\xi) \chi_i^+(k_i, r_o)$$

gives

$$t_{if} \approx \langle \chi_f^-(k_f, r_o) | V(r_o, \xi) | v_i(\xi) \chi_i^+(k_i, r_o) \rangle.$$

It is assumed that $V(r_o, \xi)$ is central and can be expanded in multipoles

$$V(r_o, \xi) = \sum_{LM} g_L(r_o, \xi) Y_L^M(\xi) Y_L^M(r_o) \quad 5.3$$

The internal states have well defined J and m , therefore

$$v_n(\xi) = \sum_{m=-n}^n J_m(\xi)$$

where n refers to the initial and final states of the nucleus.

The Wigner-Eckart Theorem is used to integrate over ξ giving

$$\begin{aligned} & \int d\xi v_f(\xi) g_L(\xi, r_o) Y_L^M(\xi) v_i \\ &= \langle J_i L m_i | J_f m_f \rangle F_L(r_o) \end{aligned} \quad 5.4$$

The term, $F_L(r_o)$, is the radially dependent form factor which depends on the model used for its explicit form.

Now the cross section is

$$\frac{d\sigma}{d\Omega} = \left(\frac{\mu}{2\pi\hbar^2} \right)^2 \frac{k_f}{k_i} \frac{(2J_f + 1)}{(2J_i + 1)} \sum_{LM} \frac{|B_{LM}|^2}{(2L + 1)} \quad 5.5$$

where

$$B_{LM} = \int dr_o \left\langle f \left| F_L(r_o) Y_L^{M*}(r_o) \right| i \right\rangle$$

5.2 Collective Model

The collective model assumes that the excited states of the nucleus are due to deformations from a spherical ground state.

The deformed nucleus is described by a deformed optical potential. A multipole expansion of the nuclear surface is made

$$R(\theta) = R_o \left[1 + \sum_L \beta_L^0 Y_L^0(\theta) \right].$$

Axial symmetry is assumed. Next the total potential is expanded

in a Taylor series about the spherical radius, R_o .

$$U(r-R) = U(r-R_o) + (R-R_o) \frac{\partial U}{\partial R} \Big|_{R=R_o} + \dots$$

The term $U(r-R_o)$ is the optical potential which describes the elastic scattering. The second term is assumed to describe the inelastic scattering, i.e. it is the interaction potential

$$V(r_o, \xi) = - \sum_L R_o \beta_L \frac{\partial U}{\partial r} Y_L^0(\theta) \quad 5.7$$

This form factor is used to calculate the cross sections for inelastic scattering using equations 5.5 and 5.6. The calculated angular distribution is normalized to the experimental angular distributions by the deformation parameter, $\delta_L = \beta_L R_o$.

5.3 Vibrational Model

The vibrational model yields the same formal results as the rotational collective model. This model relates the deformation, $\delta_L = \beta_L R_o$, to a mass transport parameter, D_L , and the surface tension parameter, C_L .

The Hamiltonian describing the multipole deformation $\delta_L = \beta_L R_o$ in the "vibrational" picture is given by (La 60):

$$H_L = \sum_M (-)^M 1/2 [D_L \dot{a}_{LM} \dot{a}_{L,-M}^* + C_L a_{LM} a_{L,-M}^*]$$

where

$$\beta_L = \sum_M |a_{LM}|^2$$

and D_L is the "mass transport" parameter and C_L is the "force constant" of the vibrator. These parameters are either calculated by more specific models or are determined by experiment.

As an example, in the classical incompressible, irrotational hydrodynamical model, $(D_L)_{\text{hyd}}$ is given by (La 60):

$$(D_L)_{\text{hyd}} = \frac{(2L+1)}{L} \frac{AM \langle r^{2L-2} \rangle}{4\pi R_o^{2L-4}}$$

where AM is the mass of the nucleus. The quantity $\langle r^{2L-2} \rangle$ is evaluated using a uniform transition density with a radius determined by comparison with the equivalent Fermi distribution. (La 60)

(Gr 69) The excitation energy of such a vibrational state is given by:

$$E_L = \hbar \omega_L = \hbar \sqrt{\frac{C_L}{D_L}}$$

The collective model for describing inelastic scattering (Ba 62) assumes the nuclear potential as viewed by the projectile undergoes a shape oscillation about a spherically symmetric potential. The form factor of such an oscillation is given by (for no spin-transfer):

$$G_{LOL}(r) = -i^L (2L+1)^{-1/2} \beta_L^R \frac{dU}{dr}$$

where

$$\beta_L^2 = \frac{(2L+1)}{2} \frac{\hbar}{\sqrt{C_L D_L}}$$

and R is the real and imaginary radii for the real and imaginary parts of G_{LOL} respectively. U is the empirically determined optical potential excluding only the spin-orbit term. For quadrupole and octopole transitions, a term in $1/r^{L+1}$ was added coherently to take into account Coulomb excitation. (Ba 62)

The multipole fractional deformation β_L is extracted from the normalization of the calculated integrated cross-section to the data. From this value, the deformation for the real part of the interaction is $\delta_L = \beta_L R_0$. Thus knowing the excitation energy, E_L , and the deformation parameter, δ_L , then the "force constant", C_L , and "mass transport" parameter, D_L , are found by:

$$C_L = \frac{(2L + 1)}{2} \frac{R_0^2}{\delta_L^2} \frac{E_L}{\hbar^2}$$

and

$$\frac{D_L}{\hbar^2} = \frac{(2L + 1)}{2} \frac{R_0^2}{\delta_L^2} \frac{1}{E_L}$$

The reduced transition probability, $B(EL; 0 \rightarrow L)$, is given (La 60) (Ow 63) in terms of the deformation parameter, δ_L , by:

$$B(EL; 0 \rightarrow L) = \frac{ze(2L + 1)}{4\pi R_0^{L-2}} \left\langle r^{2L-2} \right\rangle^2 \frac{\delta_L^2}{R_0^2}$$

We compare the results with the usual single particle estimate (Weisskopf units)

$$B_{sp} (EL; 0 \rightarrow L) = \frac{(2L+1)}{4\pi} e^2 \langle r^L \rangle^2$$

where $\langle r^L \rangle^2$ is calculated using a uniform charge distribution.

The value G_{sp} of the ratio $B(EL, 0 \rightarrow L)/B_{sp}(EL; 0 \rightarrow L)$ measures in some sense the "collective strength" of the state. Along the same vein it is of general interest to compare the reduced transition probabilities with two sum rules. The first is the non-energy-weighted sum rule, NEWSR (La 60) based on the shell model.

$$\text{NEWSR} = \sum_n B_n (EL; 0 \rightarrow L) = \frac{e^2 Z}{4\pi} \langle r^{2L} \rangle$$

where the sum is over all states with spin L. The second sum rule is an energy-weighted sum rule, (Na 65)

$$\text{EWSR} = \sum_n (E_n - E_0) B(EL; L \rightarrow 0) = \frac{Z^2 e^2 L \hbar^2}{8\pi \Delta M} (2L+1)^2 \langle r^{2L+2} \rangle$$

This sum rule is model independent in as much as the nuclear Hamiltonian does not contain velocity dependent potentials.

5.6 Calculations

The computer code JULIE (Ba 62) was used to make all DWBA calculations using the XDS Sigma-7 computer. Coulomb excitation was included for $L = 2$ and $L = 3$ cases, and the deformation of both the real and imaginary potential was used. The calculations were done with the two different sets of optical model parameters listed in Tables 4.2 and 4.3. Calculations were made at each energy for

$L = 2, 3, 4, 5$, and 6 . The results of the calculations are shown in appendix II, Figures II.1 - II.4. The angular distributions appear to be relatively insensitive to the optical model used.

The theoretical angular distributions, σ_{DWBA} , are related to the experimental angular distributions by the expression,

$$\frac{d\sigma(\text{EXP})}{d\Omega} = \frac{1}{(2L+1)} \beta_L^2 \frac{2J_B+1}{2J_A+1} \sigma_{DWBA}$$

L is the transferred orbital angular momentum, $J_A = 0$ for even-even nuclei, and $J_B = L$; therefore the expression above reduces to

$$\frac{d\sigma(\text{EXP})}{d\Omega} = \beta_L^2 \sigma_{DWBA}$$

The deformation parameter, β_L , was found for each state by comparison of the theoretical and experimental angular distributions using the computer program, SIGTOTE, written by K. N. Thompson (Th 69a). The program normalizes the integrated cross sections for the experimental and theoretical angular distributions.

The extraction of a meaningful deformation parameter depends on a knowledge of the L transfer for the observed state. When the state has been observed previously and a definite L assignment has been made there is no problem, but for a weak or previously unobserved states there may be some ambiguity concerning the L transfer of the state. The general features of the data as a function of energy and L transfer are shown in Figures 5.1 - 5.4. The states are of known L (Li 67) and the collective model fits to the data are shown.

$^{48}\text{Ca} (\text{p}, \text{p}')$
 $2^+, E^* = 3.830 \text{ MeV}$

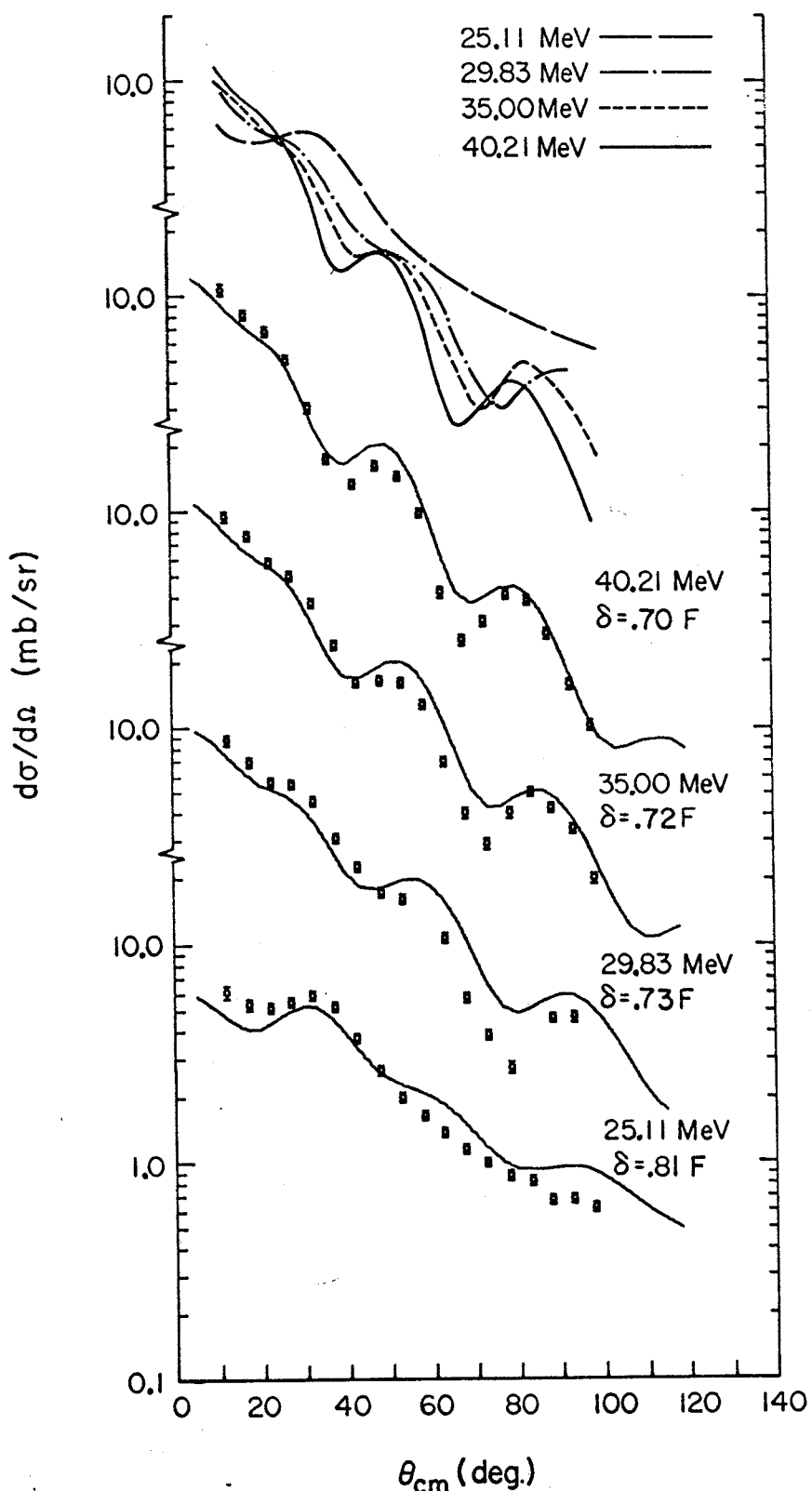


Figure 5.1 DWBA calculations for $L=2$ states..

56
 ^{48}Ca (p, p')
 $3^-, E^* = 4.502\text{ MeV}$

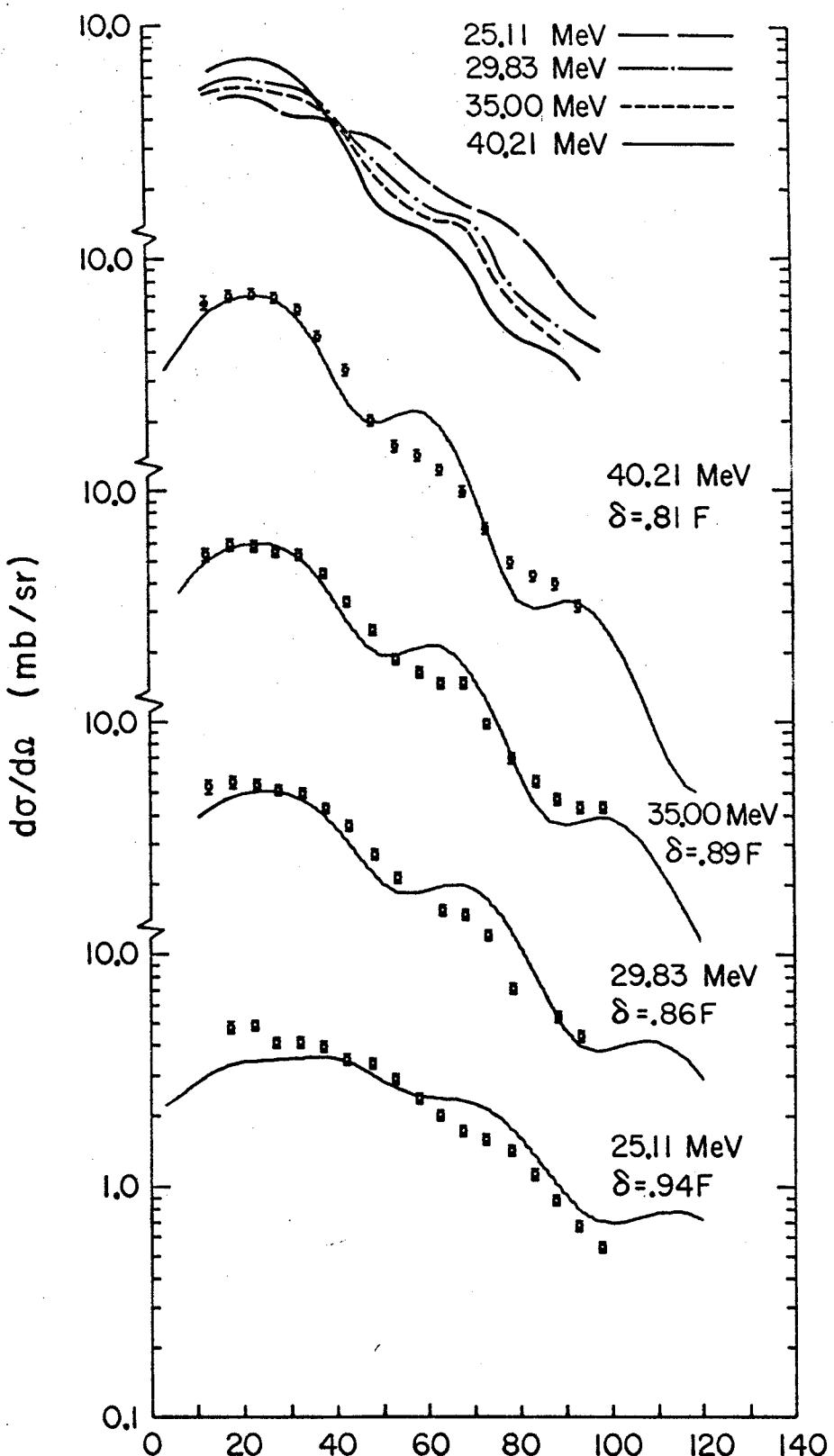


Figure 5.2 DWBA calculations for $L=3$ States.

^{48}Ca (p, p')
 $4^+, E^* = 6.335 \text{ MeV}$

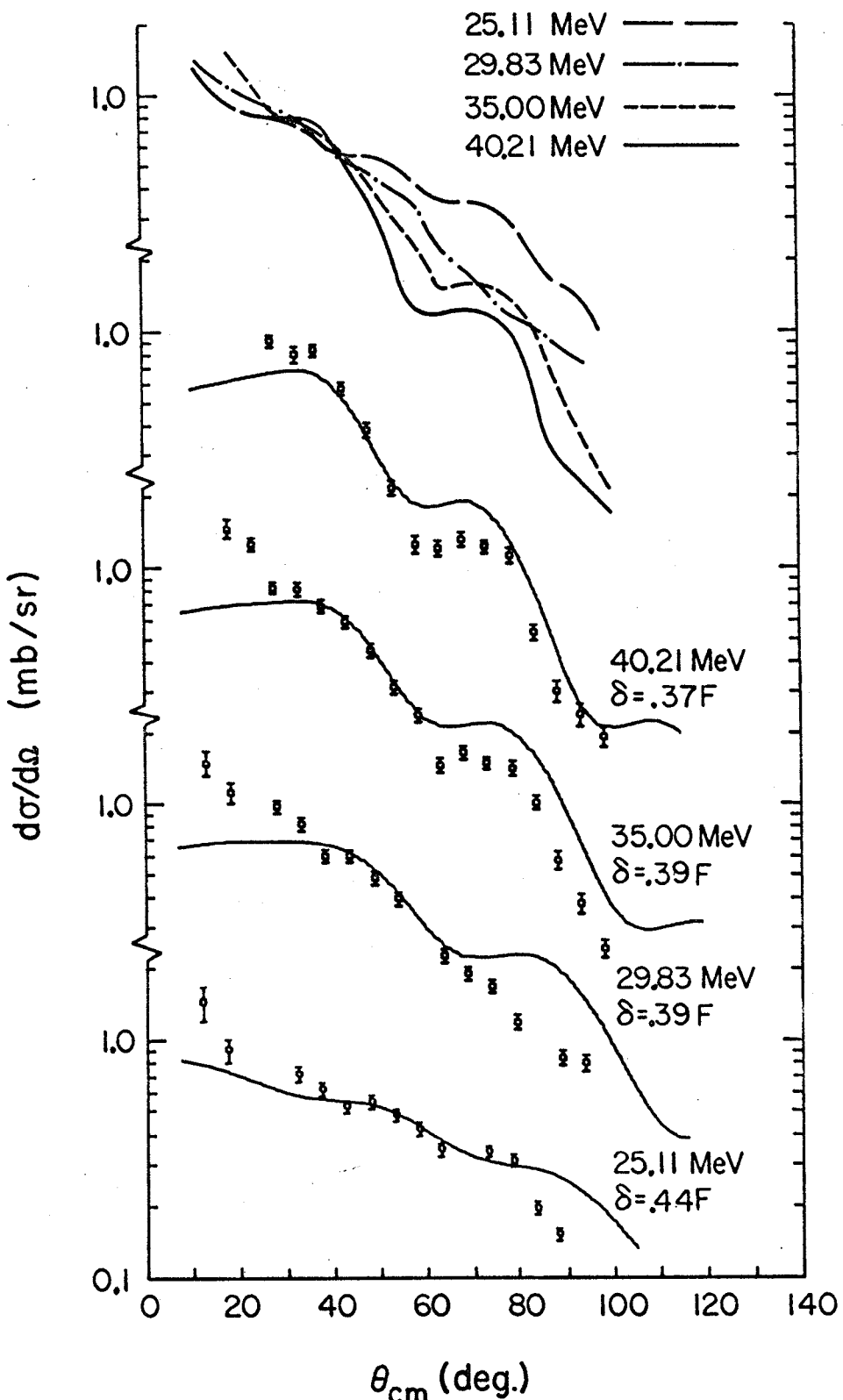


Figure 5.3 DWBA calculations for $L=4$ states.

$^{58}_{48}\text{Ca}$ (p, p')
 $5^-, E^* = 5.723 \text{ MeV}$

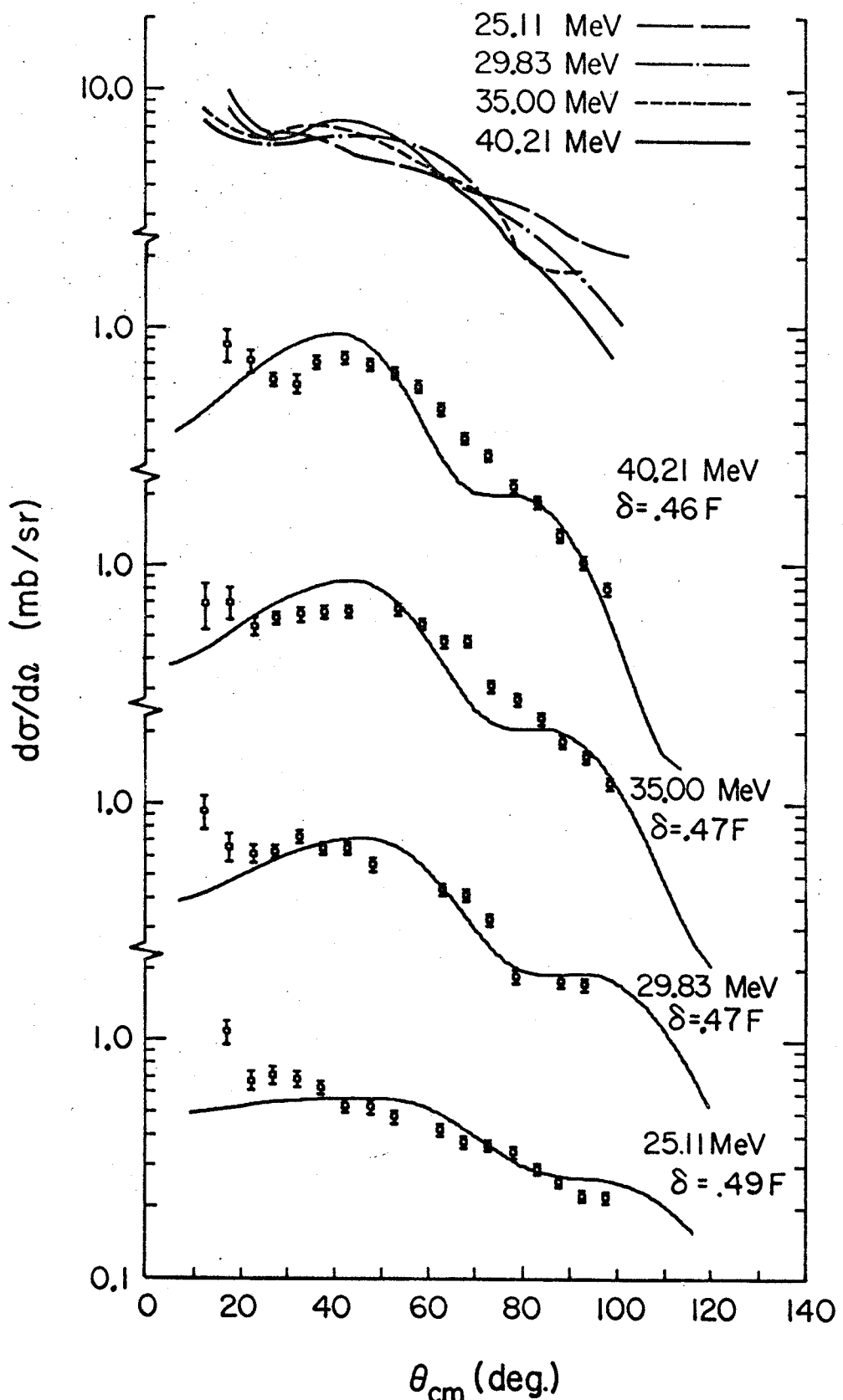


Figure 5.4 DWBA calculations for $L=5$ states.

It can be seen that as the L value increases the angular distribution peaks at successively larger angles. Also notice that the structure of the angular distribution is more pronounced for the higher energy data. For making L assignments the 35 and 40 MeV data are more useful than the 25 and 30 MeV data. The lower energy data tend to be relatively flat and structureless. The tentative L assignments made for the states observed in this experiment are shown in Figure 5.5 along with previous results for ^{48}Ca . The individual states are discussed in more detail in the following chapter.

When no L assignment could be made several different L values were tried. It was found that the ρ_L obtained was almost independent of the choice of L. This is because the theoretical angular distributions have approximately the same average cross section for various L values, but they peak at different angles.

6. RESULTS

In this chapter the individual states observed in this experiment are discussed and compared with the results obtained from other experiments. When nuclear deformations are compared the deformation, $\delta_L = \rho_{L0}^R$, for 40 MeV with real and imaginary geometries equal is used. The energy dependence of the δ_L 's is discussed later.

6.1 States below 5 MeV

3.830

The first excited state of ^{48}Ca is the strongly excited 2+ state at 3.830 MeV. The angular distribution is compared with $L = 2$ collective model calculations in Figure 5.1. The $L = 2$ assignment agrees with all the previous experiments on ^{48}Ca (Pe 65) (Li 67) (La 66) (Bj 67) (Te 68). It is interesting to compare the angular distribution with that of the first 2+ state in ^{50}Ti and ^{52}Cr . Figures 6.1 and 6.2 show that the two angular distributions are virtually the same. The figures also show the results of a microscopic calculation (Pr 70) involving the Kallio Kolltveit interaction plus exchange with core polarization. The calculation assumes excitations within the $(1f_{7/2})^2$ configuration and is seen to provide a reasonable fit to the data for the ^{48}Ca core. The core

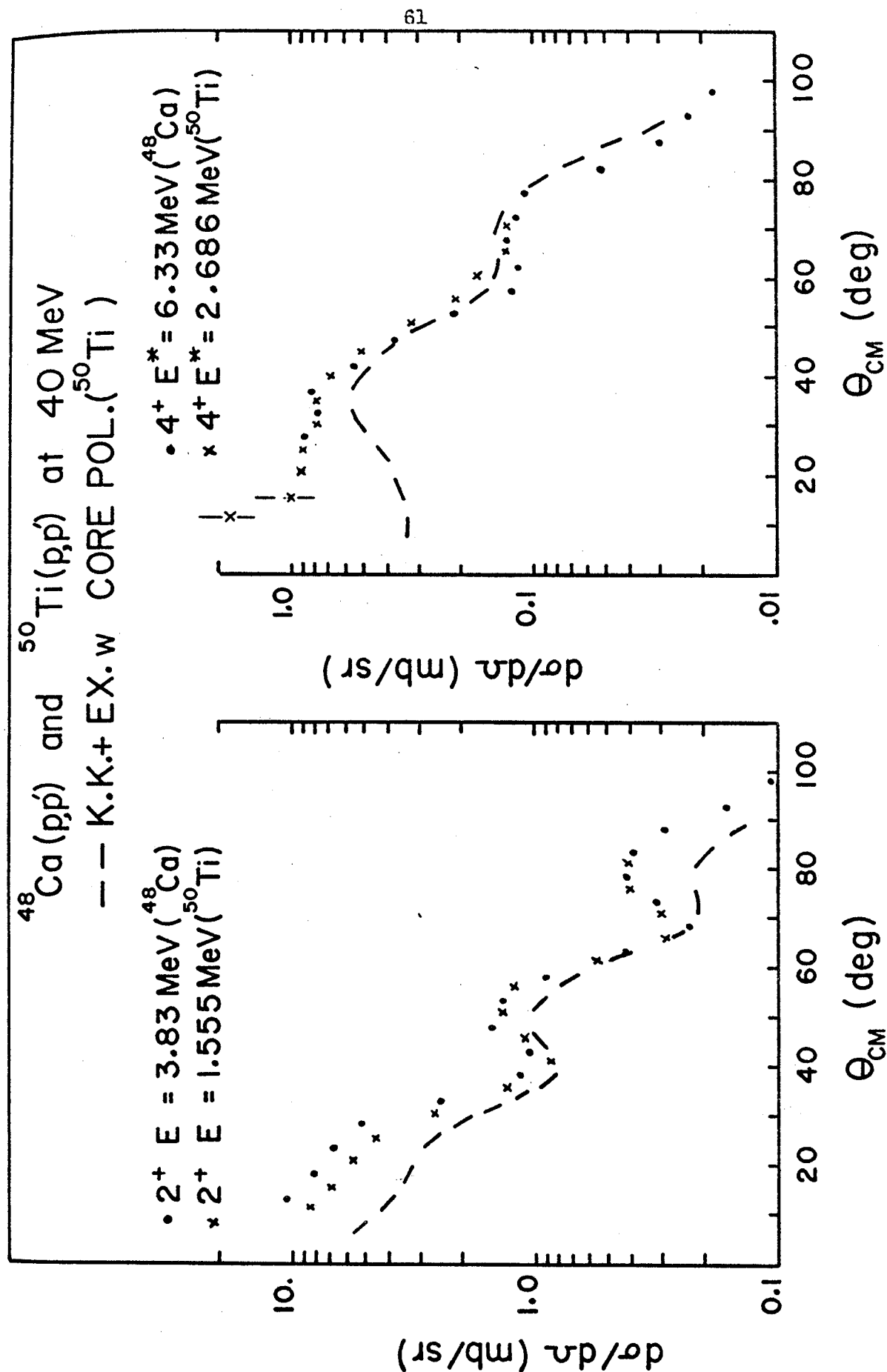


Figure 6.1 Comparison of ^{48}Ca and ^{50}Ti .

$^{48}\text{Ca}(p,p)$ AND $^{52}\text{Cr}(p,p)$ AT 40 MeV

— IMPULSE APPROX. + Ex. w CORE POL.

$$\text{FOR } ^{52}\text{Cr}: \quad |J_1\rangle = A_j |V=2\rangle + B_j |V=4\rangle$$

$$|J_2\rangle = B_j |V=2\rangle - A_j |V=4\rangle$$

$$\frac{A_j^2}{B_j^2} = \frac{\sigma_{\text{EXP}}(J_1)}{\sigma_{\text{EXP}}(J_2)} \quad \text{AND} \quad A_j^2 + B_j^2 = 1$$

$$\bullet 2^+ E^* = 3.83 \text{ MeV} (^{48}\text{Ca})$$

$$\times 2_1^+ E^* = 1.434 \text{ MeV} (^{52}\text{Cr})$$

$$A_2^2 = 0.98$$

$$\bullet 4^+ E^* = 6.33 \text{ MeV} (^{48}\text{Ca})$$

$$\times 4_1^+ E^* = 2.37 \text{ MeV} (^{52}\text{Cr})$$

$$A_4^2 = 0.53$$

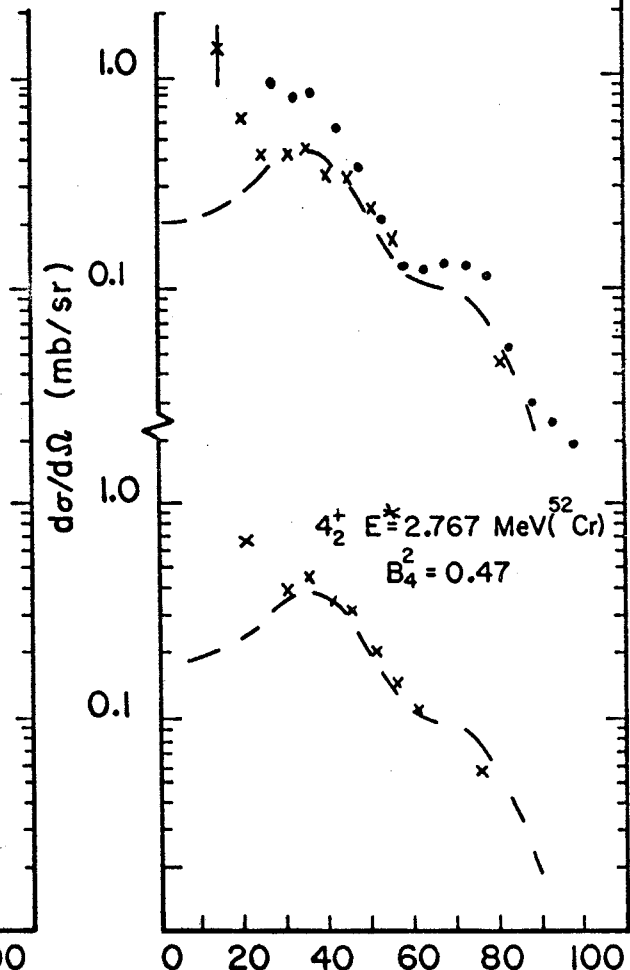
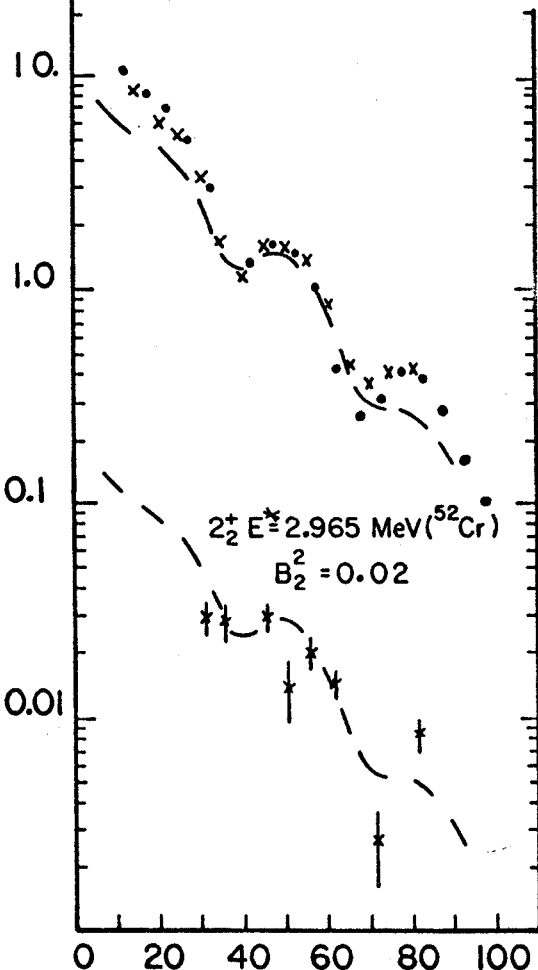


Figure 6.2 Comparison of ^{48}Ca and ^{52}Cr .

strength for each multipole and valence configuration is determined from the bound state matrix elements of Kuo and Brown (Pe 70) (Pe 69). Since the microscopic model with realistic forces contains no free parameters, the comparison of the calculations based on this model with experiment provides a direct test of the theory.

The nuclear deformation observed in this experiment of 0.65 fm is slightly higher than that observed in the inelastic alpha scattering experiments of 0.53 fm for 42 MeV α 's (Pe 65) and $f_L = 0.71$ fm for 31.5 MeV experiment (Li 66). The 12 MeV ($p, p' \gamma$) (Te 62) experiment finds a $f_L = 1.0$ fm. The reduced transition probability in Weisskopf single particle units is 4.1 for the uniform Fermi equivalent charge distribution compared with 1.7 for inelastic electron scattering (Ei 69), 5.4 for the 31.5 MeV alpha work (Be 69), and 7.70 for the 12 MeV proton work (Te 68). In general it is found that the 12 MeV ($p, p' \gamma$) experiment observes larger nuclear deformations and reduced transition probabilities. This could be due to compound nuclear effects and or two step processes.

4.281

The first 0^+ excited state in ^{48}Ca is not observed in the present experiment. Upper limits for the cross section at each energy are shown in Table 6.1, and are about 1.5%, the strength of the first 2^+ state. The (t, p) experiment observes the state with a strength of about 60% of the ground state or 150% the strength of the first 2^+ state. The fact that this first 0^+ is so weak

compared to the 0^+ state in ^{40}Ca observed with the same (p,p') reaction has been used as evidence for the existence of deformed admixture in the ^{40}Ca ground state, (Gr 70) and conversely the ground state of ^{48}Ca contains less deformed admixture.

4.502

The first 3^- state in ^{48}Ca occurs at 4.502 MeV and is strongly excited by the (p,p') reaction. A comparison with $L = 3$ collective model calculations is shown in Figure 5.2. Figure 6.3 shows the comparison of the experimental angular distribution with the known experimental angular distributions for known $L = 3$ transfers in ^{40}Ca (Ku 70). It shows that the p,p' reaction is able to make L transfer assignments based on the shape of the angular distribution, and the shape of the angular distribution is approximately independent of the target nucleus. The reduced transition probability in agreement with the (e,e') result. The deformation parameter observed here is 0.89 fm and somewhat larger than the alpha results of 0.56 fm (Pe 65) and 0.76 fm (Li 67). Again the 12 MeV proton results observe a deformation larger than our results (1.15 fm).

4.607

Analysis of the 4.607 state is complicated by the fact that the strong ^{40}Ca 5^- state at 4.48 MeV contaminates a large part of the angular distribution. The data seem to favor an $L = 4$ transfer, but $L = 3$ cannot be ruled out on the basis of these data alone.

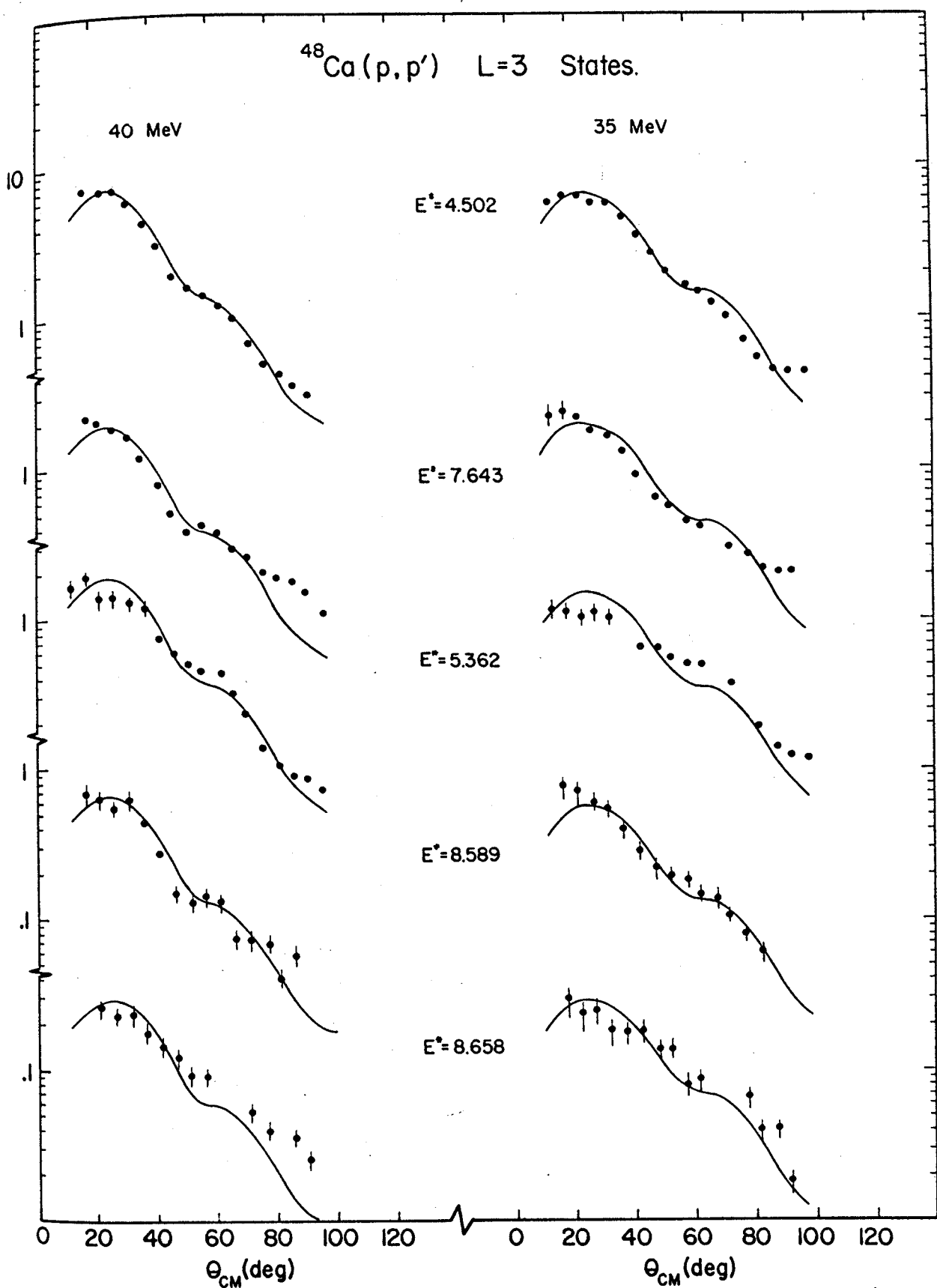


Figure 6.3 $L = 3$ states.

However, the 10 MeV proton experiment (La 66) observes an angular distribution which peaks beyond the 3 - state and is compatible with an $L = 4$ DWBA calculation. The alpha experiments were not able to resolve the state from the stronger 4.502 state, but the angular distribution obtained (Li 67) is not inconsistent with an $L = 4$ transfer. The state is not observed in the (t, p) experiment.

6.2 States between 5 and 6 MeV

5.141

In this experiment a total of 5 states are observed between 5 and 6 MeV in excitation energy. The weakly excited state at 5.141 is assigned an $L = 5$ transfer. This is not in agreement with the 42 MeV alpha work (Pe 65) which makes a tentative $L = 3$ assignment or the 31 MeV alpha work (Li 66) which is most consistent with an L transfer of 4. Lippincott's data do not rule out a possible $L = 5$ though. The present results are in agreement with the $L = 5$ assignment made in the (p, p') work of Tellez et. al. It is interesting to note that at 25 MeV the state is more strongly excited than at the higher energies ($f_L = .31$ fm at 25 MeV versus $f_L \approx .22$ fm at the other energies). The 12 MeV proton experiment observes a strength of $f_L = .87$ fm. The alpha results of Peterson agree with ours, $f_L = 0.17$ fm at 42 MeV.

5.249, 5.298

The 31 MeV alpha experiment (Li 66) was not able to resolve a

weakly excited state at 5.31 from the strong 3 - at 5.37. With our resolution it was possible to see that there are two weakly excited states in this region at 5.249 and 5.298 MeV. The 5.249 state appears to be $L = 5$ transfer but could also be $L = 4$. The 5.298 state is consistent with $L = 2$.

5.362

The 5.362 state is a strongly excited $L = 3$ state in agreement with all the previous L assignments except one (Te 68) which makes a tentative $L = 4$ assignment. The nuclear deformation observed in this experiment is about twice that observed in the alpha experiments. The state is not observed in the (t,p) experiment. A state at 5.37 MeV is observed in electron scattering, but has not been analysed (Ei 69).

The 5.48 0+ state observed in the (t,p) work (Hi 66) is not observed in this experiment. An upper limit* on the cross section at each energy is given below.

Table 6.1 Upper Limits on the 0+ Cross Sections

Incident Energy (MeV)	4.28 State % of 2^+ (3.83)	5.48 State % of 2^+ (3.83)
25	2.3	1
30	1.5	1.2
35	1.2	1.1
40	1.1	1.0

* The upper limits were obtained by taking the ratio of the background to the 2^+ cross section at 3 angles.

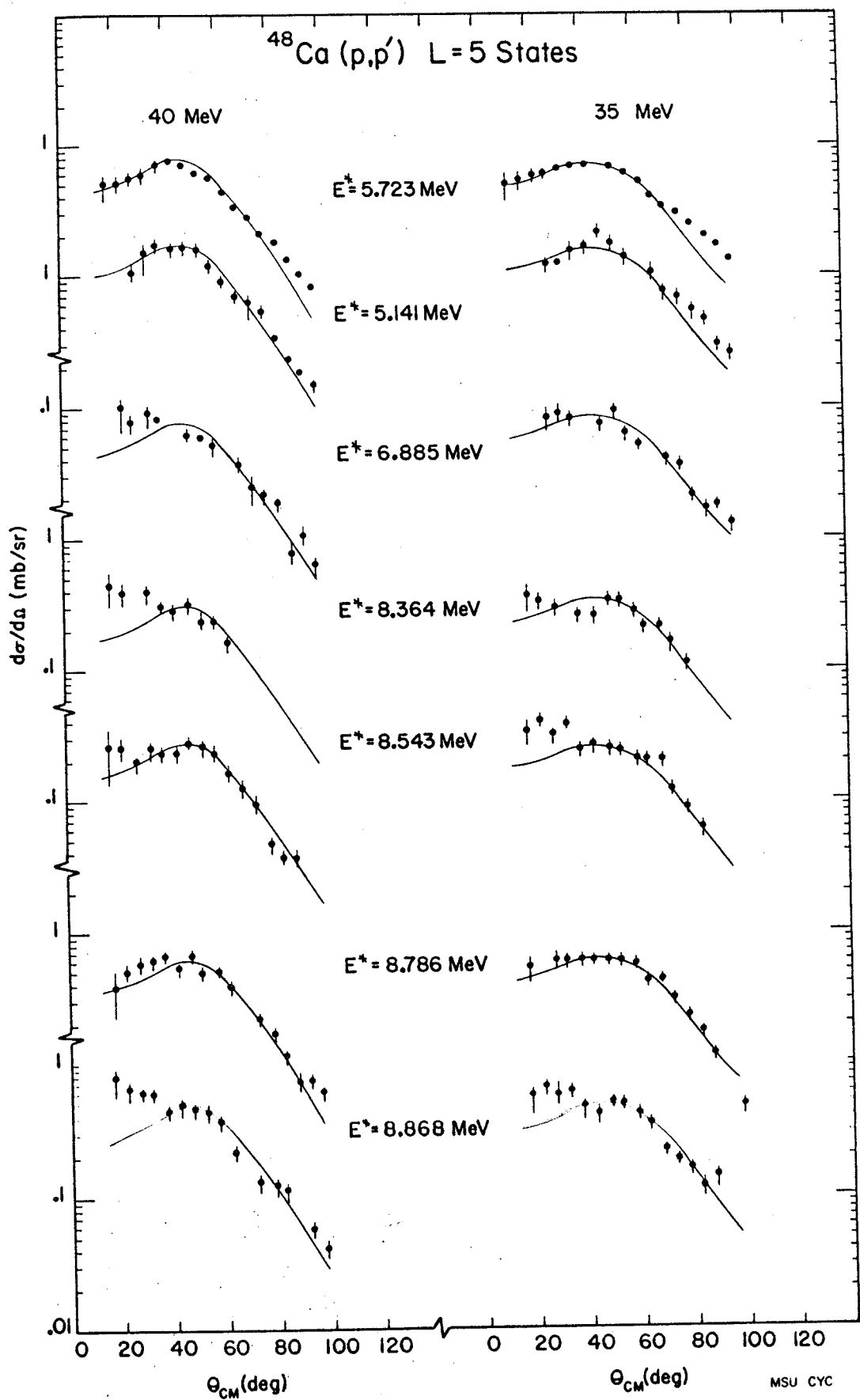
5.723

The state at 5.723 MeV is excited with an $L = 5$ transfer in agreement with the 31 MeV alpha experiment. The comparison with $L = 5$ collective model calculation is shown in Figure 5.4, and the comparison with the shape of a known $L = 5$ angular distribution from ^{40}Ca is shown in Figure 6.4. Peterson observed the state as a 2^+ and Tellez et. al. tentatively assign $L = 3$, but the present evidence for $L = 5$ seems conclusive. The deformation of 0.46 fm is again larger than that observed with alphas (0.32 fm (Li 66)). Tellez et. al. obtain a deformation of 0.44 fm in agreement with the present value, but it is not known if this is due to their different L assignment. In any case, it is the only deformation which they observe that is not substantially larger than that observed in the present experiment. The state is not observed in (t,p) or (e,e') experiments, which is also consistant with the $J^\pi = 5^-$, assignment.

6.3 States between 6 and 7 MeV

6.098

The state at 6.098 MeV is believed to correspond to the 6.11 MeV state observed in the α experiments. The state is only weakly excited and the statistics on the angular distribution are not good enough to make a positive L assignment, but the data appear to be most consistent with $L = 5$.

Figure 6.4 $L = 5$ states..

6.335

The 6.335 state angular distribution is consistent with $L = 4$ assignment made in the α experiment (Li 67). The fits to the collective model DWBA calculations are shown in Figure 5.3. Figures 6.1 and 6.2 compare the $L = 4$ states observed in ^{50}Ti and ^{52}Cr (Pr 70) with this $L = 4$ state and the overlap is seen to be almost exact.* The same theoretical calculation as used for the 2^+ states is also shown (sec 6.1). The comparison with the shape of a known $L = 4$ state in ^{40}Ca is shown in Figure 6.5 and overlap is not as good as in the case of the comparison with ^{50}Ti and ^{52}Cr . But this may be due to the different configurations giving rise to the 4^+ states in ^{40}Ca and ^{48}Ca . In ^{48}Ca the 4^+ state arises via the $(f_{7/2})^{-1} p_{3/2}$ configuration while in ^{40}Ca the configuration giving rise to 4^+ states would be $(2h-2p)$ & $(4h-4p)$. The core configurations giving rise to 4^+ states in ^{50}Ti and ^{52}Cr would be the same as for ^{48}Ca . The deformation of 0.37 fm is comparable to that observed in the 31 MeV experiment (0.38 fm). The (t,p) experiment assigns $L = 2$ for this state based on the position of the first maximum, but a second maximum at 70° as observed for the 3.83 MeV state is missing.

6.642

The state at 6.642 MeV is actually a close multiplet. It is at least a triplet of states. The resolution in this experiment was

* The two $L = 4$ states in ^{52}Cr must be added together to compare the strengths observed since the strength is divided between seniority 1 and seniority 2 states.

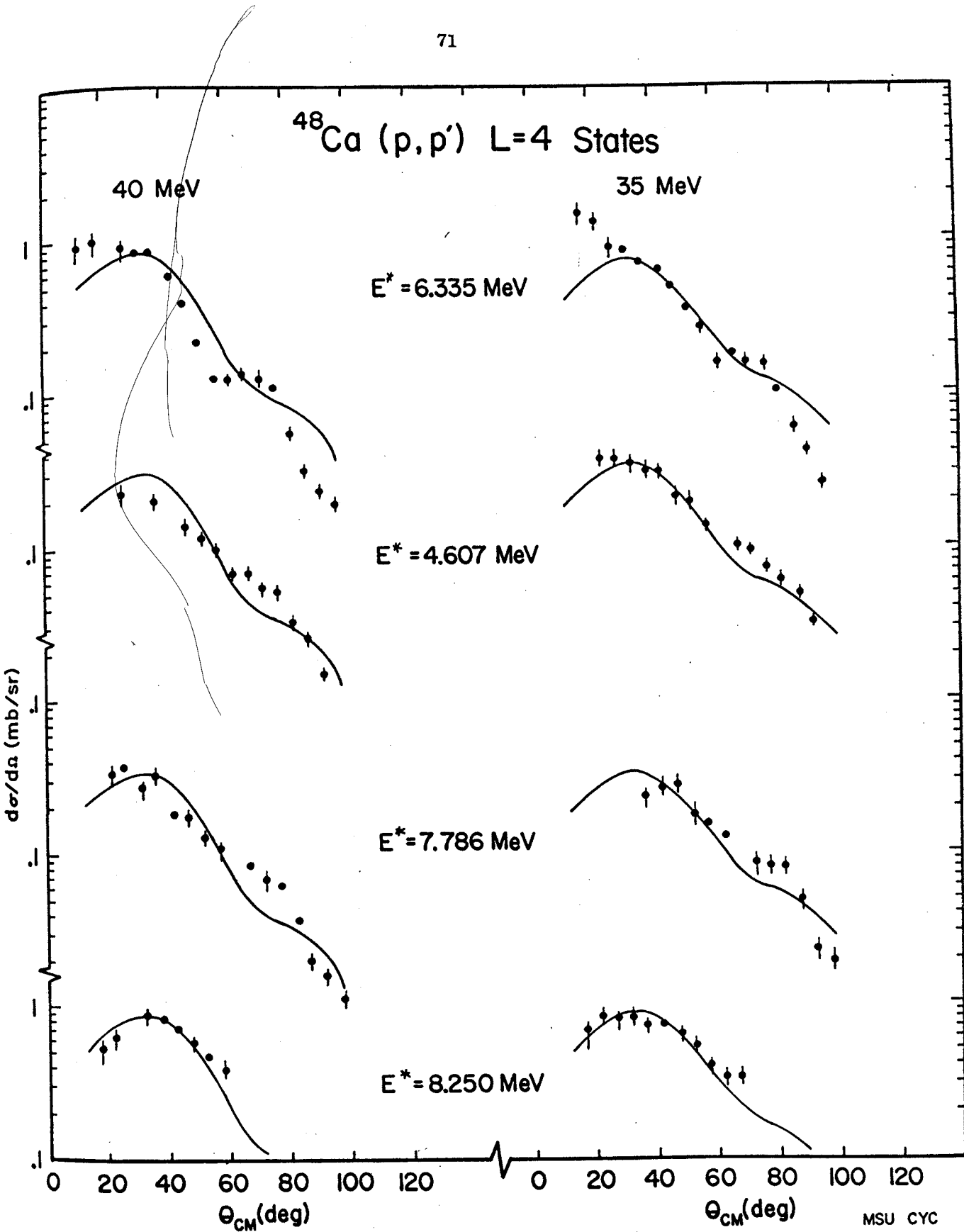


Figure 6.5 L = 4 states.

not able to resolve the individual components of the multiplet but it was able to reveal that the state was in fact a multiplet by the broadened peak shape. This is in agreement with the 12 MeV (p, p') experiment which observes a triplet at 6.618, 6.654, and 6.687 MeV. The 31 MeV alpha data for this state (Li 67) are consistent with a 4+ assignment beyond 40 degrees, but the first maximum appears to be washed out. This is what one would expect if the state were a combination of $L = 2$ and $L = 4$. The angular distribution observed in this experiment has the slope associated with a 2+ state, but the valleys are missing. This is also what one would expect if the state were a combination of $L = 2$ and $L = 4$. By combining the known $L = 2$ and $L = 4$ shapes in ratio of 1 to 1, a reasonable fit to the data could be obtained at each energy. For purposes of calculations the strength of this 6.642 state is assumed to be 50% $L = 2$ and 50% $L = 4$, and the total strength of the multiplet is the sum of the two strengths. The deformation observed in the α experiment of 0.36 fm (Li 67) is comparable to the total observed strength of the multiplet of 0.35 fm. The (t, p) experiment observes a single state at 6.645 MeV.

6.786, 6.885

The two weakly excited states at 6.786 and 6.885 MeV are tentatively assumed to be $L = 4$ and $L = 5$ respectively. These L assignments are suspicious at best, considering the poor statistics. The (t, p) tentatively assigns 2+ to the 6.793 state, but this seems

to be based on a single data point. Except for that single point the (t,p) angular distribution is the same as that for the 6.329 state which probably corresponds to the known $L = 4$ state at 6.335 MeV.

6.4 States between 7 and 8 MeV

7.009

The first state above 7 MeV is a doublet at 7.009 MeV. The angular distribution is consistent with a combination of $L = 2$ and $L = 4$ in the ratio of 1 to 1. The calculations for this state assume that 50% of the strength is $L = 2$ and 50% of the strength is $L = 4$. These L assignments should be considered very tentative at the present time. The total strength of 0.28 fm is almost twice the strength of 0.16 fm observed by Peterson with 42 MeV alphas, and who assumed an $L = 3$ state.

Lippincott reports a weak state at 7.16 MeV. No state is observed at this energy in the present experiment or by any of the other experiments.

7.320, 7.401, 7.471, 7.521

Lippincott observed a weak state at 7.53 MeV at a few large angles. Tellez et. al. observed a quartet of states in this region at 7.305, 7.402, 7.444, and 7.589 MeV. In this experiment a quartet of weakly excited states is observed in this region. Of the four states observed at 7.320, 7.401, 7.471, and 7.521 MeV,

only the strongest state at 7.401 had angular distributions at each energy consistent with a single L value. This state is tentatively assigned L = 3.

7.643

The strong L = 3 state at 7.643 MeV agrees with the L assignment obtained previously in the alpha experiments. The state is only weakly observed in the (t,p) experiment. It is observed in the electron scattering experiment, but not analysed. The nuclear deformation of 0.49 fm is comparable to that observed in the 31 MeV alpha experiment of 0.54 fm. The only state observed by Peterson in this region is a 3 - state at 7.76 with a deformation of 0.33 fm. It is probably the same state.

7.786, 7.940

The state at 7.786 has angular distributions which are consistent with an assignment of L = 4. Analysis of the 7.940 state is complicated by the fact that it is contaminated by the much larger deuteron peak over most of the angular range and could only be observed at large angles beyond 70°. No L assignment could be made.

6.5 States between 8 and 9 MeV

8.037

The analysis of the first observed state above 8 MeV is also

complicated by the deuteron peak and data could be obtained at only a few angles. No L assignment is possible from the data obtained.

At these higher excitation energies the density of states increases and it becomes difficult to make positive L assignments because most of the states are only weakly excited and often they are members of close lying multiplets which are not well resolved. The 30 keV resolution enables one to identify many of the states as multiplets by looking for broadened peak shapes.

8.250

There is a doublet observed at 8.250 MeV. This probably corresponds to the 8.268, 8.237 doublet observed in the (t,p) work (Bj 67). The angular distributions are not definitely $L = 4$ or $L = 5$, but appear to peak midway between the "classic" $L = 4$ and $L = 5$ distributions observed at 6.335 and 5.723 MeV. The analysis is again complicated by the fact that the large angle data at 40 and 35 MeV is contaminated by the much larger deuteron peak. This is the data that would allow one to determine if the doublet is $L = 4$ or $L = 5$ or a combination. A combination of 50% $L = 4$ and 50% $L = 5$ is able to fit the limited data, but there is not enough data to determine if this is the correct composition of the doublet. The (t,p) experiment observes a strength of 50% of the ground state for the 8.268 MeV state, and indicates that the 8.268 MeV state is probably a 4+ state.

8.364

The multiplet at 8.364 MeV can be fit using a combination of 20% $L = 3$ and 80% $L = 5$. These states have not been previously reported. The state has a strong $L = 5$ character as illustrated in Figure 6.4. A state at 8.473 MeV is reported by Bjerregaard et. al. in their (t,p) work, but the state is not seen in this experiment.

8.501, 8.543, 8.589

The next three states are each separated from one another by about 40 keV and are just able to be resolved by the present experiment. The 8.501 and 8.589 MeV states have $L = 3$ angular distributions. The middle state at 8.543 has an apparent $L = 5$ angular distribution. The (t,p) experiment also observes 3 states in this region at 8.513, 8.538, and 8.604 MeV which are strongly excited at 52%, 68%, and 31% of the ground state respectively. Inelastic electron scattering observes a broad bump in this energy region.

8.658

The 8.658 state is another state whose peak shape indicates that it is not a single state. A reasonable fit can be obtained using 67% $L = 3$ and 33% $L = 4$, but the evidence is not conclusive for these assignments.

8.786

The state at 8.786 MeV is a strongly excited state with an apparent $L = 5$ angular distribution. The state is well resolved with no close contaminants and the angular distribution agrees almost point for point with the $L = 5$ angular distribution at 5.723 MeV. The (t,p) experiment observes a state 8.782 MeV with a strength of 42% of the ground state indicating a sizeable 2 n particle component in the excitation.

8.868

The last strong state observed in this experiment is a very close lying doublet at 8.868 MeV. The evidence that this state is a doublet is the fact that the state consistently has a resolution about 5 to 10 keV broader than the 8.786 MeV state just below it. Also the shape of the angular distribution, while strongly $L = 5$ in character does rise at the forward angles. It is possible to fit the angular distributions at each energy assuming 20% $L = 4$ and 80% $L = 5$. The inelastic electron scattering observes a state close to 9 MeV; but it is not analysed.

With regard to the $L = 5$ assignments for the states that appear to be doublets (8.868, 8.364, and 8.250 MeV) it should be pointed out that there is no possible combination of lower L transfers which can give rise to an angular distribution which peaks around 60° as the $L = 5$ angular distribution does. It would however be possible to construct combinations with states of even higher angular momentum transfer which would peak as observed.

6.6 Summary

The p, p' reaction is able to differentiate between L transfers to a given state by the position of the first maximum in the angular distribution. In making the L assignments associated with the states observed in this experiment, consistency of L assignment at each energy was required. It was not always possible to make definite L assignments, particularly in the cases of weak states having large errors associated with the data. The distinction between $L = 3$ and $L = 4$ was often difficult to make because a 20% change in normalization would make an $L = 3$ distribution overlap an $L = 4$ distribution.

The L assignments determined in this experiment are compared with previous work in Figure 6.6. The relative strengths of the states at 40 MeV are shown in Figure 6.7. The fact which stands out is the large amount of apparent $L = 5$ strength at excitation energy above 8 MeV. These high lying apparent $L = 5$ states are not understood at the present time. If the states between 8 and 9 MeV observed in the electron scattering are the same as these apparent $L = 5$ transfer states, then it is unlikely that the J^π is greater than 3-, because of the lack of angular momentum transfer available. Furthermore, it is difficult to produce a nuclear model which would predict such a cluster of 5- states. It is for these reasons that one is led to one possible conclusion that the members of the multiplet have undetermined J^π and are excited via a 5-

^{48}Ca EXCITATION ENERGIES AND J^π

79

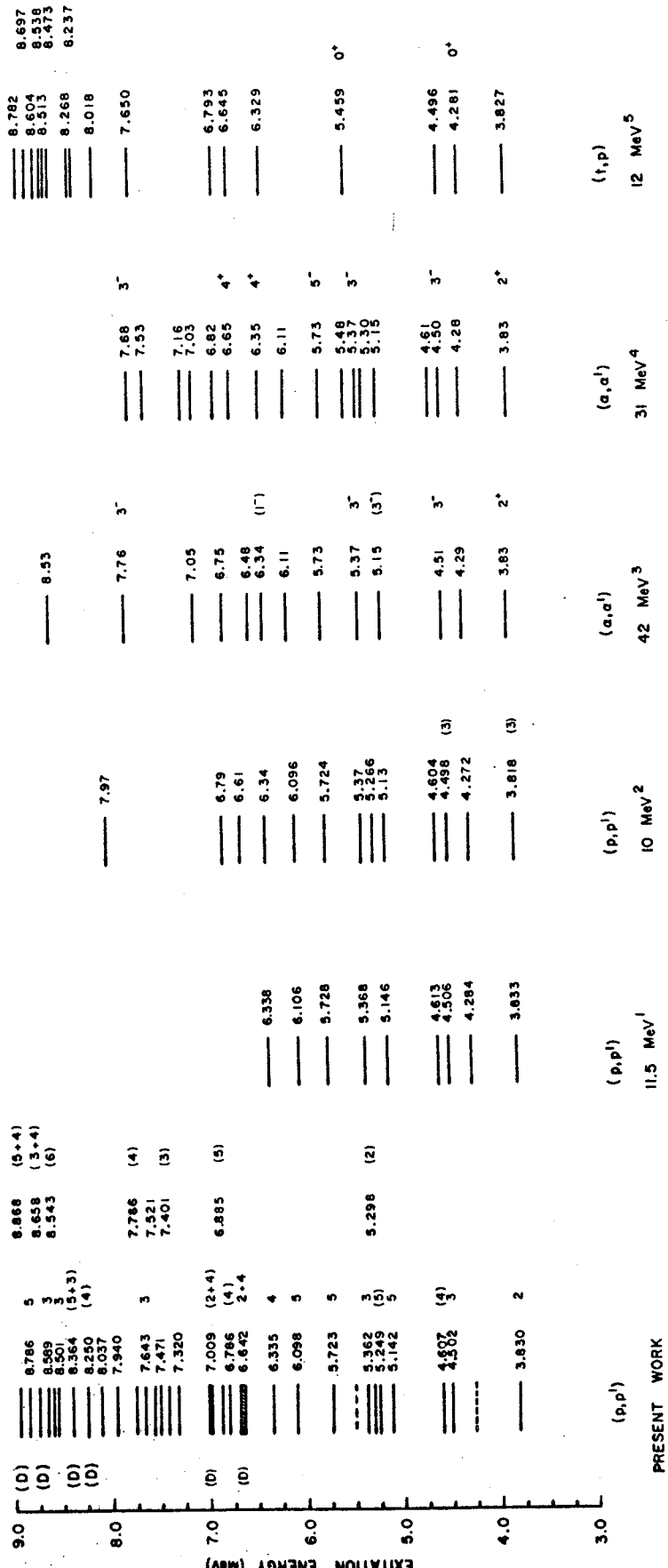


Figure 6.6 Comparison with other experiments.

Figure 6.6

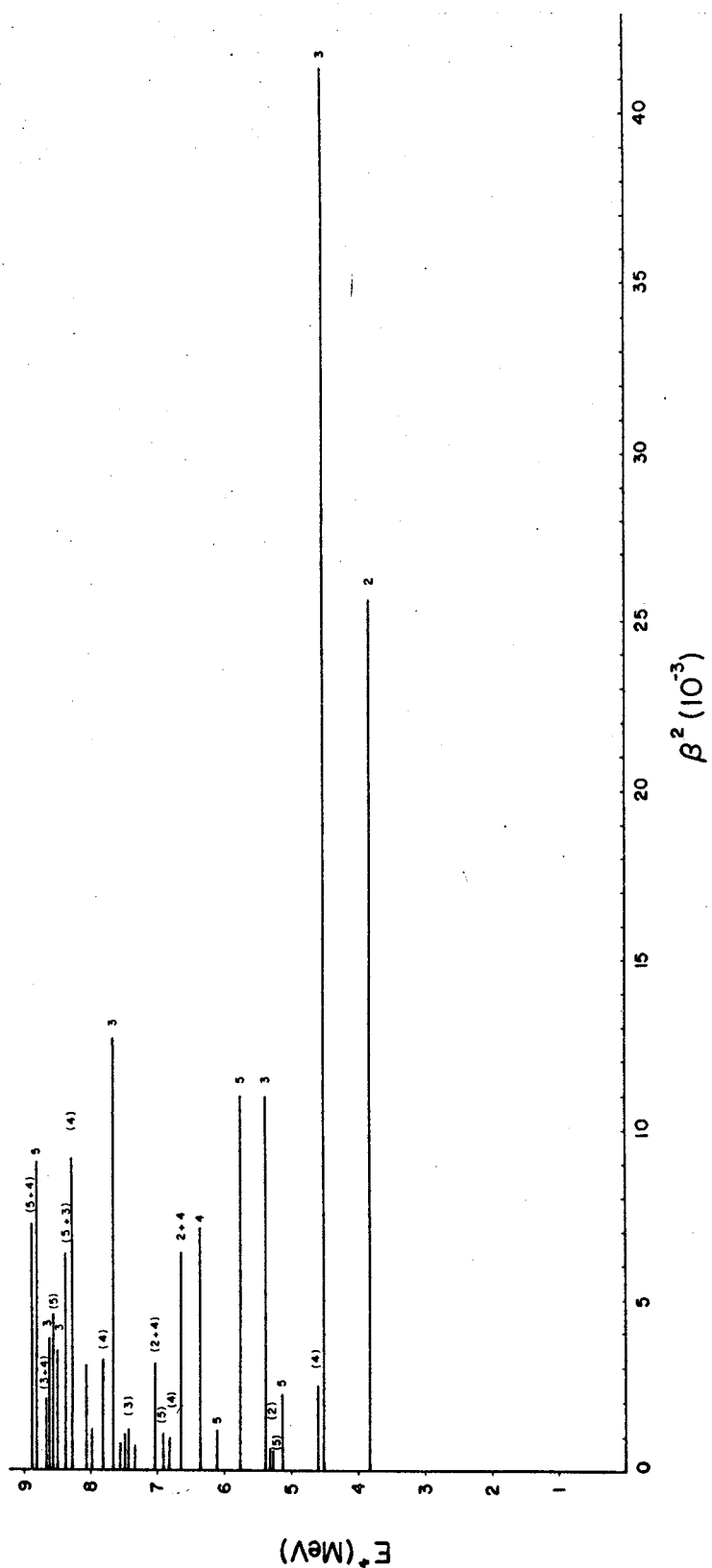


Figure 6.7 Experimentally determined β^2 .

doorway state. An alternate explanation would be that the multiplet is based on the coupling between quadrupole and octupole states with parentage in the anti-analog configuration. This interpretation could be verified by studying the γ - decay of the states.

The deformation observed in this experiment are compared with the results of previous experiments in Table 6.2. This experiment usually observes a deformation larger than that for the alpha experiments. The deformations observed in the 12 MeV ($p, p' \gamma$) experiment are always larger except for the 5 - state at 5.723 MeV.

Table 6.2 Comparison of Nuclear Deformations

E^*	$f_L(L)$ Present exp	$f_L(L)$ (Pe 65)	$f_L(L)$ (Li 67)*	$f_L(L)$ (Te 68)
3.830	0.65(2)	0.53(2)	0.71(2)	1.0(2)
4.502	0.89(3)	0.56(3)	0.76(3)	1.15(3)
4.607	0.24(4)			0.10(2)
5.141	0.22(5)	0.17(3)		0.87(5)
5.362	0.458(3)		0.26(3)	0.15(4)
5.723	0.46(5)	(2)	0.32(4)	0.44(3)
6.335	0.37(4)		0.38(4)	
6.642	0.35(2 and 4)		0.36(4)	
7.643	0.49(3)		0.54(3)	

* Calculated from the f_L using $R_o = 5.62$ fm.

This may be due to compound nuclear effects, exchange effects, or 2 step processes enhancing the cross section at lower energies.

The reduced transition probabilities are compared to the electron scattering results in Table 6.3. The values are in agreement for the 3 - state but differ by a factor of two for the 2+ state. A possible explanation might be that the electron interacts with the nucleus through the charge form factor by exciting protons while the proton can interact through both protons and neutrons, and the large number of excess neutrons in ^{48}Ca may cause some discrepancies.

It is observed that some of the 4+ states rise at forward angles. This same effect has been observed with other nuclei in this region (Ku 70) (Pr 70) (Th 69a) and is not understood at the present time.

6.7 Comparison with Theory

Jaffrin and Ripka have calculated the single particle-hole excitations giving rise to the odd parity levels in ^{48}Ca . (Ja 68). They predict two groupings of negative parity states. The lower group consists of two 3 - states, one 5 - state, two 4 - unnatural parity states, and a 2 - unnatural parity state. In the same region of excitation energy (4 to 6.5 MeV) we observe two 3 - states and four states with $L = 5$ angular momentum transfer. The $L = 5$ transfer implies that the states are negative parity, perhaps two of the $L = 5$ states are associated with the predicted 4 - states.

The reaction would occur through $L = 5$ transfer with spin flip. The same process may be occurring in the higher grouping of negative parity states between 8 and 10 MeV. The theory predicts a 5 - state, two 3 - states, two 2 - and two 4 - states. We observe several $L = 3$ and $L = 5$ states in this region which may be associated with the predicted unnatural parity states. It would be useful to have the results of a $(p, p'\gamma)$ angular correlation experiment to help determine the spins of these states.

BIBLIOGRAPHY

- Ba 62 Bassel, R. H., R. M. Drisko, and G. R. Satchler. Oak Ridge National Laboratory Report ORNL-3240 (unpublished, 1962).
- Be 69 Bernstein, A. M., M. Duffy, E. P. Lippincott. Phys. Letters 30B, 20 (1969).
- Bj 67 Bjerregaard, J. H., Ole Hansen, O. Nathan, R. Chapman, S. Hinds, and R. Middleton. Nucl. Phys. A103, 33 (1967).
- Bl 66 Blosser, H. G., and A. I. Galonsky. IEEE Trans. on Nuclear Science, NS-B, No. 4, 466 (1966).
- Bl 66a Blumberg, L.N., E. E. Gross, A van der Woude, A. Zucker, and R. H. Bassel. Phys. Rev. 147, 812 (1966).
- Ca 67 Cameron, J. Unpublished Ph.D. thesis, University of California at Los Angeles, 1967.
- Ch 65 Chasman, C. and R. A. Ristiney. Nucl. Instr. and Meth. 34, 250 (1965).
- Ei 69 Eisenstein, R. A., D. W. Madsen, H. Theissen, L. S. Cardman, and C. K. Bockelman. Phys. Rev. 188, 1815 (1969).
- El 67 Elton, Phys. Rev. 158, 970 (1967).
- Fe 70 Fernandez, B., J.S. Blair, Phys. Rev. C1, 523 (1970).
- Fr 67 Fricke, M. P., E. E. Gross, B. J. Morton, and A. Zucker. Phys. Rev. 156, 1207 (1967).
- Fr 68 Frosch, R. F., R. Hofstadter, J. S. McCarthy, G. K. Noldeke, K. J. van Oostrum, M. R. Yearian, B. C. Clark, R. Herman, and D. G. Rovenhall, Phys. Rev. 174, 1380 (1968).
"
- Gl 66 Glendenning, N. K. and M. Veneroni. Phys. Rev. 144, 839 (1966).
- Go 70 Goulding, F. S., R. H. Pehl. Lawrence Radiation Laboratory Report UCRL - 19439 (1969).
- Gr 67 Gruhn, C. R., T. Kuo, B. Gottschalk, S. Kannenberg, N.S. Wall. Phys. Letters 24B, 266 (1967).

- Gr 68 Greenlees, G. W., G. J. Pyle, Y. C. Tang. Phys. Rev. 171, 1115 (1968).
- Gr 68a Greenlees, G. W., G. J. Pyle, Y. C. Tang. Phys. Letters 26B, 658 (1968).
- Gr 68b Gruhn, C. R., T. Kuo, C. Maggiore, B. Freedman, L. Samuelson, and J. Chander. IEEE Trans. on Nuclear Science, NS-15, No. 3, 337 (1968).
- Gr 69 Gruhn, C. R., B. M. Freedman, and K. Thompson. Phys. Rev. Lett. 23, 1175 (1969).
- Gr 69a Gruhn, C. R., R. Todd, C. J. Maggiore, W. Kelly and W. McHarris. Nucl. Instr. & Meth. 75, 109 (1969).
- Gr 70 Gruhn, C. R., T. Kuo, C. J. Maggiore and B. M. Freedman. To be published.
- Ha 52 Hall, R. N. Phy. Rev. 87, 587 (1952).
- Hi 66 Hinds, S., J. H. Bjerregaard, Ole Hansen, O. Nathan. Phys. Letters 21, 328 (1966).
- Ja 68 Jaffrin, A., and G. Ripka. Nucl. Phys. 119, 529 (1968).
- Ku 70 Kuo, T., Ph.D. Thesis, Michigan State University 1970 (unpublished).
- La 60 Lane, A. M. and E. D. Pendlebury. Nucl. Phys. 15, 39 (1960).
- La 66 Lassen, L., T. Scholz and H. J. Unsold. Phys. Letters 20, 516 (1966). "
- Li 66 Lippincott, E. P. Ph.D. Thesis, Massachusetts Institute of Tech. (1966, unpublished).
- Li 67 Lippincott, E. P., and A. M. Bernstein. Phys. Rev. 163, 1170 (1967).
- Ma 67 Mackenzie, G. H., E. Kasky, M. M. Gordon and H. G. Blosser. IEEE Trans. on Nuclear Science, NS-14, No. 3, 450 (1967).
- Ma 66 Marinov, A., J. R. Erskine. Phys. Rev. 147, 826 (1966).
- Ma 66a Maples, C., G. W. Goth and J. Cerny. UCRL-16964, (1966).
- Na 65 Nathan, O. and S. G. Nilsson. In Alpha-Beta- and Gamma-ray Spectroscopy. Ed. by Kai Siegbahn. North-Holland Publishing Co., Amsterdam, 1965. Chapter X.

- No 68 Nolen, J. A., Jr., J. P. Schiffer, N. Williams. Phys. Letters 27B, 1 (1968).
- Ow 63 Owen, L. W., and G. R. Satchler. Nucl. Phys. 51, 155 (1963).
- Pe 65 Peterson, R. J. Phys. Rev. 140, B1479 (1965).
- Pe 69 Petrovich, F., H. McManus, V. A. Madsen and J. Atkinson, Phys. Rev. Letters 22, 895 (1969).
- Pe 70 Petrovich, F. Ph.D. Thesis, Michigan State University 1970 (unpublished).
- Pr 70 Freedman, B. M., C. R. Gruhn, T. Kuo and C. J. Maggiore. Phys. Rev. C2, 166 (1970).
- Ri 64 Ridley, B. W., and J. F. Turner. Nucl. Phys. 58, 497 (1964).
- Ro 61 Rost, E. Unpublished Ph.D. Thesis, University of Pittsburgh, 1961.
- Sa 64 Satchler, G. R. Nucl. Phys. 55, 1 (1964).
- Sh 52 Shockley, W. and W. T. Read. Phys. Rev. 187, 587 (1952).
- Sl 68 Slanina, D., and H. McManus. Nucl. Phys. A116, 271 (1968).
- Sn 67 Snelgrove, J. L., and E. Kasby. Nucl. Instr. and Methods 52, 153 (1967).
- Ta 68 Tarbutton, R. M., and K. T. R. Davies. Nucl. Phys. A120, 1 (1968)
- Te 69 Tellez, A., R. Ballini, J. Delaunay and J. P. Fouan. Nucl. Phys. A127, 438 (1969).
- Th 69 Thompson, K. M. Ph.D. Thesis, Michigan State University 1969 (unpublished).

APPENDICES

APPENDIX I

Detector Fabrication and Testing

In this section a detailed description of the fabrication and testing of the Ge(Li) proton detectors is presented.

1. Choice of Ge(Li)

The choice of Ge(Li) rather than Si(Li) for making counters capable of detecting protons of energy greater than 30 MeV was made for the following reasons:

1. The range of a proton in Ge is about one half of that in Si. This allows one to use a single 5 mm drifted detectors for 40 MeV protons rather than a 9 mm stack of Si(Li) detectors.
2. The resolution of Ge(Li) detectors should ultimately be better than Si(Li) detectors because the cost to form an ion pair in Ge is 20% less than in Si(2.98 vs 3.66 eV), (Pe 69a) and the maximum transfer of energy in nuclear collisions in Ge is less (X2.5) than in Si.
3. The reaction contribution to the tails should be less structured in energy and therefore more easily accounted for as a source of background.

This is because Ge has a higher density of states

of lower excitation energy and a relatively uniform spread of isotopic abundance.

4. Ge detectors appear to be less susceptible to proton radiation damage effects than Si(Li).

2. Fabrication

The starting material is horizontally grown, gallium doped germanium having a resistivity of 10 - 20 ohm - cm, an etch pit density of less than 1000 per cm^2 , and a carrier lifetime greater than 400 microseconds.

A parallel slab of suitable thickness is cut from the ingot using a diamond saw or a wire abrasive cutter. The surfaces are lapped with 600 grit and then 1000 grit to remove the saw cut damage. After taping the surfaces not to be exposed to lithium the slab is coated with lithium in a vacuum and let up to an argon atmosphere. The lithium surface is immediately coated with mineral oil and then put in a furnace being purged with argon. Diffuse at 400° for about 10 minutes and allow to cool to room temperature in about 20 minutes. After lightlylapping the diffused surface the resistance measured with an ohmmeter across 1 cm of surface should be less than 30 ohms.

Afterlapping the sides, the n-type and p-type surfaces are taped in preparation for the etches. The first etch is in 2:1(90% HNO_3 : 50% HF) for 2 minutes. After rinsing with at least 1500 ml of deionized water the crystal is etched for one minute in

1:1(50% HF : 30% H₂O₂) and rinsed well with deionized water or methyl alcohol. The sides are blown dry with dry nitrogen and the tape is removed.

The diode characteristics of the crystal are then measured at room temperature. If the saturation portion of the curve has a slope of less than 0.4 mA/100 V at 400 V bias it is suitable for drifting. The diode is placed under reverse bias (400 V, ~25 mA/cm² of diffused surface in a freon bath and drifted until the desired drift depth is achieved as observed by the copper stain test.

The solution used for the copper stain test is a saturated solution of CuSO₄ in H₂O and 10% by volume HF(50%). This stock solution is diluted 1:1 with H₂O for use. By wiping the solution on a freshly lapped surface with a cotton swab while the diode is under reverse bias a copper stain will form at the P-I junction.

The drift depth W may be calculated as follows:

$$W^2 = 2 \mu Vt$$

where

μ is the lithium mobility $\sim 4.5 \times 10^{-10}$ cm²/V-sec at 23°C.

V is reverse bias of the diode during the drift in volts.

t is the time in seconds.

The thin window geometry shown in Figure I.1 is used for

Ge(Li) Surface Barrier Geometry

90

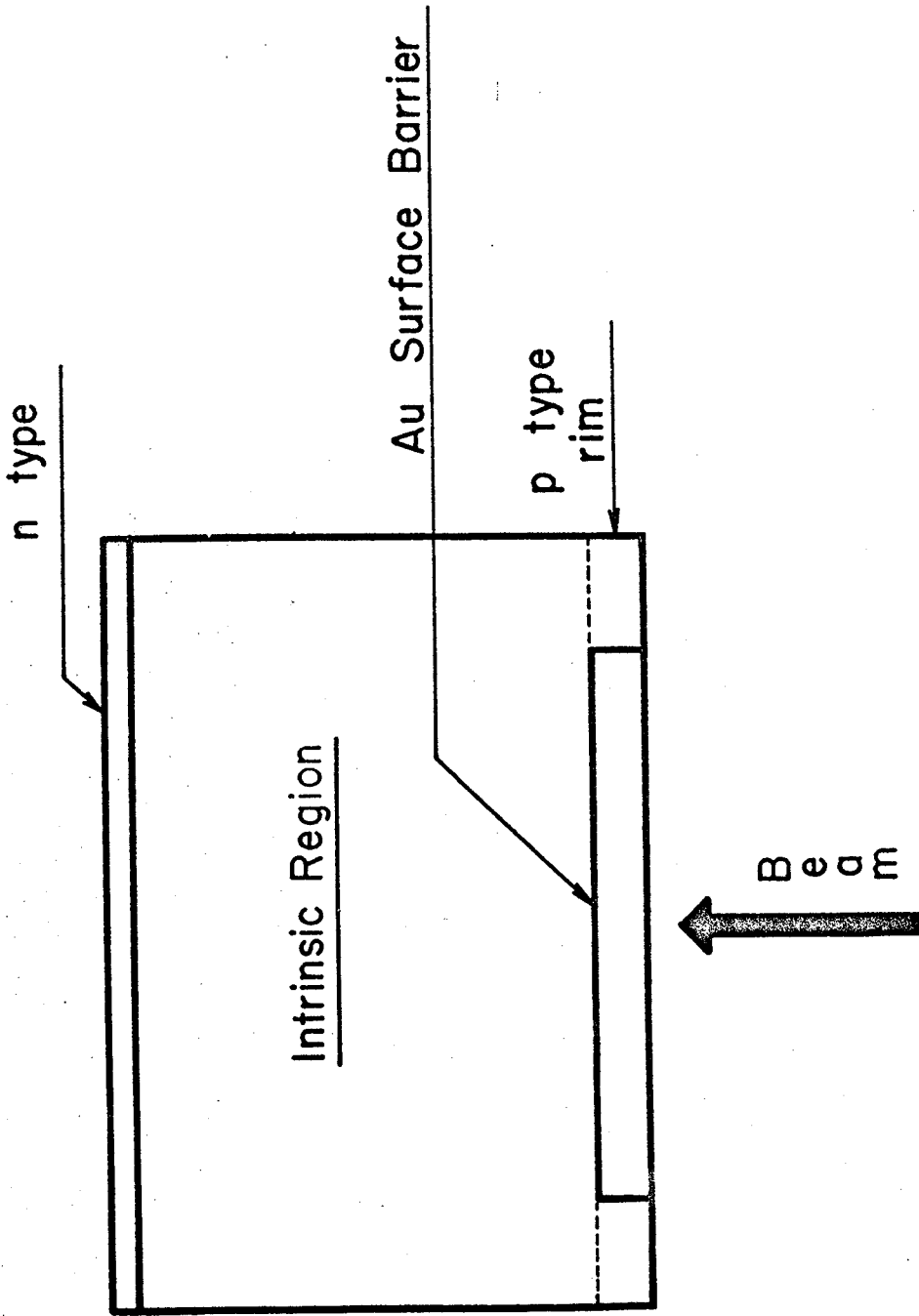


Figure I.1 Surface barrier geometry.

detecting protons in the 25 - 50 MeV range. The thin window is achieved by fabrication of a p+ contact on the intrinsic region. The procedure is as follows:

A drifted piece of Ge crystal is cut to the desired geometry. A 1-cm diameter flat ended quartz rod is chucked in a mill and is used with 600 grit abrasive and water to bore just into the intrinsic region through the p-type region. A p-type rim is thus left free to use for mechanical mounting minimizing injection of charge. The same rim has the added advantage of providing a simple means of encapsulating the p+ contact during subsequent etching of the outer surfaces. Crystal damage in the bored hole is removed by lapping with finer grits and then etching. The etching of the bored hole is rinsed and dried carefully prior to evaporation of a thin Au film onto the Ge surfaces of the hole and the exposed intrinsic region. The hole and p+ contact are then encapsulated by placing a piece of tape across the p-type rim sealing off the gold p+ contact. The n-type surface is also covered with tape before final etching with the HF : H₂O₂ etch. The diode is then mounted in the cryostat, evacuated, and cooled. When cooled to LN₂ temperature the finished detector must have a leakage current of less than 1 na at bias greater than 100V/mm drafted depth. If this low leakage current is not

obtained the diode must be recycled through the final etch procedure until it is obtained.

3. Packaging

The requirement that the Ge(Li) detector be stored in vacuum and at liquid nitrogen temperature at all times does present a packaging problem. The goniometer (Th 69) was designed to be compatible with cryostats of the Chasman design (Ch 65); therefore, this package was used.

Figure I.2 shows the mounting and collimation used with the proton detectors. The use of the thin slit in front of the collimator was found to minimize the slit scattering contribution to the "tails" of the peaks. Figure I.3 summarizes the results of a study of the slit scattering problem. The response of the detector and slits to the $^{12}\text{C}(\text{p},\text{p}')$ reaction at 40 MeV was measured at a laboratory angle of 40 degrees. The top spectrum shows the response to what was thought to be an "ideal" slit geometry. A broad satellite peak was observed to be associated with each of the excited states of ^{12}C . This satellite peak was then shown to be due to slit scattering by degrading the energy of the scattered particles which are in the region of the thick slit and using the thin slit as the effective collimator. The result is seen in the middle spectrum. The "thin" collimator was then made of Pilot B scintillator and the signal from a phototube viewing the scintillator was used to turn off the Ge(Li) detector when protons passed through it. This

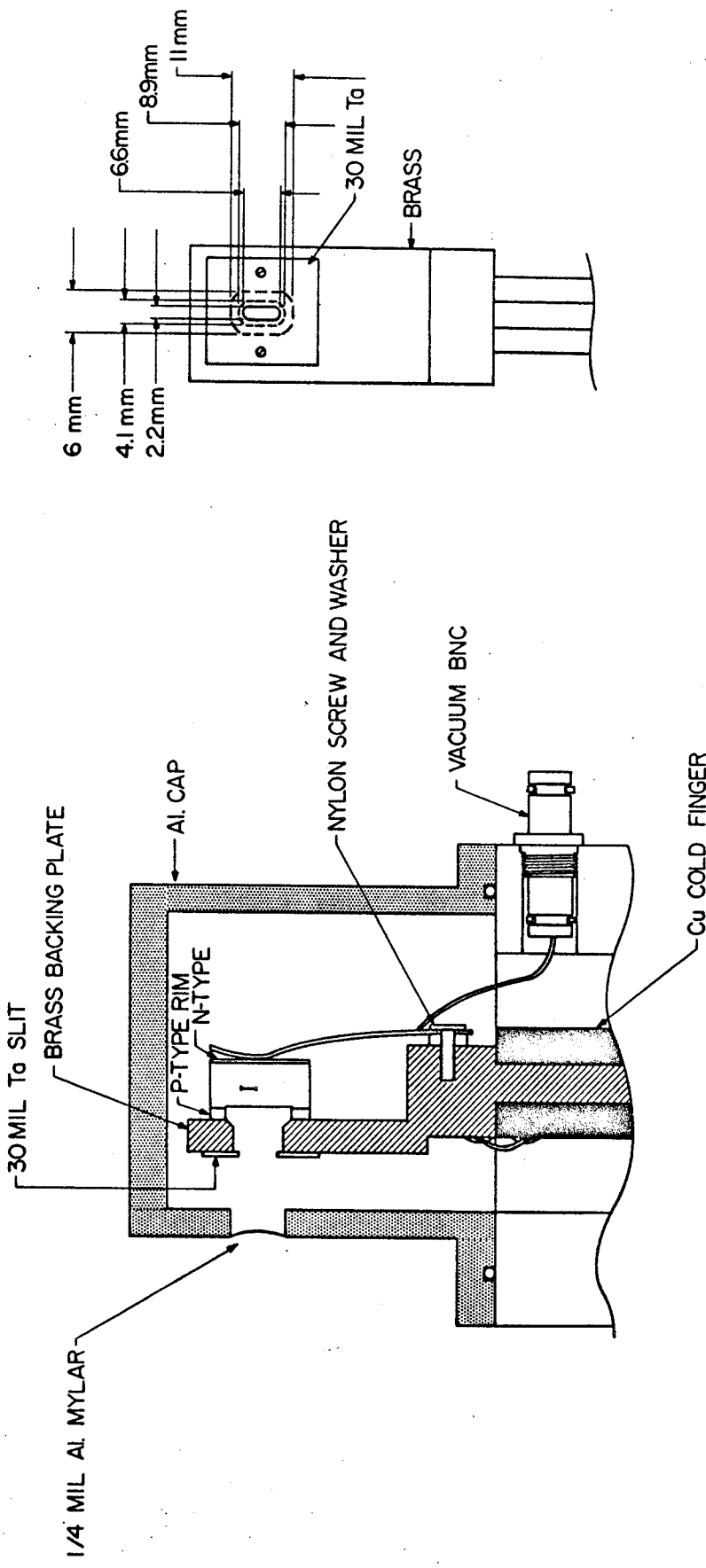
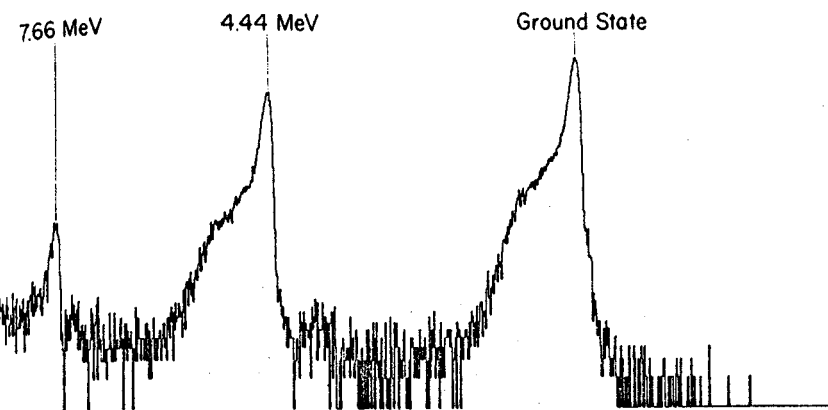


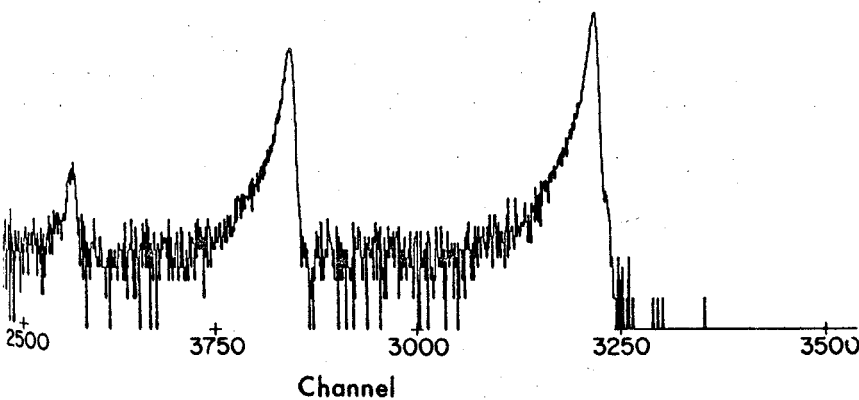
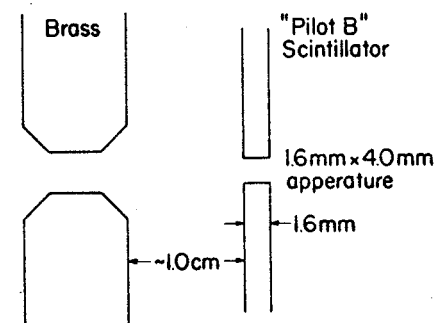
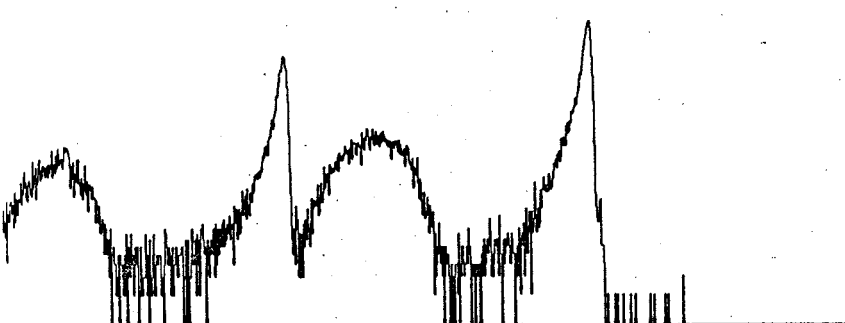
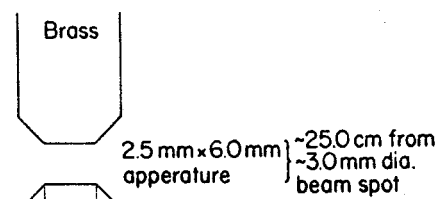
Figure 1.2 Detector mount.

Side Entry Ge(Li) Detector (130 $\frac{\text{Volts}}{\text{mm}}$ Bias)
 Slit Scattering Study, C¹² (p,p') 40 MeV 45 Degrees

Detector Response



Slit Geometry



Same as above but with
 Anticoincidence gate
 from Scintillator

Figure I.3 Slit scattering.

technique greatly reduced the slit scattering contribution to the tail as seen in the bottom spectrum of Figure I.3. This technique also allows use of relatively narrow collimation in order to reduce kinematic broadening effects and at the same time minimize the problem of slit scattering from the thick slits.

4. Testing

Once the detector is mounted there are a number of preliminary tests which the counter must pass if it is to be successful proton counter. All of these tests are necessary but not sufficient conditions to have a good proton counter. The final worth of the counter can only be determined by use with the beam.

The first test is to check the counter as a γ - detector and monitor its charge collection and resolution as a function of bias voltage. As the voltage is increased the peak height increases and the resolution improves. For a good proton counter both of these effects should show saturation at bias levels of ~ 100 V/mm drifted depth. If the peak height continues to increase as the bias is increased up to the point at which breakdown occurs, it is indicative of charge collection problems in the detector.

Figure I.4 shows the complete spectrum of ^{137}Cs obtained with one of the proton counters. An evaporated source was placed in front of the 1/4 mil aluminized mylar window; therefore, the K and L conversion electron peaks appear in the spectrum. The fact that these peaks have a resolution compatible with the straggling through the

GAMMA-RAY AND CONVERSION ELECTRON
SPECTRUM OF ^{137}Cs WITH PROTON Ge(Li)
SURFACE BARRIER DETECTOR

0.374 keV/Ch

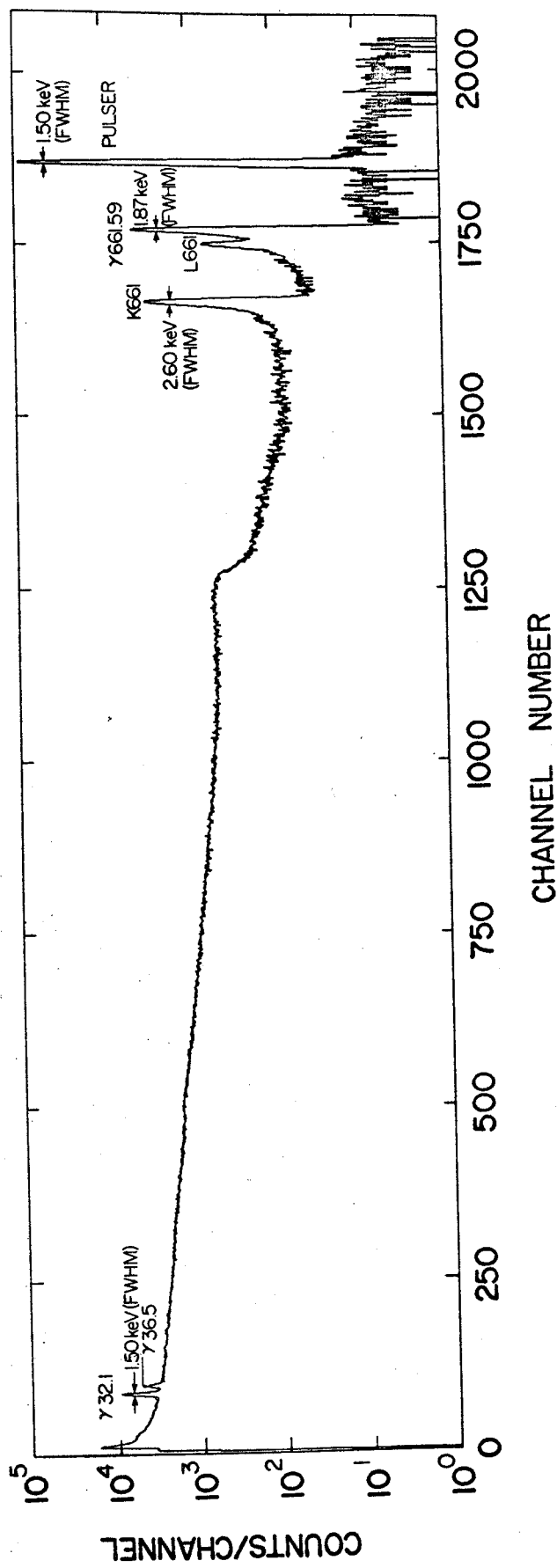


Figure I.4 ^{137}Cs spectrum.

mylar window indicates that there are no obvious problems with the collimation or detector window.

A more sensitive test of the window thickness on the counter itself is made by using a low energy alpha source. Figure I.5 illustrates the spectra taken with two different proton counters. Counter 2 has an ideal spectrum indicating the existence of a thin uniform p+ contact. The alpha peaks in the spectrum from counter 1 are asymmetric and displaced lower in energy. The displacement in energy indicates that the average window thickness for counter 1 is greater than for counter 2. The shoulder on the high side and the broad tail on the low side indicate nonuniformity of the counter window.

The final, and ultimately only, test of the proton counter is trying it with protons. Figure I.6 shows the ^{64}Ni spectrum obtained with one of the counters at 40 MeV. The spectrum from ^{12}C was used to obtain an energy and angle calibration. The sources of noise contributing to the overall 21 keV resolution are listed in Table I.1. The estimate of 9.3 keV due to the statistics of ion pair formation is based on an assumed Fano factor of 0.127. This is now known to be less than 0.084. This new Fano factor (Go 70) would lower the resulting accounted resolution to a minimum of 18.8 keV and a maximum of 19.1 keV.

5. Radiation Damage

The radiation damage studies were made with the Ge(Li)

WINDOW THICKNESS TESTS WITH ALPHA PARTICLES
FROM THE DECAY OF Th C AND Th C'

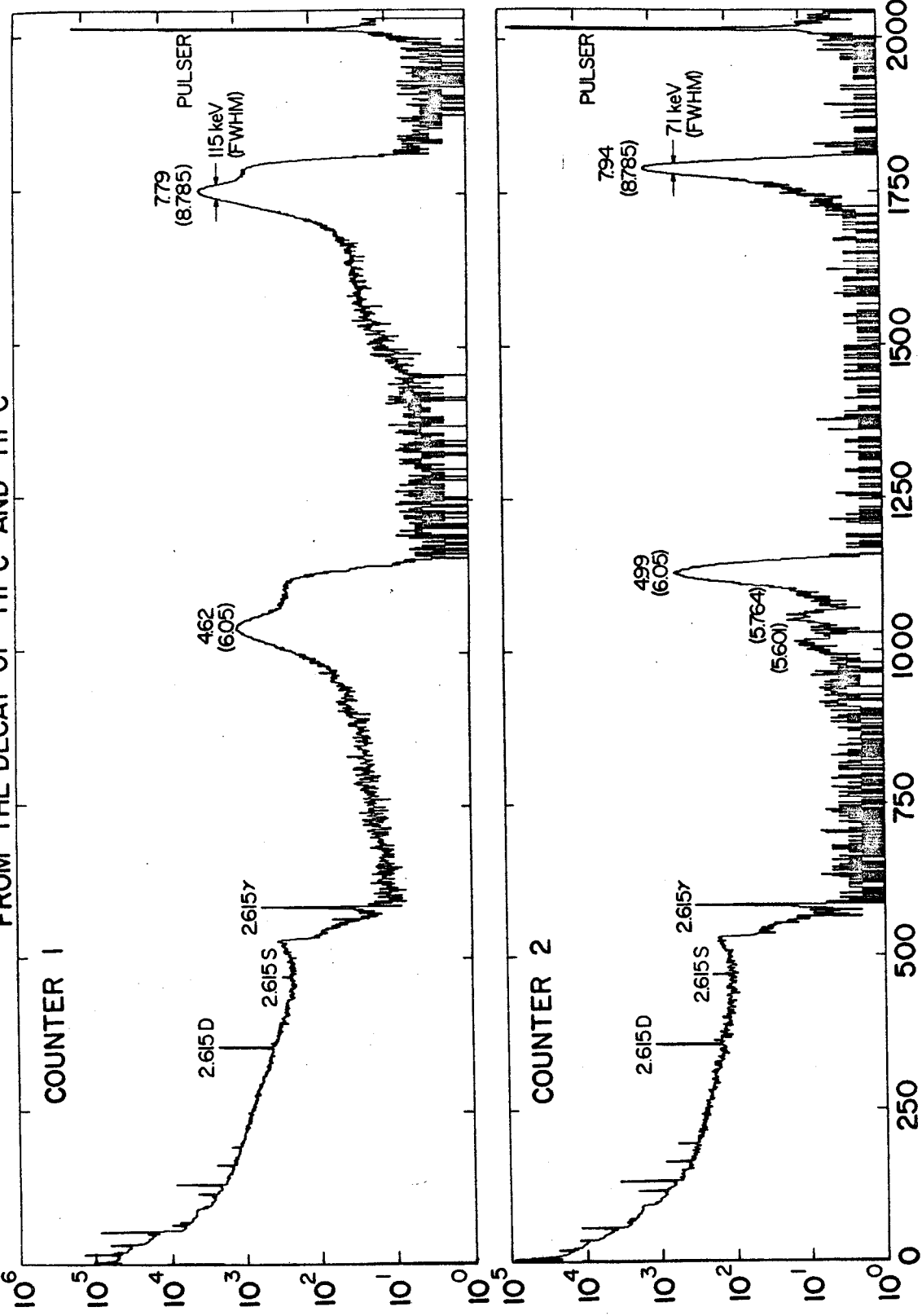


Figure 1.5 Alpha particle spectra.

RESOLUTION OF PROTON Ge(Li) SURFACE BARRIER DETECTOR

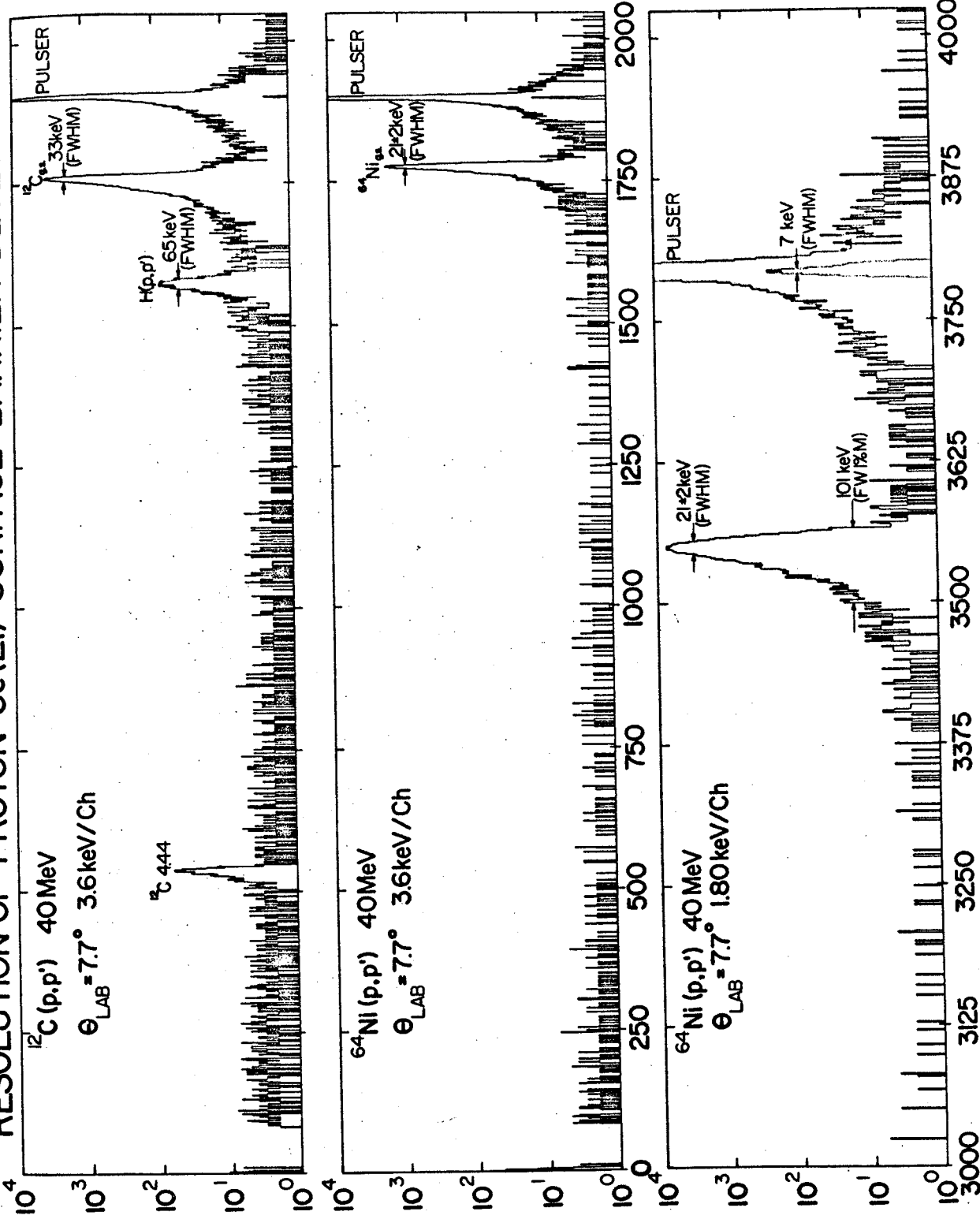


Figure I.6 Proton resolution at 40 MeV..

Table I.1 Contributions to the energy resolution.

CONTRIBUTIONS TO THE ENERGY RESOLUTION 40 MeV PROTONS IN Ge(Li) SURFACE BARRIER DETECTOR

ELEC- TRONIC	STRAGGLING			BEAM KINE- MATICS	TOTAL	MEASURED
	ION PAIR NUCLEAR	COLLISI- TION	PACKAGE- TARGET			
ΔE (keV)	7.2	9.3	0.7	2.1	5.3	8.0
ΔE^2 (keV)	51.8	86.5	0.5	15.4	237.1	36.0

detectors in the side entry geometry. Protons at 42 MeV were scattering from a 15 mil tantalum foil. All protons were counted above 160 keV. After each bombardment the response of the detector was measured with ^{137}Cs γ -rays, ^{60}Co γ -rays, and the elastic scattering of protons from Ta.

Conventional electronics were used for these experiments. The detector was operated at a bias of 100 V/mm. The response to the γ -rays was made with 7 keV (FWHM) initial limiting resolution in the electronics. The integration and differentiation time constants were set for 1.6×10^{-6} sec.

The resolution was measured as a function of total proton flux presented to the detector. A significant deterioration (~ 12 keV FWHM) in the resolution after about 10^{10} protons/cm² total flux was observed. There was no noticeable increase in reverse current after the bombardment, although during the bombardment the reverse current was proportional to the beam current presented to the target and was as large as 500 namp. In Figure I.7 a charge collection efficiency is shown as a function of total proton flux presented to the detector.

It is interesting to note the charge collection efficiency response was the same for both γ -rays and protons. The charge collection efficiency vs. total flux was observed to fit the following functional form:

$$\xi = 1 - K\phi$$

where

ξ is the pulse height normalized to its prebombarded value

ϕ is the integrated proton flux in protons/cm²

$$K = 3.2 \times 10^{-12} \pm 0.8 \times 10^{-12} \text{ cm}^2/\text{proton}$$

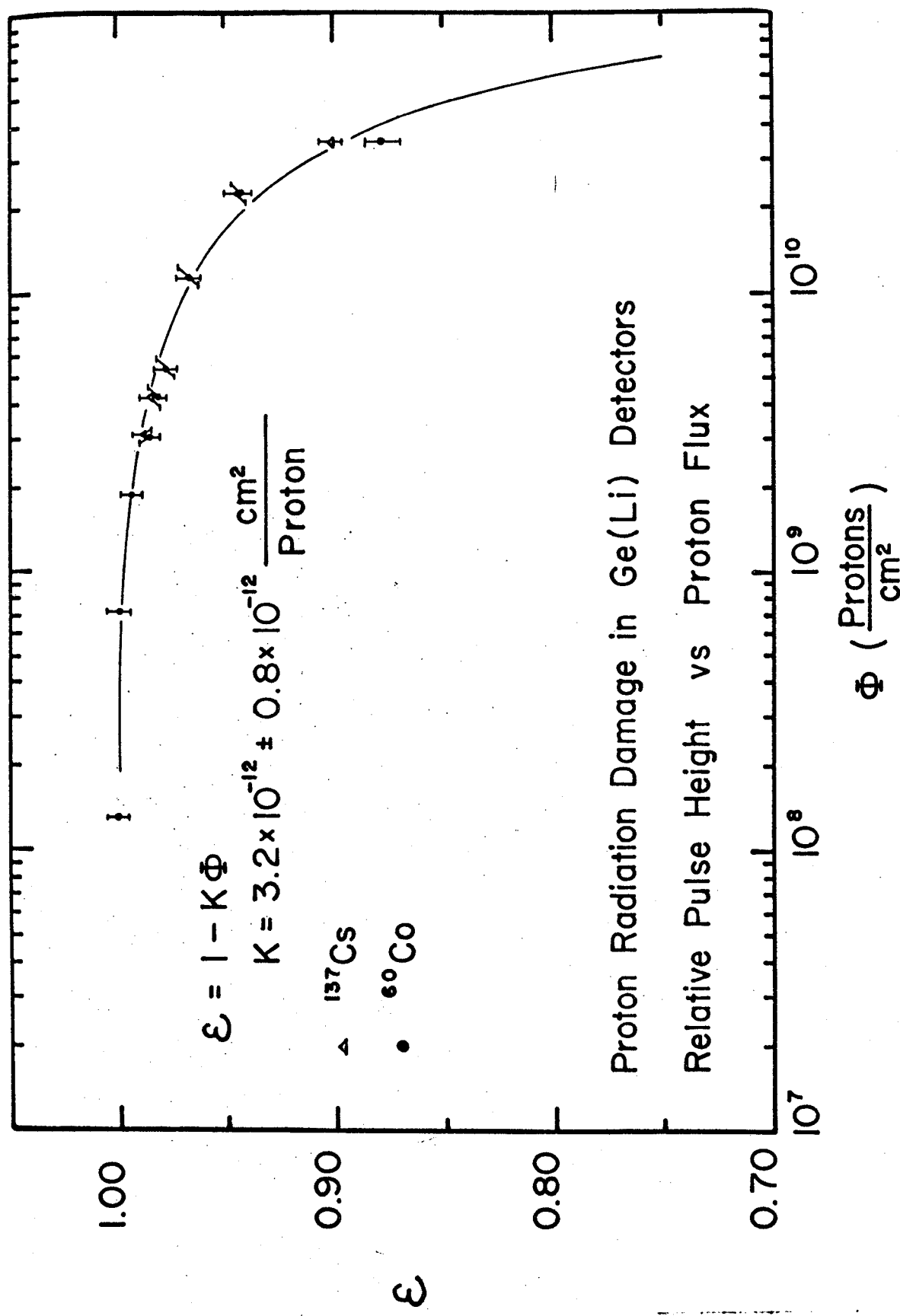


Figure 1.7 Proton radiation damage.

The previous functional form can be understood using the Hall (Ha 52) and Shockley-Read (Sh 52) single-level recombination theory. Their theory predicts the changes in free carrier lifetime, $(1/\tau - 1/\tau_0)$, is a linear function of the number of defects introduced, the capture-cross-section of the defect for minority holes or electrons, the position of the Fermi level and the position of the recombination level in the forbidden gap.

The charge collection efficiency, ξ , is related to the free carrier lifetime.

$$\xi \approx 1 - t/2 (1/\tau - 1/\tau_0)$$

and

$$(1/\tau - 1/\tau_0) \approx (2K/t)\phi$$

where

t is the charge collection time

τ_0 is the carrier lifetime before bombardment

τ is the carrier lifetime after bombardment

of Φ protons/cm².

6. Other Ge(Li) Detectors

The use of lithium drifted germanium is not restricted to making detectors of the thin window surface barrier geometry. The side entry geometry offers the possibilities of detecting higher energy particles (Gr 67) and making special purpose counters with structured electrodes to measure the density of ionization along the path of the particle (Gr 68b). The chief disadvantage of the side entry geometry is the nonuniform window on the side through which the particles pass. The

best resolution measured for this geometry is 60 keV (FWHM) for 40 MeV protons scattered from Au. A contribution of about 40 keV is attributed to this nonuniform window. The relative importance of this non-uniform window decreases as the range of the particle being detected increases.

We have also explored the feasibility of using a small side entry Ge(Li) detector in a thin-windowed mount to measure γ -ray and electron intensities simultaneously and consequently serve as a single crystal conversion-coefficient spectrometer (Gr 69a). There are several advantages to such a system, principally in the fact that it uses fewer electronics and only one analyzer, the Ge(Li)-Si(Li) system usually used can use one analyzer by measuring γ -rays and electrons sequentially, but then live-time and half-life corrections become more cumbersome. Also, a single efficiency curve can be made for the single-crystal Ge(Li) spectrometer, one that contains information about both γ -ray and electron intensities. (This is possible because the electron efficiency curve is a slowly varying function of energy.) Finally, the single-crystal spectrometer is potentially a powerful tool for coincidence experiments involving another detector because it would often mean the difference between a double and triple coincidence or, again, sequential experiments. For short-lived, difficult-to-make nuclides, this can be important. Disadvantages of such a device are source strength, i.e., the detectors are necessarily small, so strong sources are required, and the straggling experienced by the electrons in passing through the

window, which must be accounted for in stripping out the data and which affects the background of the spectra as a whole. In particular, the straggling makes it very difficult to separate the L and N electron peaks because of their small energy difference and large overlap. There also appears to be no single optimum size of detector to cover all energy regions, so one would be compelled to have an assortment of sizes.

The efficiency curve for such a detector is shown in Figure I.8. It takes the form of the relative efficiencies for γ -rays and electrons, i.e.,

$$C = \frac{D(\gamma)}{D(e^-)}$$

vs. the γ -ray energy, E_γ . [For purposes of illustration, the data has been compressed onto a single graph. In actual practice, one has to account for the differences in binding energy for different elements.] To obtain the conversion coefficient of a transition, one merely obtains an experimental intensity ratio for the γ -rays and electrons and multiplies this by the corresponding ordinate from Figure I.8 i.e.,

$$a = C \frac{A_{e^-}}{A_\gamma}$$

Because the efficiency for electrons varies very slowly, the above efficiency curve is very nearly the same as the efficiency curve for γ -rays alone. The latter curve is presented in Figure I.8 with an offset scale for comparison.

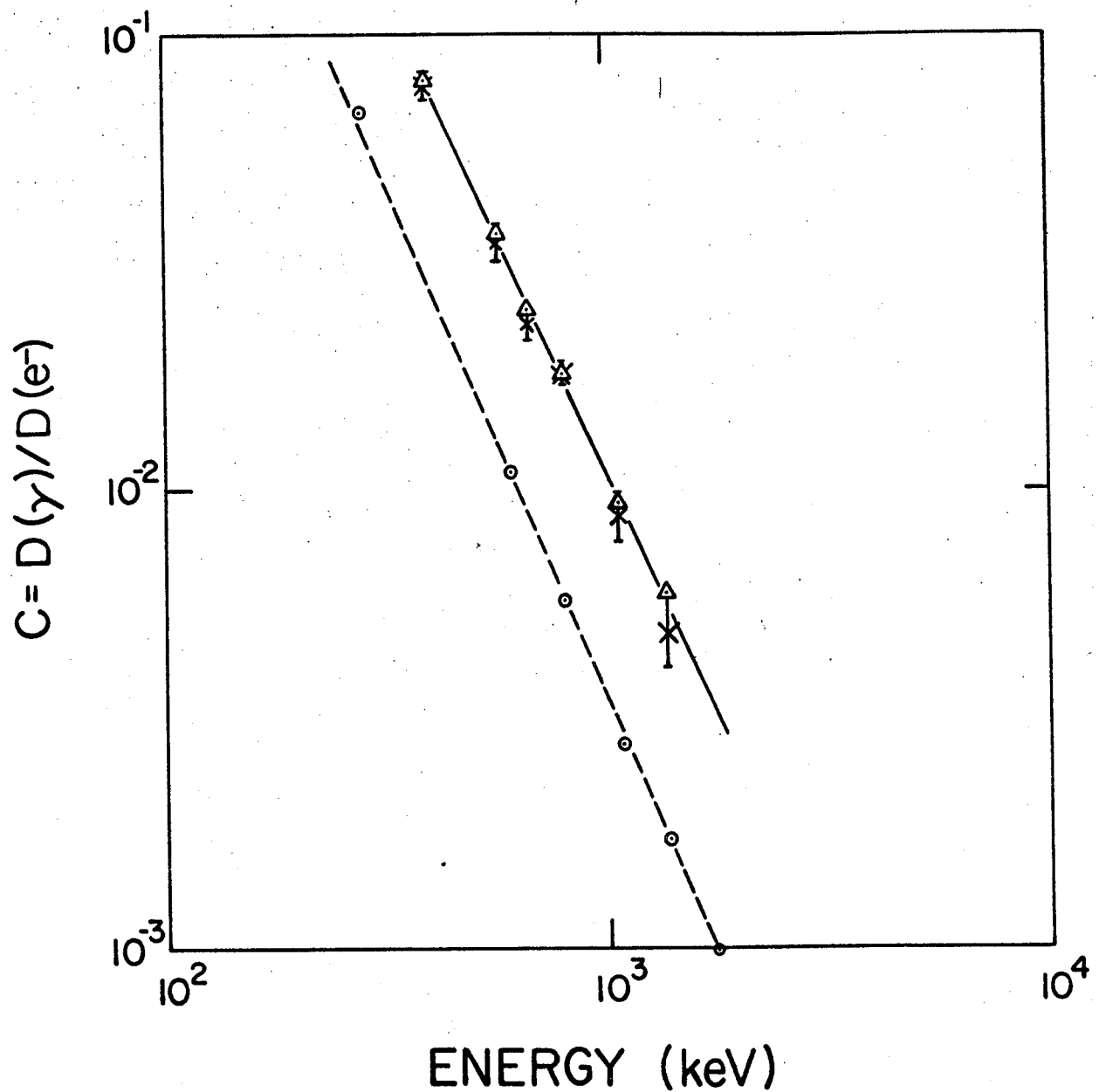


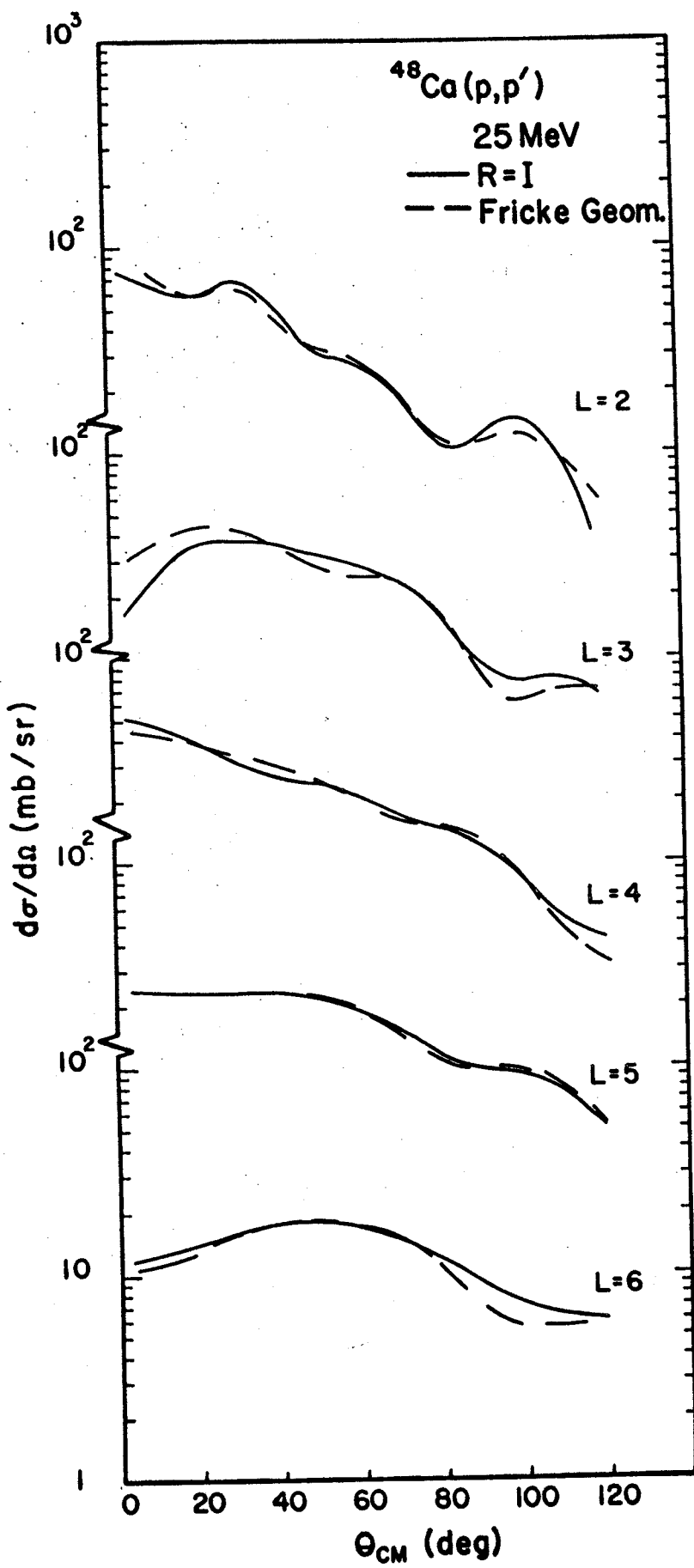
Figure I.8 Relative efficiency curve.

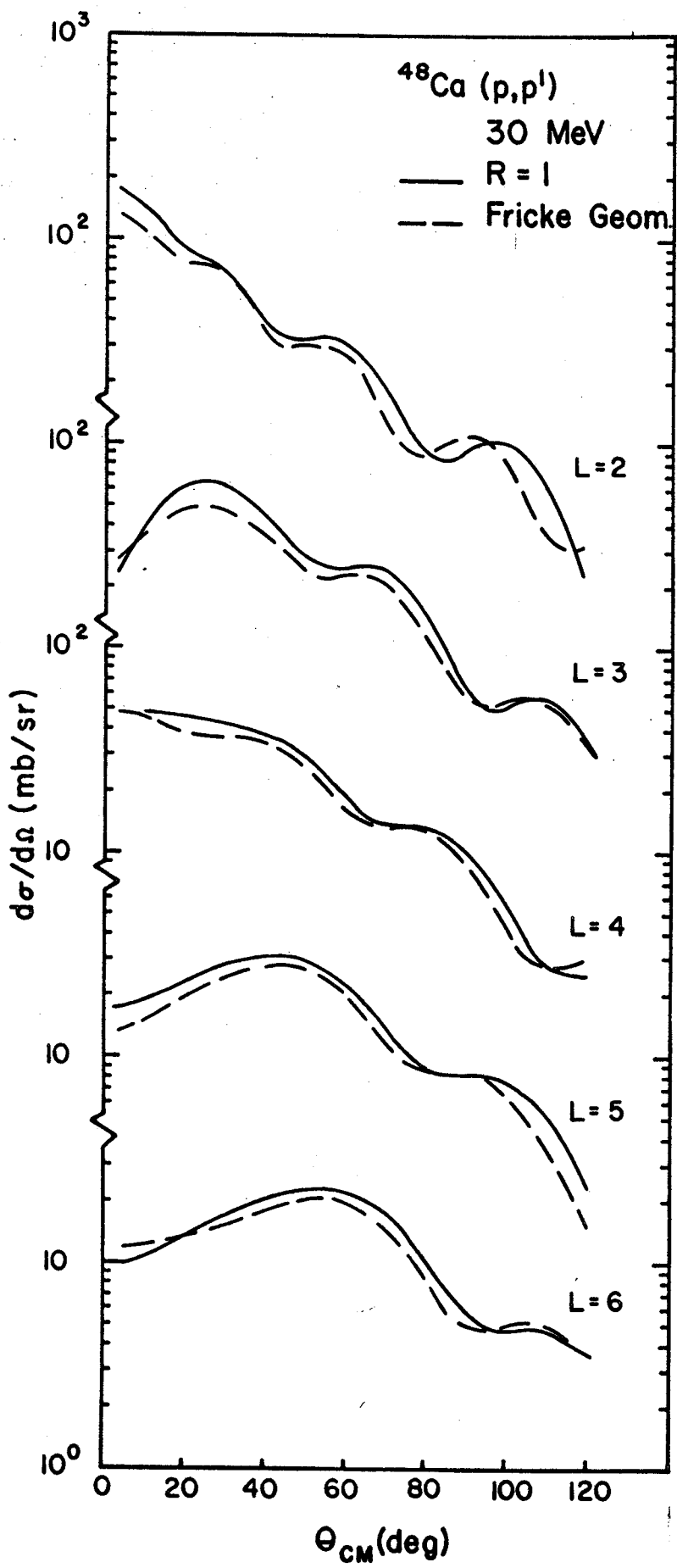
To determine conversion coefficients most precisely, the efficiencies for detecting electrons and γ -rays should be comparable, at least within several orders of magnitude. This means that a small detector is required, particularly for lower energies, where the Compton backgrounds from the γ -rays can easily obscure the electron peaks, especially when the latter have been broadened by straggling in passing through the window. At higher energies the γ -ray efficiency becomes very small and so do most conversion coefficients, so this becomes the limitation. A larger detector would be more useful for higher energies, and a smaller (thinner, to lower the γ -ray efficiency) at lower energies. In addition, the window thickness could be reduced to 0.1 mil or less, and, in fact, straggling could be essentially eliminated by using a vacuum interlock to allow one to place the source inside the can with the detector and by using a Ge(Li) detector of the surface barrier geometry.

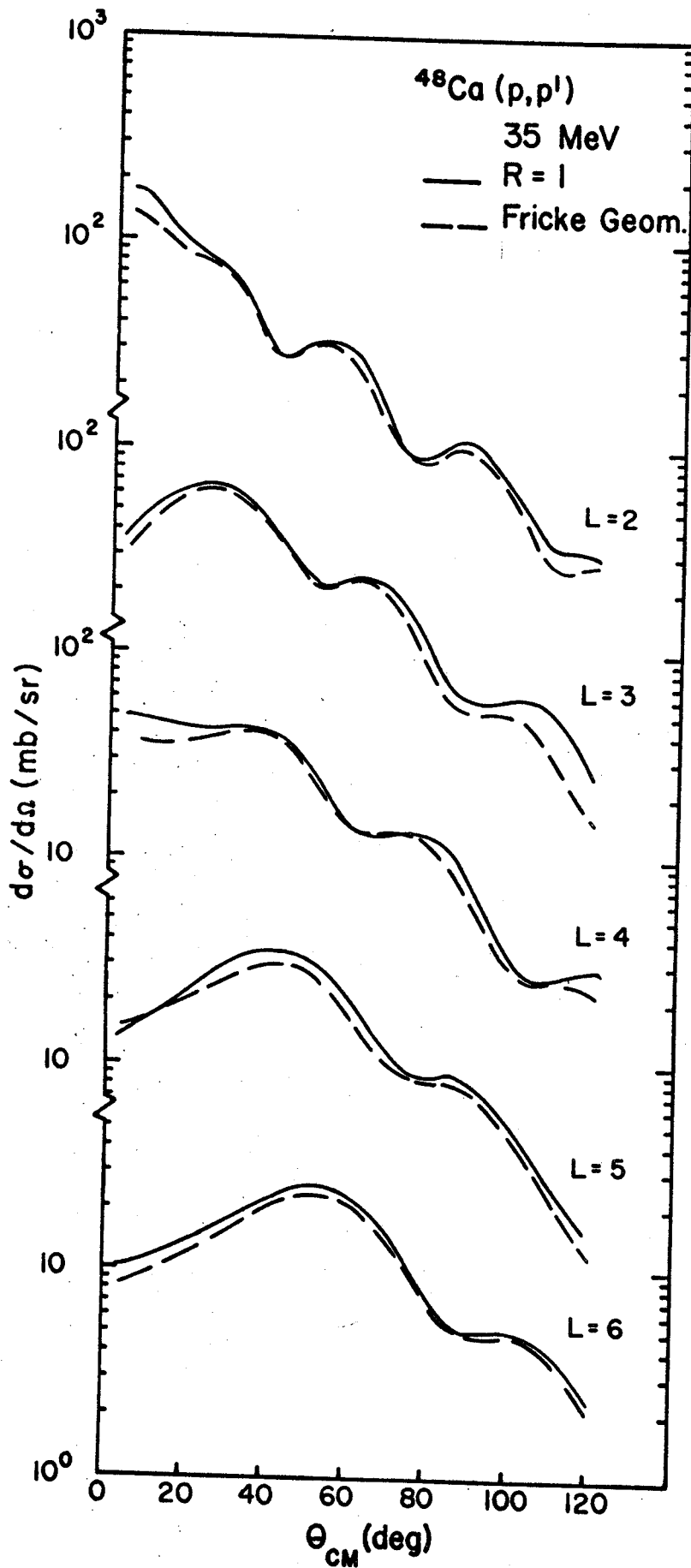
APPENDIX II

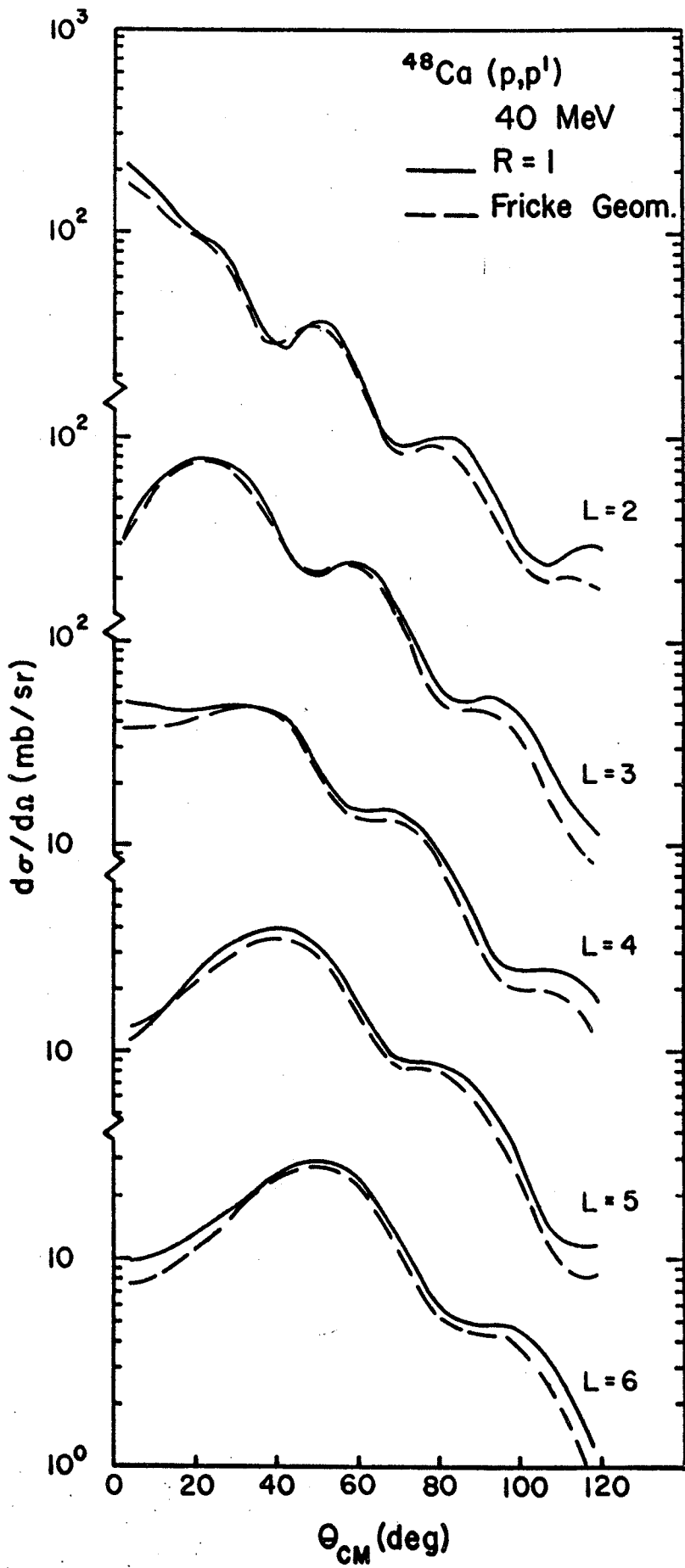
II.1 Theoretical Angular Distributions

**On the following pages are plotted the results of DWBA calculations
at each energy.**



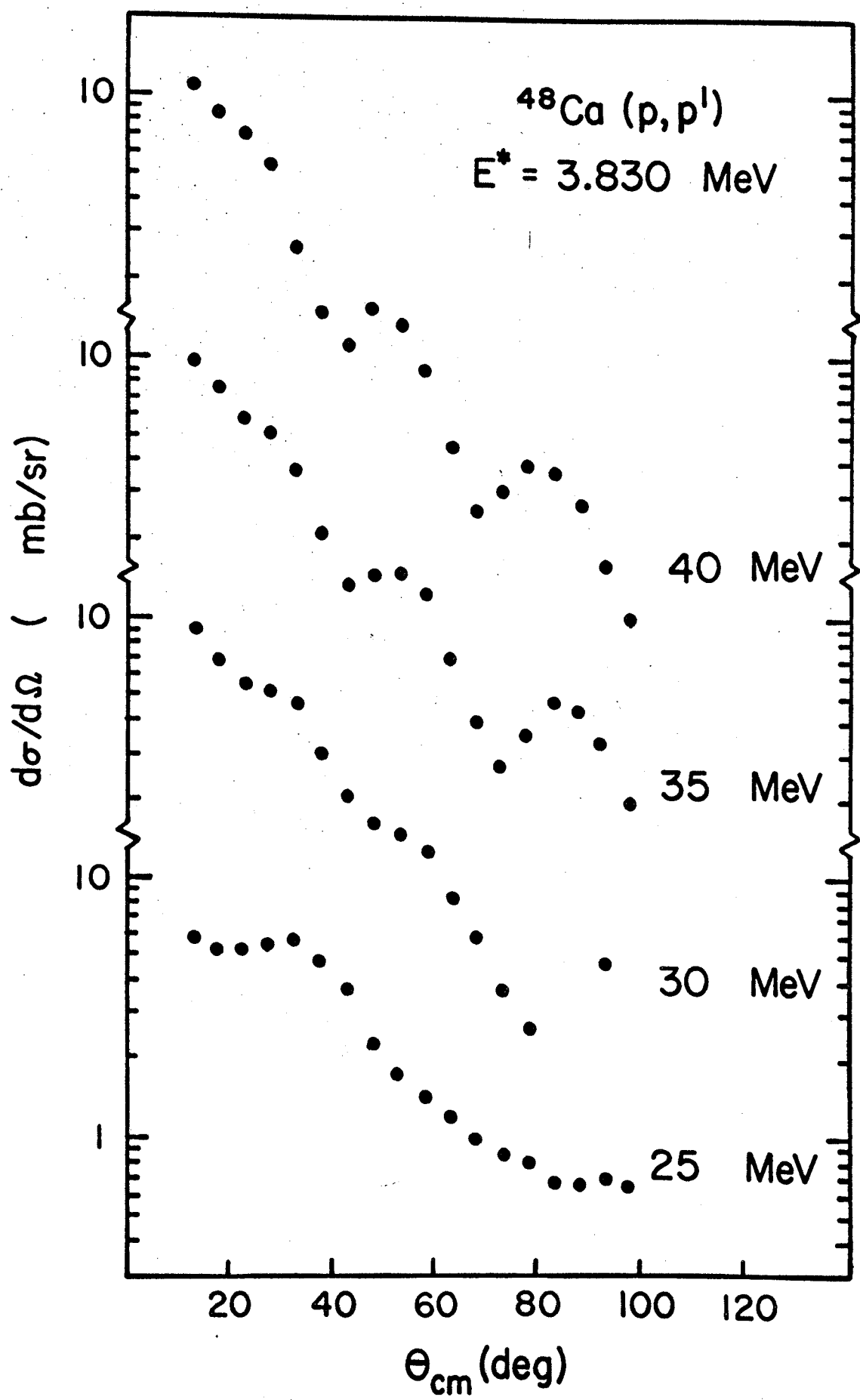


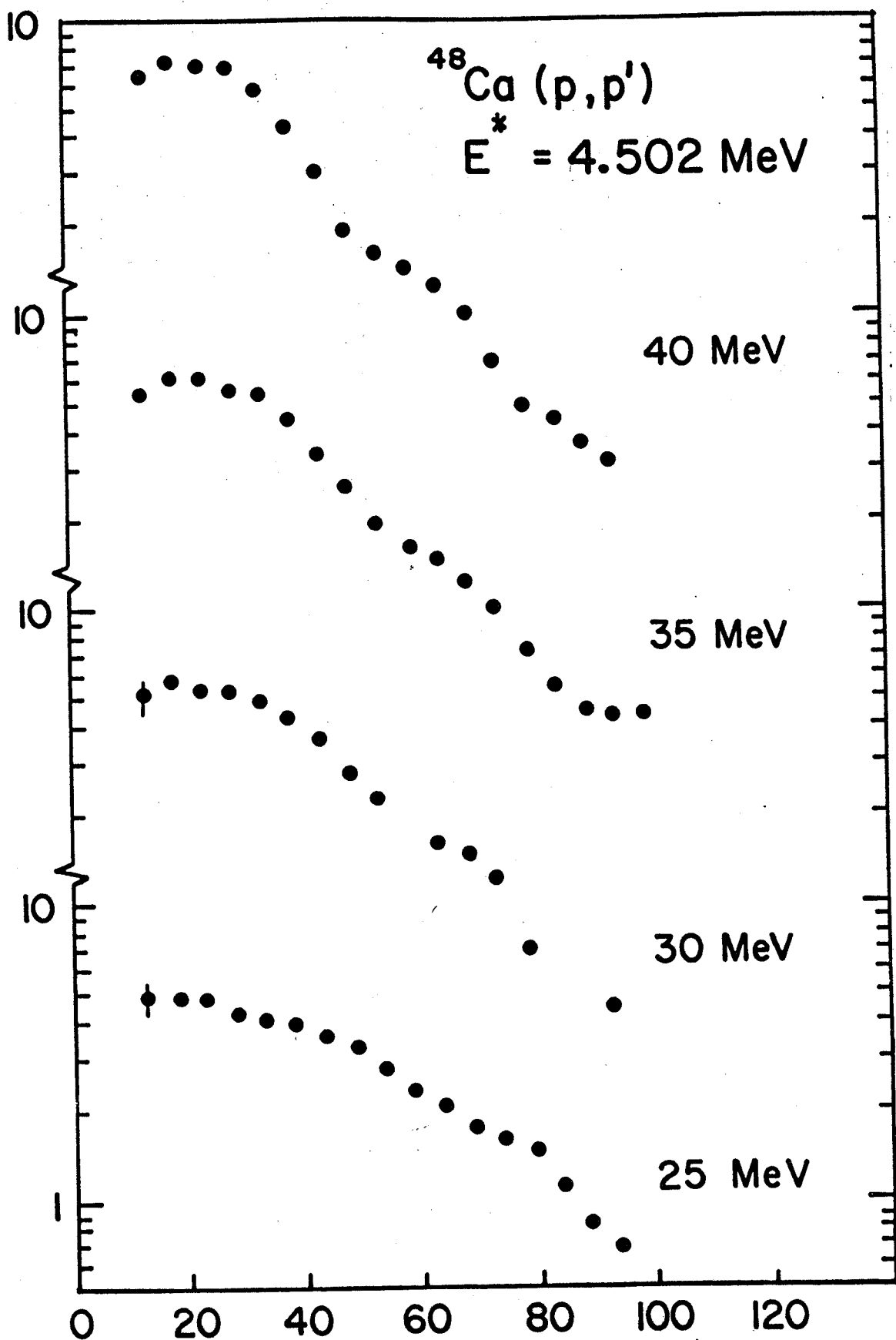




II.2 Plotted Angular Distributions

On the following pages are plotted the experimental center-of-mass angular distributions of each observed state at each of the incident beam energies.





^{48}Ca (p, p')

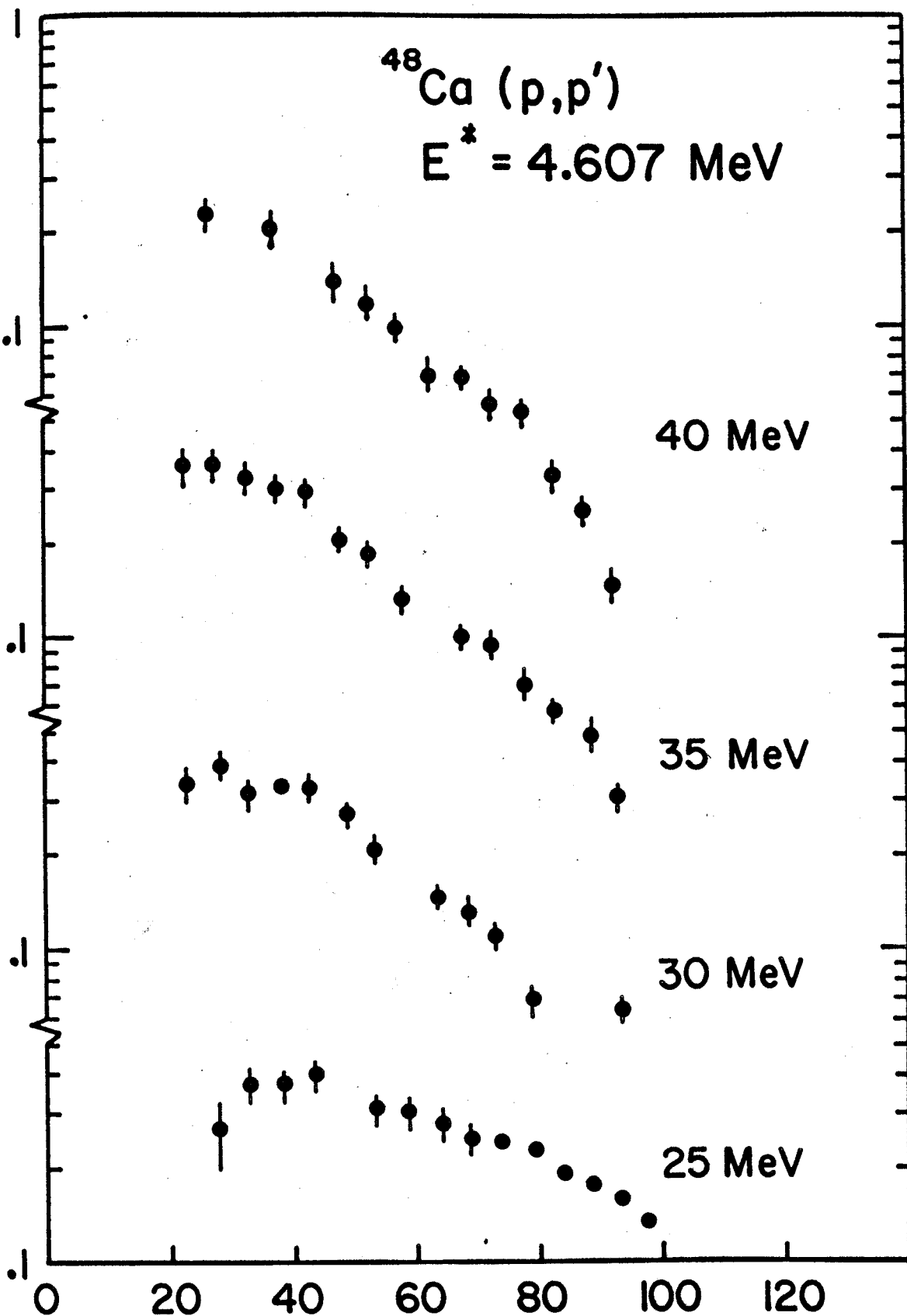
$E^* = 4.607 \text{ MeV}$

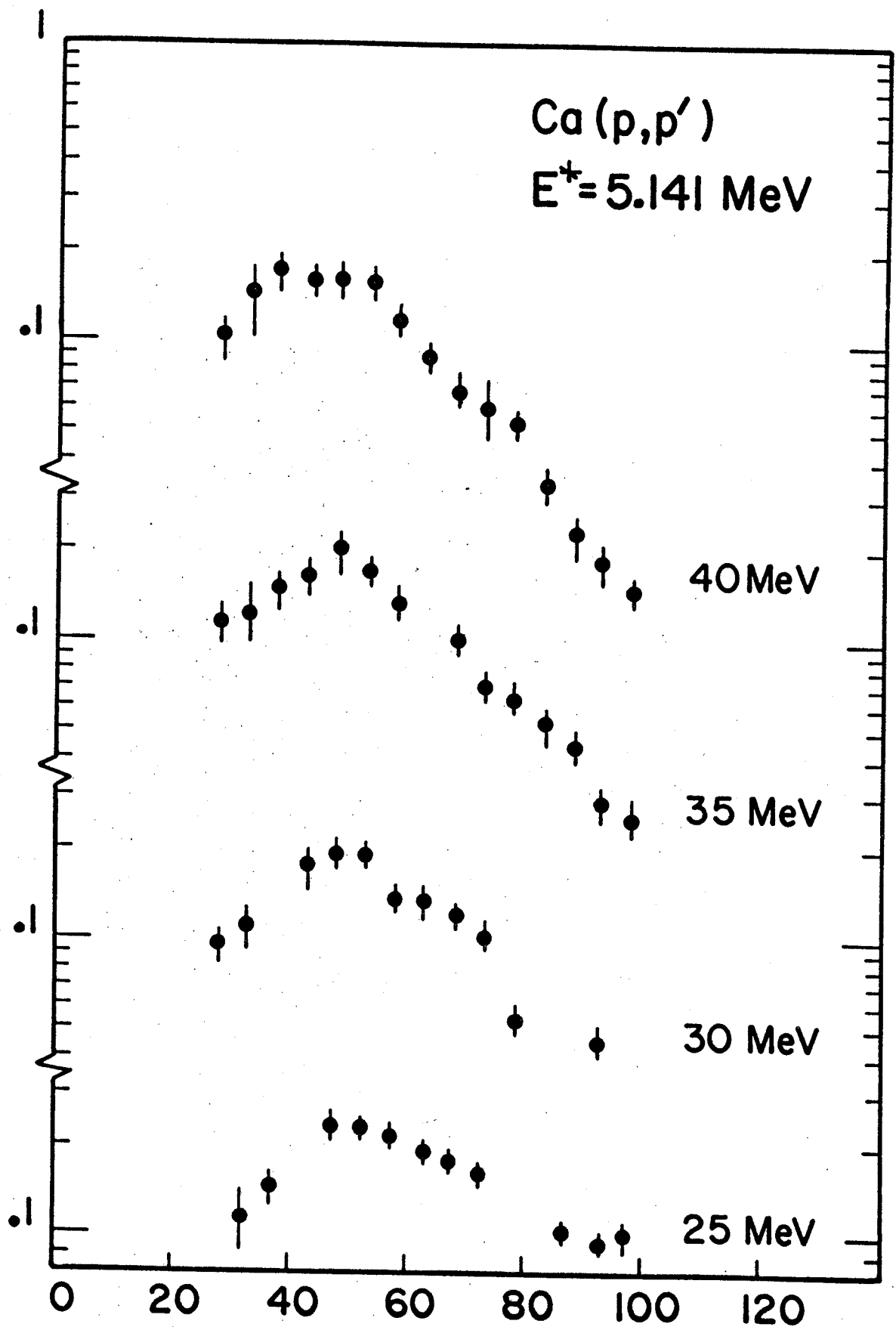
40 MeV

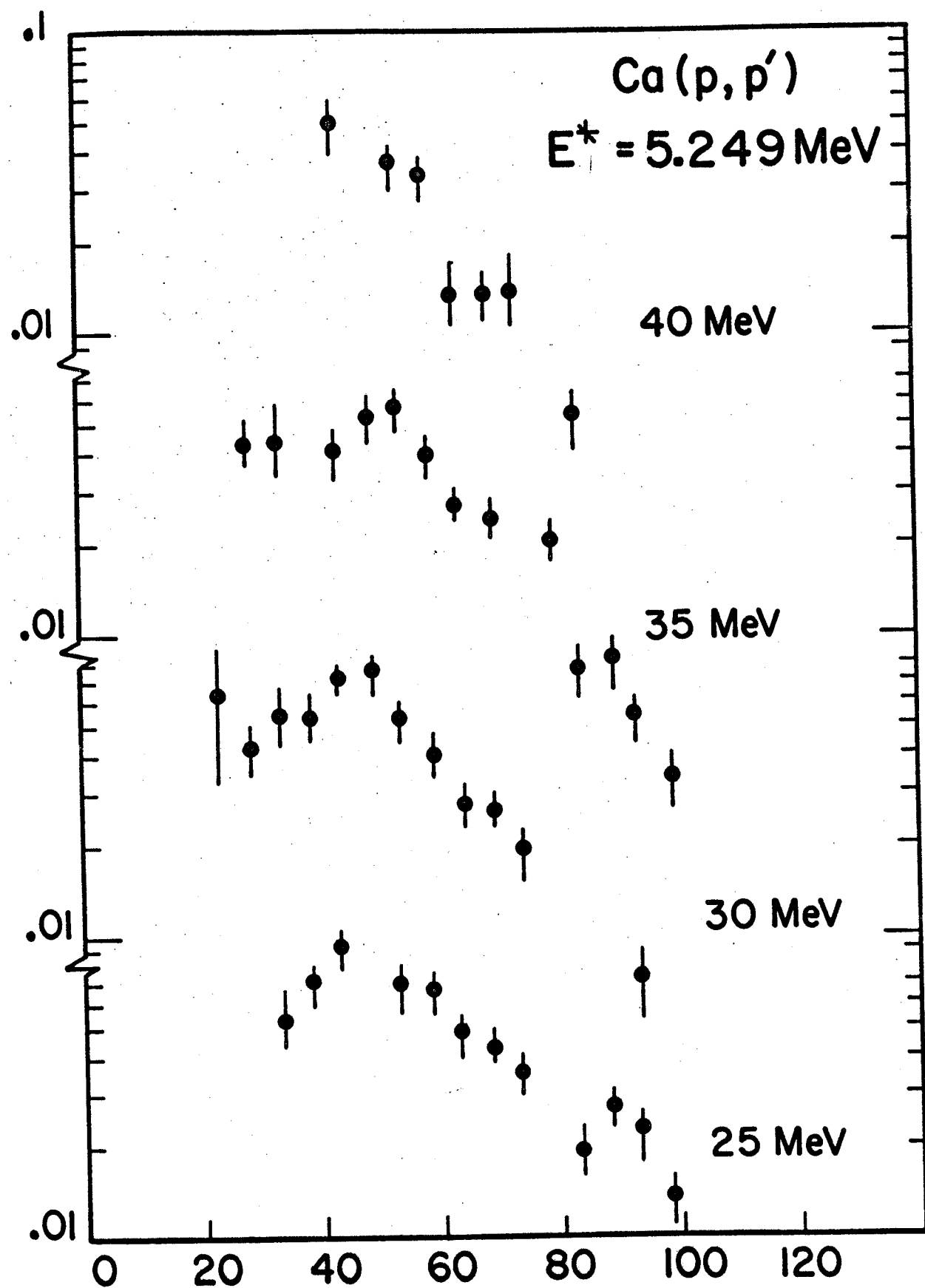
35 MeV

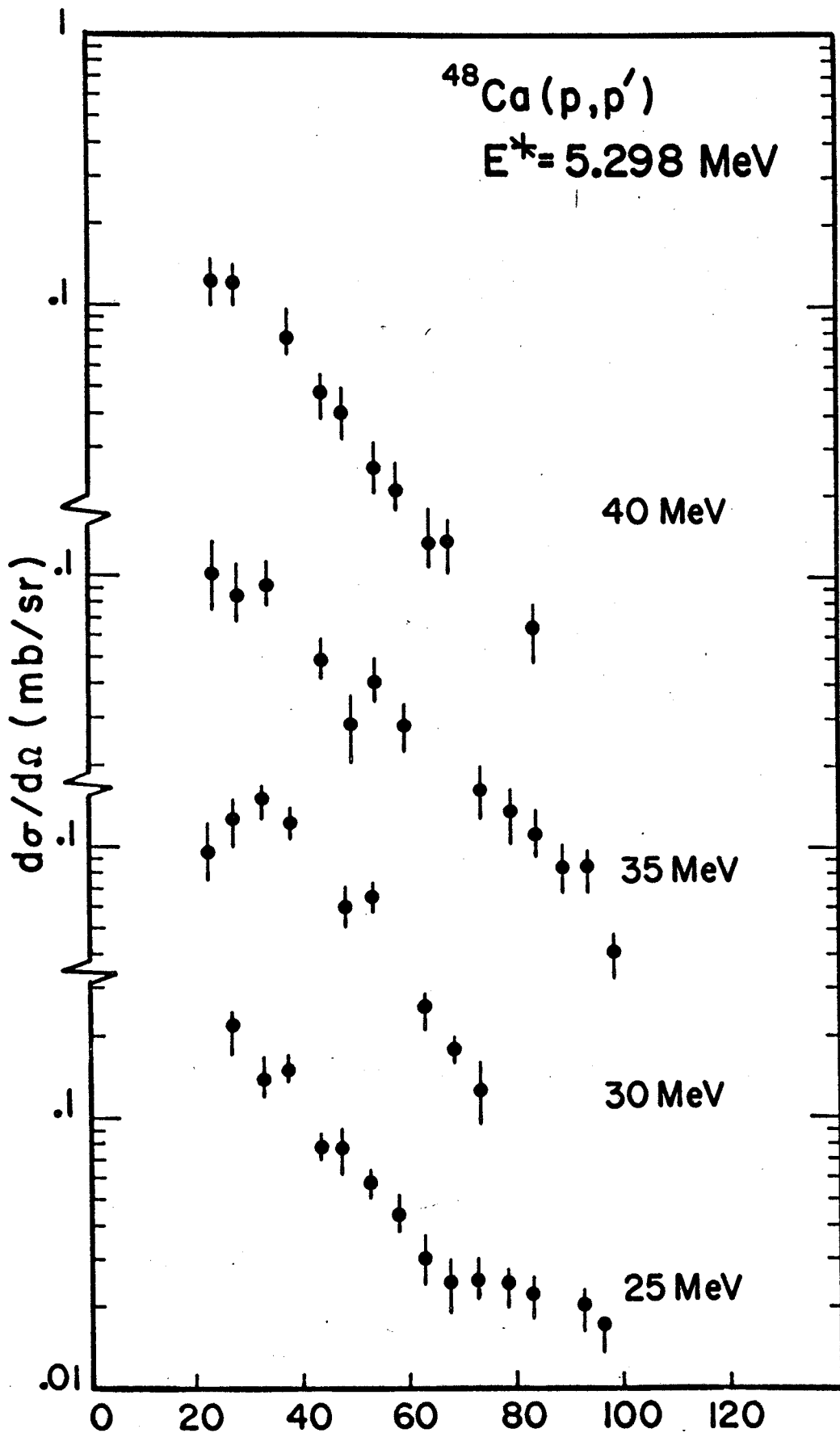
30 MeV

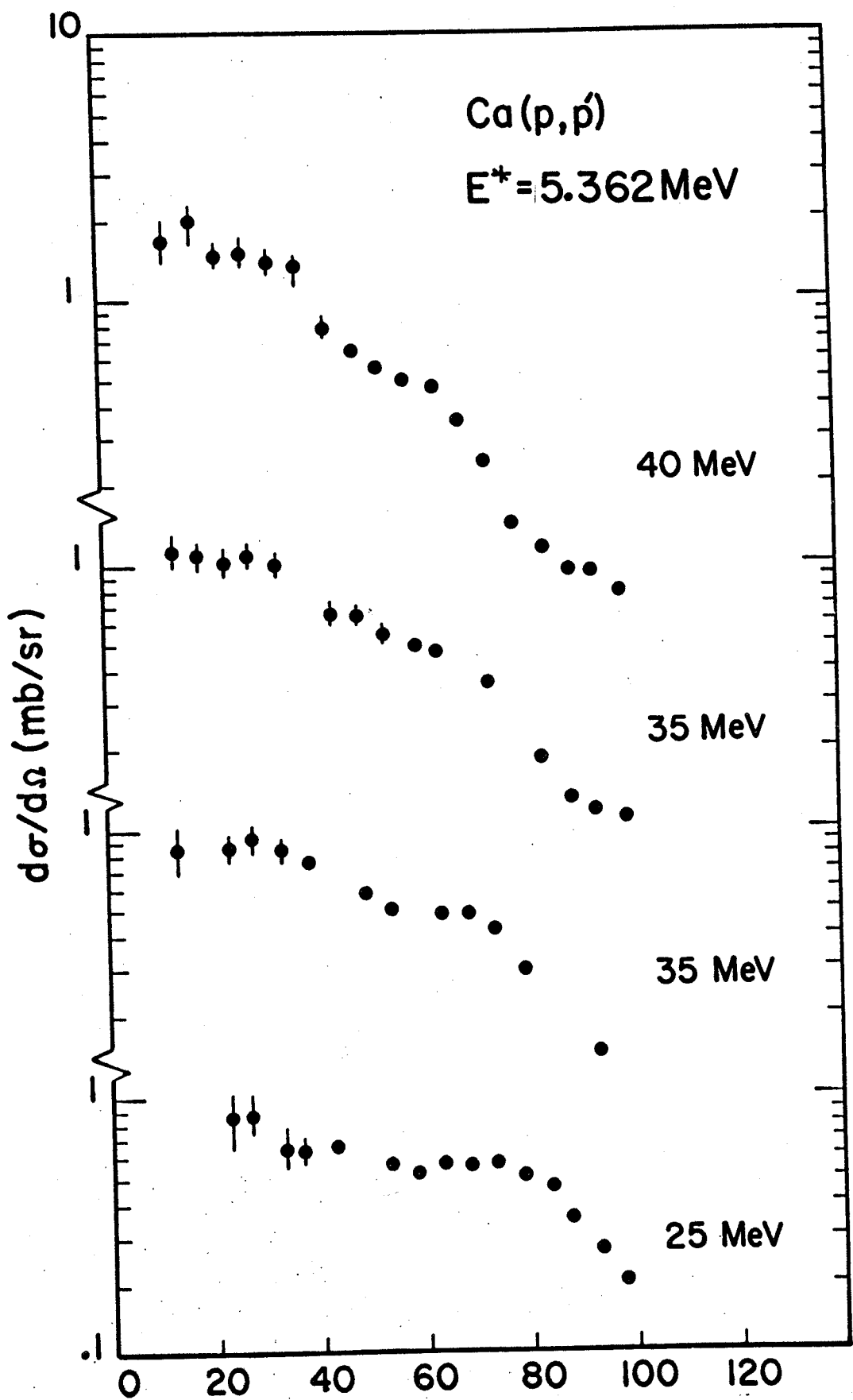
25 MeV

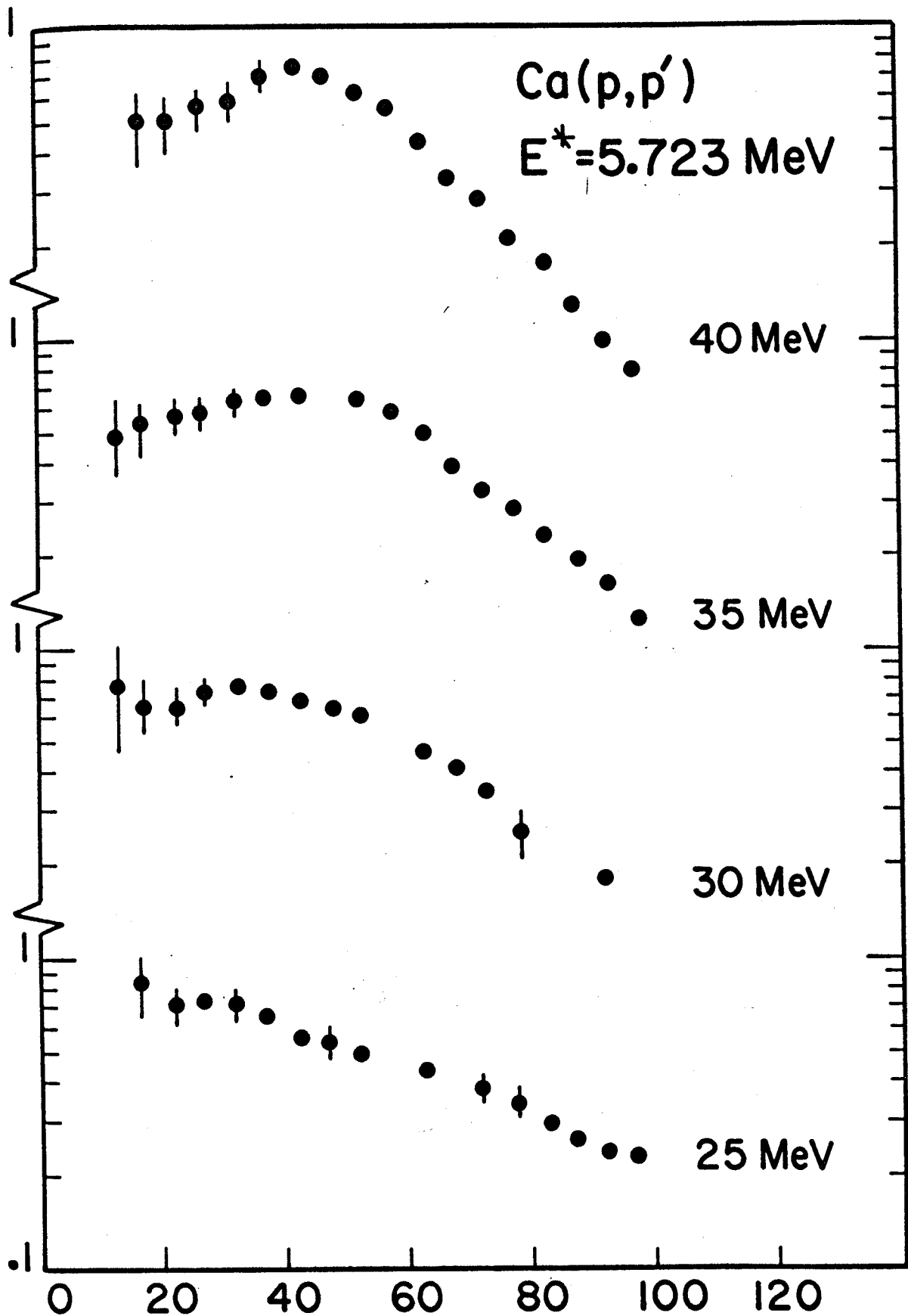


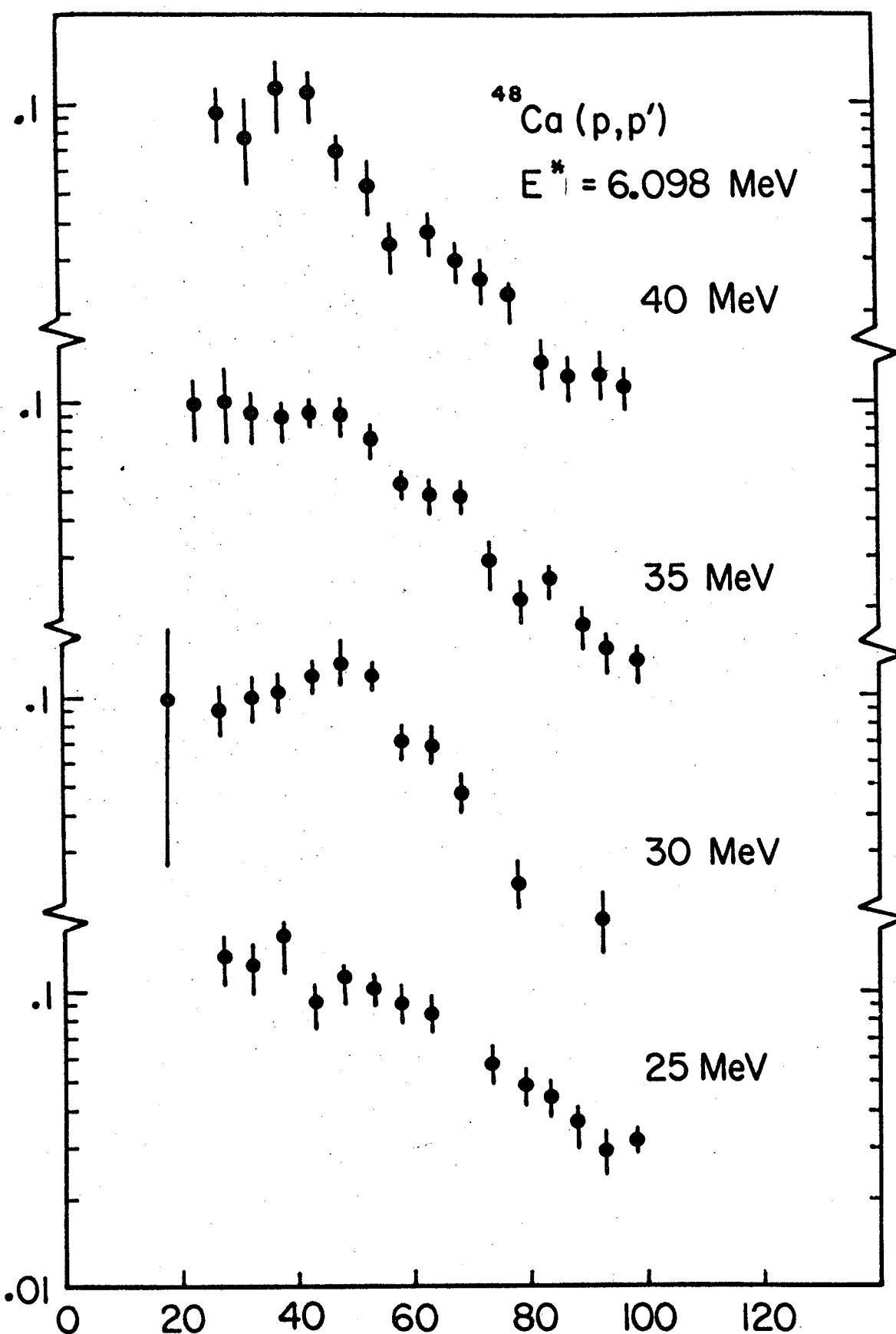


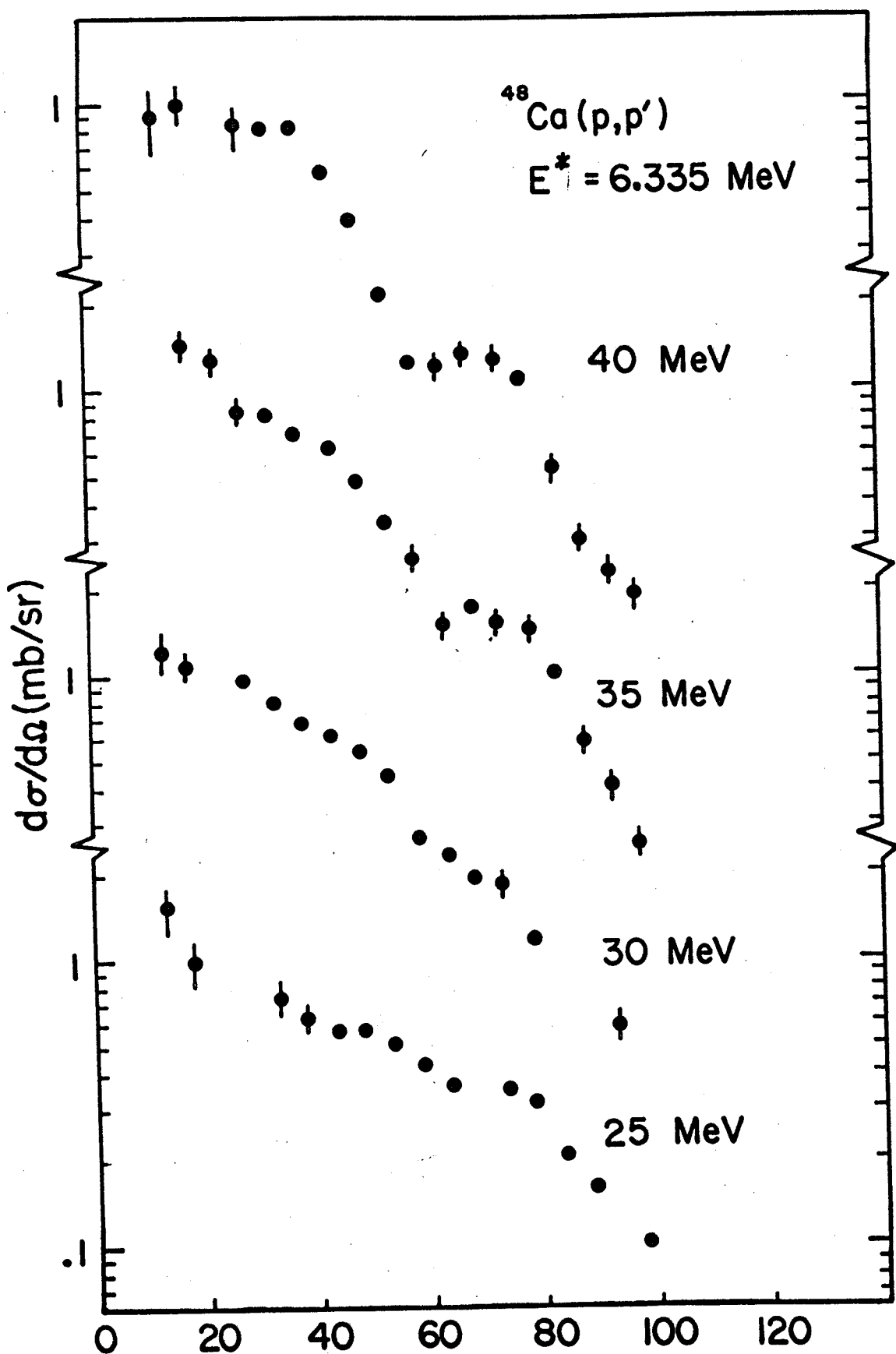


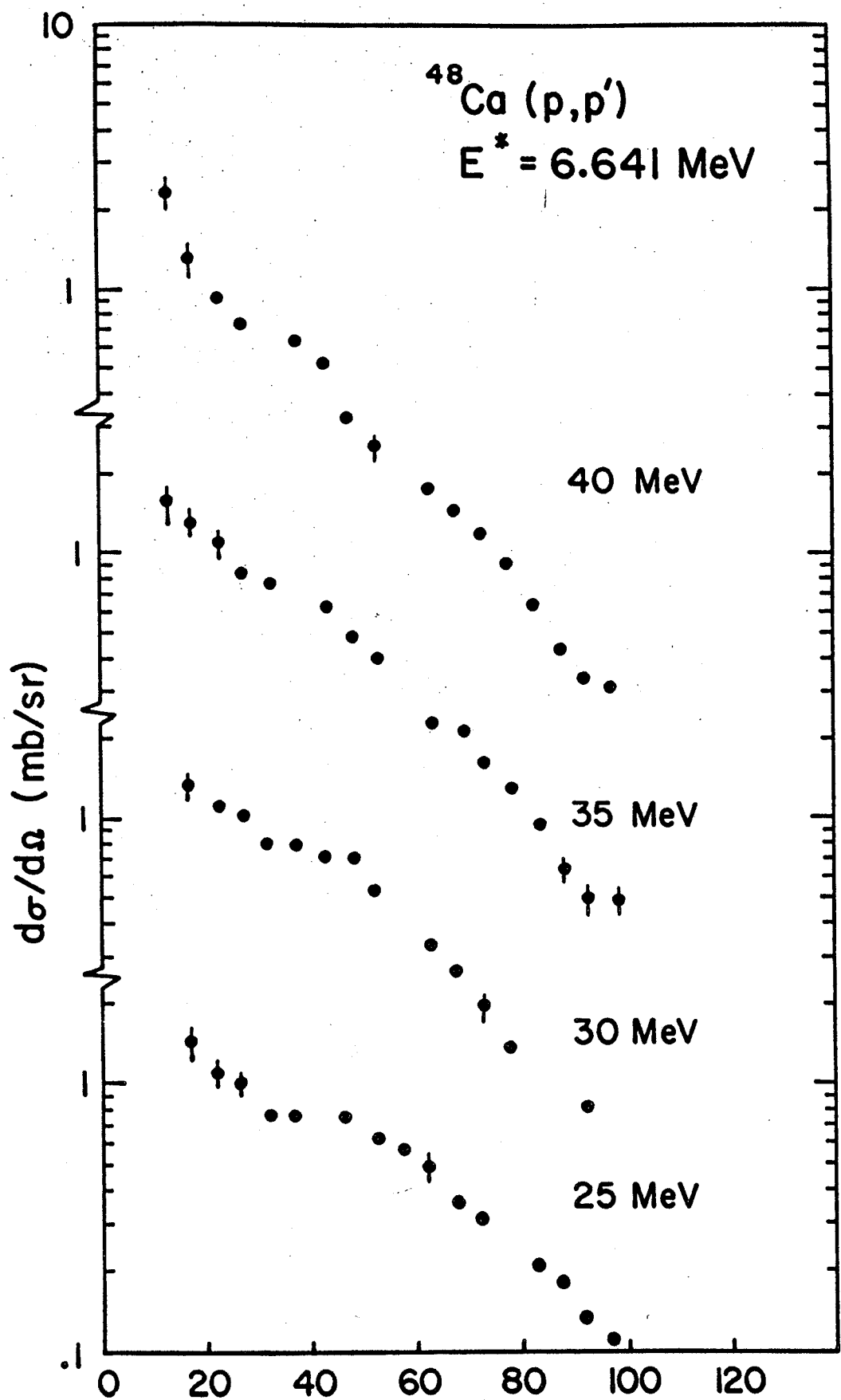


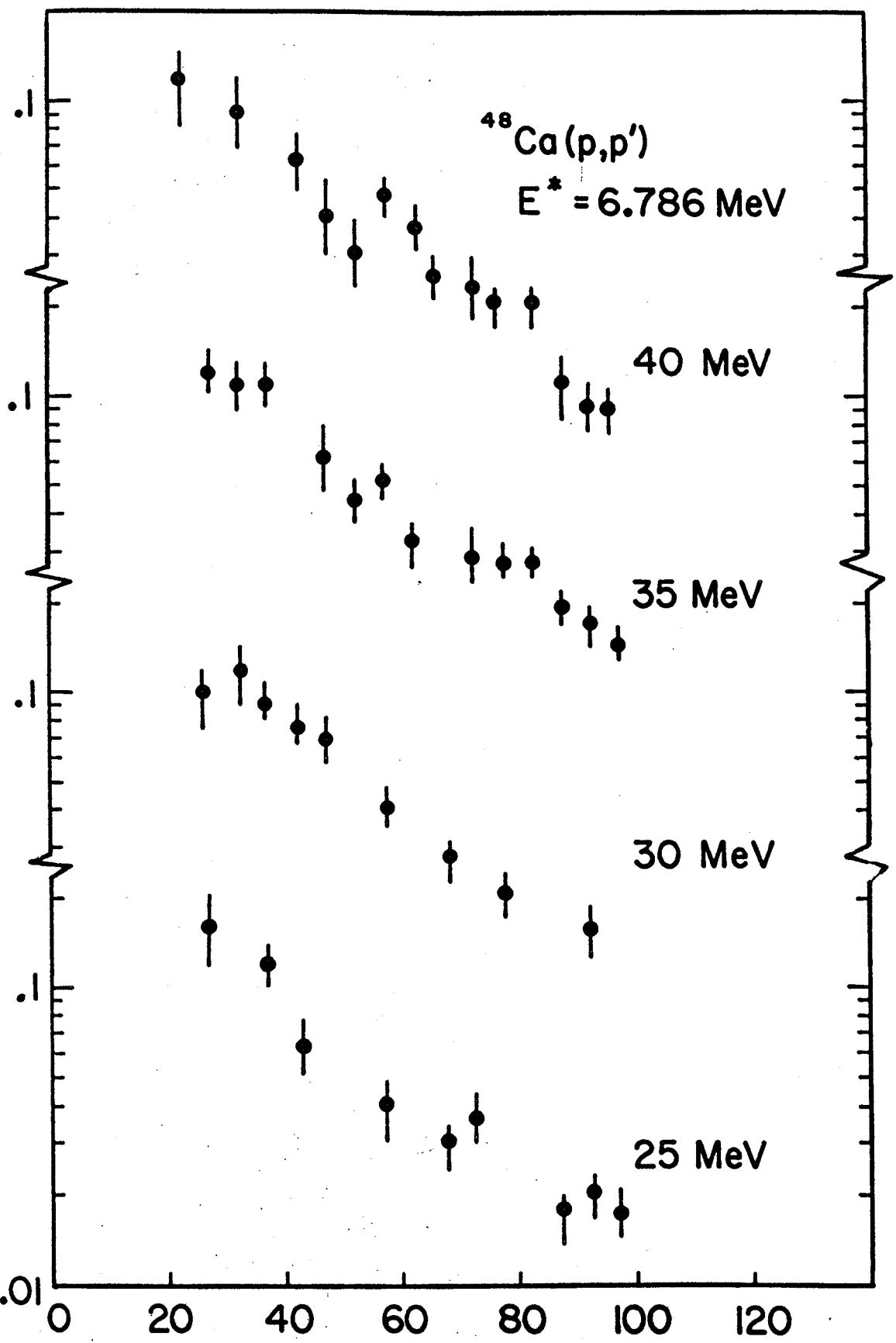


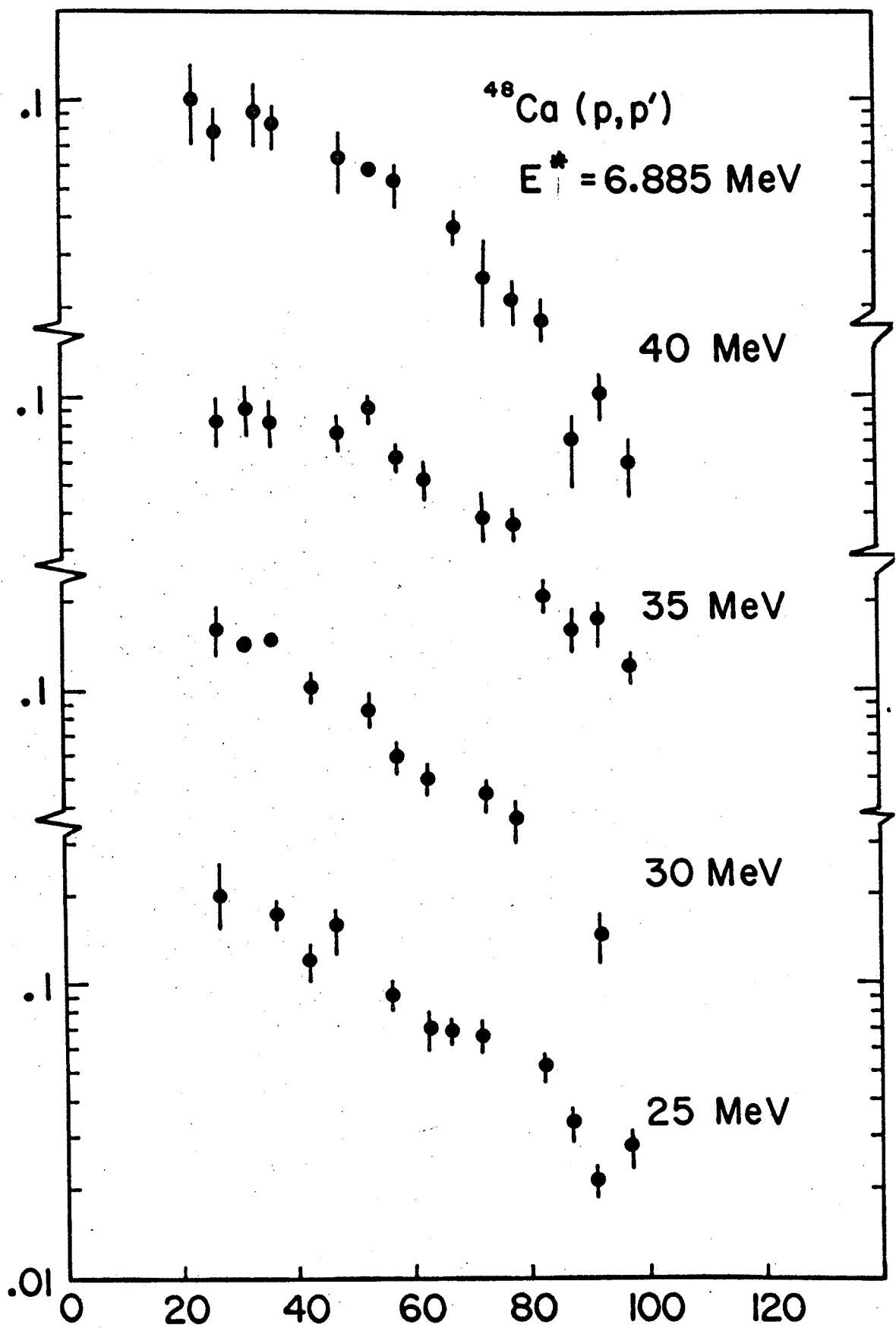


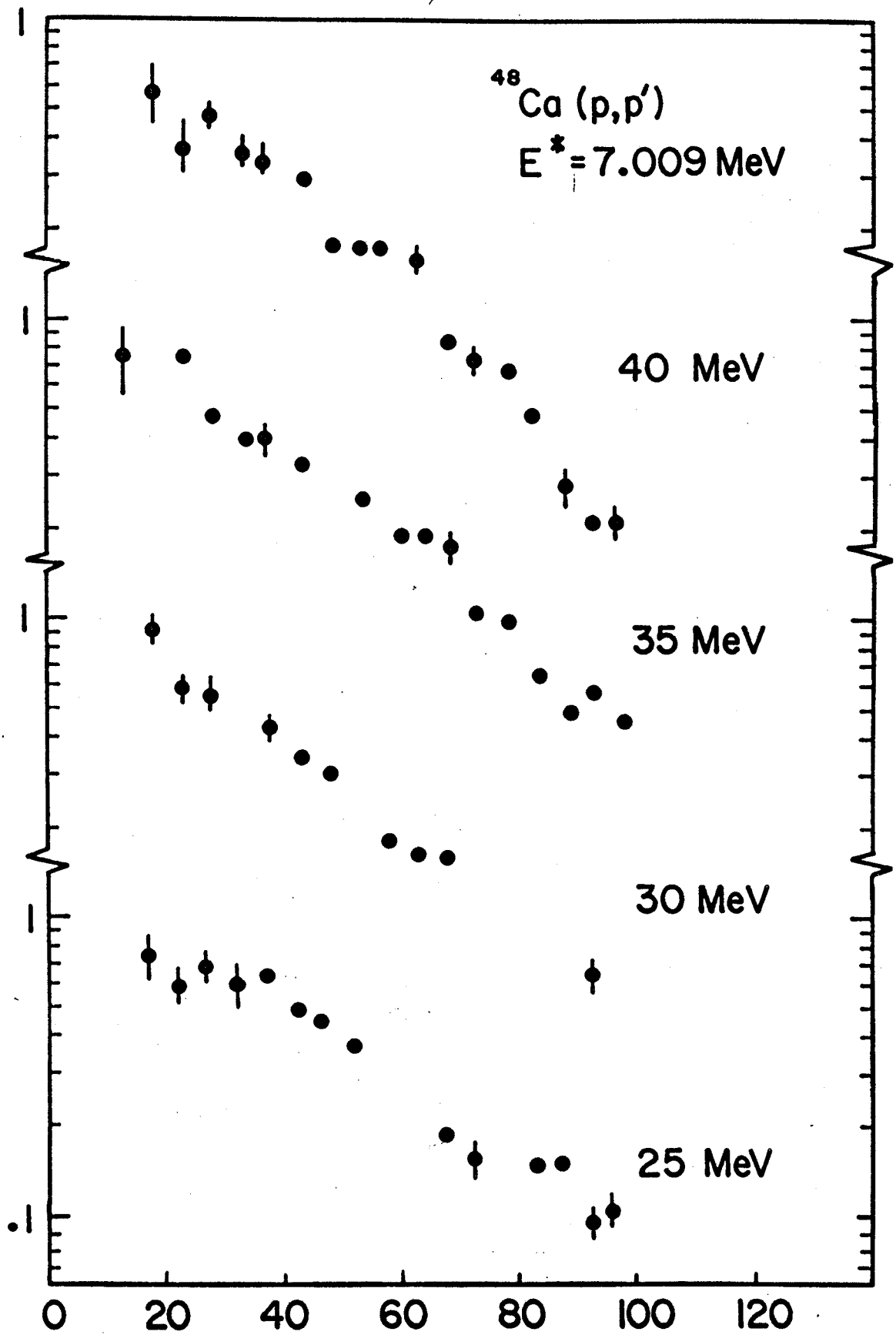


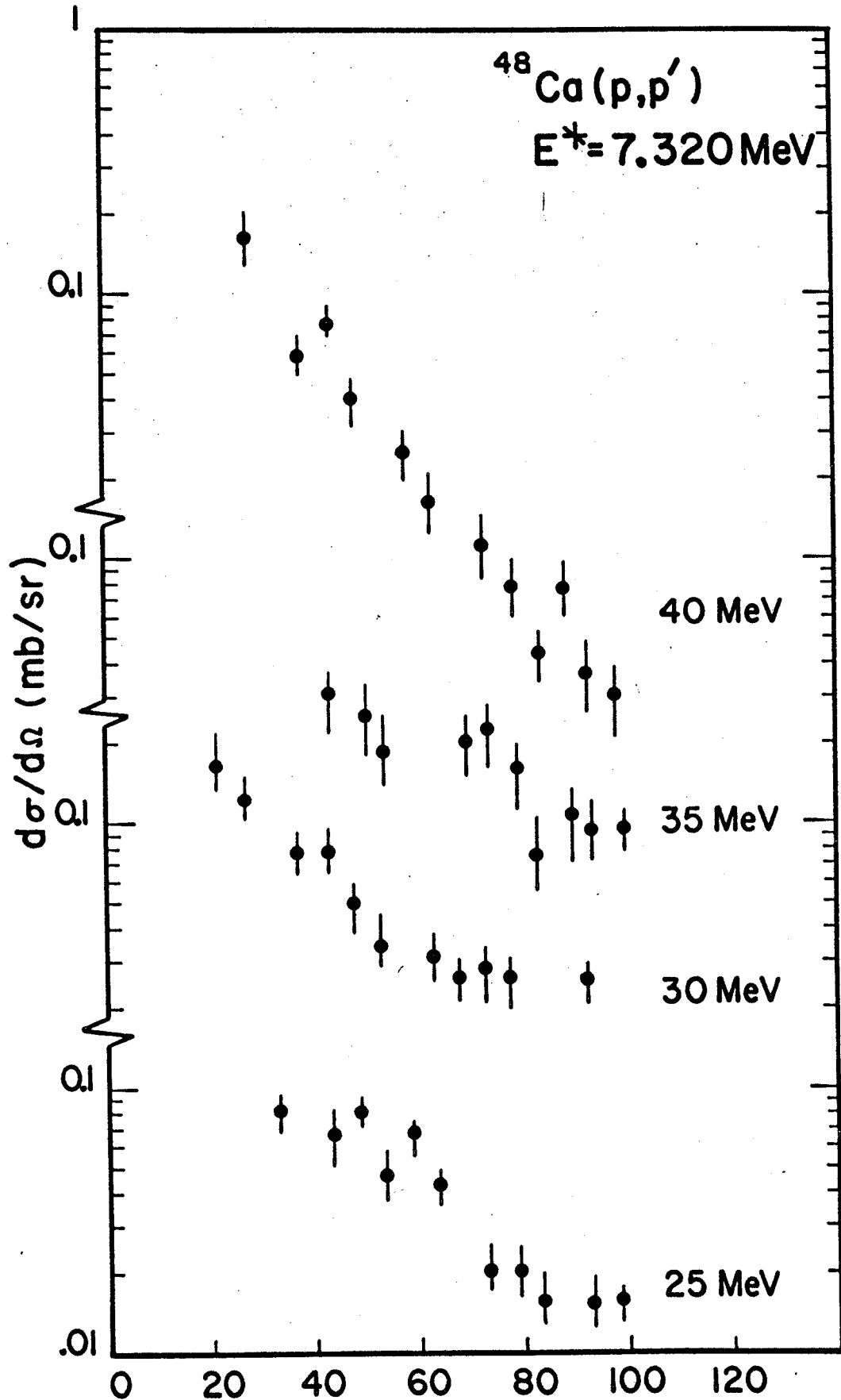


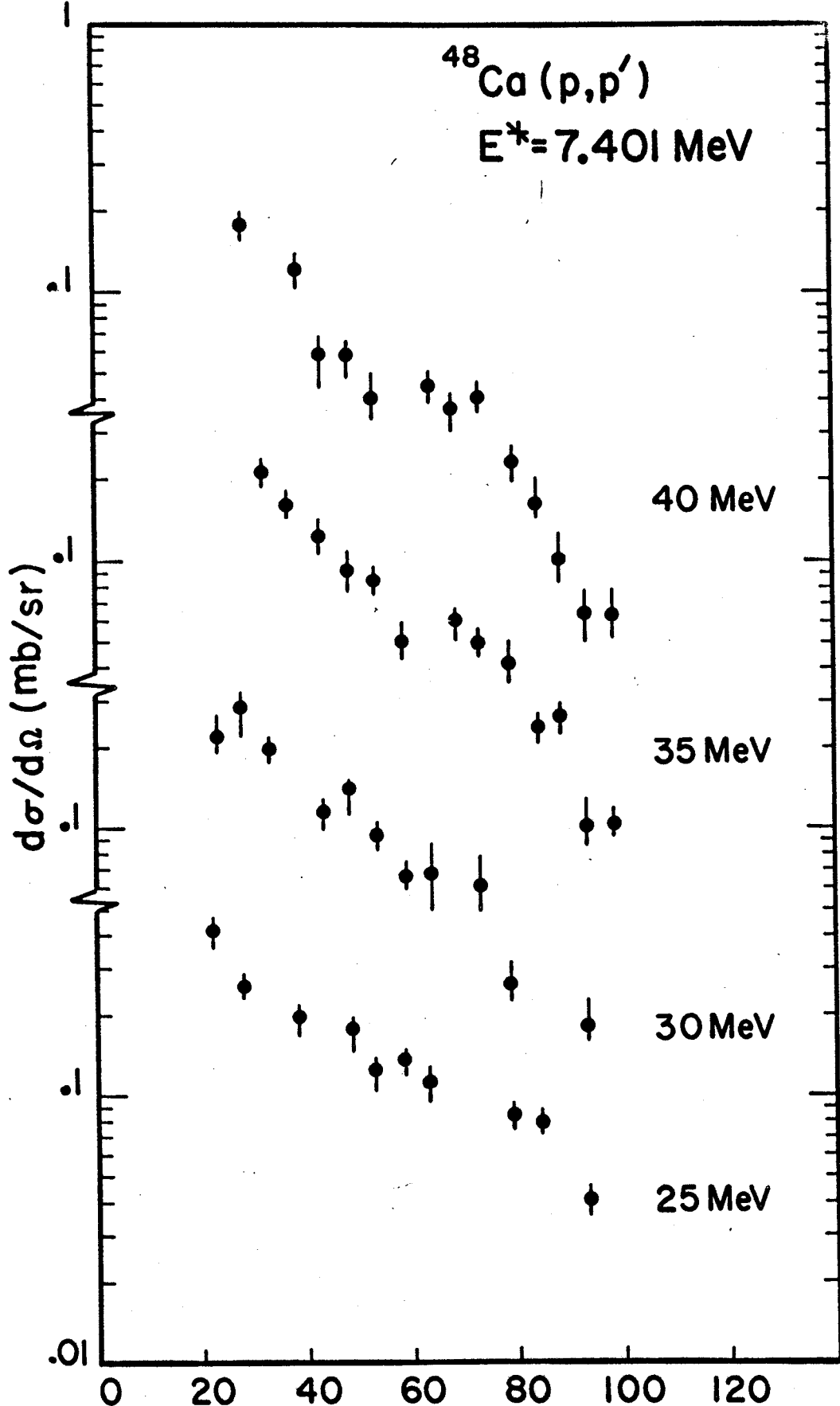


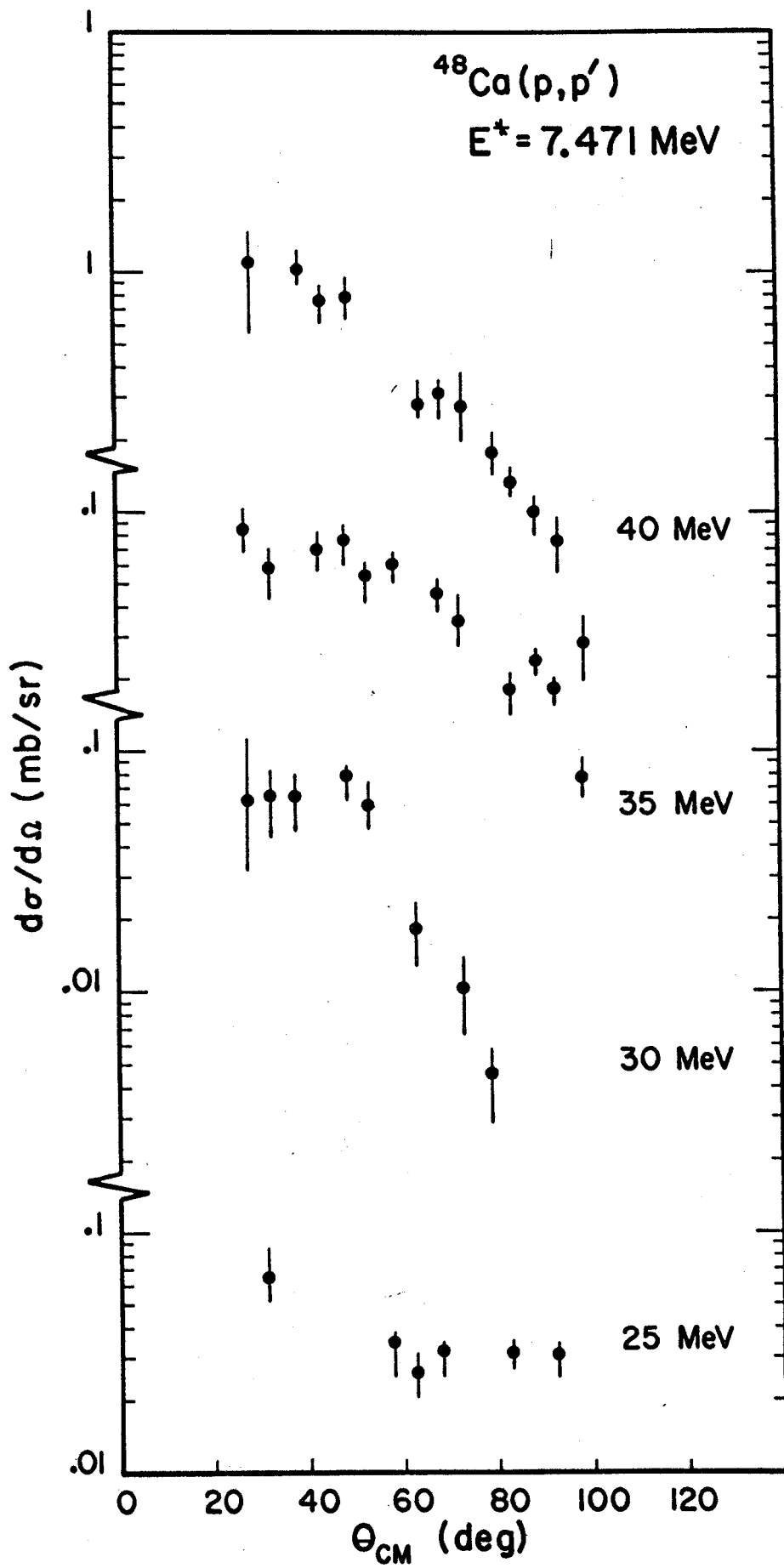


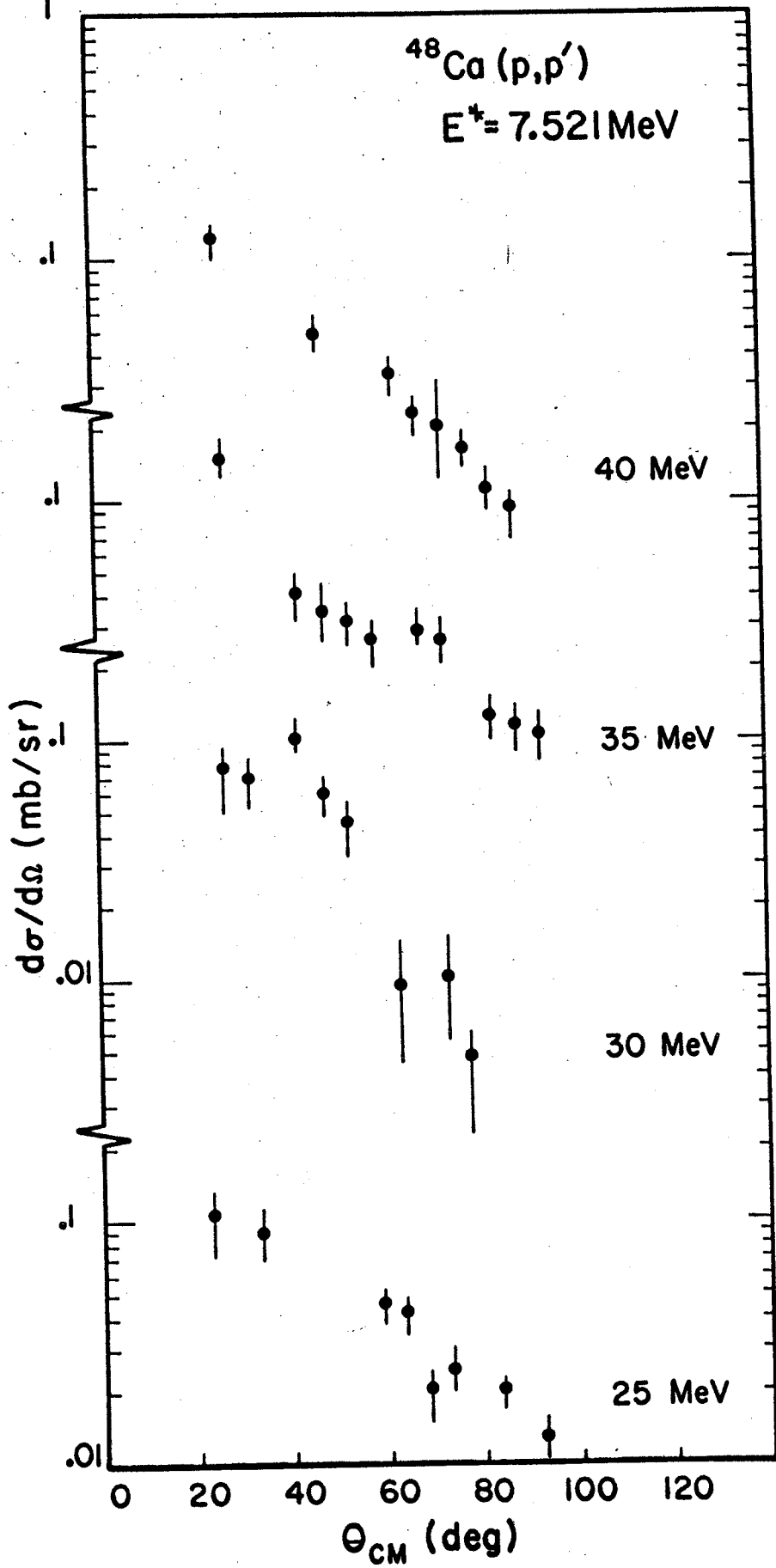


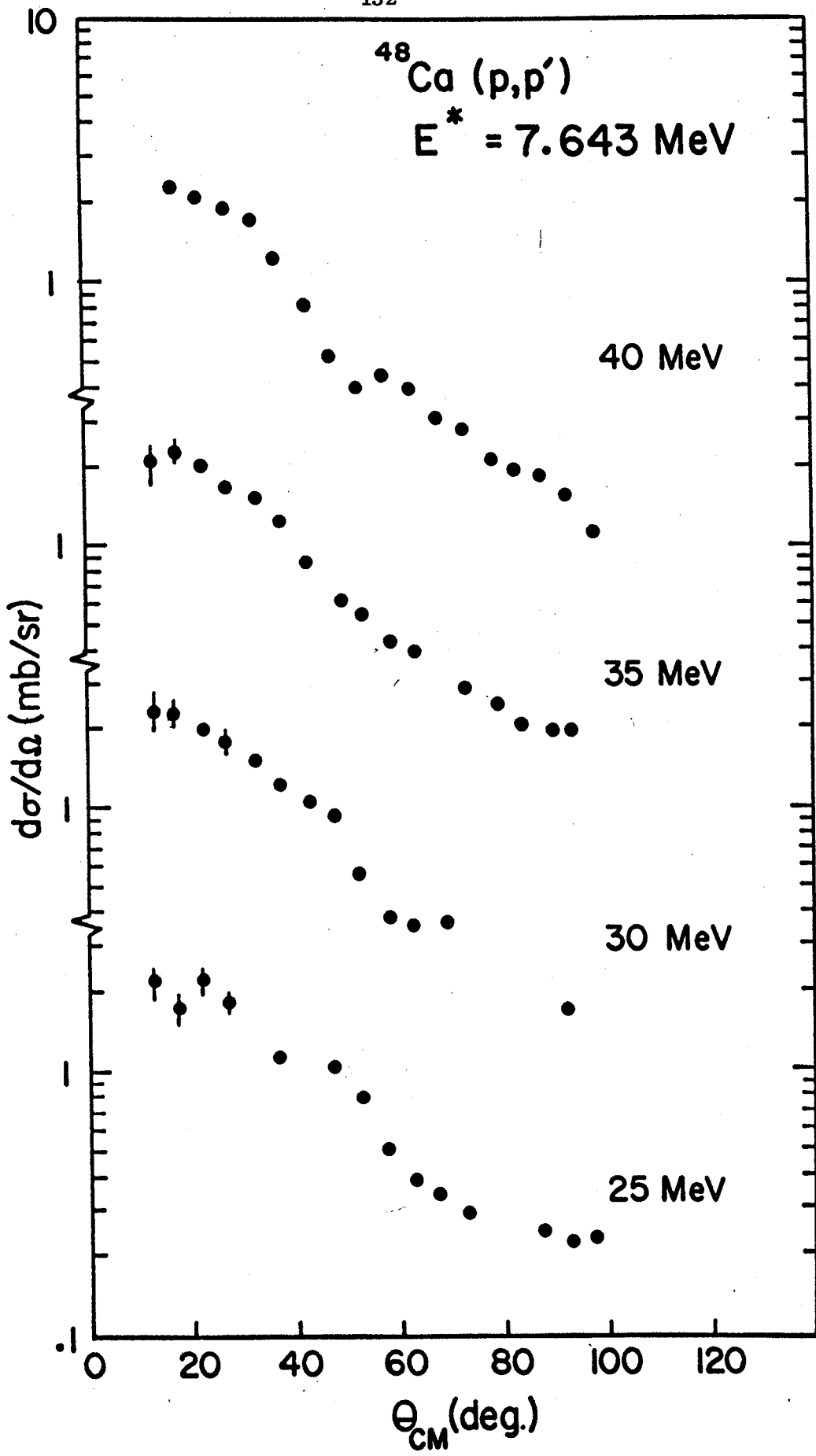


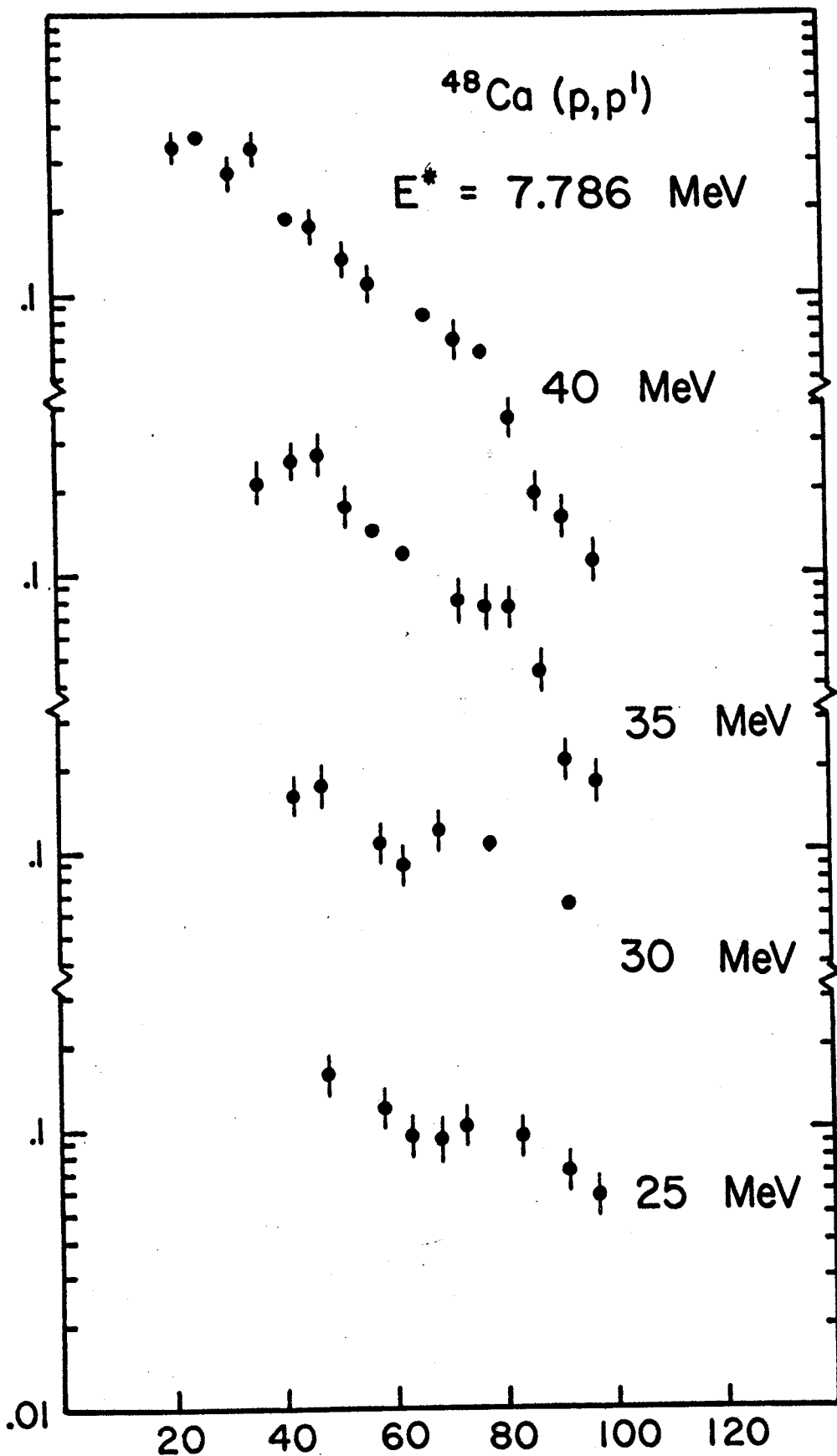


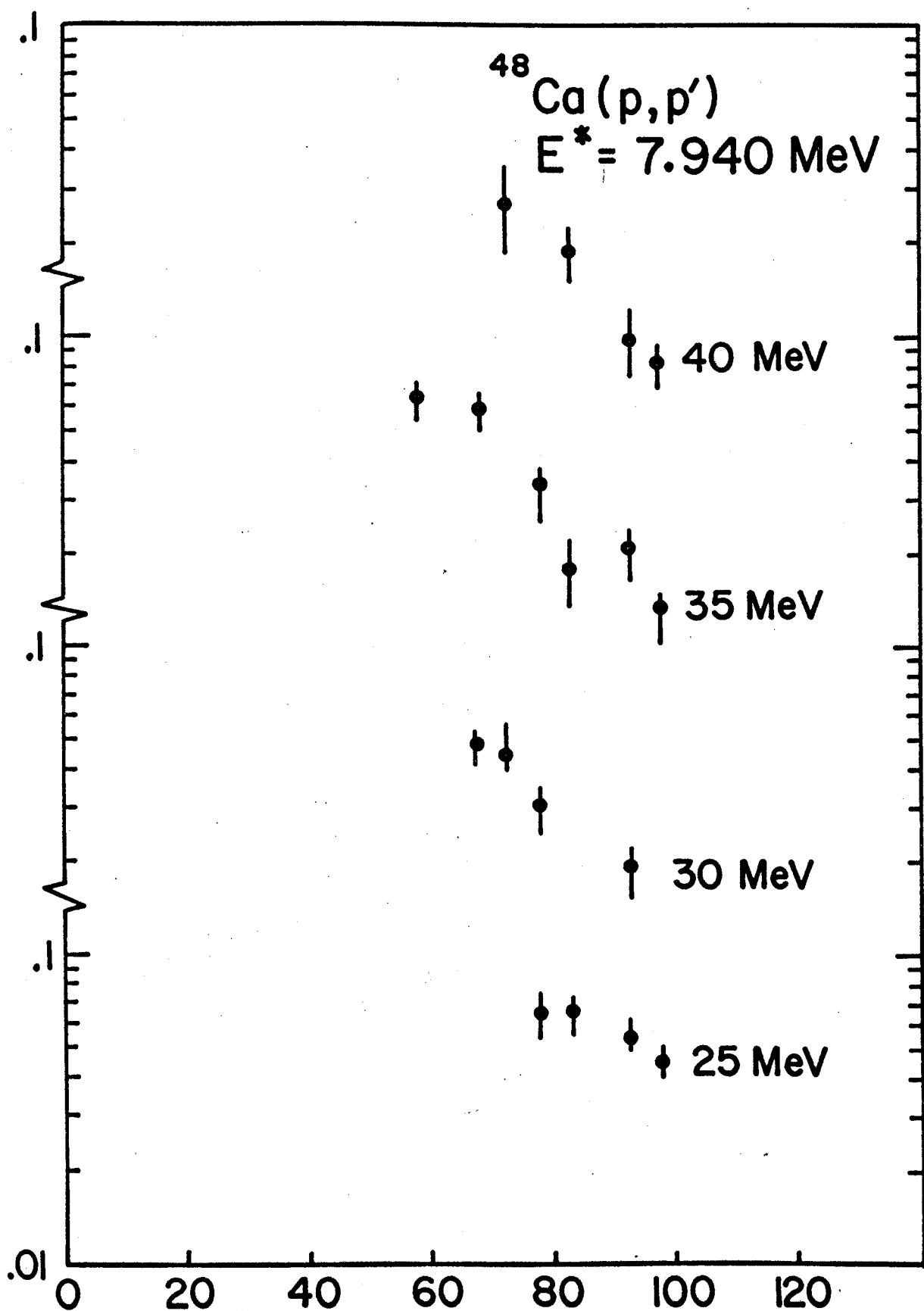


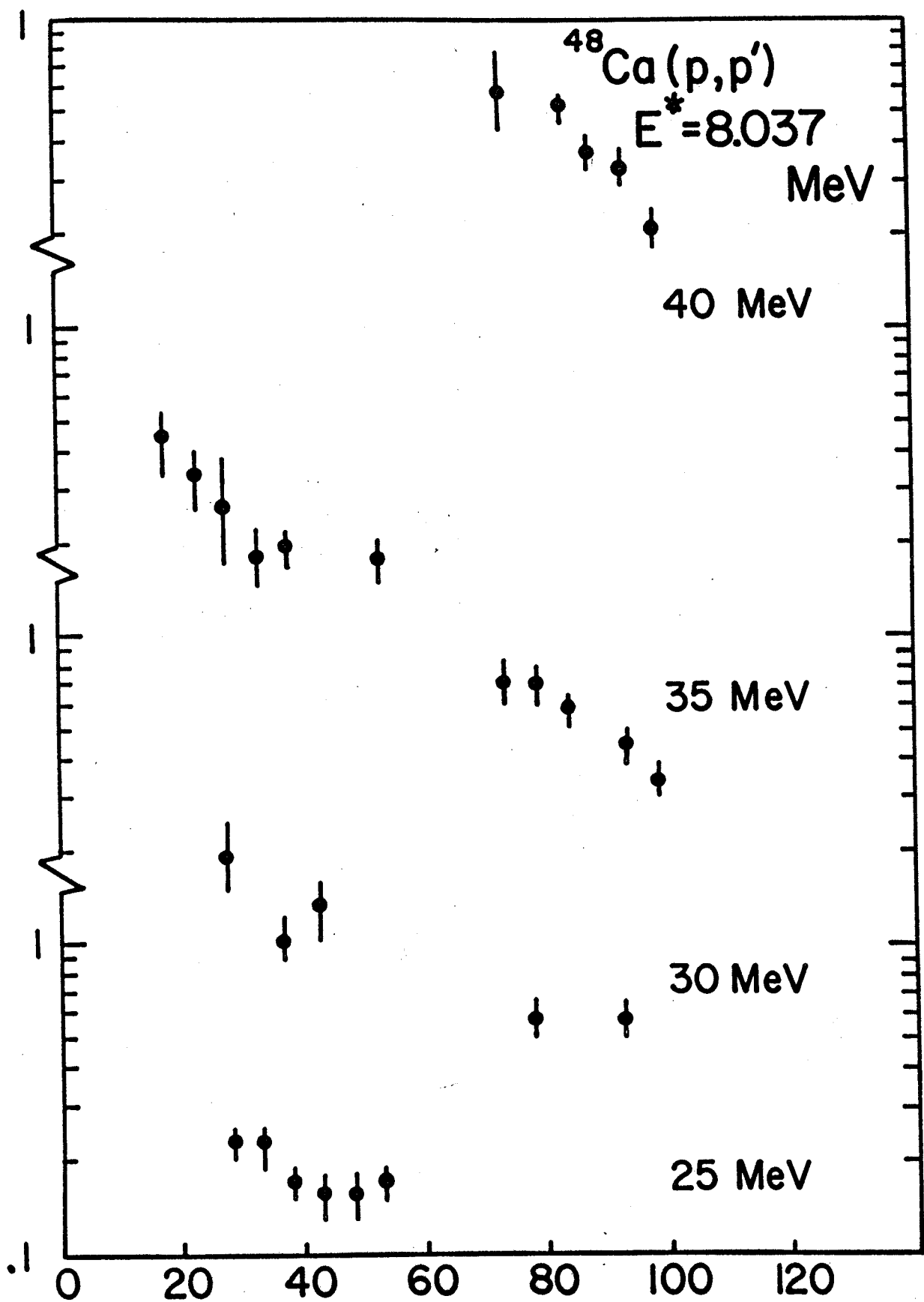












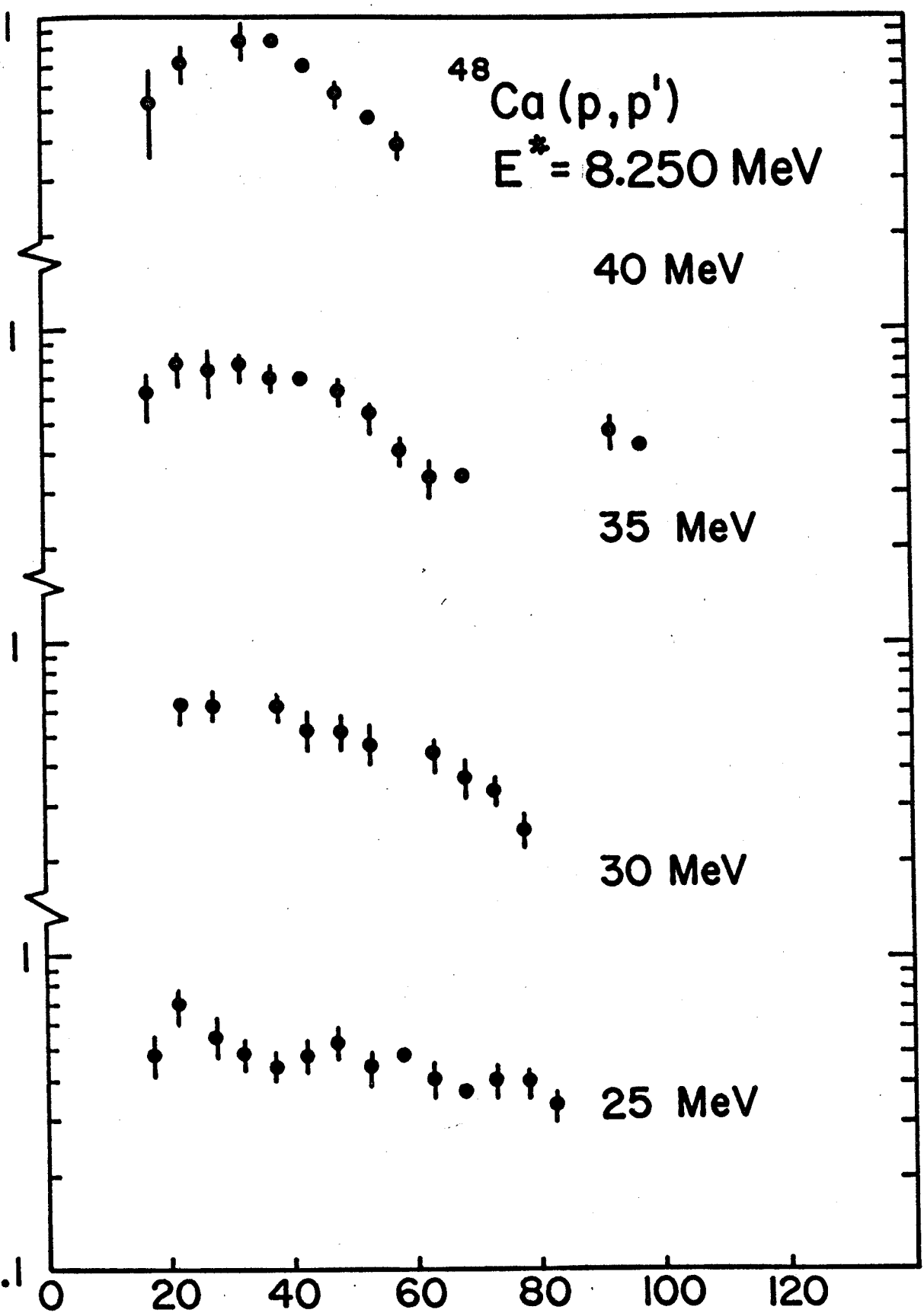
$^{48}\text{Ca}(\text{p},\text{p}')$
 $E^* = 8.250 \text{ MeV}$

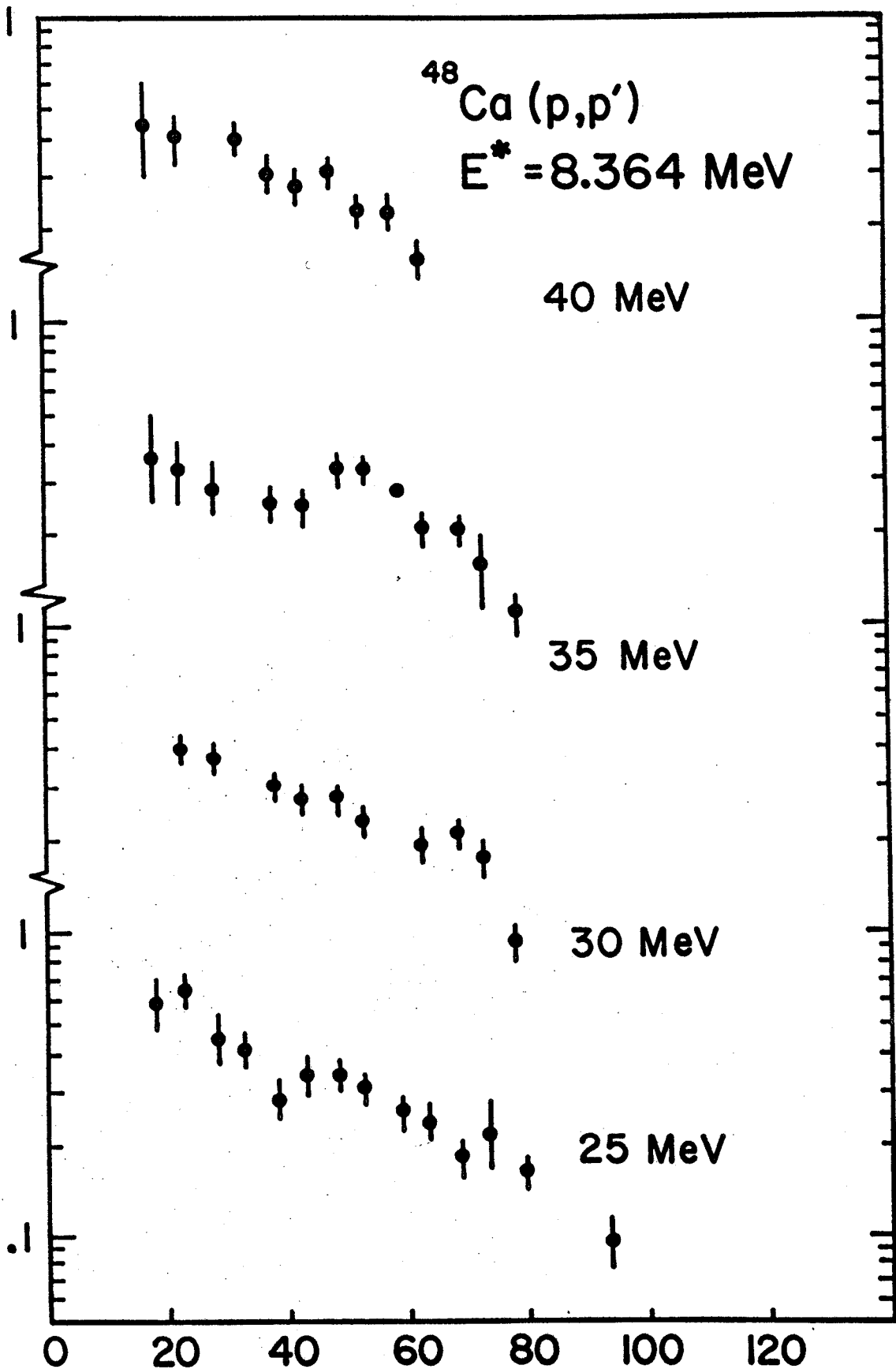
40 MeV

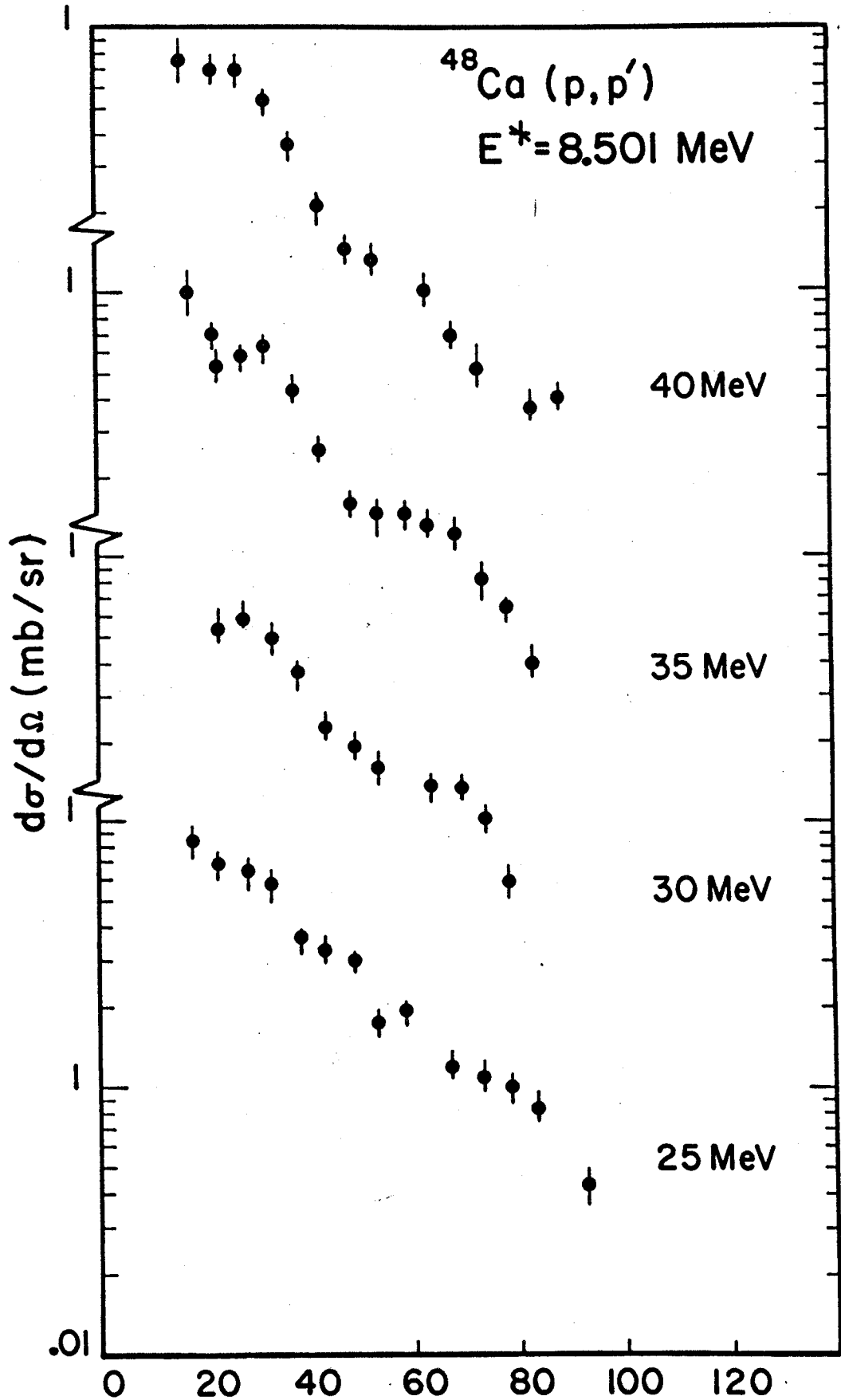
35 MeV

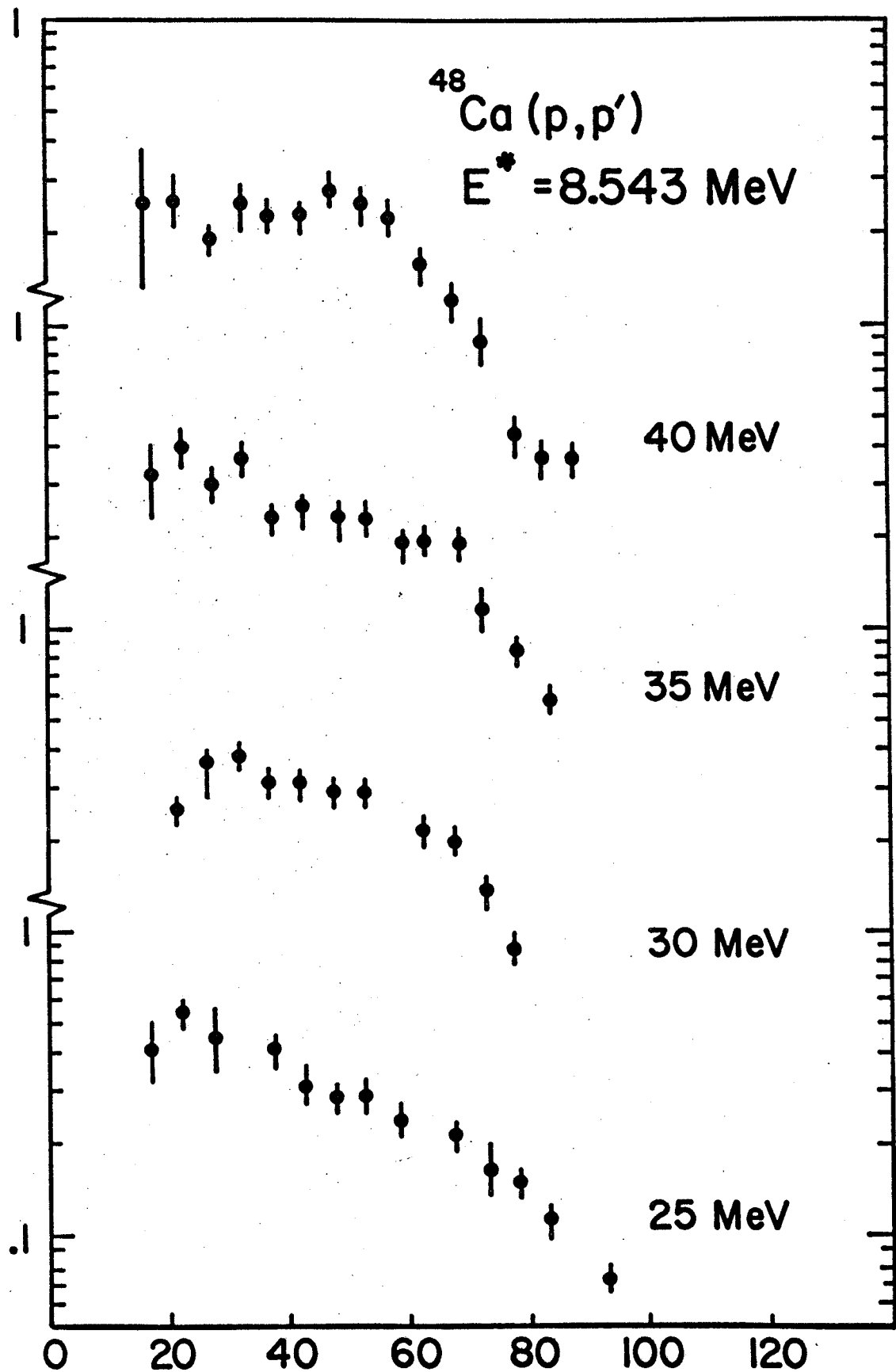
30 MeV

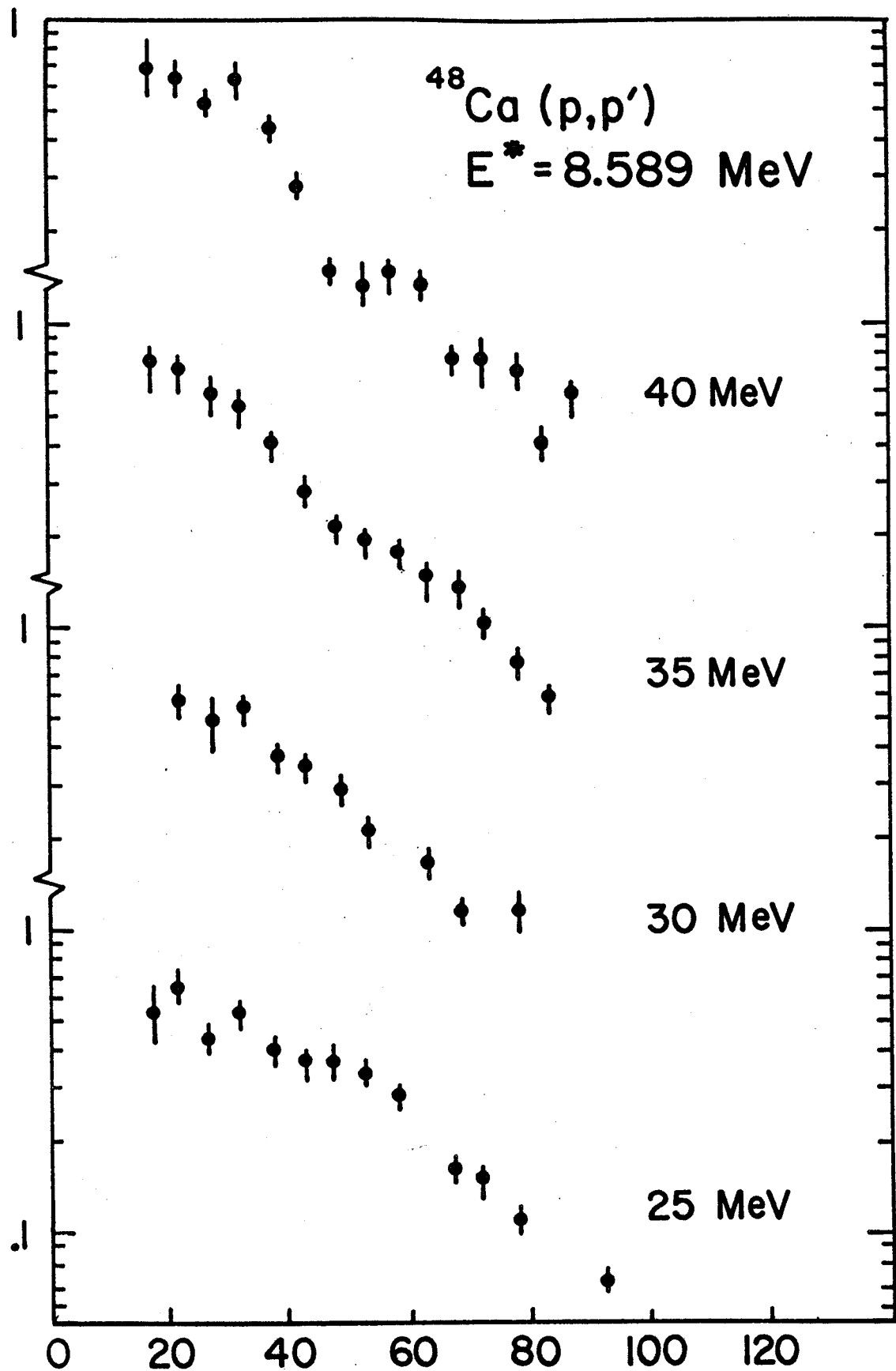
25 MeV











^{48}Ca (p, p')

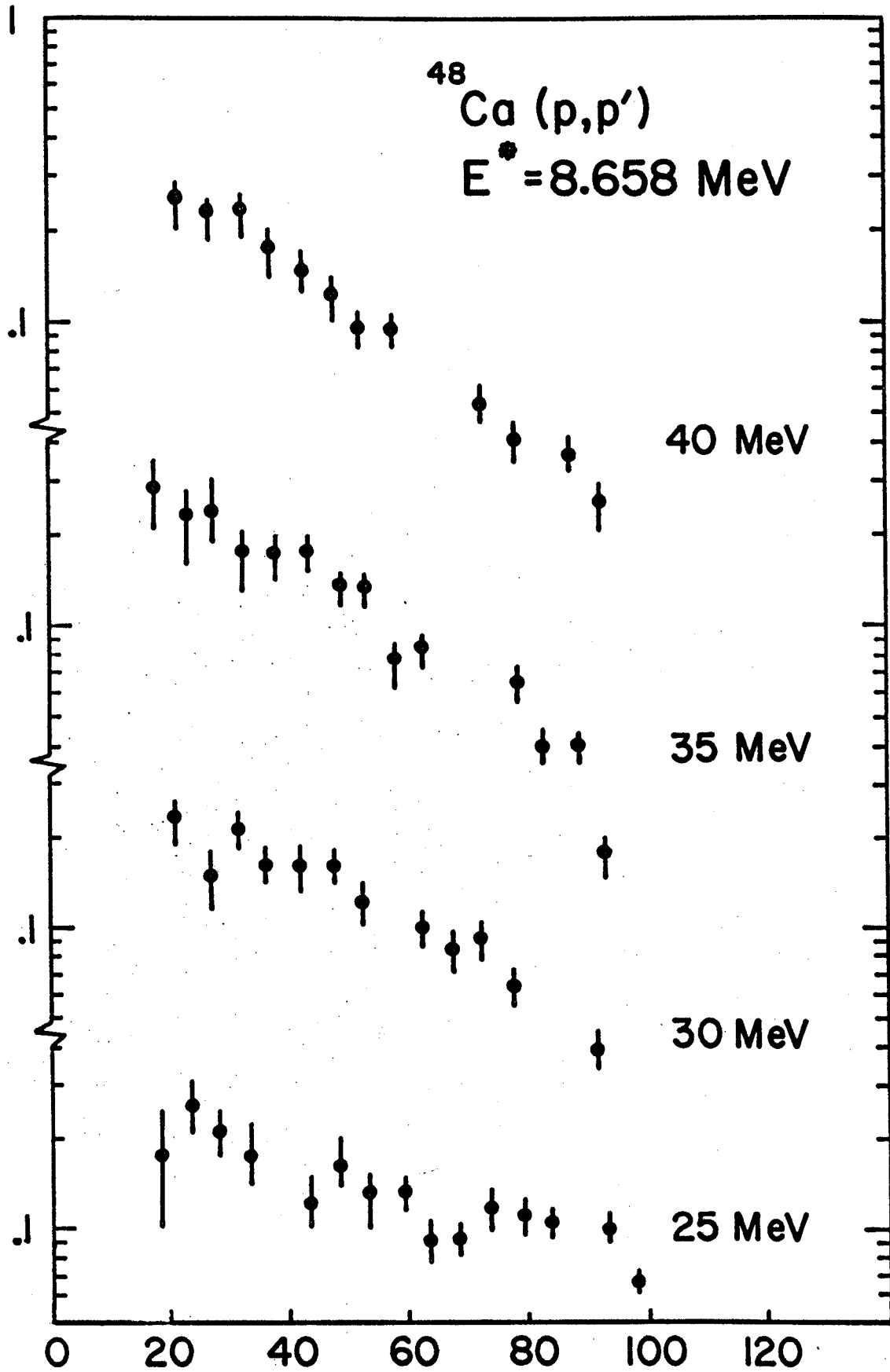
$E^* = 8.658 \text{ MeV}$

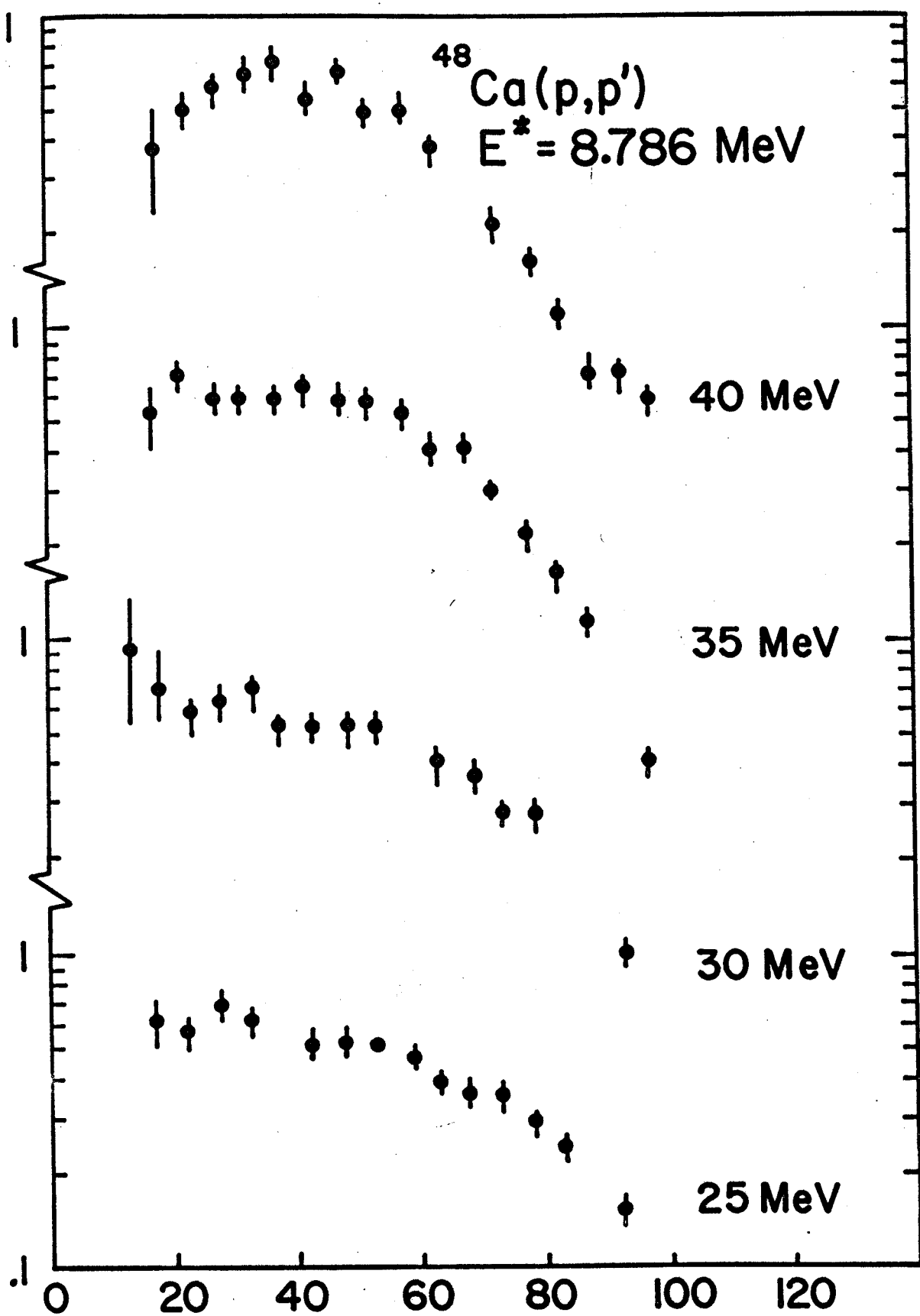
40 MeV

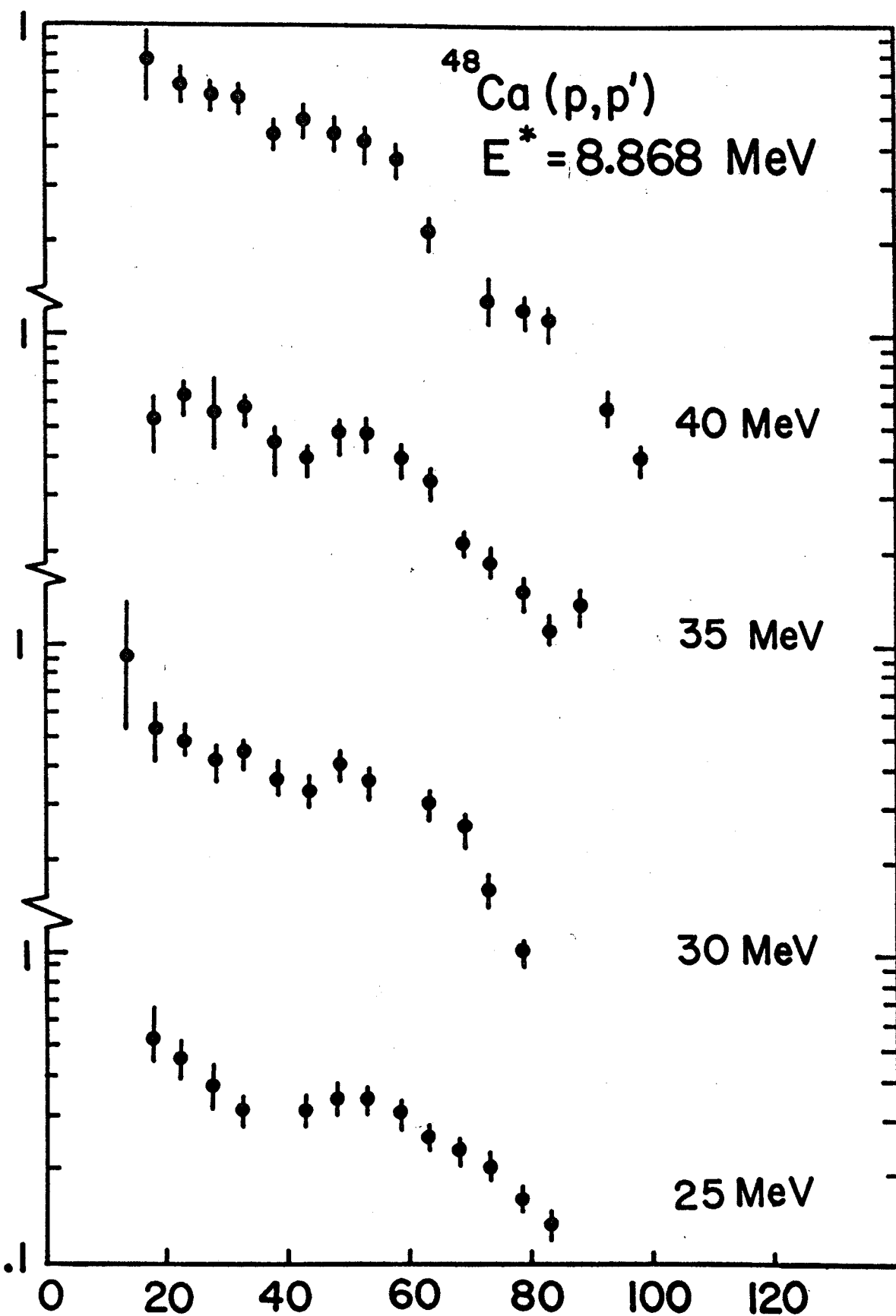
35 MeV

30 MeV

25 MeV







II.3 Tabulated Angular Distributions

The following pages contain listings of the differential cross section versus center of mass scattering angle for the excited states of ^{48}Ca at each energy. The error shown is the total relative standard error.

CA 48 (P,P) 25 MEV

0.0000

12.36	0.65507E+04	0.0901
27.25	0.16857E+03	0.4028
17.46	0.22079E+04	0.1245
32.34	0.24346E+02	0.8927
22.56	0.73801E+03	0.1356
37.43	0.90802E+02	0.2868
42.52	0.15168E+03	0.1957
48.00	0.15075E+03	0.2358
53.07	0.97593E+02	0.2241
67.83	0.95748E+01	0.5303
58.13	0.44355E+02	0.3034
72.86	0.15736E+02	0.3856
73.27	0.16888E+02	0.4198
87.92	0.17015E+02	0.3173
78.29	0.22883E+02	0.3346
83.31	0.22432E+02	0.2856
97.92	0.50529E+01	0.4559

CA 48 (P,P) 29.8 MEV

0.0000

12.77	0.54151E+04	0.0953
27.66	0.60661E+02	0.6577
17.87	0.19801E+04	0.1131
32.75	0.28622E+02	0.6892
22.97	0.50941E+03	0.1585
37.84	0.12220E+03	0.2400
28.07	0.42581E+02	0.4482
42.93	0.16318E+03	0.1656
48.41	0.12040E+03	0.2564
63.19	0.11072E+02	0.6257
53.48	0.64341E+02	0.3082
68.23	0.14841E+02	0.4827
58.54	0.19577E+02	0.5046
73.67	0.19401E+02	0.4623
78.70	0.13736E+02	0.5063
93.33	0.36306E+01	0.8584

CA48 (P,P) 35 MEV

0.0000

12.77	0.46846E+04	0.0958
27.66	0.44213E+02	0.7285
17.87	0.19897E+04	0.1187
32.76	0.55059E+02	0.5469
22.97	0.45968E+03	0.1636
37.85	0.14934E+03	0.2131
28.07	0.34817E+02	0.4920
42.93	0.15526E+03	0.1734
48.41	0.94435E+02	0.2535
63.19	0.13525E+02	0.5023
53.48	0.37824E+02	0.3878
68.24	0.20865E+02	0.4280
58.54	0.14549E+02	0.5668
73.28	0.17799E+02	0.3899
73.68	0.17164E+02	0.5300
88.34	0.35031E+01	0.8902
78.71	0.12086E+02	0.5431
93.34	0.25536E+01	0.8952
83.73	0.65410E+01	0.5616
98.33	0.27572E+01	0.6537

CA48 (P,P) 40 MEV

0.0000

12.36	0.53065E+04	0.1143
27.26	0.48270E+02	0.8735
17.47	0.20531E+04	0.1480
32.35	0.90656E+02	0.5167
22.47	0.47874E+03	0.1647
37.44	0.16777E+03	0.2085
27.57	0.41752E+02	0.4418
42.53	0.13973E+03	0.1788
47.91	0.64996E+02	0.3122
62.80	0.15553E+02	0.4709
52.98	0.21657E+02	0.4726
67.84	0.15949E+02	0.4159
58.04	0.12864E+02	0.6099
72.78	0.11576E+02	0.4864
73.18	0.11783E+02	0.5373
87.94	0.22682E+01	0.9273
78.21	0.59843E+01	0.7185
92.94	0.23551E+01	0.8686
83.23	0.30191E+01	0.7449
97.94	0.22598E+01	0.6524

* CA 48 (P,P) 25 MEV
3.830

12.38	0.60832E+01	4.9168
27.30	0.58992E+01	2.1696
17.49	0.53753E+01	3.3149
32.40	0.58799E+01	1.8070
22.60	0.51857E+01	1.8154
37.50	0.49099E+01	1.2808
27.71	0.52931E+01	1.5150
42.59	0.35240E+01	1.3537
48.07	0.23330E+01	2.1128
62.87	0.12149E+01	2.1274
53.15	0.18065E+01	1.7937
67.92	0.10029E+01	1.7871
58.22	0.14470E+01	1.8516
72.96	0.82955E+00	1.8670
73.37	0.85638E+00	2.0674
88.03	0.66280E+00	1.6303
78.40	0.70638E+00	2.1616
93.03	0.66762E+00	1.5130
83.42	0.64932E+00	1.9344
98.02	0.61102E+00	1.3355

* CA 48 (P,P) 29.83 MEV
3.830

12.79	0.88269E+01	4.3556
27.70	0.57345E+01	2.9661
17.90	0.69329E+01	2.7992
32.80	0.46192E+01	1.6883
23.00	0.56802E+01	1.5588
37.89	0.30941E+01	1.5102
28.11	0.53069E+01	1.2638
42.98	0.19756E+01	1.7025
48.47	0.15553E+01	2.4714
63.26	0.86300E+00	2.5180
53.55	0.14387E+01	2.2527
68.31	0.59963E+00	2.3471
58.61	0.12283E+01	2.0440
73.76	0.38056E+00	3.3833
78.79	0.27224E+00	3.6907
93.42	0.46182E+00	2.4425

* CA48 (P,P) 35 MEV
3.830

12.78	0.95647E+01	2.9325
27.70	0.50447E+01	2.0866
17.89	0.77539E+01	2.3239
32.80	0.37970E+01	2.0034
23.00	0.58169E+01	1.5245
37.89	0.20184E+01	2.0493
28.11	0.50372E+01	1.2501
42.98	0.13292E+01	2.1786
48.47	0.14604E+01	2.2941
63.26	0.71334E+00	2.1990
53.54	0.14993E+01	2.0602
68.31	0.40344E+00	3.1020
58.60	0.11576E+01	2.1532
73.35	0.28844E+00	3.0991
73.75	0.28912E+00	4.2433
88.41	0.46165E+00	2.3702
78.78	0.40327E+00	3.0424
93.41	0.33848E+00	2.4913
83.80	0.50213E+00	2.0587
98.40	0.19955E+00	2.4814

* CA48 (P,P) 40 MEV
3.830

12.37	0.10830E+02	3.5057
17.48	0.83091E+01	2.7754
32.39	0.25703E+01	3.4304
22.49	0.69651E+01	1.4902
37.48	0.14142E+01	2.6854
27.59	0.51058E+01	1.2390
42.57	0.10648E+01	2.5510
47.96	0.15104E+01	2.2313
62.85	0.43134E+00	2.9281
53.03	0.13524E+01	2.0323
67.90	0.25359E+00	3.4783
58.10	0.90897E+00	2.5000
72.84	0.30975E+00	3.0168
88.00	0.27129E+00	2.7707
78.27	0.41259E+00	2.8009
93.01	0.15886E+00	3.4732
83.29	0.38480E+00	2.1140
98.00	0.10265E+00	3.1771

*
CA 48 (P,P) 25 MEV
4.502

12.38	0.48215E+01	6.0392
27.31	0.43834E+01	2.5544
17.50	0.48243E+01	3.4537
32.41	0.41406E+01	2.1530
22.61	0.49267E+01	1.9011
37.51	0.39669E+01	1.3806
27.72	0.40332E+01	1.7721
42.60	0.34893E+01	1.3109
48.09	0.33482E+01	1.6302
62.89	0.19981E+01	1.5371
53.17	0.28665E+01	1.3383
67.94	0.17071E+01	1.2696
58.24	0.23571E+01	1.3494
72.98	0.15428E+01	1.2505
73.39	0.16184E+01	1.3707
88.05	0.85368E+00	1.4398
78.42	0.14120E+01	1.3617
93.05	0.66116E+00	1.5249
83.44	0.11140E+01	1.3073
98.04	0.53459E+00	1.4289

*
CA 48 (P,P) 29.8 MEV
4.502

12.79	0.52484E+01	4.8226
27.71	0.51851E+01	2.2745
17.90	0.54986E+01	2.7063
32.81	0.49630E+01	1.6350
23.01	0.53713E+01	1.6986
37.91	0.42935E+01	1.2795
28.12	0.53356E+01	1.1887
42.99	0.36181E+01	1.1460
48.48	0.27802E+01	1.6913
63.28	0.15659E+01	1.6730
53.56	0.21901E+01	1.7002
68.33	0.14967E+01	1.5281
73.77	0.12047E+01	1.8714
78.80	0.70684E+00	2.2596
93.43	0.43953E+00	2.5012

*
CA48 (P,P) 35 MEV
4.502

12.79	0.54412E+01	4.3507
27.70	0.54047E+01	2.0063
17.90	0.59864E+01	2.6882
32.80	0.53748E+01	1.6879
23.01	0.59914E+01	1.5297
37.90	0.44672E+01	1.2450
28.11	0.56364E+01	1.1795
42.99	0.33578E+01	1.2008
48.48	0.25189E+01	1.6253
63.27	0.14632E+01	1.5544
53.55	0.18770E+01	1.7553
68.32	0.12572E+01	1.8836
58.62	0.16384E+01	1.7049
73.36	0.97977E+00	1.6656
73.76	0.94626E+00	2.2928
88.42	0.45450E+00	2.4946
78.79	0.68464E+00	2.3137
93.42	0.41858E+00	2.2365
83.81	0.54273E+00	1.9711
98.41	0.41916E+00	1.7002

*
CA48 (P,P) 40 MEV
4.502

12.38	0.63802E+01	5.0179
27.29	0.70122E+01	2.2426
17.49	0.68360E+01	3.1050
32.39	0.58020E+01	2.0902
22.49	0.69739E+01	1.4561
37.49	0.45674E+01	1.2759
27.60	0.66909E+01	1.0763
42.58	0.30066E+01	1.3513
47.96	0.19787E+01	1.8180
62.86	0.12156E+01	1.7200
53.04	0.15347E+01	1.8069
67.91	0.97894E+00	1.7126
58.11	0.13958E+01	1.8915
72.85	0.67113E+00	2.0791
73.25	0.68662E+00	2.3030
88.02	0.36080E+00	2.4708
78.28	0.48543E+00	2.5700
93.02	0.31613E+00	2.4171
83.30	0.42580E+00	2.0063

* CA 48 (P,P) 25 MEV

4.607

27.31	0.26150E+00	12.1458
32.41	0.34972E+00	8.0645
37.51	0.35015E+00	5.2605
27.72	0.24091E+00	10.1475
42.60	0.38729E+00	4.5395
62.89	0.27150E+00	4.8878
53.17	0.31409E+00	4.8698
67.95	0.24190E+00	3.9611
58.24	0.29130E+00	4.6685
72.99	0.24296E+00	3.6740
73.39	0.23039E+00	4.2129
88.05	0.18149E+00	3.6321
78.42	0.23286E+00	3.6549
93.05	0.15160E+00	3.4922
83.44	0.18837E+00	3.7262
98.05	0.12598E+00	3.0017

* CA 48 (P,P) 29.8 MEV

4.607

27.71	0.3934CE+00	8.7284
32.81	0.31343E+00	7.0458
23.01	0.33644E+00	9.7709
37.91	0.31811E+00	5.0601
43.00	0.32279E+00	4.5000
48.49	0.27063E+00	6.4551
63.28	0.15011E+00	6.7586
53.56	0.21238E+00	7.1314
68.33	0.13299E+00	6.1839
73.78	0.10493E+00	8.2008
78.81	0.69805E-01	7.5377
93.44	0.63966E-01	7.0290

* CA48 (P,P) 35 MEV

4.607

32.80	0.33190E+00	8.6009
23.01	0.35172E+00	13.4433
37.90	0.28940E+00	5.6674
28.11	0.35735E+00	11.0022
42.99	0.29946E+00	4.9218
48.48	0.20019E+00	5.8215
53.55	0.18508E+00	6.9599
68.32	0.10028E+00	6.0970
58.62	0.13066E+00	7.5607
73.36	0.96132E-01	5.5000
73.76	0.91058E-01	7.8307
88.42	0.49737E-01	8.2486
78.79	0.66035E-01	7.7853
93.42	0.29274E-01	9.1597
83.81	0.55881E-01	6.4243

* CA48 (P,P) 40 MEV

4.607

37.49	0.21204E+00	7.8182
27.60	0.23450E+00	8.5367
47.97	0.13886E+00	10.0742
62.86	0.70955E-01	9.9466
53.04	0.12082E+00	8.4841
67.91	0.66419E-01	8.6722
58.11	0.10182E+00	10.1542
72.85	0.52803E-01	10.2435
73.26	0.55745E-01	9.3659
88.02	0.25353E-01	9.7308
78.29	0.50333E-01	8.6564
93.02	0.14749E-01	12.4578
83.31	0.33990E-01	7.5517

CA 48 (P,P) 25 MEV

5.141

32.42	0.11087E+00	15.9830
37.52	0.14852E+00	8.1040
48.11	0.23225E+00	8.0035
62.91	0.18280E+00	5.7374
53.18	0.22232E+00	6.2960
67.96	0.16674E+00	4.5060
58.25	0.21382E+00	5.8114
73.00	0.15392E+00	4.5797
73.41	0.15426E+00	4.9383
88.07	0.99131E-01	4.6943
93.07	0.87726E-01	4.7634
98.06	0.97408E-01	3.5200

CA 48 (P,P) 29.8 MEV

5.141

32.82	0.10704E+00	13.1341
28.12	0.94893E-01	13.2479
43.01	0.17125E+00	13.1579
48.50	0.19834E+00	7.8621
63.29	0.13326E+00	6.1489
53.57	0.18563E+00	6.9771
68.35	0.11781E+00	5.8333
58.64	0.13788E+00	6.5539
73.79	0.10120E+00	6.9633
78.82	0.54365E-01	8.7742
93.45	0.45653E-01	8.4651

CA48 (P,P) 35 MEV

5.141

32.81	0.12052E+00	15.0741
37.91	0.14498E+00	9.6227
28.12	0.11260E+00	11.3310
43.00	0.15351E+00	7.7185
48.49	0.20506E+00	6.9339
53.56	0.17823E+00	5.9904
68.33	0.10400E+00	6.4748
53.63	0.13203E+00	6.4276
73.37	0.71823E-01	6.5762
88.44	0.43141E-01	8.8471
78.81	0.61262E-01	8.4244
93.44	0.27852E-01	9.4891
83.83	0.53198E-01	6.8682
98.43	0.25816E-01	7.3790

CA48 (P,P) 40 MEV

5.141

32.40	0.14204E+00	28.0833
37.49	0.17987E+00	7.9762
27.60	0.99617E-01	12.3308
42.58	0.16158E+00	8.4328
47.97	0.15520E+00	8.0430
62.87	0.88508E-01	7.4747
53.05	0.16058E+00	6.3940
67.92	0.70819E-01	7.4747
58.12	0.12416E+00	7.2797
72.86	0.53892E-01	8.5685
73.26	0.66955E-01	8.8071
88.03	0.22233E-01	11.0263
78.30	0.50947E-01	8.9697
93.03	0.18126E-01	11.6863
83.32	0.32482E-01	7.9175
98.02	0.14240E-01	9.9324

CA 48 (P,P) 25 MEV

5.249

32.42	0.52611E-01	18.8928
37.52	0.70576E-01	12.1458
42.62	0.89976E-01	10.6164
42.91	0.47542E-01	12.3981
53.19	0.69085E-01	12.9592
67.97	0.42991E-01	9.2688
58.26	0.65567E-01	10.8447
73.01	0.32465E-01	10.8417
73.41	0.35962E-01	11.4793
88.08	0.26709E-01	10.3333
93.08	0.22373E-01	10.8487
83.46	0.19933E-01	13.1376
98.07	0.12715E-01	10.9917

CA 48 (P,P) 25.8 MEV

5.249

32.82	0.54822E-01	20.2143
23.02	0.61137E-01	45.1600
37.92	0.53903E-01	15.5570
28.13	0.41560E-01	20.4151
43.01	0.69395E-01	12.3896
48.50	0.74468E-01	13.7653
63.30	0.27168E-01	14.6349
53.58	0.50346E-01	15.0000
68.35	0.26178E-01	13.1579
58.64	0.39675E-01	12.9875
73.79	0.19000E-01	21.5217
93.45	0.71666E-02	26.9630

CA48 (P,P) 35 MEV

5.249

32.81	0.44632E-01	24.9333
28.12	0.45037E-01	17.4138
43.00	0.40064E-01	17.6629
48.49	0.54804E-01	16.6292
63.28	0.27824E-01	12.9875
53.56	0.55621E-01	11.3673
68.33	0.24690E-01	16.4545
58.63	0.38720E-01	12.5783
88.44	0.85183E-02	17.9677
78.81	0.20302E-01	15.9824
93.44	0.52858E-02	19.6154
83.83	0.74228E-02	20.7778
98.43	0.31828E-02	24.2963

CA48 (P,P) 40 MEV

5.249

42.59	0.48644E-01	17.0357
62.87	0.13775E-01	22.3500
53.05	0.34990E-01	15.0685
67.92	0.13226E-01	18.6250
58.12	0.32346E-01	15.8382
72.86	0.12857E-01	20.2979
73.27	0.16993E-01	16.5000
83.32	0.50229E-02	22.6000

CA 48 (P,P) 25 MEV

5.295

27.32	0.20415E+00	14.0533
32.42	0.13716E+00	13.2055
37.52	0.14556E+00	7.6616
42.62	0.76957E-01	11.5809
48.11	0.76325E-01	14.7447
62.91	0.30925E-01	15.1492
53.19	0.59214E-01	13.4682
67.97	0.24182E-01	22.5222
58.26	0.44389E-01	14.0642
73.01	0.25925E-01	11.7838
78.44	0.24561E-01	16.1041
93.08	0.20313E-01	10.6957
83.47	0.22858E-01	13.4800
98.07	0.16603E-01	9.4304

CA 48 (P,P) 29.8 MEV

5.295

27.72	0.12135E+00	16.6200
32.82	0.14227E+00	10.5046
23.02	0.94148E-01	22.0000
37.92	0.11667E+00	9.0000
28.13	0.12546E+00	10.0000
48.50	0.58509E-01	15.5325
63.30	0.24580E-01	15.5965
53.58	0.63083E-01	12.7596
68.35	0.16878E-01	16.4490
73.79	0.11565E-01	23.6785

CA48 (P,P) 35 MEV

5.295

27.71	0.80910E-01	16.2105
32.81	0.95212E-01	14.4844
23.01	0.10078E+00	26.0232
28.12	0.10094E+00	11.5615
43.00	0.49966E-01	14.8288
48.49	0.27709E-01	25.8222
53.56	0.40864E-01	13.0278
58.63	0.27990E-01	15.1000
73.78	0.16378E-01	17.1470
88.44	0.85182E-02	17.9677
78.81	0.13534E-01	19.6842
93.44	0.81320E-02	15.8000
83.83	0.10928E-01	17.7924
98.43	0.41259E-02	20.8000

CA48 (P,P) 40 MEV

5.295

22.50	0.12570E+00	20.3232
37.50	0.77793E-01	13.2660
27.61	0.12507E+00	9.9641
42.59	0.46472E-01	15.8318
47.97	0.41222E-01	17.3970
62.87	0.13775E-01	21.8000
53.05	0.25882E-01	18.7037
67.92	0.12675E-01	19.1956
58.12	0.20929E-01	19.8182
83.32	0.61948E-02	19.6757

*
CA 48 (P,P) 25 MEV
5.362

27.32	0.85737E+00	12.9746
32.43	0.61248E+00	5.7883
22.62	0.84172E+00	12.4946
37.53	0.64321E+00	7.4343
27.73	0.84349E+00	7.1123
42.62	0.62524E+00	3.5891
62.92	0.54786E+00	3.1356
53.19	0.54042E+00	3.4191
67.97	0.52071E+00	2.4216
58.26	0.48459E+00	3.3420
73.01	0.51054E+00	2.2900
73.41	0.55398E+00	2.4501
88.08	0.34293E+00	2.3894
78.45	0.48788E+00	2.3922
93.08	0.25185E+00	2.6826
83.47	0.42699E+00	2.1859
98.07	0.19493E+00	2.4534

CA 48 (P,P) 29.8 MEV
5.362

12.79	0.86275E+00	18.1309
27.72	0.95862E+00	5.2810
32.82	0.80268E+00	4.1431
23.02	0.84973E+00	5.0460
37.92	0.74503E+00	3.1804
28.13	0.86877E+00	3.2238
48.50	0.56987E+00	3.9467
63.30	0.46011E+00	3.1265
53.58	0.48524E+00	3.8525
68.35	0.48909E+00	2.7056
73.80	0.40726E+00	3.2677
78.83	0.27953E+00	3.6650
93.46	0.14227E+00	4.6007

*
CA48 (P,P) 35 MEV
5.362

12.79	0.11156E+01	13.8723
27.71	0.11306E+01	4.6008
17.90	0.11281E+01	9.1847
32.81	0.10443E+01	4.0043
23.01	0.10183E+01	6.9724
28.12	0.11189E+01	2.7384
43.00	0.65134E+00	2.9185
48.49	0.64899E+00	3.0806
63.29	0.46430E+00	2.7940
53.57	0.53008E+00	3.3651
58.63	0.48838E+00	3.1765
73.38	0.35376E+00	2.8166
73.78	0.34394E+00	3.8655
88.44	0.12365E+00	4.9978
93.44	0.11242E+00	4.4702
83.83	0.18041E+00	3.5543
98.43	0.10810E+00	3.4362

*
CA48 (P,P) 40 MEV
5.362

12.38	0.16196E+01	14.3725
27.30	0.14475E+01	5.2209
17.49	0.19559E+01	8.2556
32.40	0.13255E+01	4.4821
22.50	0.13865E+01	3.9643
37.50	0.12853E+01	2.5026
27.61	0.14439E+01	2.4238
42.59	0.73049E+00	2.9245
47.98	0.60861E+00	3.6135
62.87	0.45697E+00	2.9450
53.05	0.54639E+00	3.1675
67.93	0.34085E+00	3.0218
58.12	0.47280E+00	3.3702
72.87	0.22513E+00	3.7631
73.27	0.22091E+00	4.3354
88.03	0.88150E-01	5.0642
78.30	0.13709E+00	5.0653
93.03	0.89384E-01	4.7674
83.32	0.10950E+00	4.1254
98.02	0.72258E-01	3.9574

* CA 48 (P,P) 25 MEV

5.723

27.33	0.71285E+00	7.1794
17.51	0.85853E+00	13.2885
32.43	0.68738E+00	5.5191
22.62	0.67913E+00	7.5087
37.53	0.63490E+00	3.7176
42.63	0.53115E+00	4.0394
48.12	0.52678E+00	5.1402
62.93	0.42246E+00	3.6756
53.20	0.47920E+00	3.9941
73.02	0.34841E+00	2.8606
73.43	0.37888E+00	3.0792
88.09	0.25501E+00	2.9359
78.46	0.33793E+00	3.0288
93.09	0.22197E+00	2.9390
83.48	0.28690E+00	2.8082
98.08	0.21879E+00	2.3655

* CA 48 (P,P) 29.8 MEV

5.723

12.80	0.75410E+00	29.9880
27.72	0.71087E+00	6.4471
17.91	0.65631E+00	12.5424
32.83	0.72939E+00	4.4365
23.02	0.61601E+00	6.6806
37.93	0.69845E+00	3.3975
43.02	0.64868E+00	3.0507
48.51	0.62444E+00	3.8504
63.31	0.43892E+00	3.2043
53.59	0.60642E+00	6.0150
68.36	0.41361E+00	2.9500
73.80	0.32833E+00	3.6566
78.84	0.18763E+00	4.5047
93.47	0.17386E+00	4.0595

* CA48 (P,P) 35 MEV

5.723

12.79	0.49835E+00	30.2699
27.72	0.53428E+00	6.8446
17.91	0.53010E+00	19.1173
32.82	0.62615E+00	5.4014
23.02	0.55880E+00	7.1069
37.92	0.63968E+00	3.6365
28.12	0.62722E+00	3.7946
43.01	0.64311E+00	3.2169
63.29	0.48024E+00	2.7524
53.57	0.65653E+00	3.0078
68.34	0.48177E+00	2.8672
58.64	0.56950E+00	2.9476
73.39	0.32116E+00	2.9684
73.79	0.29045E+00	4.2371
88.45	0.18355E+00	4.0449
78.82	0.27387E+00	3.7490
93.45	0.15736E+00	3.7403
83.84	0.22701E+00	3.1135
98.44	0.12154E+00	3.2211

* CA48 (P,P) 40 MEV

5.723

27.30	0.53851E+00	9.0563
17.49	0.53449E+00	23.5772
32.40	0.57982E+00	7.4490
22.50	0.50141E+00	13.9468
37.50	0.71569E+00	3.6700
27.61	0.61996E+00	3.9915
42.59	0.74687E+00	2.7762
47.98	0.70004E+00	3.4139
62.88	0.45383E+00	2.9287
53.06	0.64264E+00	2.9650
67.93	0.34247E+00	3.0265
58.12	0.56454E+00	3.1238
72.87	0.27681E+00	3.4061
73.27	0.30517E+00	3.6292
88.04	0.13534E+00	4.0086
78.31	0.21612E+00	3.9743
93.04	0.10360E+00	4.3825
83.33	0.18550E+00	3.0948
98.03	0.79861E-01	3.7446

*
CA 48 (P,P) 25 MEV
6.098

32.44	0.12390E+00	17.2727
37.54	0.15205E+00	18.3333
27.74	0.13792E+00	16.6403
42.64	0.90472E-01	13.8375
48.13	0.11035E+00	13.9485
62.94	0.81198E-01	10.4148
53.21	0.10145E+00	11.6759
58.28	0.87917E-01	10.3935
73.44	0.55858E-01	10.4787
88.11	0.35267E-01	11.5485
78.47	0.49112E-01	11.3177
93.11	0.28409E-01	12.0518
83.49	0.44614E-01	9.1271
98.10	0.29847E-01	7.9824

*
CA 48 (P,P) 29.8 MEV
6.098

17.91	0.10168E+00	72.7380
32.83	0.10174E+00	16.9102
37.93	0.10365E+00	10.8487
28.14	0.90890E-01	18.2055
43.02	0.11709E+00	8.8192
48.52	0.13822E+00	9.7363
63.32	0.67680E-01	9.0764
53.59	0.11641E+00	9.9635
68.37	0.49241E-01	9.3566
58.66	0.69401E-01	9.4214
78.85	0.23145E-01	15.3030
93.48	0.18050E-01	14.7059

*
CA48 (P,P) 35 MEV
6.098

27.72	0.10427E+00	30.8367
32.82	0.92188E-01	18.9516
23.02	0.10072E+00	24.3372
37.92	0.88585E-01	15.0111
43.01	0.90438E-01	11.7861
48.50	0.89863E-01	13.0342
63.30	0.47983E-01	9.7754
53.58	0.72620E-01	9.8203
68.35	0.48246E-01	10.2558
58.65	0.51298E-01	10.6000
73.39	0.29097E-01	10.8725
73.80	0.26971E-01	17.3214
88.46	0.18135E-01	15.3030
78.83	0.21367E-01	14.9000
93.46	0.14435E-01	13.7324
83.85	0.25772E-01	10.4000
98.45	0.13440E-01	10.5965

*
CA48 (P,P) 40 MEV
6.098

32.41	0.78081E-01	31.0606
37.51	0.10630E+00	27.1275
27.61	0.88333E-01	13.6102
42.60	0.10723E+00	11.5020
47.99	0.68477E-01	15.1504
62.89	0.37183E-01	12.9629
53.06	0.53186E-01	15.3694
67.94	0.29753E-01	13.0926
58.13	0.33763E-01	16.8450
73.28	0.24806E-01	17.1644
88.05	0.11506E-01	16.3390
78.31	0.22846E-01	14.4324
93.05	0.12439E-01	15.1143
83.33	0.13393E-01	15.6125
98.04	0.11450E-01	12.2101

* CA 48 (P,P) 25 MEV
6.335

12.40	0.15424E+01	15.8287
17.52	0.96514E+00	10.5675
32.44	0.76388E+00	5.3317
37.55	0.65948E+00	3.6559
42.64	0.55515E+00	3.7800
48.14	0.58330E+00	4.4826
62.95	0.36695E+00	4.0855
53.22	0.51232E+00	3.7379
58.29	0.44684E+00	3.6448
73.05	0.33747E+00	2.9741
73.45	0.38354E+00	3.0782
88.11	0.16195E+00	3.7135
78.48	0.32739E+00	3.3860
83.50	0.20862E+00	3.5241
98.11	0.98215E-01	3.7881

* CA 48 (P,P) 29.8 MEV
6.335

12.80	0.12185E+01	13.5889
27.73	0.96753E+00	5.1779
17.92	0.11182E+01	9.1991
32.84	0.81118E+00	4.4614
37.94	0.67494E+00	3.5657
43.03	0.62138E+00	3.0623
48.52	0.53686E+00	4.1400
63.32	0.22586E+00	4.5878
53.60	0.42556E+00	4.1866
68.38	0.18903E+00	4.6412
58.67	0.25279E+00	4.6235
73.82	0.17632E+00	5.1265
78.85	0.11782E+00	5.9673
93.48	0.57866E-01	7.4816

* CA48 (P,P) 35 MEV
6.335

27.72	0.85321E+00	5.2369
17.91	0.14949E+01	7.4973
32.83	0.82659E+00	4.6349
23.02	0.12928E+01	3.7482
37.92	0.70265E+00	3.7479
28.13	0.82792E+00	3.3149
43.02	0.60599E+00	3.2925
48.51	0.45788E+00	4.3925
63.31	0.14846E+00	5.0726
53.58	0.31938E+00	4.3837
68.36	0.16754E+00	5.0112
58.65	0.24341E+00	9.6188
73.40	0.15375E+00	4.3576
73.80	0.14689E+00	6.1443
88.46	0.58527E-01	7.4366
78.83	0.14387E+00	5.2970
93.46	0.38628E-01	8.0842
83.85	0.10267E+00	4.7169
98.45	0.24994E-01	7.6368

* CA48 (P,P) 40 MEV
6.335

12.38	0.92674E+00	23.5890
27.31	0.78392E+00	7.7382
17.50	0.99906E+00	12.6522
32.41	0.80910E+00	6.2836
37.51	0.84029E+00	3.4312
27.61	0.94758E+00	3.2141
42.60	0.57909E+00	3.3291
47.99	0.38658E+00	5.0690
62.89	0.12049E+00	6.1686
53.07	0.21799E+00	5.3780
67.94	0.13140E+00	5.5178
58.13	0.12506E+00	7.2433
72.88	0.11514E+00	5.6152
73.29	0.13082E+00	5.8831
88.05	0.30032E-01	9.3636
78.32	0.11176E+00	5.7017
93.05	0.23813E-01	9.9030
83.34	0.53070E-01	6.3470
98.04	0.19148E-01	8.6884

* CA 48 (P,P) 25 MEV
6.641

27.34	0.10301E+01	5.8707
17.52	0.13886E+01	9.9786
32.45	0.78800E+00	5.3667
22.64	0.10797E+01	6.0242
37.55	0.75837E+00	3.5499
27.75	0.88957E+00	4.3101
48.15	0.74372E+00	3.9575
62.96	0.46581E+00	3.6248
53.23	0.63988E+00	3.3243
68.01	0.35954E+00	3.1568
58.30	0.55741E+00	3.2774
73.06	0.29903E+00	3.2326
73.46	0.31191E+00	3.5124
88.13	0.17582E+00	3.7575
93.13	0.12821E+00	4.1447
83.52	0.20148E+00	3.5073
98.12	0.10836E+00	3.6945

* CA 48 (P,P) 29.8 MEV
6.641

27.74	0.10327E+01	5.2277
17.92	0.13369E+01	8.4996
32.84	0.78749E+00	4.4801
23.03	0.10673E+01	5.2826
37.94	0.77087E+00	3.3095
43.04	0.71126E+00	2.8481
48.53	0.66277E+00	3.7904
63.33	0.31633E+00	3.6907
53.61	0.51335E+00	3.8383
68.38	0.25510E+00	4.0594
73.83	0.19117E+00	4.9870
78.86	0.12693E+00	5.6602
93.49	0.78838E-01	6.3973

* CA48 (P,P) 35 MEV
6.641

12.80	0.15493E+01	16.3188
27.73	0.79771E+00	5.6373
17.91	0.12757E+01	9.7606
32.83	0.72831E+00	4.9224
23.03	0.10946E+01	5.6984
28.13	0.80214E+00	3.5638
43.02	0.61937E+00	3.3413
48.51	0.46641E+00	4.6187
63.31	0.22804E+00	4.0854
53.59	0.38853E+00	3.9839
68.36	0.21090E+00	4.4858
73.41	0.16281E+00	4.2623
73.81	0.16277E+00	5.9911
88.47	0.63747E-01	7.3664
78.84	0.12855E+00	5.6842
93.47	0.48184E-01	7.2489
83.86	0.95247E-01	4.9545
98.46	0.47632E-01	5.4579

* CA48 (P,P) 40 MEV
6.641

12.38	0.23100E+01	12.5659
27.31	0.67950E+00	8.7723
17.50	0.12768E+01	13.2789
22.51	0.92929E+00	6.1106
37.51	0.65472E+00	3.8388
27.62	0.78052E+00	3.7267
42.60	0.52518E+00	3.8074
47.99	0.34472E+00	5.8682
62.90	0.16971E+00	5.1988
53.07	0.25198E+00	5.6331
67.95	0.14379E+00	5.2261
72.89	0.11295E+00	5.9855
73.29	0.12130E+00	6.3193
88.06	0.43488E-01	7.6233
78.32	0.93846E-01	6.3092
93.06	0.32699E-01	8.5598
83.35	0.60435E-01	6.1496
98.05	0.29830E-01	6.8742

CA 48 (P,P) 25 MEV
6.786

27.34	0.19022E+00	17.2571
37.56	0.11524E+00	12.6560
27.75	0.13494E+00	16.5620
42.65	0.64418E-01	20.0438
68.02	0.29266E-01	15.2660
58.30	0.38649E-01	21.5684
73.06	0.37581E-01	12.8323
73.47	0.41734E-01	12.8825
88.13	0.16606E-01	17.6495
93.13	0.20020E-01	15.7720
98.12	0.17921E-01	11.6657

CA 48 (P,P) 29.8 MEV
6.786

27.74	0.99379E-01	20.8293
32.84	0.12254E+00	15.0425
37.94	0.93366E-01	12.9927
28.15	0.99456E-01	15.4094
43.04	0.79221E-01	11.9205
48.53	0.71357E-01	15.9255
68.39	0.26851E-01	14.8461
58.68	0.40634E-01	13.1341
78.87	0.21038E-01	16.5000
93.50	0.16458E-01	17.2258

CA48 (P,P) 35 MEV
6.786

32.83	0.11147E+00	16.1600
37.93	0.11258E+00	12.4210
28.14	0.12488E+00	11.2981
48.51	0.62758E-01	20.1862
63.32	0.31633E-01	12.3846
53.59	0.44805E-01	12.5949
58.66	0.51283E-01	10.8364
73.41	0.33095E-01	10.2661
73.81	0.27448E-01	16.1754
88.47	0.18959E-01	15.5362
78.84	0.28486E-01	13.2250
93.47	0.16672E-01	13.0244
83.86	0.27522E-01	10.6592
98.46	0.15092E-01	10.0625

CA 48 (P,P) 40 MEV
6.786

32.42	0.94607E-01	26.4500
22.51	0.11544E+00	28.2967
42.61	0.63798E-01	15.6735
48.00	0.40589E-01	26.0597
62.90	0.37175E-01	12.9629
53.07	0.31136E-01	22.2461
67.95	0.26167E-01	14.7789
58.14	0.46591E-01	14.0612
72.89	0.19416E-01	19.4648
73.29	0.28540E-01	15.6071
88.06	0.10726E-01	21.1273
78.33	0.20683E-01	14.8507
93.06	0.90632E-02	18.0784
83.35	0.20591E-01	12.1382
98.05	0.91416E-02	13.9263

CA 48 (P,P) 25 MEV

6.885

27.35	0.24862E+00	14.0983
37.56	0.17615E+00	9.1083
27.76	0.16447E+00	11.7186
42.66	0.12318E+00	11.0275
48.15	0.15325E+00	11.9841
62.97	0.71014E-01	12.2143
68.02	0.70074E-01	8.9119
58.31	0.89090E-01	10.6027
73.06	0.63722E-01	8.6154
73.47	0.68613E-01	9.7429
88.14	0.34067E-01	10.3367
93.14	0.21860E-01	14.6195
83.52	0.53932E-01	7.8407
98.13	0.26698E-01	9.1654

CA 48 (P,P) 29.8 MEV

6.885

27.74	0.17693E+00	13.4931
32.84	0.14600E+00	12.5000
37.95	0.14651E+00	9.0047
28.15	0.13938E+00	12.1292
43.04	0.10442E+00	10.6983
63.34	0.48695E-01	12.9734
53.61	0.86658E-01	10.5385
58.68	0.58471E-01	10.7203
73.84	0.42525E-01	11.2815
78.87	0.35413E-01	11.7525
93.50	0.14334E-01	16.9815

CA48 (P,P) 35 MEV

6.885

32.83	0.92140E-01	16.6129
37.93	0.82287E-01	15.2400
28.14	0.84156E-01	13.9631
48.52	0.79367E-01	14.5659
63.32	0.53878E-01	9.0065
53.59	0.90741E-01	8.7500
58.66	0.65267E-01	9.6857
73.41	0.33495E-01	10.2231
73.81	0.44302E-01	12.1956
88.48	0.16211E-01	16.3390
78.84	0.35964E-01	11.8416
93.48	0.17078E-01	13.0357
83.87	0.21234E-01	12.6990
98.47	0.12026E-01	11.5196

CA48 (P,P) 40 MEV

6.885

32.42	0.92237E-01	24.4615
22.51	0.10021E+00	31.7975
37.51	0.80522E-01	15.2035
27.62	0.76320E-01	19.5588
48.00	0.60578E-01	19.8500
53.07	0.58917E-01	14.7886
67.95	0.36909E-01	12.3060
58.14	0.50393E-01	12.3019
72.89	0.22151E-01	18.0123
73.30	0.27860E-01	14.5366
88.06	0.66304E-02	29.1176
78.33	0.20374E-01	14.5303
93.06	0.10130E-01	16.7368
83.35	0.18080E-01	13.3518
98.05	0.58699E-02	18.0328

CA 48 (P,P) 25 MEV

7.009

27.35	0.65747E+00	7.6653
17.52	0.78466E+00	16.0336
32.46	0.60109E+00	18.8268
22.64	0.58795E+00	11.1822
37.56	0.61976E+00	3.9799
27.76	0.69719E+00	4.8277
42.66	0.46948E+00	4.5487
48.16	0.43295E+00	5.7659
53.24	0.35576E+00	4.7309
68.02	0.18551E+00	4.6064
73.07	0.13607E+00	5.1544
73.47	0.16930E+00	5.2105
88.14	0.14671E+00	4.3676
93.14	0.89133E-01	5.2337
83.53	0.14516E+00	4.9005
98.13	0.10348E+00	4.1727

CA 48 (P,P) 29.8 MEV

7.009

27.74	0.59132E+00	6.9057
17.92	0.93612E+00	10.0982
23.04	0.58600E+00	7.0958
37.95	0.42792E+00	5.3392
28.15	0.51598E+00	4.8634
43.04	0.33664E+00	4.6845
48.54	0.29298E+00	6.2176
63.34	0.16504E+00	5.9243
68.39	0.15593E+00	5.2472
58.68	0.18135E+00	5.8989
93.50	0.64239E-01	7.1074

CA48 (P,P) 35 MEV

7.009

12.80	0.73889E+00	24.6524
32.83	0.41311E+00	6.9928
23.03	0.72916E+00	7.1621
37.93	0.39594E+00	5.5046
28.14	0.49016E+00	4.9225
43.03	0.31839E+00	5.3489
63.32	0.18665E+00	4.6108
53.60	0.25236E+00	5.0404
68.37	0.17349E+00	9.7026
58.66	0.19066E+00	5.2424
73.41	0.98480E-01	5.7669
73.82	0.10497E+00	7.5367
88.48	0.47260E-01	8.5058
78.85	0.97206E-01	6.6044
93.48	0.55911E-01	6.5745
83.87	0.64733E-01	6.6656
98.47	0.44332E-01	5.5160

CA48 (P,P) 40 MEV

7.009

17.50	0.58616E+00	22.9852
32.42	0.35947E+00	10.2763
22.51	0.37354E+00	12.1562
37.52	0.34513E+00	6.0165
27.62	0.48707E+00	5.0276
42.61	0.29162E+00	5.3080
48.00	0.17506E+00	8.8685
62.90	0.16143E+00	10.6780
53.08	0.18153E+00	6.8549
67.95	0.80425E-01	6.6918
58.15	0.17779E+00	6.1026
72.90	0.66998E-01	8.3551
73.30	0.77802E-01	8.1572
88.06	0.26912E-01	11.0870
78.33	0.66676E-01	7.6343
93.06	0.20615E-01	10.7672
83.35	0.47041E-01	7.0534
98.06	0.20689E-01	8.2558

CA 48 (P,P) 25 MEV

7.320

32.47	0.82468E-01	20.3182
42.67	0.67207E-01	20.2941
48.17	0.84295E-01	18.1442
62.98	0.43334E-01	14.1915
53.25	0.46451E-01	19.8627
58.32	0.66287E-01	12.0675
73.49	0.21382E-01	17.1250
78.52	0.21223E-01	18.3855
93.16	0.16046E-01	15.9174
83.54	0.16453E-01	19.6888
98.15	0.15242E-01	11.8483

CA 48 (P,P) 29.8 MEV

7.320

27.74	0.11871E+00	17.4286
23.04	0.16354E+00	22.3134
37.95	0.76976E-01	16.6283
43.05	0.76489E-01	15.5412
48.54	0.46289E-01	22.0492
63.35	0.30589E-01	20.8873
53.62	0.34532E-01	22.2631
68.40	0.25469E-01	20.3108
73.85	0.26832E-01	22.6154
78.88	0.24541E-01	21.3286
93.51	0.24422E-01	12.1956

CA48 (P,P) 35 MEV

7.320

43.03	0.30124E-01	25.2836
48.52	0.25219E-01	34.0488
53.60	0.19278E-01	33.5294
68.38	0.20562E-01	19.9000
73.82	0.25037E-01	13.8654
88.49	0.10716E-01	26.1539
78.86	0.18158E-01	17.6470
93.49	0.10471E-01	19.6505
83.88	0.76275E-02	27.1622
98.48	0.10022E-01	14.5529

CA48 (P,P) 40 MEV

7.320

27.32	0.16476E+00	21.3061
37.52	0.58461E-01	20.3292
27.62	0.15634E+00	9.7703
42.61	0.78966E-01	13.7253
48.00	0.38762E-01	21.1875
62.91	0.16519E-01	25.0000
58.15	0.25192E-01	20.4151
72.90	0.90235E-02	27.9394
73.30	0.13929E-01	19.0488
88.07	0.78004E-02	23.4500
78.34	0.77168E-02	27.4400
93.07	0.37320E-02	30.4762
83.36	0.43524E-02	26.0769
98.06	0.28869E-02	29.4333

CA 48 (P,P) 25 MEV

7.401

22.65	0.39436E+00	10.4801
37.57	0.18778E+00	8.9258
27.77	0.25294E+00	9.1323
48.17	0.16776E+00	10.5507
62.99	0.10833E+00	7.6723
53.25	0.11588E+00	9.5709
58.33	0.13378E+00	8.1611
78.52	0.80543E-01	6.8444
93.16	0.40777E-01	7.8195
83.55	0.73304E-01	6.3042

CA 48 (P,P) 29.8 MEV

7.401

27.75	0.26647E+00	12.1273
32.85	0.19283E+00	10.0203
23.04	0.21416E+00	14.8832
28.16	0.27863E+00	7.8848
43.05	0.10843E+00	11.5975
48.55	0.12823E+00	10.7337
63.35	0.65052E-01	27.0993
53.63	0.93897E-01	10.5419
58.70	0.64397E-01	10.7154
73.85	0.59854E-01	21.3103
78.88	0.25242E-01	16.6666
93.52	0.17520E-01	18.5606

CA48 (P,P) 35 MEV

7.401

32.84	0.21095E+00	10.1056
37.94	0.15793E+00	8.0667
43.03	0.11779E+00	9.4580
48.53	0.87953E-01	12.8741
53.60	0.82778E-01	10.9178
68.38	0.56825E-01	9.6711
58.67	0.48939E-01	12.3810
73.42	0.48834E-01	8.7268
88.49	0.26103E-01	10.2632
78.86	0.41657E-01	10.3590
93.49	0.10369E-01	16.7451
83.88	0.23088E-01	11.7054
98.48	0.10022E-01	14.1647

CA48 (P,P) 40 MEV

7.401

37.52	0.11763E+00	10.8242
27.62	0.16905E+00	9.3850
42.61	0.55100E-01	17.4488
48.01	0.56323E-01	16.9677
62.91	0.44050E-01	12.0000
53.08	0.41663E-01	16.9310
67.96	0.34975E-01	12.0709
73.31	0.39067E-01	10.4696
88.07	0.99455E-02	16.7451
78.34	0.21915E-01	13.8732
93.07	0.63977E-02	22.2222
83.36	0.16572E-01	11.4747
98.06	0.65438E-02	17.3970

CA 48 (P,P) 25 MEV

7.471

32.47	0.65601E-01	22.6857
62.99	0.25352E-01	18.9818
68.04	0.29791E-01	13.8649
58.33	0.31716E-01	19.5256
93.16	0.29001E-01	9.8020
83.55	0.30528E-01	10.4910

CA 48 (P,P) 29.8 MEV

7.471

27.75	0.82357E-01	27.9118
32.86	0.62535E-01	28.1042
37.96	0.61980E-01	20.4725
28.16	0.46173E-01	25.9830
48.55	0.73597E-01	15.8660
63.36	0.17663E-01	26.6098
53.63	0.57547E-01	15.4316
73.86	0.99067E-02	39.0834
78.89	0.45574E-02	41.4615

CA48 (P,P) 35 MEV

7.471

27.73	0.85035E-01	19.8500
32.84	0.56448E-01	23.8421
43.03	0.66984E-01	13.2684
48.53	0.74418E-01	14.0496
53.61	0.52159E-01	14.1739
68.38	0.44113E-01	11.1780
58.68	0.55928E-01	10.2750
73.43	0.31221E-01	10.9829
73.83	0.39480E-01	11.0488
88.49	0.23355E-01	10.8471
93.49	0.17892E-01	12.3409
83.88	0.17316E-01	14.0833
98.48	0.75464E-02	16.2344

CA48 (P,P) 40 MEV

7.471

27.32	0.84052E-01	34.1600
37.52	0.10265E+00	12.8055
27.62	0.14510E+00	10.5412
42.62	0.73753E-01	15.8941
48.01	0.76911E-01	14.3228
62.91	0.28563E-01	14.4096
67.96	0.28916E-01	13.2952
72.91	0.23515E-01	13.0465
73.31	0.31253E-01	11.6087
88.07	0.97504E-02	17.2000
78.34	0.17903E-01	16.1724
93.07	0.72863E-02	21.9512
83.36	0.13392E-01	12.7500
98.07	0.27908E-02	31.0345

CA 48 (P,P) 25 MEV

7.521

32.47	0.88088E-01	19.3830
22.65	0.10575E+00	27.0741
62.99	0.42405E-01	13.9239
68.05	0.20665E-01	19.7402
58.33	0.46758E-01	14.9826
73.49	0.24943E-01	17.0000
93.16	0.13543E-01	16.1195
83.55	0.21022E-01	13.8869

CA 48 (P,P) 29.8 MEV

7.521

27.75	0.72664E-01	29.4333
32.86	0.70349E-01	22.6852
43.05	0.10437E+00	11.0043
48.55	0.56144E-01	18.3243
63.36	0.90464E-02	45.9048
53.63	0.42402E-01	18.8428
73.86	0.99065E-02	39.9583
78.89	0.49079E-02	50.5000

CA48 (P,P) 35 MEV

7.521

27.74	0.15093E+00	11.8732
43.03	0.40009E-01	19.7528
48.53	0.33826E-01	24.4545
53.61	0.30047E-01	19.5094
68.38	0.28725E-01	14.2857
58.68	0.25633E-01	15.3273
73.43	0.25084E-01	12.8510
88.49	0.10991E-01	15.8000
93.49	0.10166E-01	16.7400
83.88	0.12575E-01	18.3279

CA48 (P,P) 40 MEV

7.521

27.63	0.11892E+00	12.0503
48.01	0.47841E-01	18.8987
62.91	0.31660E-01	15.1413
67.96	0.22306E-01	16.1481
72.91	0.15038E-01	17.7272
73.31	0.27516E-01	12.7654
88.07	0.87754E-02	18.2000
78.34	0.15742E-01	17.4314
83.36	0.11048E-01	14.3788

CA 48 (P,P) 25 MEV

7.643

12.41	0.22318E+01	10.8270
27.36	0.19952E+01	3.9918
17.53	0.17161E+01	8.7562
22.65	0.23981E+01	3.0729
37.58	0.11381E+01	2.9233
27.77	0.17150E+01	2.8032
42.68	0.10072E+01	2.7416
48.18	0.10388E+01	3.3658
62.99	0.37240E+00	4.1856
53.26	0.81806E+00	2.8979
68.05	0.34056E+00	3.3010
58.33	0.48909E+00	3.4805
73.10	0.29960E+00	3.1924
73.50	0.29634E+00	3.7896
88.17	0.25387E+00	3.0418
93.17	0.22376E+00	3.0967
98.16	0.23905E+00	2.3909

CA 48 (P,P) 29.8 MEV

12.81	0.23548E+01	13.4947
27.75	0.19787E+01	3.7552
17.93	0.22481E+01	10.6710
32.86	0.15449E+01	3.0287
23.05	0.20228E+01	3.1285
37.96	0.12095E+01	2.6267
28.16	0.15904E+01	2.4221
43.06	0.10490E+01	2.4151
48.55	0.92479E+00	3.1870
63.36	0.33944E+00	3.8236
53.63	0.55603E+00	3.6427
68.41	0.36409E+00	3.5784
58.70	0.36503E+00	4.0000
93.52	0.17069E+00	4.2613

CA48 (P,P) 35 MEV

7.643

12.80	0.20259E+01	14.7953
27.74	0.16240E+01	4.0720
17.92	0.23508E+01	11.4934
32.84	0.14675E+01	3.5466
23.03	0.20097E+01	5.8463
37.94	0.12409E+01	2.7662
28.15	0.16725E+01	2.4014
43.04	0.84397E+00	2.7111
48.53	0.59898E+00	3.8932
63.33	0.38659E+00	3.1622
53.61	0.52382E+00	3.4361
58.68	0.40824E+00	3.5810
73.43	0.26604E+00	3.5446
73.83	0.28068E+00	4.3087
88.49	0.19014E+00	3.9783
78.86	0.23070E+00	4.2546
93.50	0.18380E+00	3.5055
83.88	0.19583E+00	3.5011
98.49	0.27710E-02	35.2341

CA48 (P,P) 40 MEV

7.643

27.32	0.19566E+01	4.5653
17.51	0.23827E+01	7.2605
32.42	0.17210E+01	4.0838
22.52	0.20704E+01	3.4317
37.52	0.12524E+01	2.6238
27.63	0.18884E+01	2.2182
42.62	0.80254E+00	2.9789
48.01	0.50867E+00	4.4060
62.91	0.38335E+00	3.2065
53.09	0.40223E+00	3.9345
67.97	0.30292E+00	3.3573
58.16	0.45530E+00	3.5209
72.91	0.28080E+00	3.4411
88.08	0.18526E+00	3.4947
78.34	0.21637E+00	3.9501
93.08	0.15781E+00	3.4786
83.37	0.19819E+00	3.0498
98.07	0.11452E+00	3.0412

* CA 48 (P,P) 25 MEV

	7.786	
48.18	0.15880E+00	11.1326
63.00	0.90792E-01	10.6091
68.05	0.88558E-01	7.9606
58.34	0.12156E+00	8.7793
73.10	0.10826E+00	6.1875
73.50	0.95608E-01	8.1584
93.17	0.67865E-01	6.9241
83.56	0.94504E-01	6.0464
98.16	0.56452E-01	6.4432

* CA 48 (P,P) 29.8 MEV

	7.786	
43.06	0.15743E+00	17.1428
48.55	0.17979E+00	8.1941
63.36	0.90887E-01	8.5450
68.42	0.11631E+00	12.0355
58.70	0.10896E+00	8.1318
78.89	0.10517E+00	8.2600
93.53	0.65569E-01	7.8178

* CA48 (P,P) 35 MEV

	7.786	
37.94	0.21514E+00	15.5443
43.04	0.25397E+00	11.6920
48.53	0.26750E+00	6.5149
63.34	0.11502E+00	6.4592
53.61	0.17517E+00	6.3819
58.68	0.14074E+00	6.5728
73.43	0.70711E-01	7.8717
73.83	0.89548E-01	8.8333
88.50	0.41901E-01	9.7574
78.87	0.74052E-01	7.9856
93.50	0.21653E-01	13.6526
83.89	0.74829E-01	13.8209
98.49	0.17923E-01	10.1053

* CA48 (P,P) 40 MEV

	7.786	
32.43	0.28367E+00	11.3000
22.52	0.33723E+00	11.8045
37.53	0.33999E+00	6.00000
27.63	0.35224E+00	5.6369
42.62	0.18436E+00	7.1835
48.01	0.17742E+00	8.7201
53.09	0.13407E+00	7.5750
67.97	0.85641E-01	7.2122
58.16	0.11311E+00	8.0840
72.91	0.67534E-01	7.8826
88.08	0.19501E-01	13.7100
78.34	0.60496E-01	8.5816
93.08	0.15283E-01	13.2558
83.37	0.36659E-01	8.1050
98.07	0.10778E-01	12.3750

* CA 48 (P,P) 25 MEV

7.940

78.55	0.61611E-01	8.6722
93.18	0.54764E-01	7.8468
83.57	0.62330E-01	7.6627
98.17	0.42893E-01	6.7034

* CA 48 (P,P) 29.8 MEV

7.940

68.42	0.48172E-01	10.4000
73.87	0.45399E-01	11.4273
78.90	0.29445E-01	14.0833
93.53	0.18583E-01	16.5428

* CA48 (P,P) 35 MEV

7.940

68.39	0.59057E-01	10.0886
58.68	0.62440E-01	10.3955
78.87	0.33109E-01	13.8172
93.50	0.20332E-01	11.4000
83.89	0.17521E-01	15.0235
98.49	0.12971E-01	12.6636

* CA48 (P,P) 40 MEV

7.940

72.91	0.23513E-01	15.1628
73.32	0.29552E-01	13.5517
93.08	0.97744E-02	18.8000
83.37	0.18580E-01	11.9189
98.07	0.80840E-02	14.0833

* CA 48 (P,P) 25 MEV

8.037

32.48	0.22288E+00	13.8319
37.59	0.17810E+00	11.5144
27.78	0.22813E+00	11.1897
42.69	0.15292E+00	10.3137
48.19	0.15955E+00	13.6700
53.28	0.18146E+00	7.4754

* CA 48 (P,P) 29.8 MEV

8.037

27.76	0.22756E+00	13.7021
37.97	0.10415E+00	13.1503
28.17	0.16503E+00	11.7156
43.07	0.12635E+00	11.0534
78.91	0.56785E-01	9.3642
93.54	0.55748E-01	8.4905

* CA48 (P,P) 35 MEV

8.037

27.74	0.33361E+00	7.9809
17.92	0.42652E+00	23.5316
32.85	0.17966E+00	12.5041
23.04	0.31807E+00	12.4779
37.95	0.18483E+00	9.9822
28.15	0.19993E+00	10.2403
53.62	0.17116E+00	7.1159
73.44	0.69370E-01	7.8461
73.84	0.70283E-01	9.7329
78.87	0.69775E-01	8.5969
93.51	0.45138E-01	7.4009
83.90	0.55243E-01	7.6828
98.50	0.32192E-01	7.7619

* CA48 (P,P) 40 MEV

8.037

72.92	0.47024E-01	9.4128
73.32	0.69292E-01	8.2598
88.09	0.36661E-01	8.8351
93.09	0.31989E-01	9.0944
83.37	0.50383E-01	6.5515
98.08	0.21269E-01	7.9547

CA 48 (P,P) 25 MEV
8.250

27.37	0.55871E+00	8.6019
17.54	0.49034E+00	22.3490
32.49	0.46998E+00	7.6733
22.66	0.66647E+00	7.7319
37.60	0.43233E+00	5.7729
27.78	0.50628E+00	6.4019
42.70	0.46825E+00	4.7337
48.20	0.50285E+00	5.7359
63.02	0.38836E+00	4.2491
53.28	0.43504E+00	4.2123
68.08	0.37879E+00	3.2132
58.36	0.46649E+00	3.5148
73.12	0.38769E+00	2.8538
73.53	0.38352E+00	3.2817
78.56	0.40848E+00	2.9656
83.58	0.34361E+00	2.7537

CA 48 (P,P) 29.8 MEV

8.250		
27.76	0.66076E+00	6.9963
23.05	0.60960E+00	7.6580
37.97	0.60507E+00	4.0889
28.17	0.58101E+00	4.8950
43.07	0.53454E+00	3.9579
48.57	0.52928E+00	4.7120
63.38	0.42674E+00	3.4591
53.65	0.49161E+00	4.1724
68.43	0.36777E+00	3.5585
73.88	0.32230E+00	4.2791
78.91	0.24115E+00	4.2078

CA48 (P,P) 35 MEV
8.250

27.74	0.80096E+00	5.1512
17.93	0.60459E+00	15.7455
32.85	0.75120E+00	5.0158
23.04	0.74594E+00	6.0251
37.95	0.66555E+00	3.8498
28.15	0.65703E+00	4.3302
43.05	0.68388E+00	3.1524
48.54	0.61904E+00	3.8550
63.35	0.33594E+00	3.7332
53.62	0.51854E+00	3.7301
68.40	0.34645E+00	3.7411
58.69	0.39042E+00	3.8998

CA48 (P,P) 40 MEV
8.250

17.51	0.50756E+00	29.8034
32.43	0.84597E+00	6.1844
22.52	0.68434E+00	8.1148
37.53	0.83509E+00	3.7116
42.63	0.69645E+00	3.2391
48.02	0.56662E+00	3.9914
53.10	0.47966E+00	3.8932
58.17	0.38202E+00	4.0187
93.09	0.48517E-01	6.8022
98.08	0.44174E-01	5.0959

* CA 48 (P,P) 25 MEV

8.364

27.38	0.41491E+00	9.6732
17.54	0.56924E+00	17.2717
32.49	0.41563E+00	8.6171
22.67	0.63247E+00	7.5340
37.60	0.27475E+00	7.5200
27.78	0.47967E+00	6.6721
42.70	0.33225E+00	5.9660
48.20	0.32062E+00	7.5758
63.02	0.22987E+00	5.8737
53.29	0.29953E+00	5.4413
68.08	0.17758E+00	5.0952
58.36	0.25517E+00	4.7978
73.13	0.21226E+00	4.0494
73.53	0.26180E+00	4.1565
78.56	0.16359E+00	5.0578
93.20	0.91717E-01	5.8170

* CA 48 (P,P) 29.8 MEV

8.364

27.76	0.36544E+00	9.5298
23.06	0.40473E+00	9.5946
37.98	0.31442E+00	6.2777
28.17	0.40503E+00	6.0985
43.07	0.26972E+00	6.2317
48.57	0.27372E+00	7.3130
63.38	0.19506E+00	5.3929
53.65	0.23368E+00	6.3990
68.44	0.20366E+00	5.0676
73.88	0.18116E+00	6.1913
78.92	0.93232E-01	7.3872

* CA43 (P,P) 35 MEV

8.364

27.75	0.30591E+00	8.3333
17.93	0.37784E+00	26.3929
23.04	0.33904E+00	17.3138
37.95	0.25844E+00	6.9440
28.15	0.27271E+00	7.5795
43.05	0.26104E+00	5.6850
48.54	0.31657E+00	5.9379
63.35	0.20426E+00	4.9694
53.62	0.31904E+00	5.0337
68.40	0.20144E+00	5.1373
58.69	0.27999E+00	4.7388
73.45	0.12912E+00	5.5124
73.85	0.18725E+00	5.7301
78.88	0.10501E+00	7.0373

* CA48 (P,P) 40 MEV

8.364

17.51	0.43378E+00	31.1100
32.43	0.41351E+00	10.0114
22.52	0.38523E+00	12.2368
37.53	0.30210E+00	7.2075
42.63	0.28056E+00	6.1762
48.02	0.31175E+00	5.9379
62.93	0.16582E+00	6.0207
53.10	0.23456E+00	6.0204
58.17	0.23899E+00	5.3459

CA 48 (P,P) 25 MEV
8.501

27.38	0.69678E+00	6.9922
17.54	0.85859E+00	12.0000
32.49	0.57277E+00	6.5523
22.67	0.68317E+00	6.2538
37.60	0.35381E+00	5.7930
27.79	0.62599E+00	4.9011
42.70	0.34516E+00	5.0408
48.21	0.29142E+00	6.8028
53.29	0.17528E+00	6.7861
68.09	0.12043E+00	6.2561
58.37	0.18566E+00	5.6083
73.13	0.11032E+00	5.8013
73.54	0.11130E+00	6.6240
78.57	0.10249E+00	6.8429
93.21	0.43577E-01	9.2905
83.60	0.84071E-01	6.0717

CA 48 (P,P) 29.8 MEV
8.501

32.87	0.49067E+00	5.3369
23.06	0.53630E+00	13.6750
37.98	0.35724E+00	5.1219
28.17	0.59806E+00	7.9346
43.08	0.23867E+00	5.8023
48.57	0.19181E+00	8.1858
63.39	0.13003E+00	6.0066
53.66	0.15678E+00	7.7143
68.44	0.13209E+00	5.9609
73.89	0.10110E+00	7.6694
78.92	0.58180E-01	9.0542

CA48 (P,P) 35 MEV
8.501

27.75	0.56502E+00	6.1316
17.93	0.10416E+01	15.5881
32.85	0.61747E+00	5.4062
23.04	0.70136E+00	8.3467
37.96	0.45699E+00	4.6072
28.16	0.57013E+00	4.2446
43.05	0.26146E+00	5.1890
48.55	0.15305E+00	8.8795
63.36	0.13408E+00	6.9119
53.63	0.14166E+00	14.1360
68.41	0.12332E+00	12.2515
58.70	0.14301E+00	6.7296
73.45	0.76831E-01	7.1146
73.85	0.87602E-01	8.2582
78.89	0.61938E-01	9.1609
83.91	0.39575E-01	8.9010

CA48 (P,P) 40 MEV
8.501

17.51	0.76336E+00	16.2329
32.43	0.54577E+00	7.4589
22.52	0.71210E+00	6.3719
37.54	0.35194E+00	5.7045
27.63	0.68765E+00	3.9728
42.63	0.20379E+00	6.9596
48.02	0.15011E+00	8.7218
62.93	0.98387E-01	8.0175
53.10	0.13259E+00	8.2094
67.98	0.67726E-01	8.3902
72.93	0.47566E-01	9.6494
73.33	0.58756E-01	9.3410
88.10	0.41535E-01	7.9249
83.38	0.35150E-01	8.8048

CA 48 (P,P) 25 MEV

8.543

27.38	0.50425E+00	8.3280
17.54	0.40459E+00	19.9675
22.67	0.54363E+00	7.0599
37.60	0.41678E+00	4.9982
27.79	0.36751E+00	6.4492
42.71	0.30848E+00	5.1225
48.21	0.28493E+00	6.6250
53.29	0.28447E+00	4.8781
68.09	0.20411E+00	4.2917
58.37	0.23400E+00	4.7743
73.14	0.18285E+00	4.1059
73.54	0.13712E+00	5.4675
78.57	0.14339E+00	5.0446
93.21	0.66839E-01	6.4890
83.60	0.11331E+00	4.8597

CA 48 (P,P) 29.8 MEV

8.543

27.76	0.36052E+00	9.0268
32.87	0.37742E+00	6.2276
23.06	0.25595E+00	10.9857
37.98	0.31435E+00	5.4069
28.17	0.30175E+00	6.1632
43.08	0.29349E+00	4.9219
48.57	0.28049E+00	6.2216
63.39	0.21699E+00	4.8274
53.66	0.27360E+00	5.4469
68.44	0.19848E+00	4.7296
73.89	0.12791E+00	6.6903
78.92	0.86919E-01	7.0766

CA48 (P,P) 35 MEV

8.543

17.93	0.32380E+00	19.1500
32.86	0.36067E+00	7.0206
23.04	0.40794E+00	7.6304
37.96	0.22881E+00	6.4396
28.16	0.30519E+00	5.9746
43.05	0.24663E+00	5.2131
48.55	0.23356E+00	6.3368
63.36	0.19139E+00	4.7713
53.63	0.22948E+00	5.6025
68.41	0.19058E+00	4.9216
58.70	0.18726E+00	5.4602
73.45	0.12218E+00	5.2489
73.86	0.10926E+00	7.1454
78.89	0.84719E-01	7.4916
83.91	0.60187E-01	6.8664

CA48 (P,P) 40 MEV

8.543

17.51	0.25155E+00	46.5517
32.44	0.24571E+00	11.3750
22.52	0.26101E+00	13.4369
37.54	0.23438E+00	7.0577
27.64	0.18984E+00	9.4331
42.63	0.22113E+00	5.8294
48.02	0.27661E+00	5.6937
62.93	0.15480E+00	5.5778
53.10	0.24794E+00	5.2452
67.98	0.12389E+00	5.6578
58.17	0.23374E+00	4.9451
72.93	0.81462E-01	6.7617
73.33	0.91360E-01	6.9442
88.10	0.36855E-01	8.5503
78.36	0.45366E-01	9.4966
83.39	0.34815E-01	8.5481

CA 48 (P,P) 25 MEV

8.589

17.55	0.52625E+00	17.2312
32.50	0.51092E+00	7.0366
22.67	0.62049E+00	6.8907
37.61	0.39990E+00	5.4212
27.79	0.44903E+00	6.1707
42.71	0.35752E+00	5.0079
48.21	0.36505E+00	6.0266
53.30	0.33694E+00	4.6940
68.09	0.16092E+00	4.6450
58.37	0.28070E+00	4.4631
73.14	0.14063E+00	4.8491
73.54	0.15700E+00	5.2495
78.58	0.11271E+00	5.9184
93.21	0.67281E-01	6.4573

CA 48 (P,P) 29.8 MEV

8.589

27.77	0.55405E+00	7.4236
32.88	0.51013E+00	5.4235
23.06	0.56427E+00	7.3348
37.98	0.35312E+00	5.0944
28.17	0.42602E+00	5.2055
43.08	0.31730E+00	4.9844
48.58	0.27366E+00	6.6066
63.39	0.15413E+00	5.8464
53.66	0.20337E+00	6.6815
68.44	0.11282E+00	6.6921
78.92	0.11040E+00	6.2921

CA48 (P,P) 35 MEV

8.589

27.75	0.65205E+00	5.7068
17.93	0.72852E+00	11.8185
32.86	0.52095E+00	6.0228
23.04	0.67091E+00	5.8659
37.96	0.39515E+00	4.8935
28.16	0.54220E+00	4.4257
43.05	0.28211E+00	4.8503
48.55	0.21204E+00	6.8898
63.36	0.13894E+00	10.2100
53.63	0.18301E+00	6.5170
68.41	0.13303E+00	6.0506
58.70	0.17281E+00	5.9110
73.45	0.10351E+00	5.7397
78.89	0.74395E-01	8.1340
83.91	0.57095E-01	7.1011

CA48 (P,P) 40 MEV

8.589

17.51	0.69825E+00	18.2671
32.44	0.62370E+00	7.1856
22.52	0.61956E+00	7.2842
37.54	0.42173E+00	5.2939
27.64	0.54485E+00	4.6420
42.63	0.28139E+00	5.4453
48.02	0.14647E+00	8.4876
62.93	0.13382E+00	6.2391
53.10	0.12923E+00	7.8556
67.99	0.77359E-01	7.3381
58.17	0.14062E+00	6.7230
72.93	0.69433E-01	7.4921
73.33	0.80491E-01	7.5105
88.10	0.55380E-01	6.9366
78.36	0.67894E-01	7.6045
83.39	0.39334E-01	7.8808

CA 48 (P,P) 25 MEV

8.658

17.55	0.18088E+00	44.3455
32.50	0.17778E+00	15.1474
22.67	0.25677E+00	15.1878
27.79	0.20926E+00	11.2770
42.71	0.12461E+00	11.0362
48.21	0.16511E+00	11.8873
63.04	0.92107E-01	10.2450
53.30	0.12605E+00	9.5428
68.09	0.94940E-01	7.7966
58.38	0.13445E+00	7.3444
73.14	0.11358E+00	6.0883
73.54	0.12257E+00	5.8862
78.58	0.10504E+00	6.6496
93.22	0.10026E+00	5.8752
83.60	0.10216E+00	5.6762
98.21	0.63614E-01	5.9702

CA 48 (P,P) 29.8 MEV

8.658

27.77	0.13790E+00	17.9824
32.88	0.20170E+00	9.7226
23.06	0.22545E+00	15.1243
37.98	0.16124E+00	9.6667
28.18	0.16492E+00	10.2844
43.08	0.16179E+00	7.7639
48.58	0.16070E+00	10.0283
63.39	0.10203E+00	7.8819
53.66	0.11863E+00	10.2806
68.45	0.84271E-01	8.7061
73.89	0.91599E-01	8.7568
78.93	0.61682E-01	9.5739
93.56	0.38229E-01	10.4861

CA48 (P,P) 35 MEV

8.658

27.75	0.26972E+00	8.8740
17.93	0.28060E+00	27.0385
32.86	0.17364E+00	22.8632
23.05	0.22206E+00	26.6474
37.96	0.17094E+00	15.5308
28.16	0.21764E+00	8.8683
43.06	0.17653E+00	7.5191
48.55	0.13582E+00	10.9050
63.36	0.84403E-01	8.8930
53.63	0.13258E+00	8.3761
58.70	0.72663E-01	10.8397
88.52	0.38740E-01	9.2199
78.89	0.63716E-01	9.9162
93.52	0.17486E-01	16.3604
83.91	0.41636E-01	9.1535

CA48 (P,P) 40 MEV

8.658

32.44	0.22206E+00	13.9468
22.53	0.24198E+00	16.3141
37.54	0.16669E+00	10.6752
27.64	0.21897E+00	9.2901
42.63	0.14004E+00	9.4056
48.03	0.11681E+00	11.5026
53.10	0.90936E-01	11.8842
58.18	0.88837E-01	9.5187
73.33	0.52301E-01	10.4286
88.10	0.37440E-01	8.9583
78.37	0.39810E-01	11.1550
93.10	0.24526E-01	10.7971

A 48 (P,P) 25 MEV
8.786

27.38	0.74799E+00	7.1014
17.55	0.63790E+00	16.0876
32.50	0.63055E+00	6.5074
22.67	0.56559E+00	7.5853
27.79	0.64734E+00	5.0941
42.71	0.54519E+00	4.0196
48.22	0.54301E+00	4.9493
63.04	0.41583E+00	3.8726
53.30	0.52149E+00	3.6532
68.10	0.37142E+00	3.1993
58.38	0.49105E+00	3.2341
73.15	0.36986E+00	2.8827
73.55	0.34959E+00	3.3913
78.59	0.30950E+00	3.3468
93.22	0.16577E+00	3.7842
83.61	0.24361E+00	3.3053

CA 48 (P,P) 29.8 MEV
8.786

12.82	0.94518E+00	38.3381
27.77	0.65070E+00	6.7844
17.94	0.72424E+00	23.5433
32.88	0.66358E+00	4.7627
23.06	0.55929E+00	7.5316
37.98	0.52109E+00	4.3460
28.18	0.61663E+00	4.3333
43.08	0.53654E+00	3.7379
48.58	0.50631E+00	4.5898
63.40	0.38400E+00	3.6502
53.66	0.53560E+00	3.8565
68.45	0.37181E+00	3.4126
73.90	0.28469E+00	4.3913
78.93	0.26915E+00	3.9193
93.56	0.10035E+00	5.8333

CA48 (P,P) 35 MEV
8.786

27.75	0.63496E+00	5.7826
17.93	0.51258E+00	21.6316
32.86	0.58765E+00	5.6010
23.05	0.66379E+00	6.2201
37.96	0.59626E+00	4.0132
28.16	0.53515E+00	4.6020
43.06	0.62119E+00	3.2921
48.55	0.58811E+00	3.7921
63.36	0.41054E+00	3.2039
53.63	0.56597E+00	3.4665
68.42	0.41365E+00	3.3153
58.70	0.50396E+00	3.2967
73.46	0.30090E+00	3.2500
73.86	0.28300E+00	4.3554
88.53	0.11457E+00	5.0935
78.89	0.20431E+00	4.7195
83.92	0.15149E+00	4.1156
98.52	0.39507E-01	7.6388

CA48 (P,P) 40 MEV
8.786

17.51	0.35992E+00	36.5301
32.44	0.63544E+00	7.2193
22.53	0.49533E+00	8.9284
37.54	0.66387E+00	4.1170
27.64	0.56795E+00	4.6934
42.63	0.54234E+00	3.6643
48.03	0.62940E+00	3.6740
62.94	0.35705E+00	3.6021
53.11	0.48050E+00	3.6783
58.18	0.50069E+00	3.3463
72.93	0.19462E+00	4.1952
73.34	0.21226E+00	4.4368
88.10	0.68250E-01	6.1943
78.37	0.16263E+00	4.7818
93.10	0.66823E-01	5.8138
83.39	0.11114E+00	4.4367
98.09	0.59865E-01	4.4502

CA 48 (P,P) 25 MEV

8.868

27.39	0.40375E+00	9.7047
17.55	0.53260E+00	17.6975
32.50	0.31617E+00	9.6331
22.68	0.43260E+00	11.5452
27.80	0.33786E+00	7.8750
42.72	0.31456E+00	5.6667
48.22	0.33500E+00	6.6159
63.05	0.26016E+00	5.1451
53.31	0.32607E+00	4.9267
68.10	0.23678E+00	4.3794
58.38	0.30013E+00	4.3193
73.15	0.19681E+00	4.0699
73.55	0.21633E+00	4.5556
78.59	0.16535E+00	5.0201
83.61	0.13487E+00	4.6030

CA 48 (P,P) 29.8 MEV

8.868

12.82	0.90907E+00	39.7475
27.77	0.41360E+00	8.8129
17.94	0.53829E+00	17.0089
32.88	0.42152E+00	6.0802
23.06	0.47394E+00	8.4447
37.99	0.36867E+00	5.4299
28.18	0.42746E+00	5.5667
43.09	0.33654E+00	5.1869
48.58	0.38804E+00	5.5801
63.40	0.29831E+00	4.1544
53.67	0.35220E+00	4.8780
68.45	0.24282E+00	4.3839
73.90	0.16256E+00	6.3909
78.93	0.10408E+00	6.7273

CA48 (P,P) 35 MEV

8.868

27.75	0.65402E+00	13.1656
17.93	0.51253E+00	18.1263
32.86	0.55496E+00	5.8690
23.05	0.63920E+00	6.0823
37.96	0.41939E+00	9.4765
28.16	0.49019E+00	9.5592
43.06	0.39479E+00	4.1479
48.56	0.45780E+00	4.5812
63.36	0.32543E+00	3.7449
53.64	0.49003E+00	3.7907
68.42	0.21149E+00	4.8640
58.71	0.39029E+00	3.8449
73.46	0.17659E+00	4.4758
73.86	0.19251E+00	5.4550
88.53	0.13435E+00	4.6953
78.90	0.14380E+00	5.7525
83.92	0.11274E+00	4.8958

CA48 (P,P) 40 MEV

8.868

17.51	0.73713E+00	21.5823
32.44	0.55036E+00	7.7854
22.53	0.64350E+00	8.2480
37.54	0.44018E+00	5.2136
27.64	0.57389E+00	4.6003
42.64	0.47338E+00	4.1383
48.03	0.44177E+00	4.3534
62.94	0.20328E+00	5.1066
53.11	0.39577E+00	4.1657
58.18	0.37384E+00	3.9720
72.93	0.11808E+00	5.7824
73.34	0.13312E+00	5.9490
78.37	0.11511E+00	5.8418
93.11	0.59004E-01	6.2319
83.39	0.10913E+00	4.5813
98.10	0.38306E-01	5.7186

II.4 Tabulated Nuclear Deformations

The following pages contain the tabulated nuclear deformations,
 $\delta_L = \beta_L R_0$, for the states observed in this experiment. For the
analysis labeled $R = I$, the value of R_0 is $1.20A^{1/3}$. For the analysis
labeled Fricke Geometry, $R_0 = 1.16A^{1/3}$.

⁴⁸
Ca 25 Mev R=I

Fricke

E*	L	δ_L	E*	L	δ_L
3.830	2	0.784	3.830	2	0.790
4.502	3	0.912	4.502	3	0.910
4.607	4	0.345	4.607	4	0.343
5.141	5	0.295	5.141	5	0.296
5.249	5	0.160	5.249	5	0.160
5.295	2	0.129	5.295	2	0.130
5.362	3	0.432	5.362	3	0.434
5.723	5	0.479	5.723	5	0.480
6.098	5	0.201	6.098	5	0.201
6.335	4	0.430	6.335	4	0.430
6.641	2	0.210	6.641	2	0.210
6.641	4	0.210	6.641	4	0.210
6.786	4	0.145	6.786	4	0.144
6.885	5	0.217	6.885	5	0.217
7.009	2	0.164	7.009	2	0.165
7.009	4	0.164	7.009	4	0.165
7.320	2	0.119	7.320	2	0.120
7.320	3	0.124	7.320	3	0.126
7.401	3	0.211	7.401	3	0.212
7.471	3	0.115	7.471	3	0.116
7.471	4	0.127	7.471	4	0.128
7.471	5	0.138	7.471	5	0.139
7.521	3	0.124	7.521	3	0.124
7.521	4	0.137	7.521	4	0.138
7.643	3	0.499	7.643	3	0.498
7.786	4	0.228	7.786	4	0.230
7.940	5	0.221	7.940	5	0.226
8.037	4	0.242	8.037	4	0.236
8.037	2	0.180	8.037	2	0.185
8.037	3	0.215	8.037	3	0.214
8.250	4	.235	8.250	4	.229
8.250	5	.235	8.250	5	.229
8.364	3	.074	8.364	3	.072
8.364	5	.301	8.364	5	.292
8.501	3	0.282	8.501	3	0.281
8.543	5	0.351	8.543	5	0.352
8.589	3	0.296	8.589	3	0.296
8.658	4	.074	8.658	4	.072
8.658	3	.148	8.658	3	.144
8.786	5	0.470	8.786	5	0.470
8.868	4	.074	8.868	4	.072
8.868	5	.305	8.868	5	.296

⁴⁸ Ca 30 Mev R=I

Fricke

E*	L	δ_L	E*	L	δ_L
3.830	2	0.705	3.830	2	0.737
4.502	3	0.833	4.502	3	0.921
4.607	4	0.268	4.607	4	0.284
5.141	5	0.230	5.141	5	0.246
5.249	5	0.125	5.249	5	0.134
5.295	2	0.126	5.295	2	0.130
5.362	3	0.390	5.362	3	0.431
5.723	5	0.453	5.723	5	0.485
6.098	5	0.175	6.098	5	0.187
6.335	4	0.382	6.335	4	0.407
6.641	2	0.190	6.641	2	0.200
6.641	4	0.190	6.641	4	0.200
6.641	4	0.407	6.786	4	0.146
6.786	4	0.138	6.885	5	0.185
6.885	5	0.173	7.009	2	0.150
7.009	2	0.137	7.009	4	0.150
7.009	4	0.137	7.320	2	0.126
7.320	2	0.122	7.320	3	0.134
7.320	3	0.121	7.401	3	0.184
7.401	3	0.166	7.471	3	0.117
7.471	3	0.106	7.471	4	0.126
7.471	4	0.119	7.471	5	0.133
7.471	5	0.124	7.521	3	0.119
7.521	3	0.103	7.521	4	0.127
7.521	4	0.120	7.786	4	0.253
7.786	4	0.240	7.940	5	0.174
7.940	5	0.167	8.037	4	0.191
8.037	4	0.182	8.037	2	0.191
8.037	2	0.185	8.037	3	0.192
8.037	3	0.172	8.250	4	0.229
8.250	4	0.218	8.250	5	0.229
8.250	5	0.218	8.364	3	0.068
8.364	3	0.065	8.364	5	0.263
8.364	5	0.253	8.501	3	0.270
8.501	3	0.244	8.543	5	0.331
8.543	5	0.307	8.589	3	0.284
8.589	3	0.257	8.658	4	0.072
8.658	4	0.070	8.658	3	0.144
8.658	3	0.140	8.786	5	0.461
8.786	5	0.431	8.868	4	0.076
8.868	4	0.074	8.868	5	0.309
8.868	5	0.292			

Ca⁴⁸ 35 Mev R=I

Fricke

E*	L	δ_L	E*	L	δ_L
3.830	2	0.700	3.830	2	0.729
4.502	3	0.865	4.502	3	0.893
4.607	4	0.253	4.607	4	0.265
5.141	5	0.222	5.141	5	0.237
5.249	5	0.116	5.249	5	0.124
5.295	2	0.107	5.295	2	0.111
5.362	3	0.422	5.362	3	0.438
5.723	5	0.457	5.723	5	0.487
6.098	5	0.156	6.098	5	0.167
6.335	4	0.377	6.335	4	0.396
6.641	2	0.180	6.641	2	0.190
6.641	4	0.180	6.641	4	0.190
6.785	4	0.148	6.786	4	0.154
6.885	5	0.158	6.885	5	0.168
7.009	2	0.142	7.009	2	0.147
7.009	4	0.142	7.009	4	0.147
7.320	2	0.097	7.320	2	0.101
7.320	3	0.101	7.320	3	0.106
7.401	3	0.168	7.401	3	0.175
7.471	3	0.135	7.471	3	0.140
7.471	4	0.142	7.471	4	0.148
7.471	5	0.144	7.471	5	0.154
7.521	3	0.118	7.521	3	0.122
7.521	4	0.122	7.521	4	0.128
7.643	3	0.470	7.643	3	0.487
7.785	4	0.248	7.786	4	0.260
7.940	5	0.171	7.940	5	0.181
8.037	4	0.230	8.037	4	0.242
8.037	2	0.209	8.037	2	0.216
8.037	3	0.218	8.037	3	0.227
8.250	4	0.223	8.250	4	0.229
8.250	5	0.223	8.250	5	0.229
8.364	3	0.065	8.364	3	0.068
8.364	5	0.253	8.364	5	0.263
8.501	3	0.270	8.501	3	0.280
8.543	5	0.291	8.543	5	0.311
8.589	3	0.273	8.589	3	0.282
8.658	4	0.070	8.658	4	0.072
8.658	3	0.140	8.658	3	0.144
8.786	5	0.426	8.786	5	0.454
8.868	4	0.079	8.868	4	0.080
8.868	5	0.314	8.868	5	0.326

Ca^{48} 40 Mev R=I

Fricke

E^*	L	δ_L	E^*	L	δ_L
3.830	2	0.677	3.830	2	0.702
4.502	3	0.857	4.502	3	0.884
4.607	4	0.208	4.607	4	0.216
5.141	5	0.208	5.141	5	0.220
5.249	5	0.106	5.249	5	0.112
5.295	2	0.110	5.295	2	0.113
5.362	3	0.443	5.362	3	0.458
5.723	5	0.444	5.723	5	0.469
6.093	5	0.143	6.098	5	0.151
6.335	4	0.354	6.335	4	0.369
6.641	2	0.170	6.641	2	0.180
6.641	4	0.170	6.641	4	0.180
6.786	4	0.132	6.786	4	0.138
6.885	5	0.142	6.885	5	0.150
7.009	2	0.121	7.009	2	0.127
7.009	4	0.121	7.009	4	0.127
7.320	2	0.113	7.320	2	0.117
7.320	3	0.113	7.320	3	0.117
7.401	3	0.142	7.401	3	0.147
7.471	3	0.139	7.471	3	0.144
7.471	4	0.141	7.471	4	0.146
7.471	5	0.145	7.471	5	0.153
7.521	3	0.125	7.521	3	0.129
7.521	4	0.130	7.521	4	0.135
7.643	3	0.471	7.643	3	0.486
7.786	4	0.234	7.786	4	0.243
7.940	5	0.146	7.940	5	0.155
8.037	4	0.239	8.037	4	0.258
8.037	3	0.248	8.037	2	0.244
8.037	2	0.222	8.037	3	0.277
8.250	4	.210	8.250	4	.216
8.250	5	.210	8.250	5	.216
8.364	3	.061	8.364	3	.063
8.364	5	.244	8.364	5	.250
8.501	3	0.253	8.501	3	0.261
8.543	5	0.265	8.543	5	0.279
8.589	3	0.262	8.589	3	0.270
8.653	4	.065	8.658	4	.068
8.658	3	.130	8.658	3	.136
8.786	5	0.402	8.786	5	0.424
8.868	4	.074	8.868	4	.076
8.868	5	.296	8.868	5	.305

II.5 Quantities calculated from nuclear deformations.

On the following pages are tabulated the parameters calculated from the nuclear deformations. The L is normalized to an interaction radius of $1.25A^{1/3}$. The two models used are the uniform charge distribution with $r_0 = 1.25F$ and the Wine bottle charge distribution with $r_0 = 1.03F$, $a = .52F$, and $w = -0.03$ (Fr 68).

CA48 40 MEV R=I

THE EVALUATION OF $\langle R^* L \rangle$ WAS DONE USING A UNIFORM CHARGE DISTRIBUTION.

THE NUCLEAR RADIUS PARAMETER=1.24 F THE NUCLEAR SURFACE THICKNESS PARAMETER=0.500 FWINE BOTTLE= 0.029 SEP 08, 'I

Z = 20 A = 48 BEAM ENERGY IS 40.210MEV

EX	L	BETA	B(EL)	G(SP)	G(U)	D(L)	C(L)	D(IRRF) / D(L)	B(EL) / NEWSR
3.0830	2	0.149	0.306E+03	3.6	4.1	0.289E+02	0.424E+03	0.097	0.151
4.502	3	0.189	0.994E+04	5.9	7.2	0.215E+02	0.436E+03	0.130	0.222
4.607	4	0.046	0.119E+05	0.4	0.5	0.458E+03	0.973E+04	0.006	0.012
5.141	5	0.046	0.242E+05	0.4	0.5	0.502E+03	0.133E+05	0.006	0.012
5.249	5	0.023	0.627E+05	0.1	0.1	0.189E+04	0.522E+05	0.001	0.003
5.295	2	0.024	0.807E+01	0.1	0.1	0.792E+03	0.222E+05	0.004	0.004
5.362	3	0.098	0.266E+04	1.5	1.9	0.675E+02	0.194E+04	0.041	0.059
5.723	5	0.098	0.110E+07	1.8	2.5	0.990E+02	0.324E+04	0.028	0.055
6.098	5	0.031	0.114E+06	0.2	0.3	0.896E+03	0.333E+05	0.003	0.006
6.335	4	0.078	0.345E+05	1.1	1.4	0.115E+03	0.462E+04	0.024	0.036
6.641	2	0.037	0.193E+02	0.2	0.3	0.265E+03	0.117E+05	0.011	0.010
6.641	4	0.037	0.795E+04	0.2	0.3	0.476E+03	0.210E+05	0.006	0.008
6.786	4	0.029	0.479E+04	0.1	0.2	0.773E+03	0.356E+05	0.004	0.005
6.885	5	0.031	0.113E+06	0.2	0.3	0.805E+03	0.381E+05	0.003	0.006
7.009	2	0.027	0.976E+01	0.1	0.1	0.495E+03	0.243E+05	0.006	0.005
7.009	4	0.027	0.403E+04	0.1	0.2	0.891E+03	0.437E+05	0.003	0.004
7.320	2	0.025	0.851E+01	0.1	0.1	0.543E+03	0.291E+05	0.005	0.004
7.320	3	0.025	0.173E+03	0.1	0.1	0.760E+03	0.407E+05	0.004	0.004
7.401	3	0.031	0.273E+03	0.2	0.2	0.476E+03	0.261E+05	0.006	0.006
7.471	3	0.031	0.262E+03	0.2	0.2	0.492E+03	0.275E+05	0.006	0.006
7.471	4	0.031	0.547E+04	0.2	0.2	0.615E+03	0.343E+05	0.005	0.006
7.471	5	0.032	0.117E+06	0.2	0.3	0.711E+03	0.397E+05	0.004	0.006

CA48 40 MEV R=1

THE EVALUATION OF $\langle R^* L \rangle$ WAS DONE USING A UNIFORM CHARGE DISTRIBUTION.

THE NUCLEAR RADIUS PARAMETER=1.24 F THE NUCLEAR SURFACE THICKNESS PARAMETER=0.500 FWINE BOTTLE= 0.0

Z= 20 A= 48 BEAM ENERGY IS 40.210MEV

EX	L	BETA	B(EL)	G(SP)	G(U)	D(L)	C(L)	D(IRRF) / D(L)	B(EL) / NEWSR
7.521	3	0.028	0.212E+03	0.1	0.2	0.605E+03	0.342E+05	0.005	0.005
7.521	4	0.029	0.465E+04	0.1	0.2	0.719E+03	0.407E+05	0.004	0.005
7.643	3	0.104	0.300E+04	1.8	2.2	0.419E+02	0.245E+04	0.067	0.067
7.786	4	0.052	0.151E+05	0.5	0.6	0.214E+03	0.130E+05	0.013	0.016
7.940	5	0.032	0.119E+06	0.2	0.3	0.660E+03	0.416E+05	0.004	0.006
8.037	4	0.053	0.157E+05	0.5	0.6	0.199E+03	0.129E+05	0.014	0.016
8.037	3	0.055	0.833E+03	0.5	0.6	0.144E+03	0.929E+04	0.019	0.019
8.037	2	0.049	0.329E+02	0.4	0.4	0.128E+03	0.828E+04	0.022	0.016
8.250	4	0.046	0.121E+05	0.4	0.5	0.251E+03	0.171E+05	0.011	0.013
8.250	5	0.046	0.246E+06	0.4	0.6	0.307E+03	0.209E+05	0.009	0.012
8.364	3	0.013	0.504E+02	0.0	0	0.228E+04	0.160E+06	0.001	0.001
8.364	5	0.054	0.332E+06	0.5	0.8	0.224E+03	0.157E+05	0.012	0.017
8.501	3	0.056	0.867E+03	0.5	0.6	0.131E+03	0.944E+04	0.021	0.019
8.543	5	0.058	0.392E+06	0.6	0.9	0.186E+03	0.136E+05	0.015	0.020
8.589	3	0.058	0.929E+03	0.6	0.7	0.121E+03	0.889E+04	0.023	0.021
8.658	4	0.014	0.116E+04	0.0	0	0.250E+04	0.187E+06	0.001	0.001
8.658	3	0.029	0.229E+03	0.1	0.2	0.436E+03	0.364E+05	0.006	0.005
8.786	5	0.088	0.902E+06	1.5	2.0	0.787E+02	0.607E+04	0.036	0.045
8.868	4	0.016	0.151E+04	0.0	0.1	0.188E+04	0.148E+06	0.001	0.002
8.868	5	0.065	0.489E+06	0.8	1.1	0.144E+03	0.113E+05	0.019	0.024

CA48 35 MEV R=I

THE EVALUATION OF $\langle R^* L \rangle$ WAS DONE USING A UNIFORM CHARGE DISTRIBUTION.

THE NUCLEAR RADIUS PARAMETER=1.24 F THE NUCLEAR SURFACE THICKNESS PARAMETER=0.500 FWINE BOTTLE= 0.00

Z = 20 A = 48 BEAM ENERGY IS 35.000MEV

EX	L	BETA	B(EL)	G(SP)	G(SP)	D(L)	C(L)	D(IRRθT)/D(L)	B(EL)/NEWSR
3.0830	2	0.0154	0.0327E+03	3.08	4.04	0.0271E+02	0.0397E+03	0.0103	0.0161
4.0502	3	0.0190	0.0101E+05	6.00	7.03	0.0211E+02	0.0428E+03	0.0132	0.0226
4.0607	4	0.0056	0.0176E+C5	0.05	0.07	0.0310E+03	0.0658E+04	0.009	0.018
5.0141	5	0.0049	0.0275E+C6	0.04	0.06	0.0441E+C3	0.0117E+05	0.006	0.014
5.0249	5	0.0026	0.0751E+C5	0.01	0.02	0.0158E+04	0.0436E+05	0.002	0.004
5.0295	2	0.0024	0.0763E+01	0.01	0.01	0.0837E+03	0.0235E+05	0.003	0.004
5.0362	3	0.0093	0.0241E+04	1.04	1.07	0.0744E+02	0.0214E+04	0.038	0.054
5.0723	5	0.0101	0.0117E+07	1.09	2.06	0.0934E+02	0.0306E+04	0.030	0.058
6.0098	5	0.0034	0.0136E+06	0.02	0.03	0.0753E+03	0.0280E+05	0.004	0.007
6.0335	4	0.0083	0.0391E+05	1.02	1.06	0.0101E+03	0.0407E+04	0.028	0.041
6.0641	2	0.0040	0.0216E+02	0.03	0.03	0.0236E+03	0.0104E+05	0.012	0.011
6.0641	4	0.0040	0.0891E+C4	0.03	0.04	0.0425E+03	0.0137E+05	0.007	0.009
6.0786	4	0.0033	0.0602E+C4	0.02	0.02	0.0615E+03	0.0283E+05	0.005	0.006
6.0885	5	0.0035	0.0139E+06	0.02	0.03	0.0650E+03	0.0398E+05	0.004	0.007
7.0009	2	0.0031	0.0134E+02	0.02	0.02	0.0359E+03	0.0176E+05	0.008	0.007
7.0009	4	0.0031	0.0554E+04	0.02	0.02	0.0647E+03	0.0318E+05	0.004	0.006
7.0320	2	0.0021	0.0627E+01	0.01	0.01	0.0737E+03	0.0395E+05	0.004	0.003
7.0320	3	0.0022	0.0138E+03	0.01	0.01	0.0952E+03	0.0510E+05	0.003	0.003
7.0401	3	0.0037	0.0382E+03	0.02	0.03	0.0340E+03	0.0186E+05	0.008	0.009
7.0471	3	0.0030	0.0247E+03	0.01	0.02	0.0522E+03	0.0291E+05	0.005	0.006
7.0471	4	0.0031	0.0554E+04	0.02	0.02	0.0607E+03	0.0339E+05	0.005	0.006
7.0471	5	0.0032	0.0116E+06	0.02	0.03	0.0721E+03	0.0402E+05	0.004	0.006

CA48 35 MEV R=1

04:30 SEP '08, '

THE EVALUATION OF $\langle R^* L \rangle$ WAS DONE USING A UNIFORM CHARGE DISTRIBUTION.

THE NUCLEAR RADIUS PARAMETER=1.24 F THE NUCLEAR SURFACE THICKNESS PARAMETER=0.500 FWINE BOTTLE= 0.0

Z= 20 A= 48 BEAM ENERGY IS 35.000MEV

EX	L	BETA	B(EL)	G(SP)	GU(SP)	D(L)	C(L)	D(IRR&T)/D(L)	B(EL)/NEWSR
7.521	3	0.026	0.189E+03	0.1	0.1	0.1	0.679E+03	0.384E+05	0.004
7.521	4	0.027	0.409E+04	0.1	0.2	0.2	0.816E+03	0.462E+05	0.004
7.643	3	0.0103	0.299E+04	1.8	0.5	0.7	0.421E+02	0.246E+04	0.067
7.786	4	0.055	0.169E+05	0.5	0.5	0.7	0.191E+03	0.116E+05	0.018
7.940	5	0.038	0.163E+06	0.3	0.4	0.4	0.481E+03	0.303E+05	0.008
8.037	4	0.051	0.145E+05	0.5	0.6	0.6	0.215E+03	0.139E+05	0.015
8.037	2	0.046	0.291E+02	0.3	0.4	0.4	0.145E+03	0.934E+04	0.014
8.037	3	0.048	0.643E+03	0.4	0.5	0.5	0.186E+03	0.120E+05	0.014
8.250	4	0.049	0.137E+05	0.4	0.6	0.6	0.223E+03	0.152E+05	0.014
8.250	5	0.049	0.278E+06	0.5	0.6	0.6	0.272E+03	0.185E+05	0.014
8.364	3	0.014	0.572E+C2	0.0	0.0	0.0	0.201E+04	0.141E+06	0.001
8.364	5	0.056	0.357E+06	0.6	0.6	0.8	0.209E+03	0.146E+05	0.018
8.501	3	0.059	0.987E+03	0.6	0.7	0.7	0.115E+03	0.829E+04	0.022
8.543	5	0.064	0.473E+06	0.8	1.1	1.1	0.154E+03	0.113E+05	0.024
8.589	3	0.060	0.101E+04	0.6	0.7	0.7	0.111E+03	0.819E+04	0.023
8.658	4	0.015	0.135E+04	0.0	0.1	0.1	0.215E+04	0.161E+06	0.001
8.658	3	0.031	0.265E+03	0.2	0.2	0.2	0.419E+03	0.314E+05	0.006
8.786	5	0.094	0.101E+07	1.7	2.3	2.3	0.701E+02	0.541E+04	0.050
8.868	4	0.017	0.172E+C4	0.1	0.1	0.1	0.165E+04	0.130E+06	0.002
8.868	5	0.069	0.550E+06	0.9	1.2	0.9	0.128E+03	0.100E+05	0.027

CA48 30 MEV R=1

04:29 SEP 08, 1

THE EVALUATION OF <R*L> WAS DONE USING A UNIFORM CHARGE DISTRIBUTION.

THE NUCLEAR RADIUS PARAMETER=1.24 F THE NUCLEAR SURFACE THICKNESS PARAMETER=0.500 F WINE BOTTLE= 0.0

Z= 20 A= 48 BEAM ENERGY IS 29.830MEV

EX	L	BETA	B(EL)	G(SP)	G(SP)	D(L)	C(L)	D(IRROT)/D(L)	B(EL)/NEWSR
3.0830	2	0.155	0.331E+03	3.9	4.4	0.257E+02	0.391E+03	0.105	0.164
4.0502	3	0.183	0.939E+04	5.6	6.8	0.228E+02	0.461E+03	0.123	0.210
4.0607	4	0.059	0.197E+05	0.6	0.8	0.276E+03	0.586E+04	0.010	0.021
5.0141	5	0.051	0.295E+06	0.5	0.7	0.411E+03	0.109E+05	0.007	0.015
5.0249	5	0.028	0.872E+05	0.1	0.2	0.136E+04	0.375E+05	0.002	0.004
5.0295	2	0.028	0.106E+02	0.1	0.1	0.604E+03	0.169E+05	0.005	0.005
5.0362	3	0.086	0.206E+04	1.2	1.5	0.872E+02	0.251E+04	0.032	0.046
5.0723	5	0.100	0.115E+07	1.9	2.6	0.951E+02	0.311E+04	0.029	0.057
6.0098	5	0.039	0.171E+06	0.3	0.4	0.538E+03	0.222E+05	0.005	0.009
6.0335	4	0.084	0.401E+05	1.2	1.6	0.939E+02	0.397E+04	0.028	0.042
6.0641	2	0.042	0.241E+02	0.3	0.3	0.212E+03	0.934E+04	0.013	0.012
6.0641	4	0.042	0.992E+04	0.3	0.4	0.381E+03	0.168E+05	0.007	0.010
6.0641	4	0.090	0.455E+05	1.4	1.8	0.831E+02	0.366E+04	0.034	0.048
6.0786	4	0.030	0.524E+04	0.2	0.2	0.707E+03	0.326E+05	0.004	0.005
6.0885	5	0.038	0.167E+06	0.3	0.4	0.542E+03	0.257E+05	0.005	0.008
7.0009	2	0.030	0.125E+02	0.1	0.2	0.336E+03	0.190E+05	0.007	0.006
7.0009	4	0.030	0.516E+04	0.2	0.2	0.695E+03	0.341E+05	0.004	0.005
7.0320	2	0.027	0.992E+01	0.1	0.1	0.466E+03	0.250E+05	0.006	0.005
7.0320	3	0.027	0.198E+03	0.1	0.1	0.663E+03	0.355E+05	0.004	0.004
7.0401	3	0.037	0.373E+03	0.2	0.3	0.349E+03	0.191E+05	0.008	0.008
7.0471	3	0.023	0.152E+03	0.1	0.1	0.847E+03	0.473E+05	0.003	0.003
7.0471	4	0.026	0.389E+04	0.1	0.2	0.864E+03	0.482E+05	0.003	0.004
7.0471	5	0.027	0.858E+05	0.1	0.2	0.972E+03	0.543E+05	0.003	0.004

CA48 30 MEV R=1

04:30 SEP 08, 1

THE EVALUATION OF $\langle R^* L \rangle$ WAS DONE USING A UNIFORM CHARGE DISTRIBUTION.

THE NUCLEAR RADIUS PARAMETER=1.24 F THE NUCLEAR SURFACE THICKNESS PARAMETER=0.500 FWINE BFTTLE= 0.00

Z= 20 A= 48 BEAM ENERGY IS 29.830MEV

EX	L	BETA	B(EL)	G(SP)	G(U)	D(L)	C(L)	D(IIRR&T)/D(L)	B(EL)/NEWSR
7.521	3	0.024	0.158E+03	0.1	0.1	0.810E+03	0.458E+05	0.003	0.004
7.521	4	0.026	0.396E+03	0.1	0.2	0.844E+03	0.477E+05	0.003	0.004
7.786	4	0.053	0.158E+03	0.5	0.6	0.204E+03	0.124E+05	0.017	0.017
7.940	5	0.037	0.156E+03	0.3	0.4	0.504E+03	0.318E+05	0.006	0.008
8.037	4	0.040	0.911E+03	0.3	0.4	0.343E+03	0.222E+05	0.008	0.010
8.037	2	0.041	0.228E+02	0.3	0.3	0.185E+03	0.119E+05	0.015	0.011
8.037	3	0.038	0.401E+03	0.2	0.3	0.299E+03	0.193E+05	0.009	0.009
8.250	4	0.048	0.131E+05	0.4	0.5	0.233E+03	0.159E+05	0.012	0.014
8.250	5	0.048	0.265E+05	0.4	0.6	0.285E+03	0.194E+05	0.010	0.013
8.364	3	0.014	0.572E+02	0.0	0.0	0.201E+04	0.141E+06	0.001	0.001
8.364	5	0.056	0.357E+06	0.6	0.8	0.209E+03	0.146E+05	0.013	0.018
8.501	3	0.054	0.806E+03	0.5	0.6	0.140E+03	0.101E+05	0.020	0.018
8.543	5	0.068	0.526E+05	0.9	1.2	0.139E+03	0.101E+05	0.020	0.026
8.589	3	0.057	0.894E+03	0.5	0.6	0.125E+03	0.924E+04	0.022	0.020
8.658	4	0.015	0.135E+04	0.0	0.1	0.215E+04	0.161E+06	0.001	0.001
8.658	3	0.031	0.265E+03	0.2	0.2	0.419E+03	0.314E+05	0.007	0.006
8.786	5	0.095	0.194E+07	1.7	2.4	0.684E+02	0.528E+04	0.052	0.041
8.868	4	0.016	0.151E+04	0.0	0.1	0.188E+04	0.148E+06	0.001	0.002
8.868	5	0.064	0.476E+06	0.8	1.1	0.148E+03	0.116E+05	0.019	0.024

CA48 25 MEV R=1

THE EVALUATION OF $\langle R^* L \rangle$ WAS DONE USING A UNIFORM CHARGE DISTRIBUTION.

THE NUCLEAR RADIUS PARAMETER=1.24 F THE NUCLEAR SURFACE THICKNESS PARAMETER=0.500 FWINE BOTTLE= 0.000

Z= 20 A= 48 BEAM ENERGY IS 25.110MEV

EX	L	BETA	B(EL)	G(SP)	GU(SP)	D(L)	C(L)	D(IRRFIT)/D(L)	B(EL)/NEWSR
3.830	2	0.173	0.410E+03	4.8	5.5	0.216E+02	0.316E+03	0.129	0.202
4.502	3	0.201	0.113E+05	6.7	8.2	0.190E+02	0.385E+03	0.147	0.251
4.607	4	0.076	0.327E+05	1.0	1.3	0.167E+03	0.354E+04	0.017	0.034
5.141	5	0.065	0.486E+06	0.8	1.1	0.250E+03	0.660E+04	0.011	0.024
5.249	5	0.035	0.143E+06	0.2	0.3	0.831E+03	0.229E+05	0.003	0.007
5.295	2	0.028	0.111E+02	0.1	0.1	0.576E+03	0.162E+05	0.005	0.005
5.362	3	0.095	0.253E+04	1.5	1.8	0.710E+02	0.204E+04	0.039	0.056
5.723	5	0.105	0.128E+07	2.1	2.9	0.851E+02	0.279E+04	0.033	0.064
6.098	5	0.044	0.226E+06	0.4	0.5	0.453E+03	0.169E+05	0.006	0.011
6.335	4	0.095	0.508E+05	1.6	2.1	0.780E+02	0.313E+04	0.036	0.053
6.641	2	0.046	0.294E+02	0.3	0.4	0.173E+03	0.765E+04	0.016	0.015
6.641	4	0.046	0.121E+05	0.4	0.5	0.312E+03	0.138E+05	0.009	0.013
6.786	4	0.032	0.578E+04	0.2	0.2	0.641E+03	0.295E+05	0.004	0.006
6.885	5	0.048	0.263E+06	0.4	0.6	0.345E+03	0.163E+05	0.008	0.013
7.009	2	0.036	0.179E+02	0.2	0.2	0.269E+03	0.132E+05	0.010	0.009
7.009	4	0.036	0.739E+04	0.2	0.3	0.485E+03	0.238E+05	0.006	0.008
7.320	2	0.026	0.944E+01	0.1	0.1	0.490E+03	0.262E+05	0.006	0.005
7.320	3	0.027	0.208E+03	0.1	0.2	0.631E+03	0.338E+05	0.004	0.005
7.401	3	0.046	0.603E+03	0.4	0.4	0.216E+03	0.118E+05	0.013	0.013
7.471	3	0.025	0.179E+03	0.1	0.1	0.719E+03	0.402E+05	0.004	0.004
7.471	4	0.028	0.443E+04	0.1	0.2	0.758E+03	0.423E+05	0.004	0.005
7.471	5	0.030	0.106E+06	0.2	0.2	0.785E+03	0.433E+05	0.004	0.005

CA48 25 MEV R=1

04:30 SEP 08, 1

THE EVALUATION OF $\langle R^* L \rangle$ HAS DONE USING A UNIFORM CHARGE DISTRIBUTION.

THE NUCLEAR RADIUS PARAMETER=1.24 F THE NUCLEAR SURFACE THICKNESS PARAMETER=0.500 FWINE BOTTLE= 0.0

Z= 20 A= 48 BEAM ENERGY IS 25.110MEV

EX	L	BETA	B(L)	G(SP)	G(SP)	D(L)	C(L)	D(IRR&T)/D(L)	B(L)/NEWSR
7.521	3	0.027	0.208E+03	0.1	0.2	0.2	0.615E+03	0.348E+05	0.005
7.521	4	0.030	0.516E+04	0.2	2.0	2.4	0.647E+03	0.366E+05	0.005
7.643	3	0.110	0.337E+04	0.4	0.4	0.6	0.373E+02	0.218E+04	0.075
7.786	4	0.050	0.143E+05	0.5	0.4	0.6	0.226E+03	0.137E+05	0.015
7.940	5	0.049	0.273E+06	0.6	0.4	0.6	0.288E+03	0.182E+05	0.014
8.037	4	0.053	0.161E+05	0.5	0.5	0.6	0.194E+03	0.125E+05	0.017
8.037	2	0.040	0.216E+02	0.3	0.3	0.3	0.195E+03	0.126E+05	0.011
8.037	3	0.047	0.626E+03	0.4	0.5	0.5	0.191E+03	0.124E+05	0.014
8.250	4	0.052	0.152E+05	0.5	0.5	0.6	0.201E+03	0.137E+05	0.016
8.250	5	0.052	0.308E+06	0.5	0.5	0.7	0.245E+03	0.167E+05	0.015
8.364	3	0.016	0.741E+02	0.0	0.1	0.1	0.155E+04	0.109E+06	0.002
8.364	5	0.066	0.566E+06	0.8	0.8	1.1	0.147E+03	0.103E+05	0.025
8.501	3	0.062	0.108E+04	0.6	0.6	0.8	0.105E+03	0.760E+04	0.024
8.543	5	0.077	0.688E+05	1.1	1.1	1.6	0.106E+03	0.774E+04	0.034
8.589	3	0.065	0.119E+04	0.7	0.9	0.9	0.944E+02	0.697E+04	0.026
8.658	4	0.016	0.151E+04	0.0	0.1	0.1	0.193E+04	0.144E+06	0.002
8.658	3	0.033	0.297E+03	0.2	0.2	0.2	0.375E+03	0.281E+05	0.007
8.786	5	0.103	0.123E+07	2.0	2.0	2.8	0.575E+02	0.444E+04	0.061
8.868	4	0.016	0.151E+04	0.0	0.1	0.1	0.188E+04	0.148E+06	0.002
8.868	5	0.067	0.519E+06	0.8	1.2	0.1	0.135E+03	0.106E+05	0.026

CA48 40 MEV FRICKE

THE EVALUATION OF $\langle R^* L \rangle$ WAS DONE USING A UNIFORM CHARGE DISTRIBUTION.

THE NUCLEAR RADIUS PARAMETER=1.24 F THE NUCLEAR SURFACE THICKNESS PARAMETER=0.500 FINE BOTTLE= 0.00

Z= 20 A= 48 BEAM ENERGY IS 40.210MEV

EX	L	BETA	B(EL)	G(SP)	GU(SP)	D(L)	C(L)	D(IIRRGT)/D(L)	B(EL)/NEWSR
3.830	2	0.155	0.329E+03	3.9	4.4	0.269E+02	0.395E+03	0.104	0.162
4.502	3	0.195	0.106E+05	6.3	7.7	0.202E+02	0.409E+03	0.138	0.236
4.607	4	0.048	0.128E+05	0.4	0.5	0.425E+03	0.902E+04	0.007	0.013
5.141	5	0.048	0.270E+05	0.4	0.6	0.449E+03	0.119E+05	0.006	0.013
5.249	5	0.025	0.700E+05	0.1	0.2	0.170E+04	0.467E+05	0.002	0.003
5.295	2	0.025	0.851E+04	0.1	0.1	0.751E+03	0.211E+05	0.004	0.004
5.362	3	0.101	0.284E+04	1.7	2.1	0.632E+02	0.182E+04	0.044	0.063
5.723	5	0.103	0.123E+07	2.0	2.8	0.887E+02	0.291E+04	0.031	0.061
6.098	5	0.033	0.127E+06	0.2	0.3	0.803E+03	0.299E+05	0.003	0.006
6.335	4	0.081	0.374E+05	1.2	1.5	0.106E+03	0.425E+04	0.026	0.039
6.641	2	0.040	0.216E+02	0.3	0.3	0.236E+03	0.104E+05	0.012	0.011
6.641	4	0.040	0.891E+04	0.3	0.4	0.425E+03	0.187E+05	0.007	0.009
6.786	4	0.030	0.524E+04	0.2	0.2	0.707E+03	0.326E+05	0.004	0.005
6.885	5	0.033	0.126E+06	0.2	0.3	0.721E+03	0.342E+05	0.004	0.006
7.009	2	0.028	0.108E+02	0.1	0.1	0.449E+03	0.221E+05	0.006	0.005
7.009	4	0.028	0.443E+04	0.1	0.2	0.808E+03	0.397E+05	0.003	0.005
7.320	2	0.026	0.913E+04	0.1	0.1	0.507E+03	0.271E+05	0.006	0.005
7.320	3	0.026	0.185E+03	0.1	0.1	0.709E+03	0.380E+05	0.004	0.004
7.401	3	0.032	0.293E+03	0.2	0.2	0.444E+03	0.243E+05	0.006	0.007
7.471	3	0.032	0.281E+03	0.2	0.2	0.459E+03	0.256E+05	0.006	0.006
7.471	4	0.032	0.586E+04	0.2	0.3	0.574E+03	0.320E+05	0.005	0.006
7.471	5	0.034	0.131E+06	0.2	0.3	0.639E+03	0.356E+05	0.004	0.007

CA48 40 MEV FRICKE

04:30 SEP 08, 1

THE EVALUATION OF $\langle R^* L \rangle$ WAS DONE USING A UNIFORM CHARGE DISTRIBUTION.

THE NUCLEAR RADIUS PARAMETER=1.24 F THE NUCLEAR SURFACE THICKNESS PARAMETER=0.500 FWINE BOTTLE= 0.0

Z= 20 A= 48 BEAM ENERGY IS 40.210MEV

EX	L	BETA	B(L)	G(SP)	G(SP)	D(L)	C(L)	D(IRRGT)/D(L)	B(L)/NEWSR
7.521	3	0.028	0.225E+03	0.1	0.2	0.568E+03	0.321E+05	0.005	0.005
7.521	4	0.030	0.501E+04	0.2	0.2	0.667E+03	0.377E+05	0.004	0.005
7.643	3	0.107	0.320E+04	1.9	2.3	0.394E+02	0.230E+04	0.071	0.071
7.786	4	0.053	0.162E+05	0.5	0.7	0.199E+03	0.120E+05	0.017	0.017
7.940	5	0.034	0.134E+06	0.2	0.3	0.586E+03	0.369E+05	0.005	0.007
8.037	4	0.057	0.183E+05	0.6	0.7	0.171E+03	0.110E+05	0.016	0.019
8.037	2	0.054	0.397E+02	0.5	0.5	0.106E+03	0.685E+04	0.026	0.020
8.037	3	0.061	0.104E+04	0.6	0.8	0.115E+03	0.744E+04	0.024	0.023
8.250	4	0.048	0.128E+05	0.4	0.5	0.237E+03	0.162E+05	0.012	0.013
8.250	5	0.048	0.269E+06	0.4	0.6	0.290E+03	0.193E+05	0.010	0.013
8.364	3	0.014	0.537E+02	0.0	0.0	0.214E+04	0.150E+06	0.001	0.001
8.364	5	0.055	0.349E+06	0.6	0.8	0.214E+03	0.149E+05	0.013	0.017
8.501	3	0.057	0.922E+03	0.5	0.7	0.123E+03	0.87E+04	0.023	0.021
8.543	5	0.061	0.435E+06	0.7	1.0	0.168E+03	0.123E+05	0.017	0.022
8.589	3	0.059	0.987E+03	0.6	0.7	0.114E+03	0.837E+04	0.025	0.022
8.658	4	0.015	0.127E+04	0.0	0.1	0.228E+04	0.171E+06	0.001	0.004
8.658	3	0.030	0.250E+03	0.1	0.2	0.444E+03	0.333E+05	0.006	0.006
8.786	5	0.093	0.100E+07	1.6	2.3	0.707E+02	0.546E+04	0.039	0.050
8.868	4	0.017	0.159E+04	0.0	0.1	0.178E+04	0.149E+06	0.002	0.002
8.868	5	0.067	0.519E+06	0.8	1.2	0.135E+03	0.105E+05	0.021	0.026

CA48 35 MEV FRICKE

THE EVALUATION OF $\langle R^* L \rangle$ WAS DONE USING A UNIFORM CHARGE DISTRIBUTION.
 THE NUCLEAR RADIUS PARAMETER=1.24 F THE NUCLEAR SURFACE THICKNESS PARAMETER=0.500 F WINE BOTTLE = 0.000

Z = 20	A = 48	BEAM ENERGY IS	35.000MEV	EX	L	BETA	B(EL)	G(SP)	G(U SP)	D(L)	C(L)	D(IRRET)/D(L)	B(EL)/NEWSR
3.830	2	0.160	0.354E+03	4.2	4.7	0.249E+02	0.366E+03	0.112	0.175	0.196E+02	0.397E+03	0.143	0.244
4.502	3	0.198	0.109E+05	6.5	7.9	0.196E+02	0.397E+03	0.143	0.143	0.282E+03	0.600E+04	0.010	0.020
4.607	4	0.058	0.193E+05	0.6	0.8	0.282E+03	0.102E+05	0.007	0.016	0.138E+04	0.381E+05	0.002	0.004
5.141	5	0.052	0.314E+06	0.5	0.7	0.387E+03	0.218E+05	0.004	0.004	0.138E+04	0.218E+05	0.004	0.004
5.249	5	0.027	0.858E+05	0.1	0.2	0.691E+02	0.199E+04	0.040	0.058	0.823E+02	0.270E+04	0.034	0.066
5.295	2	0.024	0.821E+C1	0.1	0.1	0.778E+03	0.920E+02	0.004	0.004	0.657E+03	0.244E+05	0.004	0.008
5.362	3	0.096	0.260E+04	1.5	1.9	0.691E+02	0.199E+04	0.040	0.058	0.431E+05	0.369E+04	0.030	0.045
5.723	5	0.107	0.132E+07	2.2	3.0	0.823E+02	0.270E+04	0.034	0.066	0.920E+02	0.369E+04	0.013	0.012
6.098	5	0.037	0.156E+06	0.3	0.4	0.920E+02	0.934E+04	0.013	0.012	0.920E+02	0.344E+04	0.013	0.010
6.335	4	0.087	0.431E+05	1.3	1.7	0.920E+02	0.934E+04	0.013	0.012	0.657E+03	0.272E+05	0.005	0.007
6.641	2	0.042	0.241E+02	0.3	0.3	0.212E+03	0.168E+05	0.007	0.010	0.381E+03	0.168E+05	0.005	0.008
6.641	4	0.042	0.992E+04	0.3	0.4	0.568E+03	0.261E+05	0.005	0.007	0.568E+03	0.261E+05	0.005	0.008
6.786	4	0.034	0.652E+04	0.2	0.3	0.575E+03	0.272E+05	0.005	0.008	0.680E+03	0.172E+05	0.005	0.007
6.885	5	0.037	0.158E+06	0.3	0.4	0.864E+03	0.165E+05	0.008	0.007	0.335E+03	0.165E+05	0.005	0.006
7.009	2	0.032	0.144E+02	0.2	0.2	0.603E+03	0.296E+05	0.005	0.006	0.415E+03	0.364E+05	0.004	0.003
7.009	4	0.032	0.594E+04	0.2	0.2	0.680E+03	0.463E+05	0.003	0.003	0.680E+03	0.463E+05	0.003	0.003
7.320	2	0.022	0.680E+01	0.1	0.1	0.864E+03	0.864E+05	0.008	0.009	0.314E+03	0.172E+05	0.009	0.009
7.320	3	0.023	0.152E+03	0.1	0.1	0.864E+03	0.864E+05	0.008	0.008	0.485E+03	0.271E+05	0.006	0.006
7.401	3	0.039	0.415E+03	0.2	0.3	0.558E+03	0.558E+05	0.005	0.005	0.558E+03	0.312E+05	0.005	0.006
7.471	4	0.033	0.602E+04	0.2	0.2	0.630E+03	0.352E+05	0.004	0.007	0.630E+03	0.352E+05	0.004	0.007
7.471	5	0.034	0.132E+06	0.2	0.3	0.630E+03	0.352E+05	0.004	0.007	0.630E+03	0.352E+05	0.004	0.007

CA48 35 MEV FRICKE

04:30 SEP 08, 17

THE EVALUATION OF $\langle R^* \cdot L \rangle$ WAS DONE USING A UNIFORM CHARGE DISTRIBUTION.

THE NUCLEAR RADIUS PARAMETER=1.24 F THE NUCLEAR SURFACE THICKNESS PARAMETER=0.500 FWINE BOTTLE= 0.00

Z = 20 A = 48 BEAM ENERGY IS 35.000MEV

EX	L	BETA	B(EL)	G(SP)	GU(SP)	D(L)	C(L)	D(IRRAT)/D(L)	B(EL)/NEWSR
7.521	3	0.027	0.202E+03	0.1	0.1	0.635E+03	0.359E+05	0.004	0.004
7.521	4	0.028	0.450E+04	0.1	0.2	0.742E+03	0.419E+05	0.005	0.005
7.643	3	0.107	0.321E+04	1.9	2.3	0.392E+02	0.229E+04	0.071	0.072
7.786	4	0.057	0.186E+05	0.6	0.7	0.174E+03	0.105E+05	0.016	0.019
7.940	5	0.040	0.183E+06	0.3	0.4	0.429E+03	0.271E+05	0.007	0.009
8.037	4	0.053	0.161E+05	0.5	0.6	0.194E+03	0.125E+05	0.014	0.017
8.037	2	0.048	0.311E+02	0.4	0.4	0.135E+03	0.875E+04	0.021	0.015
8.037	3	0.050	0.698E+03	0.4	0.5	0.172E+03	0.111E+05	0.016	0.016
8.250	4	0.050	0.144E+05	0.4	0.6	0.211E+03	0.144E+05	0.013	0.015
8.250	5	0.050	0.293E+06	0.5	0.7	0.258E+03	0.176E+05	0.011	0.015
8.364	3	0.015	0.626E+02	0.0	0.0	0.184E+04	0.129E+06	0.002	0.001
8.364	5	0.058	0.386E+06	0.6	0.9	0.193E+03	0.135E+05	0.014	0.019
8.501	3	0.052	0.106E+04	0.6	0.8	0.107E+03	0.771E+04	0.026	0.024
8.543	5	0.068	0.540E+06	0.9	1.2	0.135E+03	0.987E+04	0.021	0.027
8.589	3	0.062	0.108E+04	0.6	0.8	0.104E+03	0.768E+04	0.027	0.024
8.658	4	0.016	0.143E+04	0.0	0.1	0.204E+04	0.153E+06	0.001	0.001
8.658	3	0.032	0.281E+03	0.2	0.2	0.396E+03	0.297E+05	0.007	0.006
8.786	5	0.100	0.115E+07	1.9	2.6	0.617E+02	0.476E+04	0.045	0.057
8.868	4	0.018	0.176E+04	0.1	0.1	0.161E+04	0.127E+06	0.002	0.002
8.868	5	0.072	0.593E+06	1.0	1.3	0.119E+03	0.932E+04	0.024	0.030

CA48 30 MEV FRICKE

THE EVALUATION OF $\langle R^* L \rangle$ WAS DONE USING A UNIFORM CHARGE DISTRIBUTION.

THE NUCLEAR RADIUS PARAMETER=1.24 F THE NUCLEAR SURFACE THICKNESS PARAMETER=0.500 FWINE BOTTLE= 0.0

Z= 20 A= 48 BEAM ENERGY IS 29.830MEV

EX	L	BETA	B(EL)	G(SP)	GU(SP)	D(L)	C(L)	D(IRRFIT)/D(L)	B(EL)/NEWSR
3.830	2	0.162	0.362E+03	4.3	4.9	0.244E+02	0.358E+03	0.114	0.179
4.502	3	0.203	0.115E+05	6.8	8.3	0.186E+02	0.377E+03	0.150	0.256
4.607	4	0.063	0.222E+05	0.7	0.9	0.246E+03	0.522E+04	0.011	0.023
5.141	5	0.054	0.338E+06	0.6	0.8	0.359E+03	0.949E+04	0.008	0.017
5.249	5	0.029	0.100E+06	0.2	0.2	0.119E+04	0.327E+05	0.002	0.005
5.295	2	0.029	0.113E+02	0.1	0.2	0.567E+03	0.159E+05	0.005	0.006
5.362	3	0.095	0.251E+04	1.5	1.8	0.714E+02	0.205E+04	0.039	0.056
5.723	5	0.107	0.131E+07	2.1	3.0	0.830E+02	0.272E+04	0.034	0.065
6.098	5	0.041	0.195E+06	0.3	0.4	0.524E+03	0.195E+05	0.005	0.010
6.335	4	0.090	0.455E+05	1.4	1.8	0.871E+02	0.349E+04	0.032	0.048
6.641	2	0.044	0.267E+02	0.3	0.4	0.191E+03	0.843E+04	0.015	0.013
6.641	4	0.044	0.110E+05	0.3	0.4	0.344E+03	0.152E+05	0.008	0.011
6.786	4	0.032	0.586E+04	0.2	0.2	0.632E+03	0.291E+05	0.004	0.006
6.885	5	0.041	0.191E+06	0.3	0.4	0.474E+03	0.225E+05	0.006	0.010
7.009	2	0.033	0.150E+02	0.2	0.2	0.322E+03	0.158E+05	0.009	0.007
7.009	4	0.033	0.619E+04	0.2	0.2	0.579E+03	0.285E+05	0.005	0.006
7.320	2	0.028	0.106E+02	0.1	0.1	0.437E+03	0.234E+05	0.006	0.005
7.320	3	0.029	0.243E+03	0.1	0.2	0.541E+03	0.290E+05	0.005	0.005
7.401	3	0.041	0.458E+03	0.3	0.3	0.284E+03	0.155E+05	0.010	0.010
7.471	3	0.026	0.185E+03	0.1	0.1	0.695E+03	0.388E+05	0.004	0.004
7.471	4	0.028	0.436E+04	0.1	0.2	0.770E+03	0.430E+05	0.004	0.005
7.471	5	0.029	0.988E+05	0.2	0.2	0.845E+03	0.472E+05	0.003	0.005

CA48 30 MEV FRICKE

THE EVALUATION OF $\langle R^* L \rangle$ WAS DONE USING A UNIFORM CHARGE DISTRIBUTION.

THE NUCLEAR RADIUS PARAMETER=1.24 F THE NUCLEAR SURFACE THICKNESS PARAMETER=0.500 F WINE BOTTLE= 0.0004

Z = 20 A = 48 BEAM ENERGY IS 29.830MEV

EX	L	BETA	B(EL)	G(SP)	GU(SP)	D(L)	C(L)	D(RRBT)/D(L)	B(EL)/NEWSR
7.521	3	0.026	0.192E+03	0.1	0.1	0.667E+03	0.377E+05	0.004	0.004
7.521	4	0.028	0.443E+04	0.1	0.2	0.753E+03	0.426E+05	0.005	0.005
7.786	4	0.056	0.176E+05	0.5	0.7	0.183E+03	0.111E+05	0.015	0.018
7.940	5	0.038	0.169E+06	0.3	0.4	0.465E+03	0.293E+05	0.006	0.008
8.037	4	0.042	0.100E+05	0.3	0.4	0.312E+03	0.201E+05	0.009	0.010
8.037	2	0.042	0.243E+02	0.3	0.3	0.173E+03	0.112E+05	0.016	0.012
8.037	3	0.042	0.499E+03	0.3	0.4	0.240E+03	0.155E+05	0.012	0.011
8.250	4	0.050	0.144E+05	0.4	0.6	0.211E+03	0.144E+05	0.013	0.015
8.250	5	0.050	0.293E+06	0.5	0.7	0.258E+03	0.176E+05	0.011	0.015
8.364	3	0.015	0.626E+02	0.0	0.0	0.184E+04	0.129E+06	0.002	0.001
8.364	5	0.058	0.386E+06	0.6	0.9	0.193E+03	0.135E+05	0.014	0.019
8.501	3	0.059	0.987E+03	0.6	0.7	0.115E+03	0.829E+04	0.024	0.022
8.543	5	0.073	0.612E+06	1.0	1.4	0.119E+03	0.871E+04	0.023	0.030
8.589	3	0.063	0.109E+04	0.7	0.8	0.103E+03	0.757E+04	0.027	0.024
8.658	4	0.016	0.143E+04	0.0	0.1	0.204E+04	0.153E+06	0.001	0.001
8.658	3	0.032	0.281E+03	0.2	0.2	0.396E+03	0.297E+05	0.007	0.006
8.786	5	0.101	0.119E+07	1.9	2.7	0.598E+02	0.462E+04	0.047	0.059
8.868	4	0.017	0.159E+04	0.0	0.1	0.178E+04	0.140E+06	0.002	0.002
8.868	5	0.068	0.533E+06	0.9	1.2	0.132E+03	0.104E+05	0.021	0.027

CA48 25 MEV FRICKE

04:29 SEP 08, 1

THE EVALUATION OF $\langle R^* L \rangle$ WAS DONE USING A UNIFORM CHARGE DISTRIBUTION.

THE NUCLEAR RADIUS PARAMETER=1.24 F. THE NUCLEAR SURFACE THICKNESS PARAMETER=0.500 FWINE BOTTLE= 0.0

Z= 20 A= 48 BEAM ENERGY IS 25.110MEV

EX	L	BETA	B(EL)	G(SP)	GU(SP)	D(L)	C(L)	D(IRRET)/D(L)	B(EL)/NEWSR
3.830	2	0.174	0.416E+03	4.9	5.6	0.212E+02	0.312E+03	0.131	0.205
4.502	3	0.200	0.112E+05	6.7	8.1	0.191E+02	0.386E+03	0.146	0.250
4.607	4	0.076	0.323E+05	1.0	1.3	0.169E+03	0.358E+04	0.017	0.034
5.141	5	0.065	0.489E+06	0.8	1.1	0.248E+03	0.655E+04	0.011	0.024
5.249	5	0.035	0.143E+06	0.2	0.3	0.831E+03	0.229E+05	0.003	0.007
5.295	2	0.029	0.113E+02	0.1	0.2	0.567E+03	0.159E+05	0.005	0.006
5.362	3	0.096	0.255E+04	1.5	1.8	0.704E+02	0.202E+04	0.040	0.057
5.723	5	0.106	0.129E+07	2.1	2.9	0.847E+02	0.277E+04	0.033	0.064
6.098	5	0.044	0.226E+06	0.4	0.5	0.453E+03	0.169E+05	0.006	0.011
6.335	4	0.095	0.508E+05	1.6	2.1	0.780E+02	0.313E+04	0.036	0.053
6.641	2	0.046	0.294E+02	0.3	0.4	0.173E+03	0.765E+04	0.016	0.015
6.641	4	0.046	0.121E+05	0.4	0.5	0.312E+03	0.138E+05	0.009	0.013
6.786	4	0.032	0.570E+04	0.2	0.2	0.649E+03	0.299E+05	0.004	0.006
6.885	5	0.048	0.263E+06	0.4	0.6	0.345E+03	0.163E+05	0.008	0.013
7.009	2	0.036	0.181E+02	0.2	0.2	0.266E+03	0.131E+05	0.010	0.009
7.009	4	0.036	0.748E+04	0.2	0.3	0.479E+03	0.235E+05	0.006	0.008
7.320	2	0.026	0.960E+C1	0.1	0.1	0.482E+03	0.258E+05	0.006	0.005
7.320	3	0.028	0.215E+C3	0.1	0.2	0.612E+03	0.328E+05	0.005	0.005
7.401	3	0.047	0.608E+C3	0.4	0.4	0.214E+03	0.117E+05	0.013	0.014
7.471	3	0.026	0.182E+C3	0.1	0.1	0.707E+03	0.395E+05	0.004	0.004
7.471	4	0.028	0.450E+C4	0.1	0.2	0.747E+03	0.417E+05	0.004	0.005
7.471	5	0.031	0.108E+C6	0.2	0.2	0.774E+03	0.432E+05	0.004	0.005

CA48 25 MEV FRICKE

04:30 SEP 08, 197

THE EVALUATION OF $\langle R^* L \rangle$ WAS DONE USING A UNIFORM CHARGE DISTRIBUTION.

THE NUCLEAR RADIUS PARAMETER=1.024 FOR THE NUCLEAR SURFACE THICKNESS PARAMETER=0.500 FINE BOTTLE= 0.000

Z= 20 A= 48 BEAM ENERGY IS 25.110³EV

EX	L	BETA	B(EL)	G(SP)	G0(SP)	D(L)	C(L)	D(IRRET)/D(L)	B(EL)/NEWSR
7.521	0.027	0.208E+03	0.1	0.615E+03	0.348E+05	0.005			
7.521	0.030	0.524E+04	0.2	0.638E+03	0.361E+05	0.005			
7.643	3	0.110	0.336E+04	2.0	0.375E+02	0.219E+04	0.075		
7.786	4	0.051	0.145E+05	0.5	0.222E+03	0.135E+05	0.015		
7.940	5	0.050	0.285E+06	0.5	0.275E+03	0.174E+05	0.014		
8.037	4	0.052	0.153E+05	0.5	0.204E+03	0.132E+05	0.016		
8.037	2	0.041	0.228E+02	0.3	0.185E+03	0.119E+05	0.011		
8.037	3	0.047	0.620E+03	0.4	0.193E+03	0.125E+05	0.014		
8.250	4	0.050	0.144E+05	0.4	0.211E+03	0.144E+05	0.015		
8.250	5	0.050	0.293E+06	0.5	0.258E+03	0.176E+05	0.015		
8.364	3	0.016	0.702E+02	0.0	0.164E+04	0.115E+06	0.002		
8.364	5	0.064	0.476E+06	0.8	0.157E+03	0.110E+05	0.018		
8.501	3	0.062	0.107E+04	0.6	0.106E+03	0.765E+04	0.024		
8.543	5	0.077	0.692E+06	1.1	0.106E+03	0.770E+04	0.026		
8.589	3	0.065	0.119E+04	0.7	0.944E+02	0.697E+04	0.030		
8.658	4	0.016	0.143E+04	0.0	0.204E+04	0.153E+06	0.001		
8.658	3	0.032	0.281E+03	0.2	0.396E+03	0.297E+05	0.007		
8.786	5	0.103	0.123E+07	2.0	0.575E+02	0.444E+04	0.049		
8.868	4	0.016	0.143E+04	0.0	0.199E+04	0.156E+06	0.001		
8.868	5	0.065	0.489E+06	0.8	0.144E+03	0.113E+05	0.019		

CA48 40 MEV R=1

THE EVALUATION OF $\langle R^2 \rangle L$ HAS BEEN USING A FERMI CHARGE DISTRIBUTION.

04:24 SEP 08, '17

THE NUCLEAR RADIUS PARAMETER=1.03 F . THE NUCLEAR SURFACE THICKNESS PARAMETER=0.520 FWINE BOTTLE= -0.03

Z= 20 A= 48 BEAM ENERGY IS 40.210MEV

EX	L	BETA	B(EL)	G(SP)	GU(SP)	D(L)	C(L)	D(IRRIT)/D(L)	B(EL)/NEWSR
3.830	2	0.149	0.450E+03	5.2	5.2	0.200E+02	0.293E+03	0.141	0.181
4.502	3	0.189	0.314E+05	15.9	15.9	0.148E+02	0.301E+03	0.335	0.384
4.607	4	0.046	0.121E+05	2.5	2.5	0.316E+03	0.671E+04	0.034	0.037
5.141	5	0.046	0.122E+08	9.4	9.4	0.346E+03	0.916E+04	0.083	0.076
5.249	5	0.023	0.318E+07	2.4	2.4	0.131E+04	0.360E+05	0.022	0.020
5.295	2	0.024	0.119E+02	0.1	0.1	0.547E+03	0.153E+05	0.005	0.005
5.362	3	0.098	0.839E+04	4.2	4.2	0.466E+02	0.134E+04	0.106	0.103
5.723	5	0.098	0.558E+08	42.9	42.9	0.683E+02	0.224E+04	0.422	0.349
6.098	5	0.031	0.579E+07	4.5	4.5	0.618E+03	0.230E+05	0.047	0.036
6.335	4	0.078	0.350E+06	7.2	7.2	0.794E+02	0.319E+04	0.135	0.108
6.641	2	0.037	0.284E+02	0.3	0.3	0.183E+03	0.805E+04	0.015	0.011
6.641	4	0.037	0.806E+05	1.7	1.7	0.329E+03	0.145E+05	0.033	0.025
6.786	4	0.029	0.486E+05	1.0	1.0	0.533E+03	0.246E+05	0.020	0.015
6.885	5	0.031	0.571E+07	4.4	4.4	0.555E+03	0.263E+05	0.052	0.036
7.009	2	0.027	0.144E+02	0.2	0.2	0.341E+03	0.168E+05	0.008	0.006
7.009	4	0.027	0.408E+05	0.8	0.8	0.614E+03	0.302E+05	0.017	0.013
7.320	2	0.025	0.125E+02	0.1	0.1	0.375E+03	0.201E+05	0.008	0.005
7.320	3	0.025	0.546E+02	0.3	0.3	0.525E+03	0.281E+05	0.009	0.007
7.401	3	0.031	0.862E+02	0.4	0.4	0.329E+03	0.180E+05	0.015	0.011
7.471	3	0.031	0.826E+03	0.4	0.4	0.340E+03	0.190E+05	0.015	0.010
7.471	4	0.031	0.555E+05	1.1	1.1	0.425E+03	0.237E+05	0.025	0.017
7.471	5	0.032	0.595E+07	4.6	4.6	0.491E+03	0.274E+05	0.059	0.037

CA48 40 MEV R=1

THE EVALUATION OF $\langle R^* L \rangle$ WAS DONE USING A FERMI CHARGE DISTRIBUTION.

THE NUCLEAR RADIUS PARAMETER=1.03 F THE NUCLEAR SURFACE THICKNESS PARAMETER=0.520 FWINE BOTTLE = -0.03

Z = 20 A = 48 BEAM ENERGY IS 40.210MEV

EX	L	BETA	B(EL)	G(SP)	GU(SP)	D(L)	C(L)	D(IRRGT)/D(L)	B(EL)/NEWSR
7.521	3	0.028	0.668E+03	0.3	0.3	0.417E+03	0.236E+05	0.012	0.008
7.521	4	0.029	0.472E+05	1.0	1.0	0.496E+03	0.281E+05	0.022	0.015
7.643	3	0.104	0.948E+04	4.8	4.8	0.289E+02	0.169E+04	0.172	0.116
7.786	4	0.052	0.153E+06	3.2	3.2	0.148E+03	0.897E+04	0.072	0.047
7.940	5	0.032	0.603E+07	4.6	4.6	0.455E+03	0.287E+05	0.063	0.038
8.037	4	0.053	0.159E+06	3.3	3.3	0.137E+03	0.887E+04	0.078	0.049
8.037	3	0.055	0.263E+04	1.3	1.3	0.992E+02	0.641E+04	0.050	0.032
8.037	2	0.049	0.483E+02	0.6	0.6	0.884E+02	0.571E+04	0.032	0.019
8.250	4	0.046	0.123E+06	2.5	2.5	0.173E+03	0.118E+05	0.062	0.038
8.250	5	0.046	0.125E+08	9.6	9.6	0.212E+03	0.144E+05	0.136	0.078
8.364	3	0.013	0.159E+03	0.1	0.1	0.158E+04	0.110E+06	0.003	0.002
8.364	5	0.054	0.168E+08	13.0	13.0	0.155E+03	0.123E+05	0.186	0.105
8.501	3	0.056	0.274E+04	1.4	1.4	0.901E+02	0.651E+04	0.055	0.033
8.543	5	0.058	0.199E+C8	15.3	15.3	0.128E+03	0.937E+04	0.224	0.124
8.589	3	0.058	0.293E+04	1.5	1.5	0.832E+02	0.614E+04	0.060	0.036
8.658	4	0.014	0.118E+05	0.2	0.2	0.172E+04	0.122E+06	0.006	0.004
8.658	3	0.029	0.723E+03	0.4	0.4	0.35E+03	0.251E+05	0.015	0.009
8.786	5	0.088	0.457E+08	35.2	35.2	0.543E+02	0.419E+04	0.531	0.286
8.868	4	0.016	0.153E+05	0.3	0.3	0.130E+04	0.122E+06	0.008	0.005
8.868	5	0.065	0.248E+C8	19.1	19.1	0.992E+02	0.780E+04	0.291	0.155

CA48 35 MEV R=1

04:24 SEP 08, 17

THE EVALUATION OF $\langle R^* L \rangle$ WAS DONE USING A FERMI CHARGE DISTRIBUTION.

THE NUCLEAR RADIUS PARAMETER = 1.03 F THE NUCLEAR SURFACE THICKNESS PARAMETER = 0.520 FWINE BOTTLE = -0.03

Z = 20 A = 48 BEAM ENERGY IS 35.0000MEV

EX	L	BETA	B(EL)	G(SP)	GU(SP)	D(L)	C(L)	D(IRRBT)/D(L)	B(EL)/NEWSR
3.830	2	0.154	0.481E+03	5.6	0.187E+02	0.274E+03	0.151	0.194	
4.502	3	0.190	0.320E+05	16.2	0.146E+02	0.295E+03	0.341	0.391	
4.607	4	0.056	0.179E+06	3.7	0.214E+03	0.454E+04	0.050	0.055	
5.141	5	0.049	0.139E+08	10.7	0.304E+03	0.804E+04	0.095	0.087	
5.249	5	0.026	0.381E+07	2.9	0.109E+04	0.301E+05	0.026	0.024	
5.295	2	0.024	0.112E+02	0.1	0.578E+03	0.162E+05	0.005	0.005	
5.362	3	0.093	0.761E+04	3.9	0.514E+02	0.148E+04	0.097	0.093	
5.723	5	0.101	0.591E+08	45.5	0.645E+02	0.211E+04	0.447	0.369	
6.098	5	0.034	0.689E+07	5.3	0.519E+03	0.193E+05	0.055	0.043	
6.335	4	0.083	0.397E+C6	8.2	0.700E+02	0.281E+04	0.153	0.122	
6.641	2	0.040	0.318E+C2	0.4	0.163E+03	0.718E+04	0.017	0.013	
6.641	4	0.040	0.904E+C5	1.9	0.293E+03	0.129E+05	0.037	0.028	
6.786	4	0.033	0.611E+C5	1.3	0.424E+03	0.195E+05	0.025	0.019	
6.885	5	0.035	0.706E+C7	5.4	0.448E+03	0.213E+05	0.064	0.044	
7.009	2	0.031	0.198E+C2	0.2	0.248E+03	0.122E+05	0.011	0.008	
7.009	4	0.031	0.563E+C5	1.2	0.446E+03	0.219E+05	0.024	0.017	
7.320	2	0.021	0.923E+C1	0.1	0.509E+03	0.273E+05	0.006	0.004	
7.320	3	0.022	0.436E+C3	0.2	0.657E+03	0.352E+05	0.008	0.005	
7.401	3	0.037	0.121E+C4	0.6	0.235E+C3	0.129E+05	0.021	0.015	
7.471	3	0.030	0.779E+C3	0.4	0.360E+C3	0.201E+05	0.014	0.010	
7.471	4	0.031	0.563E+C5	1.2	0.419E+C3	0.234E+05	0.026	0.017	
7.471	5	0.032	0.587E+C7	4.5	0.497E+C3	0.278E+05	0.058	0.037	

CA48 35 MEV R=1

04:25 SEP 08, 17

THE EVALUATION OF <R**L> HAS BEEN USING A FERMI CHARGE DISTRIBUTION.

THE NUCLEAR RADIUS PARAMETER=1.03 F THE NUCLEAR SURFACE THICKNESS PARAMETER=0.520 FWINE BOTTLE=-0.03

Z= 20 A= 48 BEAM ENERGY IS 35.000MEV

EX	L	BETA	B(EL)	S(SP)	GU(SP)	D(L)	C(L)	D(IRRBT)/D(L)	B(EL)/NEWSR
7.521	3	0.026	0.595E+03	0.3	0.3	0.468E+03	0.265E+05	0.007	0.011
7.521	4	0.027	0.415E+03	0.9	0.9	0.563E+03	0.319E+05	0.013	0.019
7.643	3	0.103	0.944E+04	4.8	4.8	0.290E+02	0.170E+04	0.116	0.171
7.786	4	0.055	0.172E+04	3.5	3.5	0.132E+03	0.798E+04	0.053	0.081
7.940	5	0.038	0.827E+04	6.4	6.4	0.332E+03	0.209E+05	0.052	0.087
8.037	4	0.051	0.148E+04	3.0	3.0	0.148E+03	0.958E+04	0.046	0.072
8.037	2	0.046	0.429E+04	0.5	0.5	0.998E+02	0.645E+04	0.017	0.028
8.037	3	0.048	0.203E+04	1.0	1.0	0.128E+03	0.829E+04	0.025	0.039
8.250	4	0.049	0.139E+04	2.9	2.9	0.154E+03	0.105E+05	0.043	0.070
8.250	5	0.049	0.141E+04	10.8	10.8	0.188E+03	0.128E+05	0.153	0.088
8.364	3	0.014	0.181E+04	0.1	0.1	0.139E+04	0.971E+05	0.004	0.002
8.364	5	0.056	0.181E+04	13.9	13.9	0.144E+03	0.101E+05	0.113	0.200
8.501	3	0.059	0.312E+04	1.6	1.6	0.791E+02	0.572E+04	0.038	0.063
8.543	5	0.064	0.240E+04	13.4	18.4	0.107E+03	0.777E+04	0.150	0.270
8.589	3	0.060	0.319E+04	1.6	1.6	0.766E+02	0.565E+04	0.065	0.095
8.658	4	0.015	0.137E+04	0.3	0.3	0.149E+04	0.111E+06	0.007	0.004
8.658	3	0.031	0.838E+04	0.4	0.4	0.289E+03	0.217E+05	0.010	0.017
8.786	5	0.094	0.513E+04	39.5	39.5	0.483E+02	0.373E+04	0.321	0.596
8.868	4	0.017	0.174E+04	0.4	0.4	0.114E+04	0.896E+05	0.009	0.027
8.868	5	0.069	0.279E+04	21.5	21.5	0.881E+02	0.693E+04	0.174	0.327

CA48 30 MEV R=1

THE EVALUATION OF $\langle R^* L \rangle$ WAS DONE USING A FERMIC CHARGE DISTRIBUTION.

THE NUCLEAR RADIUS PARAMETER=1.03 F THE NUCLEAR SURFACE THICKNESS PARAMETER=0.520 FWINE BOTTLE=-0.03

Z= 20 A= 48 BEAM ENERGY IS 29.830MEV

EX	L	BETA	B(EL)	G(SP)	GU(SP)	D(L)	C(L)	D(IRRF)/D(L)	B(EL)/NEWSR
3•830	2	0•155	0•488E+03	5•6	5•6	0•184E+02	0•270E+03	0•153	0•196
4•502	3	0•183	0•297E+05	15•0	15•0	0•157E+02	0•318E+03	0•316	0•363
4•607	4	0•059	0•200E+06	4•1	4•1	0•191E+03	0•404E+04	0•056	0•062
5•141	5	0•051	0•150E+08	11•5	11•5	0•283E+03	0•749E+04	0•102	0•094
5•249	5	0•028	0•442E+07	3•4	3•4	0•940E+03	0•259E+05	0•031	0•028
5•295	2	0•028	0•156E+02	0•2	0•2	0•417E+03	0•117E+05	0•007	0•006
5•362	3	0•036	0•650E+04	3•3	3•3	0•601E+02	0•173E+04	0•083	0•080
5•723	5	0•100	0•581E+08	44•7	44•7	0•656E+02	0•215E+04	0•439	0•363
6•098	5	0•039	0•867E+07	6•7	6•7	0•413E+03	0•153E+05	0•070	0•054
6•335	4	0•084	0•407E+06	8•4	8•4	0•682E+02	0•274E+04	0•157	0•126
6•641	2	0•042	0•354E+02	0•4	0•4	0•146E+03	0•644E+04	0•019	0•014
6•641	4	0•042	0•191E+06	2•1	2•1	0•263E+03	0•116E+05	0•041	0•031
6•641	4	0•090	0•462E+06	9•5	9•5	0•573E+02	0•253E+04	0•187	0•143
6•786	4	0•030	0•531E+05	1•1	1•1	0•488E+03	0•225E+05	0•022	0•016
6•885	5	0•038	0•847E+07	6•5	6•5	0•374E+03	0•177E+05	0•077	0•053
7•009	2	0•030	0•184E+02	0•2	0•2	0•266E+03	0•131E+05	0•011	0•007
7•009	4	0•030	0•524E+05	1•1	1•1	0•479E+03	0•235E+05	0•022	0•016
7•320	2	0•027	0•146E+02	0•2	0•2	0•322E+03	0•172E+05	0•009	0•006
7•320	3	0•027	0•626E+03	0•3	0•3	0•458E+03	0•245E+05	0•011	0•008
7•401	3	0•037	0•118E+04	0•6	0•6	0•240E+03	0•132E+05	0•021	0•014
7•471	3	0•023	0•480E+03	0•2	0•2	0•584E+03	0•326E+05	0•008	0•006
7•471	4	0•026	0•395E+05	0•8	0•8	0•596E+03	0•333E+05	0•018	0•012
7•471	5	0•027	0•435E+07	3•3	3•3	0•671E+03	0•374E+05	0•043	0•027

CA48 30 MEV R=1

THE EVALUATION OF $\langle R^* L \rangle$ WAS DONE USING A FERMI CHARGE DISTRIBUTION.

THE NUCLEAR RADIUS PARAMETER=1.0C3 F THE NUCLEAR SURFACE THICKNESS PARAMETER=0.520 FWINE BOTTLE=-0.03

Z = 20 A = 48 BEAM ENERGY IS 29.830MEV

EX	L	BETA	B(EL)	G(SP)	GU(SP)	D(L)	C(L)	D(IRROT)/D(L)	B(EL)/NEWSR
7.521	3	0.024	0.499E+03	0.3	0.3	0.559E+03	0.316E+05	0.009	0.006
7.521	4	0.026	0.402E+05	0.8	0.8	0.582E+03	0.329E+05	0.018	0.012
7.786	4	0.053	0.161E+C6	3.3	3.3	0.141E+03	0.852E+04	0.076	0.050
7.940	5	0.037	0.789E+C7	6.1	6.1	0.348E+03	0.219E+05	0.083	0.049
8.037	4	0.040	0.924E+05	1.9	1.9	0.237E+03	0.153E+05	0.045	0.029
8.037	2	0.041	0.336E+C2	0.4	0.4	0.127E+03	0.823E+04	0.022	0.014
8.037	3	0.038	0.126E+C4	0.6	0.6	0.206E+03	0.133E+05	0.024	0.015
8.250	4	0.048	0.133E+06	2.7	2.7	0.161E+03	0.109E+05	0.067	0.041
8.250	5	0.048	0.134E+08	10.3	10.3	0.197E+03	0.134E+05	0.147	0.084
8.364	3	0.014	0.181E+03	0.1	0.1	0.139E+04	0.971E+05	0.004	0.002
8.364	5	0.056	0.181E+08	13.9	13.9	0.144E+03	0.101E+05	0.200	0.113
8.501	3	0.054	0.255E+04	1.3	1.3	0.969E+02	0.700E+04	0.051	0.031
8.543	5	0.068	0.267E+08	20.5	20.5	0.957E+02	0.699E+04	0.301	0.167
8.589	3	0.057	0.282E+04	1.4	1.4	0.864E+02	0.638E+04	0.057	0.035
8.658	4	0.015	0.137E+05	0.3	0.3	0.149E+04	0.111E+06	0.007	0.004
8.658	3	0.031	0.838E+03	0.4	0.4	0.289E+03	0.217E+05	0.017	0.010
8.786	5	0.095	0.526E+08	40.4	40.4	0.472E+02	0.364E+04	0.610	0.328
8.868	4	0.016	0.153E+05	0.3	0.3	0.130E+04	0.102E+06	0.008	0.005
8.868	5	0.064	0.241E+08	18.6	18.6	0.102E+03	0.802E+04	0.283	0.151

CA48 25 MEV R=1

THE EVALUATION OF $\langle R^* L \rangle$ WAS DONE USING A FERMI CHARGE DISTRIBUTION.

THE NUCLEAR RADIUS PARAMETER=1.03 F THE NUCLEAR SURFACE THICKNESS PARAMETER=0.520 FWINE BOTTLE=

Z = 20 A = 48 BEAM ENERGY IS 25.110MEV

EX	L	BETA	B(EL)	G(SP)	GU(SP)	D(L)	C(L)	D(IRR0T)/D(L)	B(EL)/NEWSR
3.0830	2	0.173	0.603E+03	7.0	7.0	0.149E+02	0.218E+03	0.189	0.243
4.502	3	0.201	0.356E+05	1.8.0	18.0	0.131E+02	0.265E+03	0.379	0.435
4.607	4	0.076	0.332E+06	5.9	6.9	0.115E+03	0.244E+04	0.093	0.102
5.141	5	0.065	0.246E+08	18.9	18.9	0.172E+03	0.455E+04	0.167	0.154
5.249	5	0.035	0.724E+07	5.6	5.6	0.574E+03	0.158E+05	0.050	0.045
5.295	2	0.028	0.163E+02	0.2	0.2	0.398E+03	0.111E+05	0.007	0.007
5.362	3	0.095	0.798E+04	4.0	4.0	0.490E+02	0.141E+04	0.101	0.098
5.723	5	0.105	0.649E+08	49.9	49.9	0.587E+02	0.192E+04	0.491	0.406
6.098	5	0.044	0.114E+08	8.8	8.8	0.313E+03	0.116E+05	0.092	0.071
6.335	4	0.095	0.516E+06	10.7	10.7	0.538E+02	0.215E+04	0.199	0.159
6.641	2	0.046	0.433E+02	0.5	0.5	0.120E+03	0.528E+04	0.024	0.017
6.641	4	0.046	0.123E+06	2.5	2.5	0.215E+03	0.950E+04	0.050	0.038
6.786	4	0.032	0.587E+05	1.2	1.2	0.442E+03	0.204E+05	0.024	0.018
6.885	5	0.048	0.133E+08	10.2	10.2	0.238E+03	0.113E+05	0.121	0.083
7.009	2	0.036	0.264E+02	0.3	0.3	0.186E+03	0.913E+04	0.015	0.011
7.009	4	0.036	0.750E+05	1.5	1.5	0.34E+03	0.164E+05	0.032	0.023
7.320	2	0.026	0.139E+02	0.2	0.2	0.338E+03	0.181E+05	0.008	0.006
7.320	3	0.027	0.657E+03	0.3	0.3	0.436E+03	0.233E+05	0.011	0.008
7.401	3	0.046	0.190E+04	1.0	1.0	0.149E+03	0.815E+04	0.033	0.023
7.471	3	0.025	0.565E+03	0.3	0.3	0.496E+03	0.277E+05	0.010	0.007
7.471	4	0.028	0.450E+05	0.9	0.9	0.523E+03	0.292E+05	0.020	0.014
7.471	5	0.030	0.539E+07	4.1	4.1	0.542E+03	0.302E+05	0.053	0.034

CA48 25 MEV R=1

04:25 SEP 08, 17

THE EVALUATION OF $\langle R^* * L \rangle$ WAS DONE USING A FERMI CHARGE DISTRIBUTION.

THE NUCLEAR RADIUS PARAMETER=1.03 F THE NUCLEAR SURFACE THICKNESS PARAMETER=0.520 FWINE BOTTLE=-0.03

Z= 20 A= 48 BEAM ENERGY IS 25.110MEV

EX	L	BETA	B(EL)	G(SP)	GU(SP)	D(L)	C(L)	D(IRRBT)/D(L)	B(EL)/NEWSR
7.521	3	0.027	0.657E+03	0.3	0.3	0.424E+03	0.240E+05	0.012	0.008
7.521	4	0.030	0.524E+05	1.1	1.1	0.447E+03	0.253E+05	0.024	0.016
7.643	3	0.110	0.105E+05	5.4	5.4	0.258E+02	0.151E+04	0.193	0.130
7.786	4	0.050	0.145E+06	3.0	3.0	0.156E+03	0.944E+04	0.069	0.045
7.940	5	0.049	0.138E+08	10.6	10.6	0.199E+03	0.125E+05	0.145	0.086
8.037	4	0.053	0.163E+06	3.4	3.4	0.134E+03	0.865E+04	0.080	0.050
8.037	2	0.040	0.318E+02	0.4	0.4	0.135E+03	0.869E+04	0.021	0.013
8.037	3	0.047	0.198E+04	1.0	1.0	0.132E+03	0.853E+04	0.038	0.024
8.250	4	0.052	0.154E+06	3.2	3.2	0.138E+03	0.942E+04	0.077	0.048
8.250	5	0.052	0.156E+08	12.0	12.0	0.169E+03	0.115E+05	0.170	0.098
8.364	3	0.016	0.234E+03	0.1	0.1	0.107E+04	0.749E+05	0.005	0.003
8.364	5	0.066	0.256E+08	19.7	19.7	0.102E+03	0.711E+04	0.283	0.160
8.501	3	0.062	0.340E+04	1.7	1.7	0.725E+02	0.524E+04	0.068	0.042
8.543	5	0.077	0.349E+08	26.8	26.8	0.732E+02	0.534E+04	0.394	0.218
8.589	3	0.065	0.375E+04	1.9	1.9	0.652E+02	0.481E+04	0.076	0.046
8.658	4	0.016	0.153E+05	0.3	0.3	0.133E+04	0.997E+05	0.008	0.005
8.658	3	0.033	0.937E+03	0.5	0.5	0.259E+03	0.194E+05	0.019	0.011
8.786	5	0.103	0.625E+08	48.1	48.1	0.397E+02	0.307E+04	0.726	0.391
8.868	4	0.016	0.153E+05	0.3	0.3	0.130E+04	0.102E+06	0.008	0.005
8.868	5	0.067	0.263E+08	20.2	20.2	0.934E+02	0.735E+04	0.308	0.164

CA48 40 MEV FRICKE

THE EVALUATION OF $\langle R^* L \rangle$ WAS DONE USING A FERMI CHARGE DISTRIBUTION.

THE NUCLEAR RADIUS PARAMETER=1.03 F THE NUCLEAR SURFACE THICKNESS PARAMETER=0.520 FWINE BOTTLE=-0.0300

Z = 20 A = 48 BEAM ENERGY IS 40.210MEV

EX	L	BETA	B(EL)	G(SP)	G(SP)	D(L)	C(L)	D(IRRBT)/D(L)	B(EL)/NEWSR
3.0830	2	0.155	0.483E+03	5.6	5.6	0.186E+02	0.272E+03	0.152	0.195
4.0502	3	0.195	0.334E+05	16.9	16.9	0.139E+02	0.283E+03	0.356	0.409
4.0607	4	0.048	0.130E+06	2.7	2.7	0.293E+03	0.623E+04	0.037	0.040
5.0141	5	0.048	0.137E+08	10.5	10.5	0.310E+03	0.819E+04	0.093	0.086
5.0249	5	0.025	0.355E+07	2.7	2.7	0.117E+04	0.322E+05	0.025	0.022
5.0295	2	0.025	0.125E+02	0.1	0.1	0.518E+03	0.145E+05	0.005	0.005
5.0362	3	0.101	0.897E+04	4.5	4.5	0.436E+02	0.125E+04	0.114	0.110
5.0723	5	0.103	0.622E+08	47.9	47.9	0.612E+02	0.201E+04	0.471	0.389
6.0098	5	0.033	0.645E+07	5.0	5.0	0.554E+03	0.206E+05	0.052	0.040
6.0335	4	0.081	0.380E+06	7.8	7.8	0.731E+02	0.293E+04	0.147	0.117
6.0641	2	0.040	0.318E+02	0.4	0.4	0.163E+03	0.718E+04	0.017	0.013
6.0641	4	0.040	0.904E+05	1.9	1.9	0.293E+03	0.129E+05	0.037	0.028
6.0786	4	0.030	0.531E+05	1.1	1.1	0.488E+03	0.225E+05	0.022	0.016
6.0885	5	0.033	0.637E+07	4.9	4.9	0.497E+03	0.236E+05	0.058	0.040
7.0009	2	0.028	0.158E+02	0.2	0.2	0.310E+03	0.152E+05	0.009	0.006
7.0009	4	0.028	0.450E+05	0.9	0.9	0.558E+03	0.274E+05	0.019	0.014
7.0320	2	0.026	0.134E+02	0.2	0.2	0.350E+03	0.187E+05	0.008	0.005
7.0320	3	0.026	0.585E+03	3	3	0.489E+03	0.262E+05	0.010	0.007
7.0401	3	0.032	0.924E+03	0.5	0.5	0.307E+03	0.158E+05	0.016	0.011
7.0471	3	0.032	0.887E+03	0.4	0.4	0.317E+03	0.177E+05	0.016	0.011
7.0471	4	0.032	0.595E+05	1.2	1.2	0.396E+03	0.221E+05	0.027	0.018
7.0471	5	0.034	0.662E+07	5.1	5.1	0.441E+03	0.246E+05	0.065	0.041

CA48 40 MEV FRICKE

04:24 SEP 08, 1700

THE EVALUATION OF $\langle R^* L \rangle$ WAS DONE USING A FERMI CHARGE DISTRIBUTION.

THE NUCLEAR RADIUS PARAMETER=1.03 F THE NUCLEAR SURFACE THICKNESS PARAMETER=0.520 FWINE BOTTLE= -0.0300

Z = 20 A = 48 BEAM ENERGY IS 40.210MEV

EX	L	BETA	B(EL)	S(SP)	G(SP)	D(L)	C(L)	D(IRRGT)/D(L)	B(EL)/NEWSR
7.521	3	0.028	0.711E+03	0.4	0.392E+03	0.222E+05	0.013	0.009	0.016
7.521	4	0.030	0.508E+03	1.0	0.460E+03	0.260E+05	0.023	0.023	0.124
7.643	3	0.107	0.101E+05	5.1	0.272E+02	0.159E+04	0.183	0.078	0.051
7.786	4	0.053	0.165E+06	3.4	0.137E+03	0.831E+04	0.071	0.042	0.042
7.940	5	0.034	0.680E+07	5.2	0.404E+03	0.255E+05	0.091	0.057	0.057
8.037	4	0.057	0.186E+06	3.8	0.118E+03	0.761E+04	0.038	0.024	0.024
8.037	2	0.054	0.584E+02	0.7	0.732E+02	0.473E+04	0.062	0.040	0.040
8.037	3	0.061	0.328E+04	1.7	0.795E+02	0.514E+04	0.065	0.040	0.040
8.250	4	0.048	0.130E+06	2.7	0.164E+03	0.111E+05	0.144	0.082	0.082
8.250	5	0.048	0.132E+08	10.2	0.200E+03	0.136E+05	0.003	0.002	0.002
8.364	3	0.014	0.170E+03	0.1	0.148E+04	0.103E+06	0.195	0.110	0.110
8.364	5	0.055	0.177E+08	13.6	0.147E+03	0.103E+05	0.612E+04	0.36	0.36
8.501	3	0.057	0.291E+04	1.5	0.847E+02	0.846E+04	0.249	0.138	0.138
8.543	5	0.061	0.220E+08	16.9	0.116E+03	0.578E+04	0.063	0.038	0.038
8.589	3	0.059	0.312E+04	1.6	0.783E+02	0.118E+06	0.097	0.04	0.04
8.658	4	0.015	0.129E+05	0.3	0.157E+04	0.306E+03	0.230E+05	0.10	0.10
8.658	3	0.030	0.791E+03	0.4	0.488E+02	0.377E+04	0.591	0.318	0.318
8.786	5	0.093	0.509E+08	39.1	0.123E+04	0.968E+05	0.009	0.005	0.005
8.868	4	0.017	0.161E+05	0.3	0.934E+02	0.735E+04	0.308	0.164	0.164
8.868	5	0.067	0.263E+08	20.2	0.2				

CA48 35 MEV FRICKE

04:25 SEP 08, 1971

THE EVALUATION OF $\langle R^* L \rangle$ WAS DONE USING A FERMI CHARGE DISTRIBUTION.

THE NUCLEAR RADIUS PARAMETER=1.03 F THE NUCLEAR SURFACE THICKNESS PARAMETER=0.520 FWINE BOTTLE = -0.03

Z = 20	A = 48	BEAM ENERGY IS	35.000MEV	EX	L	B(L)	G(SP)	GU(SP)	D(L)	C(L)	D(IRRGT)/D(L)	B(L)/NEWSR
3.830	2	0.160	0.521E+03	6.0	6.0	0.172E+02	0.252E+03	0.164	0.210	0.210	0.367	0.422
4.502	3	0.198	0.345E+05	17.4	17.4	0.135E+02	0.274E+03	0.055	0.060	0.060	0.055	0.060
4.607	4	0.058	0.196E+06	4.0	4.0	0.195E+03	0.414E+04	0.108	0.099	0.099	0.108	0.099
5.141	5	0.052	0.159E+08	12.2	12.2	0.267E+03	0.705E+04	0.030	0.027	0.027	0.030	0.030
5.249	5	0.027	0.435E+07	3.3	3.3	0.955E+03	0.263E+05	0.005	0.005	0.005	0.005	0.005
5.295	2	0.024	0.121E+02	0.1	0.1	0.537E+03	0.151E+05	0.005	0.005	0.005	0.005	0.005
5.362	3	0.096	0.820E+04	4.1	4.1	0.477E+02	0.137E+04	0.104	0.100	0.100	0.104	0.100
5.723	5	0.107	0.671E+08	51.6	51.6	0.568E+02	0.186E+04	0.508	0.419	0.419	0.508	0.419
6.098	5	0.037	0.789E+07	6.4	6.4	0.453E+03	0.169E+05	0.064	0.049	0.049	0.064	0.049
6.335	4	0.087	0.438E+06	9.0	9.0	0.635E+02	0.255E+04	0.169	0.135	0.135	0.169	0.135
6.641	2	0.042	0.354E+02	0.4	0.4	0.146E+03	0.644E+04	0.019	0.014	0.014	0.019	0.014
6.641	4	0.042	0.101E+06	2.1	2.1	0.263E+03	0.116E+05	0.041	0.031	0.031	0.041	0.031
6.786	4	0.034	0.662E+05	1.4	1.4	0.392E+03	0.180E+05	0.027	0.020	0.020	0.027	0.020
6.885	5	0.037	0.799E+07	6.1	6.1	0.397E+03	0.188E+05	0.073	0.050	0.050	0.073	0.050
7.009	2	0.032	0.212E+02	0.2	0.2	0.231E+03	0.114E+05	0.012	0.009	0.009	0.012	0.009
7.009	4	0.032	0.603E+05	1.2	1.2	0.416E+03	0.205E+05	0.026	0.019	0.019	0.026	0.019
7.320	2	0.022	0.100E+02	0.1	0.1	0.469E+03	0.251E+05	0.006	0.004	0.004	0.006	0.004
7.320	3	0.023	0.480E+03	0.2	0.2	0.596E+03	0.319E+05	0.008	0.006	0.006	0.008	0.006
7.401	3	0.039	0.131E+04	0.7	0.7	0.216E+03	0.119E+05	0.023	0.016	0.016	0.023	0.016
7.471	3	0.031	0.838E+03	0.4	0.4	0.335E+03	0.187E+05	0.015	0.010	0.010	0.015	0.010
7.471	4	0.033	0.611E+05	1.3	1.3	0.385E+03	0.215E+05	0.028	0.019	0.019	0.028	0.019
7.471	5	0.034	0.671E+07	5.2	5.2	0.435E+03	0.243E+05	0.066	0.042	0.042	0.066	0.042

CA48 35 MEV FRICKE

04:24 SEP 08, 1974

THE EVALUATION OF $\langle R^* \cdot L \rangle$ WAS DONE USING A FERMI CHARGE DISTRIBUTION.

THE NUCLEAR RADIUS PARAMETER=1.03 F THE NUCLEAR SURFACE THICKNESS PARAMETER=0.520 FWINE BOTTLE=-0.0320

Z = 20 A = 48 BEAM ENERGY IS 35.000MEV

EX	L	BETA	B(L)	G(SP)	G(U,SP)	D(L)	C(L)	D(IRRGT)/D(L)	B(EL)/NEWSR
7.521	3	0.027	0.636E+03	0.3	0.438E+03	0.3	0.248E+05	0.011	0.008
7.521	4	0.028	0.457E+05	0.9	0.512E+03	0.289E+05	0.021	0.014	0.014
7.643	3	0.107	0.101E+05	5.1	0.271E+02	0.158E+04	0.183	0.124	0.124
7.786	4	0.057	0.189E+06	3.9	0.120E+03	0.726E+04	0.089	0.058	0.058
7.940	5	0.040	0.927E+07	7.1	0.296E+03	0.187E+05	0.097	0.058	0.058
8.037	4	0.053	0.163E+06	3.4	0.134E+03	0.865E+04	0.080	0.050	0.050
8.037	2	0.048	0.458E+02	0.5	0.934E+02	0.603E+04	0.030	0.018	0.018
8.037	3	0.050	0.220E+04	1.1	0.118E+03	0.765E+04	0.042	0.027	0.027
8.250	4	0.050	0.146E+06	3.0	0.146E+03	0.992E+04	0.073	0.045	0.045
8.250	5	0.050	0.148E+08	11.4	0.178E+03	0.121E+05	0.162	0.093	0.093
8.364	3	0.015	0.198E+03	0.1	0.127E+04	0.887E+05	0.004	0.002	0.002
8.364	5	0.058	0.196E+08	15.1	0.133E+03	0.932E+04	0.216	0.122	0.122
8.501	3	0.062	0.335E+04	1.7	0.736E+02	0.532E+04	0.067	0.041	0.041
8.543	5	0.068	0.274E+08	21.0	0.933E+02	0.681E+04	0.309	0.171	0.171
8.589	3	0.062	0.340E+C4	1.7	0.718E+02	0.530E+04	0.069	0.042	0.042
8.658	4	0.016	0.145E+C5	0.3	0.140E+04	0.105E+06	0.008	0.004	0.004
8.658	3	0.032	0.887E+C3	0.4	0.273E+C3	0.205E+05	0.018	0.011	0.011
8.786	5	0.100	0.583E+C8	44.9	0.426E+02	0.328E+04	0.677	0.364	0.364
8.868	4	0.018	0.179E+C5	0.4	0.111E+04	0.874E+05	0.010	0.006	0.006
8.868	5	0.072	0.301E+08	23.1	0.818E+02	0.643E+04	0.352	0.188	0.188

CA48 30 MEV ERICKE

04:25 SEP 08, 17

THE EVALUATION, EF <R*EL> WAS DONE USING A FERMI CHARGE DISTRIBUTION.

THE NUCLEAR RADIUS PARAMETER=1.03 F THE NUCLEAR SURFACE THICKNESS PARAMETER=0.520 FWINE BOTTLE=-0.030

Z= 20 A= 43 BEAM ENERGY IS 29.830MEV

EX	L	BETA	B(EL)	G(SP)	GU(SP)	D(L)	C(L)	D(IRROT)/D(L)	B(EL)/NEWSR
3.830	2	0.162	0.533E+03	6.2	6.2	0.168E+02	0.247E+03	0.167	0.215
4.502	3	0.203	0.363E+05	18.3	18.3	0.128E+02	0.260E+03	0.386	0.444
4.607	4	0.263	0.225E+06	4.6	4.6	0.170E+03	0.360E+04	0.63	0.69
5.141	5	0.354	0.171E+08	13.2	13.2	0.248E+03	0.655E+04	0.116	0.107
5.249	5	0.229	0.508E+07	3.9	3.9	0.818E+03	0.225E+05	0.035	0.032
5.295	2	0.029	0.166E+02	0.2	0.2	0.391E+03	0.110E+05	0.007	0.007
5.362	3	0.295	0.794E+04	4.0	4.0	0.492E+02	0.142E+04	0.101	0.097
5.723	5	0.127	0.666E+03	51.2	51.2	0.572E+02	0.187E+04	0.503	0.416
6.098	5	0.41	0.989E+07	7.6	7.6	0.361E+03	0.134E+05	0.080	0.062
6.335	4	0.090	0.462E+06	9.5	9.5	0.601E+02	0.241E+04	0.178	0.143
6.641	2	0.044	0.392E+02	0.5	0.5	0.132E+03	0.582E+04	0.021	0.016
6.641	4	0.044	0.112E+06	2.3	2.3	0.237E+03	0.105E+05	0.045	0.034
6.786	4	0.032	0.595E+05	1.2	1.2	0.436E+03	0.201E+05	0.025	0.018
6.885	5	0.041	0.968E+07	7.4	7.4	0.327E+03	0.155E+05	0.088	0.061
7.009	2	0.033	0.221E+02	0.3	0.3	0.222E+03	0.109E+05	0.013	0.009
7.009	4	0.033	0.628E+05	1.3	1.3	0.400E+03	0.196E+05	0.027	0.019
7.320	2	0.028	0.156E+02	0.2	0.2	0.301E+03	0.162E+05	0.009	0.006
7.320	3	0.029	0.768E+03	0.4	0.4	0.373E+03	0.200E+05	0.013	0.009
7.401	3	0.041	0.145E+04	0.7	0.7	0.196E+03	0.107E+05	0.025	0.018
7.471	3	0.026	0.585E+03	0.3	0.3	0.480E+03	0.268E+05	0.010	0.007
7.471	4	0.028	0.443E+05	0.9	0.9	0.532E+03	0.297E+05	0.020	0.014
7.471	5	0.029	0.501E+07	3.8	3.8	0.583E+03	0.325E+05	0.049	0.031

CA48 30 MEV FRICKE

THE EVALUATION OF $\langle R^* L \rangle$ WAS DONE USING A FERMI CHARGE DISTRIBUTION.

04:24 SEP 08, 1970

THE NUCLEAR RADIUS PARAMETER=1.03 F THE NUCLEAR SURFACE THICKNESS PARAMETER=0.520 FINE BOTTLE= -0.0303

Z = 20 A = 48 BEAM ENERGY IS 29.830MEV

EX	L	BETA	B(EL)	G(SP)	GU(SP)	D(L)	C(L)	D(IRRGT)/D(L)	B(EL)/NEWSR
7.521	3	0.026	0.605E+03	0.3	0.460E+03	0.260E+05	0.011	0.007	0.014
7.521	4	0.028	0.450E+05	0.9	0.520E+03	0.294E+05	0.021	0.021	0.055
7.786	4	0.056	0.179E+06	3.7	0.127E+03	0.767E+04	0.085	0.085	0.054
7.940	5	0.038	0.857E+07	6.6	0.321E+03	0.202E+05	0.090	0.090	0.031
8.037	4	0.042	0.102E+06	2.1	0.215E+03	0.139E+05	0.050	0.050	0.014
8.037	2	0.042	0.358E+02	0.4	0.119E+03	0.772E+04	0.024	0.024	0.019
8.037	3	0.042	0.158E+04	0.8	0.166E+03	0.107E+05	0.030	0.030	0.045
8.250	4	0.050	0.146E+06	3.0	0.146E+03	0.992E+04	0.073	0.073	0.093
8.250	5	0.050	0.148E+08	11.4	0.178E+03	0.121E+05	0.162	0.162	0.002
8.364	3	0.015	0.198E+03	0.1	0.127E+04	0.887E+05	0.004	0.004	0.122
8.364	5	0.058	0.196E+08	15.1	0.133E+03	0.932E+04	0.216	0.216	0.038
8.501	3	0.059	0.312E+04	1.6	0.791E+02	0.572E+04	0.063	0.063	0.194
8.543	5	0.073	0.310E+08	23.8	0.823E+02	0.601E+04	0.350	0.350	0.042
8.589	3	0.063	0.345E+04	1.7	0.708E+02	0.522E+04	0.070	0.070	0.004
8.658	4	0.016	0.145E+05	0.3	0.140E+04	0.105E+06	0.008	0.008	0.011
8.658	3	0.032	0.887E+03	0.4	0.4	0.205E+05	0.018	0.018	0.376
8.786	5	0.101	0.601E+08	46.3	0.413E+02	0.319E+04	0.698	0.698	0.005
8.868	4	0.017	0.161E+05	0.3	0.3	0.968E+05	0.009	0.009	0.169
8.868	5	0.068	0.270E+08	20.8	0.910E+02	0.716E+04	0.317	0.317	

CA48 25 MEV FRICKE

THE EVALUATION OF $\langle R^* L \rangle$ WAS DONE USING A FERMI CHARGE DISTRIBUTION.

THE NUCLEAR RADIUS PARAMETER=1.03 F THE NUCLEAR SURFACE THICKNESS PARAMETER=0.520 FWINE BOTTLE = -0.03171

Z= 20 A= 48 BEAM ENERGY IS 25.110MEV

EX	L	BETA	B(EL)	G(SP)	G(SP)	D(L)	C(L)	D(IRRET)/D(L)	B(EL)/NEWSR
3.830	2	0.174	0.612E+03	7.1	7.1	0.147E+02	0.215E+03	0.192	0.247
4.502	3	0.220	0.354E+05	17.9	17.9	0.132E+02	0.267E+03	0.377	0.433
4.607	4	0.076	0.328E+06	6.8	6.8	0.116E+03	0.247E+04	0.092	0.101
5.141	5	0.065	0.248E+08	19.1	19.1	0.171E+03	0.452E+04	0.168	0.155
5.249	5	0.035	0.724E+07	5.6	5.6	0.574E+03	0.158E+05	0.050	0.045
5.295	2	0.029	0.166E+02	0.2	0.2	0.391E+03	0.110E+05	0.007	0.007
5.362	3	0.096	0.805E+04	4.1	4.1	0.486E+02	0.140E+04	0.102	0.098
5.723	5	0.106	0.652E+08	50.1	50.1	0.584E+02	0.191E+04	0.493	0.407
6.098	5	0.044	0.114E+08	8.8	8.8	0.313E+03	0.116E+05	0.092	0.071
6.335	4	0.095	0.516E+06	10.7	10.7	0.538E+02	0.216E+04	0.199	0.159
6.641	2	0.046	0.433E+02	0.5	0.5	0.120E+03	0.528E+04	0.024	0.017
6.641	4	0.046	0.123E+06	2.5	2.5	0.215E+03	0.950E+04	0.050	0.038
6.786	4	0.032	0.579E+05	1.2	1.2	0.448E+03	0.206E+05	0.024	0.018
6.885	5	0.048	0.133E+08	10.2	10.2	0.238E+03	0.113E+05	0.121	0.083
7.009	2	0.036	0.267E+02	0.3	0.3	0.184E+03	0.902E+04	0.015	0.014
7.009	4	0.036	0.760E+05	1.6	1.6	0.330E+03	0.162E+05	0.032	0.023
7.320	2	0.026	0.141E+02	0.2	0.2	0.332E+03	0.178E+05	0.008	0.006
7.320	3	0.028	0.679E+03	0.3	0.3	0.422E+03	0.226E+05	0.012	0.008
7.401	3	0.047	0.192E+04	1.0	1.0	0.147E+03	0.808E+04	0.034	0.024
7.471	3	0.026	0.575E+03	0.3	0.3	0.488E+03	0.272E+05	0.010	0.007
7.471	4	0.028	0.457E+05	0.9	0.9	0.515E+03	0.288E+05	0.021	0.014
7.471	5	0.031	0.547E+07	4.2	4.2	0.534E+03	0.298E+05	0.054	0.034

CA48 25 MEV FRICKE

THE EVALUATION OF $\langle R^* L \rangle$ WAS DONE USING A FERMI CHARGE DISTRIBUTION.

THE NUCLEAR RADIUS PARAMETER=1.03 F THE NUCLEAR SURFACE THICKNESS PARAMETER=0.520 FWINE BOTTLE= -0.03

Z= 20 A= 48 BEAM ENERGY IS 25.110MEV

EX	L	BETA	B(EL)	G(SP)	GU(SP)	D(L)	C(L)	D(IRRST)/D(L)	B(EL)/NEWSR
7.521	3	0.027	0.657E+03	0.3	0.3	0.424E+03	0.240E+05	0.012	0.008
7.521	4	0.030	0.531E+05	1.1	1.1	0.440E+03	0.249E+05	0.024	0.016
7.643	3	0.110	0.106E+05	5.4	5.4	0.259E+02	0.151E+04	0.192	0.130
7.786	4	0.051	0.148E+06	3.0	3.0	0.153E+03	0.928E+04	0.070	0.046
7.940	5	0.050	0.145E+08	11.1	11.1	0.190E+03	0.120E+05	0.152	0.090
8.037	4	0.052	0.155E+06	3.2	3.2	0.141E+03	0.910E+04	0.076	0.048
8.037	2	0.041	0.336E+02	0.4	0.4	0.127E+03	0.823E+04	0.022	0.014
8.037	3	0.047	0.196E+04	1.0	1.0	0.133E+03	0.861E+04	0.037	0.024
8.250	4	0.050	0.146E+06	3.0	3.0	0.146E+03	0.992E+04	0.073	0.045
8.250	5	0.050	0.148E+08	11.4	11.4	0.178E+03	0.121E+05	0.162	0.093
8.364	3	0.016	0.222E+03	0.1	0.1	0.113E+04	0.791E+05	0.004	0.003
8.364	5	0.064	0.241E+08	18.6	18.6	0.108E+03	0.756E+04	0.267	0.151
8.501	3	0.062	0.338E+04	1.7	1.7	0.731E+02	0.528E+04	0.068	0.041
8.543	5	0.077	0.351E+08	27.0	27.0	0.728E+02	0.531E+04	0.396	0.219
8.589	3	0.065	0.375E+04	1.9	1.9	0.652E+02	0.481E+04	0.076	0.046
8.658	4	0.016	0.145E+05	0.3	0.3	0.140E+04	0.105E+06	0.008	0.004
8.658	3	0.032	0.887E+03	0.4	0.4	0.273E+03	0.205E+05	0.018	0.011
8.786	5	0.103	0.625E+08	48.1	48.1	0.397E+02	0.307E+04	0.726	0.391
8.868	4	0.016	0.145E+05	0.3	0.3	0.137E+04	0.108E+06	0.008	0.004
8.868	5	0.065	0.248E+08	19.1	19.1	0.992E+02	0.780E+04	0.291	0.155